

Application and assessment of multi-wavelength
measurements of variable chlorophyll *a* fluorescence
for analysis of irradiance stress, physiological state and
community composition in freshwater phytoplankton

by

Laura Beecraft

A thesis
presented to the University of Waterloo
in fulfillment of the
thesis requirement for the degree of
Doctor of Philosophy
in
Biology

Waterloo, Ontario, Canada, 2018

©Laura Beecraft 2018

Examining Committee Membership

The following served on the Examining Committee for this thesis. The decision of the Examining Committee is by majority vote.

External Examiner	Dr. Rolf Vinebrooke Professor, Department of Biological Sciences University of Alberta
Supervisor(s)	Dr. Ralph Smith Professor, Department of Biology University of Waterloo
Internal Member	Dr. Simon Chuong Associate Professor, Undergraduate Advisor Department of Biology, University of Waterloo
Internal-external Member	Dr. Claude Duguay Professor, University Research Chair and Associate Dean, Research Department of Geography and Environmental Management University of Waterloo
Other Member(s)	Dr. Susan Watson Adjunct Faculty, Department of Biology University of Waterloo Dr. Kirsten Müller Professor and Associate Dean, Graduate Studies Department of Biology, University of Waterloo

AUTHOR'S DECLARATION

I hereby declare that I am the sole author of this thesis. This is a true copy of the thesis, including any required final revisions, as accepted by my examiners.

I understand that my thesis may be made electronically available to the public.

Abstract

Phytoplankton are a diverse group of organisms of fundamental importance in aquatic ecosystems. Exposure to high levels of photosynthetically active and ultraviolet radiation (PAR and UVR) is unavoidable for most phytoplankton and can result in photoinhibition, an irradiance-dependent loss of photosynthetic capacity that leads to decreased growth and productivity. Chlorophyll *a* (Chl *a*) fluorescence can provide fast and efficient measurements of the abundance, composition and photosynthetic ability of phytoplankton, with the maximum quantum yield of photochemistry ($F_v:F_m$) providing quantification of photoinhibition and other stresses. Multi-wavelength fluorometry targeting photosynthetic accessory pigments characteristic of major phytoplankton groups has potential to provide estimates of group-specific abundance and photosynthetic performance.

A multi-wavelength Pulse Amplitude Modulated fluorometer (Phyto-PAM) was used in this thesis to measure the sensitivity of $F_v:F_m$ of phytoplankton pigment groups in natural assemblages to photoinhibition by PAR and UVR, while simultaneously assessing the group-discrimination abilities of the instrument when applied to complex assemblages. Analogous experiments were used to evaluate the PAR and UVR responses of thirteen laboratory cultures, comparing sunlight sensitivity within and among pigment groups, and with the examined natural communities. The effects of taxon and light exposure on multi-wavelength fluorescence excitation spectra (FES) and associated uncertainty in pigment-group estimates were tested, and Phyto-PAM discrimination abilities were further challenged using different FES settings, relative pigment-group contribution and light exposures.

Estimates of pigment group abundance in natural communities (Hamilton Harbour) were similar to independent measurements by microscopic analysis, but the instrument could usually estimate $F_v:F_m$ only for the dominant group. Light treatments including the UVR wavebands caused the highest levels of photoinhibition. Relative pigment group sensitivity was consistent between laboratory cultures and field data, with cyanobacteria the most sensitive, chlorophytes the least, and chromophytes intermediate but variable. The results suggested that the sunlight tolerance allowing some cyanobacteria to form surface blooms is not due to innate resistance of Photosystem II (PSII) to photoinhibition, but supported observations of resistance to sunlight stress in chlorophytes.

In laboratory populations (cultures), variation of FES among taxa within pigment groups was greater than the variation induced by experimental irradiance exposures, especially for variable fluorescence spectra, and posed the larger challenge to correct measurements of group composition and photosynthetic ability. Group-specific fluorescence estimates were within 10% of true values on average using a variety of FES settings. However, up to 20% of fluorescence was mis-attributed in some cases, and $F_v:F_m$ was estimated for a group not present up to 30% of the time on average. In simple mixtures of two or three uni-algal cultures, group-specific abundance estimates were within 10% of true values 61 to 74% of the time. $F_v:F_m$ estimates were often within 10% of true values for the dominant taxon, but errors increased for taxa at low levels of relative abundance. Group-specific estimates of abundance by Phyto-PAM proved robust, but the scope for errors in quantifying composition and assigning $F_v:F_m$ in some cases was large and highlighted the value of replicate measurements and the continued need for independent verification.

Acknowledgements

There are many to whom I owe thanks for help and support in pursuing my PhD. First, I wish to express my sincere gratitude to my supervisor Dr. Ralph Smith; for his calm and insightful guidance throughout all of my graduate career, and his support and encouragement of both my academic goals and, at times substantial, extracurricular commitments. Funding for all research conducted towards this thesis was supported by an NSERC Discovery Grant to Dr. Ralph Smith, and two Ontario Graduate Scholarships. Thank you to my committee member and collaborator/co-author Dr. Susan Watson, for use of the Phyto-PAM and access to phytoplankton cultures, for sharing her considerable knowledge and expertise in ‘all things algae’, and for introducing the opportunity to serve on the IAGLR board of directors.

Thank you to those with whom I have shared the Smith lab over the years, Joel and Lisa, and especially to Joanna, who showed me the ropes in the lab, and has been a tremendous friend and lab mate throughout the ups and downs of grad school. Thank you to Joanna and Sameer for assistance with laboratory culture work and experiments when I did not have enough hands or time. There are many friends and family to thank for their support during my time in Waterloo, but special thanks go to my dear friends Jessica, Stephanie, Mercedes, Kelly and Ashley.

I am extremely thankful to Matthieu, for his love, support and patience. And finally, I am inexpressibly grateful to my parents, Lloyd and Lois, for their steadfast love, support and inspiration – in all things.

Table of Contents

Examining Committee Membership.....	ii
AUTHOR'S DECLARATION	iii
Abstract	iv
Acknowledgements	vi
Table of Contents	vii
List of Figures	x
List of Tables.....	xiii
List of Abbreviations.....	xvii
Chapter 1 Introduction.....	1
1.1 Phytoplankton and their aquatic environment	1
1.2 Solar radiation and climate warming in aquatic environments	5
1.3 Phytoplankton irradiance responses	8
1.4 Chlorophyll <i>a</i> fluorometry.....	12
1.5 Research objectives	15
Chapter 2 Differential sensitivity of Photosystem II activity to ultraviolet radiation among phytoplankton pigment groups from natural communities.....	18
2.1 Summary	18
2.2 Introduction	18
2.3 Methods.....	21
2.3.1 Sample collection and analyses	21
2.3.2 Irradiance exposure experiments	22
2.3.3 ¹⁴ C-assimilation experiments	23
2.3.4 Phyto-PAM fluorescence parameters and Reference spectra.....	23
2.3.5 Data and statistical analysis.....	24
2.4 Results	24
2.4.1 Environmental conditions.....	24
2.4.2 Community composition and group discrimination	25
2.4.3 Phytoplankton spectral responses and sensitivity.....	28
2.4.4 Irradiance responses of $F_v:F_m$ and ¹⁴ C uptake.....	34
2.5 Discussion	35
2.5.1 Community composition and group discrimination	35

2.5.2 Phytoplankton spectral responses and UVR sensitivity	36
2.5.3 Significance of $F_v:F_m$ for photosynthetic C fixation.....	39
2.6 Acknowledgements.....	41
Chapter 3 Effects of solar radiation stress on Photosystem II efficiency in freshwater phytoplankton pigment groups.....	42
3.1 Summary.....	42
3.2 Introduction.....	42
3.3 Methods.....	45
3.3.1 Culture conditions	45
3.3.2 Irradiance exposures experiments	47
3.3.3 Statistical analyses	48
3.4 Results.....	50
3.4.1 Cumulative inhibition of $F_v:F_m$ in acute exposure experiments	50
3.4.2 Kinetics of F_0 and F_m	52
3.4.3 Modeling kinetics and estimating repair and damage rates	54
3.4.4 Comparisons between laboratory and natural populations	60
3.5 Discussion.....	60
Chapter 4 Quantifying the challenges of taxon- and irradiance-dependent variability for multi-wavelength PAM fluorometry: patterns in excitation spectra and consequences for pigment group estimation.....	66
4.1 Summary.....	66
4.2 Introduction.....	66
4.3 Methods.....	69
4.3.1 Phytoplankton cultures and irradiance exposure conditions	69
4.3.2 Chl <i>a</i> variable fluorescence measurements	70
4.3.3 Statistical analyses	70
4.3.4 Reference Spectra selection	71
4.4 Results and Discussion	73
4.4.1 Taxonomic variation of Reference Spectra.....	73
4.4.2 Effects of Reference Spectra selection on algal group assignment in monocultures.....	79
4.4.3 Effects of PAR and UVR on fluorescence excitation spectra.....	83
4.5 Conclusions and recommendations.....	88

Chapter 5 Quantifying the challenges of taxon- and irradiance-dependent variability for multi-wavelength PAM fluorometry in phytoplankton mixtures	90
5.1 Summary	90
5.2 Introduction	90
5.3 Methods	93
5.3.1 Growth conditions and experimental design	93
5.3.2 Chlorophyll fluorescence measurements	95
5.3.3 Testing effects of taxon abundance and irradiance exposure on estimates of F_0 and $F_v:F_m$	96
5.4 Results	97
5.5 Discussion	110
Chapter 6 Conclusions and future outlook	116
Bibliography	123
Appendix A Chapter 2 Supplementary Tables and Figures	152
Appendix B Chapter 3 Supplementary Tables and Figures	154
Appendix C Chapter 4 Supplementary Tables and Figures	161
Appendix D Chapter 5 Supplementary Tables and Figures	168

List of Figures

- Figure 2.1. Relative $F_v:F_m$ (normalized to time 0 values) after 75 min irradiance exposure averaged across all sampling dates for each spectral treatment P (PAR only), PA (PAR + UV-A) and PAB (PAR + UV-A + UV-B) and algal group (Bl - blues, Gr - greens, Br - browns). Error bars indicate standard deviation..... 30
- Figure 2.2. Kinetics of relative $F_v:F_m$ for the dominant algal group, where symbols represent average values and error bars indicate standard deviation, on (A) July 11, 2012 (green) and (B) August 1, 2012 (blue), with fitted values from the Kok model for treatments PA and PAB and a linear trend line for treatment P. 32
- Figure 2.3. Rate constants of repair (A) and damage (B) compared to post-exposure relative $F_v:F_m$ for PA (open symbols) and PAB (shaded symbols) spectral treatments. Linear regression analyses yielded significant relationships between damage rate and relative $F_v:F_m$ (PA $r^2 = 0.724$, $p = 0.032$, dashed line; PAB $r^2 = 0.894$, $p = 0.001$, solid line). 33
- Figure 3.1 Spectral irradiance of experimental treatments P (PAR only), PA (PAR + UV-A) and PAB (PAR + UV-A + UV-B). Complete spectral irradiance data available electronically upon request..... 48
- Figure 3.2 95% Confidence intervals for post-exposure (75 min) relative $F_v:F_m$ of experimental taxa, separated by spectral treatment P – PAR only (A), PA – PAR + UV-A (B), PAB – PAR + UV-A + UV-B (C), and algal group (Blue – black fill, Brown – no fill, Green – grey fill). Note: *A. oscillarioides* bar represents the range of values rather than the 95% confidence interval, as only 2 experimental replicates were used..... 52
- Figure 3.3 Minimum (F_0) and maximum (F_m) fluorescence over time for *Synechococcus rhodobaktron* (A. F_0 , B. F_m), *Microcystis aeruginosa* (C. F_0 , D. F_m), and *Synura petersenii*. (E. F_0 , F. F_m) with fitted polynomial regressions for each spectral treatment (P - dotted line, PA - dashed line, PAB - solid line)..... 53
- Figure 3.4 Kinetics of relative $F_v:F_m$ for (A) *Dolichospermum lemmermannii*, (B) *Scenedesmus obliquus*, and (C) *Peridinium inconspicuum* with fitted Kok model values for each spectral treatment (P, PA, PAB)..... 57
- Figure 3.5 Repair (upper panel) and damage (lower panel) rate constants for culture strains compared to post-exposure relative $F_v:F_m$ for PA (A,C) and PAB (B,D) spectral treatments. Linear

regression analyses yielded significant relationships between damage rate and relative $F_v:F_m$ for PA and PAB (PA $r^2 = 0.561$, $p = 0.003$, dashed line; PAB $r^2 = 0.748$, $p < 0.003$, solid line). Relationships between repair rate and relative $F_v:F_m$ were non-significant ($p > 0.2$). ... 58

Figure 4.1 Average Reference Spectra (RS) for each algal group (Bl – blues, N = 28, circles and solid line; Bl-sp – special case blues (PE-rich taxa), N = 4, diamonds and dotted line; Gr – greens, N = 13, squares and short-dashed line; Br – browns, N = 12, triangles and dashed line) with error bars representing 95% confidence intervals. (A) F_0 RS, (B) F_v RS. 74

Figure 4.2 Minimum, F_0 (A) and variable, F_v (B) fluorescence RS for 13 monoculture experimental taxa, with line type distinguishing algal group: dashed line – blue, short-dashed line – green, solid line – brown. Note: *S. rhodobaktron* is included with the blue group here, though it does not exhibit the typical blue RS shape. 75

Figure 4.3 NMDS ordination of Phyto-PAM minimum, F_0 (A) and variable, F_v (B) fluorescence Reference Spectra (RS) for freshwater phytoplankton taxa. Solid symbols: RS of 13 experimental taxa, open symbols: remaining library RS (both created using the same Phyto-PAM fluorometer). Stress type 1. Groupings indicated are from hierarchical cluster analysis, with solid lines indicating groups with 90% similarity, and dashed lines around groups with 80% similarity. 77

Figure 4.4 Normalized response spectra from different light treatments (Pre-exposure, P – PAR only, PA – PAR + UV-A, PAB – PAR + UV-A + UV-B) for F_0 (A, C, E) and F_v (B, D, F) for *A. oscillarioides* (A, B), *P. simplex* (C, D) and *S. petersenii* (E,F). 84

Figure 4.5 NMDS ordination of response spectra for F_0 (A) and F_v (B) of 13 experimental taxa (distinguished by Phyto-PAM pigment group: blue, green, brown) following different light exposure treatments (Pre-exposure, P – PAR only, PA – PAR + UV-A, PAB – PAR + UV-A + UV-B). Stress type 1. Groupings indicated are from hierarchical cluster analysis, with solid lines indicating groups with 90% similarity, and dashed lines around groups with 80% similarity. 85

Figure 5.1 Estimated algal F_0 (as percentage of total F_0 signal) compared to true proportions at different contribution levels in binary mixtures. 1:1 line is shown in black, and 1:1 $\pm 10\%$ lines are shown in gray. Solid symbols are matching Reference Spectra (RS) scenarios, open symbols are non-matching RS scenarios. 98

Figure 5.2 Relative offset between observed algal $F_v:F_m$ compared to true $F_v:F_m$ (expressed as percentage of true $F_v:F_m$) in binary mixtures at different contribution levels. Solid symbols are matching RS scenarios; open symbols are non-matching RS scenarios.	100
Figure 5.3 Estimated Algal F_0 (as percentage of total F_0 signal) compared to True proportions at different contribution levels in ternary mixtures. 1:1 line is shown in black, and 1:1 $\pm 10\%$ lines are shown in gray. Solid symbols are matching RS scenarios, open symbols are non-matching RS scenarios.	101
Figure 5.4 Relative offset between observed algal $F_v:F_m$ compared to true $F_v:F_m$ (expressed as percentage of true $F_v:F_m$) in ternary mixtures at different contribution levels. Solid symbols are matching RS scenarios, open symbols are non-matching RS scenarios.	105
Figure A.1 Spectral irradiance of 100% intensity experimental treatments (PAB – PAR + UV-A + UV-B, PA – PAR + UVA-A, and P – PAR only).....	153
Figure B.2 Box plot (Tukey) of relative $F_v:F_m$ (normalized to initial) after 75 min irradiance exposure for all taxa in each spectral treatment (P – PAR only, PA – PAR + UV-A, PAB – PAR + UV-A + UV-B) and algal group, left to right: blues, browns, greens. Boxes represent the median within the first and third quartiles, whiskers represent the lowest and highest points within 1.5 times the first and third quartiles, respectively, with outliers (asterisks) falling beyond this range (outliers not present).	155
Figure B.3 Sample residual plots from Kok model non-linear regression analysis for (A) <i>P. simplex</i> treatment P, (B) <i>D. lemmermannii</i> treatment PA, (C) <i>P. inconspicuum</i> treatment PAB	158

List of Tables

Table 2.1. Light, temperature and chlorophyll a (Chl <i>a</i>) at Station 1001, Hamilton Harbour (SML - surface mixed layer)	25
Table 2.2. Algal group classification by fluorescence (Percentage of Ft) and microscopy (Biomass), and the identity of dominant classes (defined as >10% of total biomass) within each Phyto-PAM pigment group.....	27
Table 2.3. Initial $F_v:F_m$ and post exposure relative $F_v:F_m$ (normalized to initial) of the algal group(s) resolved for each sampling date for treatments P (PAR only), PA (PAR + UV-A) and PAB (PAR + UV-A + UV-B). Values represent mean (\pm standard deviation).....	29
Table 2.4. Group-specific damage and repair rate constants (rate constant, 95% confidence interval) estimated by fitting the Kok model to $F_v:F_m$ exposure response kinetics.....	31
Table 2.5. Phyto-PAM group-specific fluorescence (Ft) proportions as percentages (mean \pm standard deviation) separated by size class.....	33
Table 2.6. Community (645 nm diode) $F_v:F_m$ and ^{14}C uptake spectral responses normalized to PAR-only (P) treatment (mean \pm standard deviation) for different size classes.	34
Table 3.1 Phytoplankton species used in irradiance exposure experiments.....	46
Table 3.2 Broadband PFD for UV-B, UV-A and PAR in the three experimental spectral treatments.	48
Table 3.3 Group-specific initial $F_v:F_m$ and post-exposure relative $F_v:F_m$ (normalized to initial) of phytoplankton taxa for spectral treatments P (PAR only), PA (PAR + UV-A), and PAB (PAR + UV-A + UV-B). Values are mean (\pm standard deviation). Algal Group refers to Phyto-PAM designated groups (Bl - blues, Gr - greens, Br - browns).....	51
Table 3.4 Percent change in minimal fluorescence (F_0) and maximum fluorescence (F_m) (endpoint relative to initial) during experimental irradiance exposures (P, PA, PAB) for each algal group.....	54
Table 3.5 Kok model damage and repair rate constants and r/k ratio of relative $F_v:F_m$ exposure response kinetics for the PAB treatment. (complete results in Table B.5).....	55
Table 3.6 Average rate constants of damage and repair (\pm standard deviation) for each spectral treatment and pigment group.....	56
Table 3.7 Comparison of irradiance response metrics ($F_v:F_m$ and Kok model coefficients) between laboratory monocultures (“Culture”), Hamilton Harbour field assemblages (“Field”1), and	

field results adjusted for comparison to the lower-irradiance laboratory experiments (“Adjusted Field”, see Methods). Values are pigment-group averages (95% confidence interval, or range in cases where $n=2$, indicated by ²).	59
Table 4.1 Experimental Freshwater Phytoplankton Taxa	69
Table 4.2 Scenarios to assess uncertainty in Phyto-PAM estimates of group-specific fluorescence arising from variability of reference spectra (RS), illustrated with <i>Asterionella formosa</i> as the taxon presented to the instrument.	72
Table 4.3 Offset in Algal F_0 and $F_v:F_m$ estimates (as percentage of true values) using different Reference Spectra (RS) scenarios, with minimum and maximum parameters summarizing relative offsets, and mean values summarizing absolute offsets.....	79
Table 4.4 Algal F_0 proportions estimated for each algal group in Reference Spectra (RS) scenarios 2 and 3. Proportions were calculated from replicate measurements for a given case, N, and summary statistics were calculated for all cases for a given algal group.....	81
Table 4.5 Frequency of $F_v:F_m$ estimation for each algal group in Reference Spectra (RS) scenarios 2 and 3. Frequencies were calculated from replicate measurements for a given case, N, and summary statistics were calculated for all cases for a given algal group.....	82
Table 4.6 Interaction probabilities between diode and light treatment for minimum (F_0) and variable (F_v) fluorescence response spectra for each taxon from 2-way ANOVA.	87
Table 5.1 Experimental binary (A-J) and ternary (K, L) mixtures of freshwater phytoplankton.	94
Table 5.2 Differences (expressed as percentage) of estimated F_0 proportions from true values in binary mixtures using matching and non-matching Reference Spectra (RS). Different superscript letters (^{A,B}) indicate groups (contribution levels) that are significantly different ($p<0.05$).....	97
Table 5.3 Relative differences (expressed as percentage) of Estimated $F_v:F_m$ from True Values in Binary Mixtures using matching and non-matching RS. Different superscript letters (^{A,B}) indicate groups (contribution levels) that are significantly different ($p<0.05$).	99
Table 5.4 Main and interaction effects of RS selection (RS), algal group (AG) and taxon contribution level (TC) on estimation errors of F_0 and $F_v:F_m$ in binary and ternary mixtures.	103
Table 5.5 Differences (expressed as percentage) of estimated F_0 proportions from true values in ternary mixtures using matching and non-matching RS. Different superscript letters (^{A,B}) indicate groups (contribution levels) that are significantly different ($p > 0.05$)	104

Table 5.6	Relative differences (expressed as percentage) of estimated $F_v:F_m$ from true values in ternary mixtures using matching and non-matching RS. Different superscript letters (^{A,B}) indicate groups (contribution levels) that are significantly different ($p < 0.05$)......	106
Table 5.7	Relative offset in F_0 estimates (compared to pre-exposure proportions) following acute irradiance exposure (P – PAR only, PA – PAR + UVA, PAB – PAR + UVA + UVB) in mixtures. Mixture codes and taxa correspond to experimental mixtures in Table 5.1. Symbols indicate (^γ) significant light treatment effects (1-way ANOVA, $p < 0.05$), and (^β) light treatments producing algal proportions significantly different from pre-exposure values (Tukey HSD, $p < 0.05$). Taxon 1 of each mixture is shown, taxon 2 offsets are complementary.	107
Table 5.8	Signed and absolute average change in post-exposure F_0 proportions compared to pre-exposure values for each algal group in binary and ternary mixtures. Different superscript letters (^{A,B,C}) indicate algal groups that are significantly different ($p < 0.05$).	108
Table 5.9	Relative difference in observed $F_v:F_m$ between monoculture and binary mixture (expressed as percentage of monoculture values) following irradiance exposures, with interaction effect (IE) p-values for suspension type and light treatment (2-way ANOVA).....	109
Table 5.10	Relative difference in observed $F_v:F_m$ between monoculture and ternary mixture (expressed as percentage of monoculture values) following irradiance exposures, with interaction effect (IE) p-values for suspension type and light treatment.....	109
Table A.1	Broadband photon flux density (PFD) for UV-B, UV-A and PAR in 100% intensity experimental spectral treatments. (Complete radiometric data used to calculate waveband PFD available electronically.)	152
Table A.2	Frequency of group-specific $F_v:F_m$ measurement for each experiment date, where frequencies <95% (grey text) were considered unreliable and not analyzed further (groups >95% shown in black text).....	152
Table B.3	Broadband photon flux density (PFD) for UV-B, UV-A and PAR in experimental spectral treatments. (Complete radiometric data used to calculate waveband PFD available electronically.)	154
Table B.4	Polynomial regression analysis results of minimal fluorescence (F_0) and maximal fluorescence (F_m) during experimental irradiance exposures (P – PAR only, PA – PAR + UV-A, PAB – PAR + UV-A + UV-B) for all taxa examined, and percent change between	

endpoint and initial (normalized to endpoint) and percent change between initial and point of maximum change (normalized to point of maximum change).	156
Table B.5 Damage and repair rate constants (rate constants, 95% confidence interval) estimated by fitting the Kok model to relative $F_v:F_m$ exposure response kinetics, for all taxa and spectral treatments (P, PA, PAB).	159
Table C.6 Phyto-PAM minimum (F_0) and variable (F_v) fluorescence Reference Spectra.	161
Table C.7 Reference Spectra (RS) scenarios applied to each experimental taxon.	164
Table C.8 Effect of excitation wavelength (Exc LED: 470, 520, 645, 665 nm) and light treatment (LightTr: Pre-exposure and post-exposure P, PA, PAB) on normalized minimum (F_0) and variable (F_v) fluorescence for each taxon, based on two-way ANOVA.	166
Table D.9 Phytoplankton Taxa used in Binary and Ternary Experimental Mixtures	168
Table D.10 Reference Spectra (RS) Scenarios applied to each binary and ternary mixture (Taxa presented), with the matching RS scenario for each mixture highlighted in grey.	168
Table D.11 Average estimated algal group F_0 proportions (expressed as percentage of total F_0 signal) at different levels of relative taxon contribution, for taxon 1 in binary mixtures with matching RS applied. Symbols indicate estimated proportions different from true proportions by 5% (γ) and 10% (β), respectively.	170
Table D.12 $F_v:F_m$ of pure culture ('true' $F_v:F_m$, first row and shaded) and relative difference in estimated $F_v:F_m$ (as percentage of pure culture $F_v:F_m$) at different levels of relative contribution in binary mixtures with matching RS applied. Symbols (γ) indicating significant differences in estimated $F_v:F_m$ from true $F_v:F_m$ based on 1-way ANOVA and Tukey's HSD post-hoc analysis ($p < 0.05$).	171
Table D.13 $F_v:F_m$ of pure culture ('true' $F_v:F_m$, first row and shaded) and relative difference in estimated $F_v:F_m$ at different levels of relative contribution in ternary mixtures (K and L, Table 5.1), with symbols (γ) indicating significant differences in estimated $F_v:F_m$ from true $F_v:F_m$ based on 1-way ANOVA and Tukey's HSD post-hoc analysis ($p < 0.05$).	172
Table D.14 Pre-exposure $F_v:F_m$ and post-exposure relative $F_v:F_m$ from independently conducted binary mixture and monoculture irradiance exposure experiments. Average (\pm standard deviation). Letter/number represents mixture code and taxon number.	173
Table D.15 Pre-exposure $F_v:F_m$ and post-exposure relative $F_v:F_m$ from independently conducted ternary mixture and monoculture irradiance exposure experiments. Average (\pm standard deviation).	174

List of Abbreviations

AOA: Algae Online Analyzer

APC: allophycoyanin

ATP: adenosine triphosphate

C: carbon

¹⁴C: radioactive isotope of carbon

Chl *a*: chlorophyll *a*

CBB cycle: Calvin-Benson-Bassham cycle

CCIW: Canadian Center for Inland Waters

CDOM: chromophoric dissolved organic matter

CPCC: Canadian Phycological Culture Center

CPD: cyclobutane pyrimidine dimer

DNA: deoxyribonucleic acid

DOM: dissolved organic matter

E₀: PAR at depth zero (surface irradiance)

ETC: electron transport chain

F₀, F_m, F_v: minimum, maximum and variable fluorescence of Photosystem II Chl *a*

F_v:F_m: dark-adapted maximum quantum yield of photochemistry/of Photosystem II

Fe: iron

FES: fluorescence excitation spectrum/spectra

FP: Fluoroprobe

FRRF: fast repetition rate fluorometry

GHGs: green house gas(es)

HABS: harmful algal bloom(s)

HPLC: high profile liquid chromatography

k: rate constant for damage, as estimated using the Kok model (1956)

K_d: attenuation coefficient of PAR

LED: light emitting diode

LGLs: Laurentian Great Lakes

LHC (LCHI, LCHII): light harvesting complex (of Photosystem I and Photosystem II, respectively)

MAA: mycosporine-like amino acid

N: nitrogen

NADPH: (reduced) nicotinamide adenine dinucleotide phosphate

NPQ: non-photochemical quenching

OCP: orange carotenoid protein

P: phosphorus (when discussed with nutrients)

P, PA, PAB: PAR only, PAR + UV-A and PAR + UV-A + UV-B, respectively (abbreviations for experimental light treatments)

PAM: pulse amplitude modulation

PAR: photosynthetically active radiation

PBS: phycobilisome(s)

PBP: phycobiliprotein(s)

PC: phycocyanin

PE: phycoerythrin

PEC: phycoerythrocyanin

PFD: photon flux density

POM: particulate organic matter

PSI, PSII: Photosystem I, Photosystem II

r: rate constant for repair, as estimated using the Kok model (1956)

ROS: reactive oxygen species

RS: (Phyto-PAM) Reference Spectrum/Spectra

SML: surface mixed layer

UV-A, UV-B, UV-C: ultraviolet-A radiation (320-400 nm), ultraviolet-B radiation (280-320 nm), ultraviolet-C radiation (100-280nm)

UVR: ultraviolet radiation

Z_e: mixed layer depth

Chapter 1

Introduction

Phytoplankton comprise only 1% of the total photosynthetic biomass on Earth, but are responsible for 40-50% of global primary production (Falkowski & Raven 2007). They are a diverse group of organisms found in many environments, and are of critical importance in aquatic ecosystems. Phytoplankton require sunlight for photosynthesis, making them susceptible to stress and cellular damage (photoinhibition) from excess visible light and ultraviolet radiation (UVR). While considerable research has been conducted assessing the effects of photosynthetically active radiation (PAR) and UVR on phytoplankton and primary production (Harrison & Smith 2009; Beardall et al., 2014), particularly in marine environments, there has been no systematic comparison of UVR sensitivity among multiple freshwater taxa spanning the major phytoplankton pigment groups.

Climate warming and anthropogenic impacts strongly influence aquatic systems (McKenzie et al., 2011; Häder et al., 2015; O'Reilly et al., 2015), and growing human populations have resulted in both increased use, and eutrophication, of water – in particular freshwater – resources (Wilhelm et al., 2004). Numerous technologies are used by scientific researchers and environmental resource managers to measure phytoplankton in aquatic systems; chlorophyll *a* (Chl *a*) fluorescence in particular is widely used (Huot & Babin 2010), but there remains considerable uncertainty in parameters estimated from it. The need for reliable and detailed data are an on-going challenge, made difficult by the range of natural variation of phytoplankton themselves, and of their environments. This thesis investigates irradiance stress responses of freshwater phytoplankton and evaluates the use of multi-wavelength variable Chl *a* fluorescence technology to measure them. Knowledge of the comparative response to sunlight stress among different phytoplankton groups and taxa, and the mechanisms involved, is important to understanding current and predicting future phytoplankton dynamics under changing irradiance conditions in aquatic environments. Furthermore, quantifying the reliability and limitations of Chl *a* fluorescence measurements used to estimate phytoplankton abundance and photophysiology is essential for those using and applying these technologies.

1.1 Phytoplankton and their aquatic environment

Phytoplankton are unattached and free-floating, usually microscopic, aquatic organisms typically capable of photosynthesis. Some species can influence their position in the water column through buoyancy control, flagellar motion or gliding motility, but in general phytoplankton move passively

with water currents (Falkowski & Raven 2007). Algae is a term used to refer to both phytoplankton (microalgae) and macroalgae, and describes a polyphyletic group of organisms that typically exhibit common ecophysiological traits: aquatic habitats, oxygenic photosynthesis and relatively simple structural organization (Graham et al., 2016).

Phytoplankton exhibit a tremendous amount of diversity and occupy almost every habitat on Earth. There are roughly a dozen divisions (phyla) of algae (Graham et al., 2016), although a range of classification schemes exist and algal taxonomy is frequently revised and updated. Cyanobacteria are the sole prokaryotic division (Domain Bacteria) of phytoplankton and are commonly referred to as blue-green algae. They have a variety of morphologies (unicellular, colonial and filamentous) and occur in both marine and freshwater environments. Most cyanobacteria contain Chl *a* and phycobilins, or in some cases Chl *b*, as their major light-harvesting pigments (Campbell et al., 1998; Graham et al., 2016). Phycobilins are also important light-harvesting pigments in Rhodophyta, or red algae (primarily marine macroalgae), and Cryptophyta or cryptophytes – unicellular flagellates found in both marine and freshwater habitats (Kirk 1994; Schagerl & Donabaum 2003; Graham et al., 2016).

Chlorophytes, or green algae, are eukaryotic algae containing Chl *a* and *b* as the major light harvesting pigments (Schagerl et al., 2003), and predominantly refers to members of division Chlorophyta. Members of Chlorarachniophyta and some cyanobacteria also contain Chl *a* and *b*. Chlorophyta are both marine and freshwater, and exhibit a range of morphologies: unicellular, colonial, macroalgae, flagellated or non-flagellated (Graham et al., 2016). Euglenophyta are primarily freshwater, unicellular flagellates that utilize Chl *a* and *b* for light harvesting, and also have a number of heterotrophic members. Chromophytes refer to eukaryotic algae containing Chl *a*, *c*, and often different xanthophylls as the major light harvesting pigments, and include several taxonomic divisions: Haptophyta, Ochrophyta and Dinophyta. The majority of dinoflagellates (Dinophyta) are unicellular flagellates, with many marine and some freshwater genera, and with or without thecal plates. Haptophytes (Haptophyta) are primarily marine flagellates, as well as and non-flagellate unicells and colonies. Members of Ochrophyta are distinguished by heterokont flagella at some point in their life cycle, and include several classes of phytoplankton present in marine and freshwater environments: Bacillariophyceae, Chrysophyceae, Synurophyceae, Raphidophyceae and Eustigmatophyceae (Graham et al., 2016).

Phytoplankton abundance and composition are influenced by numerous, interacting factors, but the primary controls of growth and abundance are nutrients, light, temperature and grazing pressure (Helbling & Zagarese 2003; Sommer et al., 2012). The large diversity of phytoplankton species found in a seemingly homogeneous environment produces the potential for high species richness, however communities tend to be dominated by only a handful of species at a given time. Species-specific differences in optima for different factors, as well as competition and consumption by zooplankton, determine the dominant taxa at a given place and time, and contribute to seasonal succession of algal communities (Falkowski & Raven 2007; Sommer et al., 2012). Phytoplankton growth and biomass are supported by sufficient sunlight for photosynthesis, and the availability of nitrogen and phosphorus, with phosphorus the limiting nutrient in many freshwater systems (Kalf 2002; Falkowski & Raven 2007). Other abiotic factors affecting algal growth and photosynthesis include: the availability of macronutrients (as mentioned) and micronutrients, form and concentration of inorganic carbon, pH, and turbulence (Helbling & Zagarese 2003; Falkowski & Raven 2007; Häder et al., 2015). The focus here will be on sunlight, both PAR and UVR, essential to photosynthesis and primary production.

Photosynthesis is the biological conversion of light energy into chemical bond energy, using sunlight, water and carbon dioxide to produce organic carbon compounds and oxygen. In eukaryotic photoautotrophs, photosynthesis takes place within the chloroplasts: membrane-enclosed organelles that contain the thylakoid membranes, with an internal aqueous phase, the lumen, surrounded by an aqueous stroma (Falkowski & Raven 2007). Cyanobacteria do not have chloroplasts and the thylakoid membranes are in the cytoplasm, often located around the periphery of the cell (Campbell et al., 1998; Falkowski & Raven 2007). The organization of the photosynthetic process is highly conserved and involves two major processes: the light-dependent (photochemical) and light-independent (carbon reduction) reactions. The light reactions involve two sequential photoreactions that occur on and within the thylakoid membranes, which contain integral membrane protein complexes and prosthetic groups that facilitate these reactions. Critical components include the D1 and D2 proteins, which provide scaffolding for Photosystems II and I (PSII and PSI) and the electron transport chain (ETC) components. Energy from PAR (and some UVR) is used by PSII to oxidize water, extracting electrons which then move through the ETC for the eventual formation of reduced nicotinamide adenine dinucleotide phosphate (NADPH), and protons, which are used to produce adenosine triphosphate (ATP) (Falkowski & Raven 2007).

The light-independent reactions, or Calvin-Benson-Bassham (CBB) cycle, while not directly dependent on light energy, use the products of the light reactions and thus only occur during light exposure. The CBB cycle uses ATP, NADPH, water and several enzymes to produce organic carbon compounds and water via a carboxylation step, followed by a series of reduction reactions. The fixation and biochemical reduction of carbon dioxide takes place in the aqueous phase, called the stroma (Falkowski & Raven 2007). The photochemical reactions of photosynthesis require electronic transitions within molecules, which begin with the absorption of electromagnetic radiation by pigments.

Pigments are organic molecules that absorb light energy due to the conjugated pi-orbital system of a chromophore (the part of the molecule that absorbs light), and the chemical composition and degree of conjugation result in wavelength-specific absorption. Pigments with a rigid molecular structure must use changes in chemical states (i.e. photochemistry or fluorescence) to release absorbed excitation energy, while molecules with more flexible molecular structures and vibrational states (i.e. carotenoids) can release excitation energy as infrared radiation or heat (Rabinowitch & Govindjee 1970). Autotrophic phytoplankton contain pigments that can be classified as photosynthetic (absorbing radiation with the energy for photochemistry) and non-photosynthetic. There are three types of photosynthetic pigments: chlorophylls, carotenoids, and biliproteins. Non-photosynthetic pigments, often types of carotenoids, have a higher degree of conjugation resulting in absorption of longer wavelength radiation. This longer wavelength radiation does not have a high enough energy to excite Chl *a*, and therefore does not contribute to photosynthesis (Rabinowitch & Govindjee 1970; Kirk 1994). The majority of light absorption is by photosynthetic accessory or antenna pigments, which transfer excitation energy to the reaction centers; together these form light-harvesting complexes for PSII and PSI, (LHCII and LHCI).

Chl *a* is the ubiquitous pigment found in all oxygenic photoautotrophs, and is an essential and highly conserved component of PSI and PSII. Chl *a* has strong absorption in the blue (ca. 465 nm) and red region (670-680 nm) of the visible spectrum, and absorbs weakly in the green and yellow portions. When present, Chl *b* and *c* help to increase absorption within this window at both the short- and long-wavelength ends due to differences in chemical structure, increasing the absorption efficiency of visible light (Kirk 1994; Falkowski & Raven 2007). Carotenoids are C₄₀ (40 carbon) isoprenoid compounds that absorb strongly in the blue and green region of the spectrum, producing their characteristic yellow-orange colours. There are numerous carotenoids, which can be further

classified as carotenes (do not contain oxygen) and xanthophylls (contain oxygen) (Rabinowitch & Govindjee 1970). A variety of xanthophylls are photosynthetic, functioning as accessory pigments for light absorption, and are often characteristic of different phytoplankton groups (Armstrong & Hearst 1996). Carotenoids also function as quenchers of excess excitation energy, releasing energy vibrationally as heat, and acting as antioxidants, neutralizing damaging reactive oxygen species (ROS) and triplet state Chl *a* (Kirk 1994; Helbling & Zagarese 2003).

Phycobilin pigments combine with proteins to form multimeric pigment-protein complexes, the phycobiliproteins (PBP), of which there are four basic types: phycoerythrin (PE, absorption peak approx. 560 nm) and phycoerythrocyanin (PEC) which appear red, and phycocyanin (PC, 625 nm) and allophycocyanin (APC, 650-655 nm), which absorb at longer wavelengths and appear blue (Kirk 1994; Callieri et al., 2014; Rastogi et al., 2015). Small linker proteins further organize PBPs into macromolecular structures, the phycobilisomes (PBSs), consisting of rods extending radially from a core. The shorter wavelength absorbing pigments are at the distal ends of the rods, with increasing wavelength absorbance towards the core, to facilitate energy transfer.

1.2 Solar radiation and climate warming in aquatic environments

The sun emits electromagnetic radiation over a range of wavelengths and energy levels. UVR, specifically UV-B (280-320 nm) and UV-A (320-400 nm), PAR and infra-red (IR) radiation pass through the Earth's atmosphere to the biosphere. The amount and type of radiation entering the water column is affected by: absorption of UVR by the Earth's atmosphere, in particular UV-B by the ozone (O₃) layer; cloud cover; season; reflectance at the water's surface, depending on the angle of incidence (Kirk 1994; Falkowski & Raven 2007; Madronich et al., 2011), and latitude and altitude among other factors. Of the light entering the water, red light is attenuated most quickly because the longer wavelengths of PAR have higher absorption coefficients in water, while shorter wavelength PAR has lower absorption (Kirk 1994). Thus, blue light and long-wavelength UVR (UV-A) travel deeper into the water column.

Light traveling through water interacts with living and non-living matter: particulate organic matter (POM), chromophoric/coloured dissolved organic matter (CDOM, or DOM), and phytoplankton, and these constituents play a role in the effects and attenuation of radiation in the water column (Helbling & Zagarese 2003). POM decreases water clarity, absorbing and to a smaller extent reflecting incoming PAR and UVR and decreasing light penetration in the water column. CDOM significantly

decreases light penetration, in particular UVR and short wavelength PAR (Scott et al., 2009; Häder et al., 2015). UVR also reacts with CDOM causing photobleaching, resulting in destruction of the coloured component and increasing light penetration, and potentially producing ROS and free radicals (Zhang et al., 2013). The density and location of phytoplankton affect PAR and UVR penetration, with absorbance spectra maximal in the blue, and to a lesser extent the red, region of the spectrum due to absorbance by Chl *a* (Millie et al., 2002). In some instances, the density of buoyant phytoplankton can be so high at or near the water's surface that appreciable light penetration is reduced to the top few centimeters of the water column.

UVR is effectively absorbed by a variety of macromolecules in addition to phytoplankton pigments, such as proteins, nucleic acids and lipids, which are necessary for correct genetic, chemical and physiological functioning of cells (He & Hader 2002; Beardall et al., 2014). Higher energy UV-B can produce genetic mutations such as cyclobutane pyrimidine dimers (CPDs) in deoxyribonucleic acid (DNA), and form ROS and free radicals, which can lead to cellular damage such as lipid peroxidation. While longer wavelength UV-A is less damaging compared to equal amounts of UV-B, it comprises a larger proportion of incoming UVR and is transmitted through both the atmosphere and water more effectively than UV-B. Therefore, UV-A can often produce more cumulative biological damage and photoinhibition in phytoplankton compared to UV-B (Kalf 2002; Harrison & Smith 2009; Beardall et al., 2014).

Decreased levels of stratospheric ozone have resulted in increased levels of incident UVR reaching the Earth's surface over the past thirty years (Doyle et al., 2005; McKenzie et al., 2011). While ozone depletion has slowed following the Vienna Convention (1988) and accompanying Montreal Protocol (1989), recovery is slow and varies with latitude due to global tropospheric warming and the feedback mechanisms between greenhouse gases (GHGs), temperature and ozone levels (McKenzie et al., 2011; Beardall et al., 2014; Häder et al., 2015). Aquatic systems are still experiencing increased exposure to PAR and UVR due to the effects of and interactions with climate warming, which are expected to have a greater effect on current and future levels of UVR exposure in the water column compared to ozone depletion (Helbling & Zagarese 2003; Beardall et al., 2014).

Climate warming, or climate change, is the increase in the Earth's average atmospheric temperature, resulting in corresponding changes in climate, including rising ocean surface water temperatures and increases in severe weather patterns (McKenzie et al., 2011). Lakes and inland water bodies can be very sensitive to climate effects, responding quickly to changes in solar

irradiance, precipitation, wind, hydrology, and terrestrial and atmospheric inputs (Williamson et al., 2009). Aquatic systems can experience climate change-related increases in sunlight exposure due to decreases in the amount of snow and ice cover, earlier ice-off events, and earlier onset of stratification (McKenzie et al., 2011; O'Reilly et al., 2015). Populations that typically experienced minimal light exposure under ice cover or during mixis periods are becoming exposed to light sooner, and at higher intensities. Earlier ice-off, earlier onset of stratification and warmer epilimnetic temperatures have been documented in the Laurentian Great Lakes (LGLs) and elsewhere (Austin & Colman 2008; Williamson et al., 2009; O'Reilly et al., 2015). Changing precipitation patterns can increase CDOM delivery during intense rain events, while long dry periods will increase photobleaching, increase surface water temperatures and decrease the depth of the surface mixed layer (SML) (Häder et al., 2015).

An important environmental and water management concern is bloom forming and toxin producing phytoplankton, also referred to as nuisance or harmful algal blooms (HABs). Climate warming and anthropogenic eutrophication contribute to increased proliferation, seasonal dominance and changing/increasing biogeography of nuisance/harmful algae. In marine environments, these are usually species from the Dinophyta and Ochrophyta divisions, while in freshwater systems they are predominantly members of the cyanobacteria. The latter will be examined in more detail. Cyanobacteria have several traits which can directly and indirectly promote their growth under climate warming conditions. Increased epilimnetic water temperatures tend to favour growth of cyanobacteria over other eukaryotic phytoplankton, as many of the bloom-forming taxa have higher optimum growth temperatures (Carey et al., 2012; Paerl & Otten 2013). Earlier and stronger stratification favours gas vesicle-containing buoyant taxa; they can adjust position in the photic zone which facilitates competitive dominance for light (Qin et al., 2015). Cyanobacteria are generally strong competitors for nutrients at both low and high concentrations, with fast uptake rates and the capacity for luxury nutrient storage (Carey et al., 2012; Xiao et al., 2017).

Cyanobacteria are able to maintain maximal rates of photosynthesis and growth at relatively low light, and have been described as low-light adapted (Schwaderer et al., 2011; Carey et al., 2012; Xiao et al., 2017). Marine studies of cyanobacteria have demonstrated a high sensitivity to UVR exposure and limited potential for photoacclimation compared to co-occurring eukaryotic taxa (Kulk et al., 2011; Neale et al., 2014). Conversely, many cyanobacteria possess a variety of mechanisms to cope with high irradiance exposure, including production of photoprotective carotenoids and UV-

absorbing compounds, antioxidant enzymes and molecules, increased rates of protein repair, and the capacity for vertical migration (Paerl & Paul 2012; Fragoso et al., 2014; Qin et al., 2015; Roshan et al., 2015). The ability of bloom-forming Cyanobacteria to tolerate high PAR and UVR exposure is often described as one of the factors contributing to successful bloom formation and competition with eukaryotic phytoplankton (Wulff et al., 2007; Xenopoulos et al., 2009; Paerl & Paul 2012; Häder et al., 2015), though not always with clear evidence. These contradictory observations on cyanobacterial light tolerance may be due to variation among species, strains or ecotypes (Moore & Chisholm 1999; Six et al., 2009; Xiao et al., 2017), and indicate the need for standardized comparisons across a larger sampling of species using both PAR and UVR treatments.

Research is still needed to compare differential PAR and UVR sensitivity among and within phytoplankton groups, as controlled studies examining a broad range of species are still limited, particularly for freshwater phytoplankton. It will be more challenging to observe and understand how the varying sensitivities among algal species interact with other environmental factors, such as temperature, mixing conditions and nutrients in natural systems. The direct and indirect effects of climate warming very likely will have strong effects on the abundance and species composition of both marine and freshwater phytoplankton communities, which may cascade through different trophic levels, and is of concern to researchers, managers and commercial industries utilizing water resources.

1.3 Phytoplankton irradiance responses

Algae must have strategies to balance the absorption and use of incoming radiant energy in the highly fluctuating conditions of aquatic environments, where the quantity and spectral composition of light exposure changes on the course of minutes (vertical mixing, cloud cover), to hours, to seasons. Phytoplankton characteristics which affect their response to PAR and UVR include cell size, growth form (single cell versus colonial), motility, cell covering (e.g. presence of mucilage or sheath, silica or CaCO₃ scales or coccoliths) and the structure and composition of the photosynthetic apparatus and light harvesting antennae (Brunet et al., 2011; Graham et al., 2016). Phytoplankton also have short- and long-term response mechanisms to adapt to sub-optimal, supra-optimal and rapidly fluctuating intensities, and to reduce light-induced damage to photosynthetic and other cellular components.

Irradiance responses of phytoplankton are also influenced by other abiotic factors, such as temperature, salinity and the chemical form and concentration of nutrients. These effects are often

species-specific, with both synergistic and antagonist responses with the effects of light, and in particular UVR, exposure (Litchman et al., 2002; Sobrino et al., 2005; Marcoval et al., 2007; Sobrino et al., 2009; Xenopoulos et al., 2009; Halac et al., 2013; Cabrerizo et al., 2014). High PAR and UVR exposure can impact planktonic organisms in a variety of ways: growth reduction, changes in the uptake of inorganic nutrients, reduced swimming speed, increased cell volume, altered fatty acid composition and increased susceptibility to pollutants (Harrison & Smith 2009; Oberegger et al., 2011; Häder et al., 2015). These irradiance-induced effects on phytoplankton can have subsequent effects at higher trophic levels (e.g. consumption by zooplankton) and/or ecosystem level effects (e.g. carbon cycle and carbon sequestration).

Light is one of the primary factors controlling phytoplankton growth in the water column – they are restricted to the photic zone and light becomes limiting with depth. The most common response by photosynthetic phytoplankton to prolonged low light is an increase in the amounts light harvesting pigments or in the number of reaction centers, to capture more of the available light energy (Falkowski & Raven 2007; Deblois et al., 2013). Motile cells will often move towards a more favourable depth on shorter time scales (minutes) using phototaxis or buoyancy control (Whittington et al., 2000; Richter et al., 2007; Graham et al., 2016). The responses of phytoplankton to high light conditions can be divided into rapid responses, which result in decreased function of PSII: photodamage and photoinhibition, and responses to maintain function: repair, photoprotection and photoacclimation (MacIntyre et al., 2002; Moore et al., 2006; Brunet et al., 2011). These responses act over a range of time scales, vary with other abiotic factors such as temperature and nutrient availability, are often species-specific in type and magnitude. Beyond responses at the organism level, prolonged changes in light conditions can lead to evolutionary responses at the genotypic level, or photoadaptation (Moore et al., 2006).

The inhibition of photoautotrophs by light has been recognized for a century, with experimentation and observation continuing over the past sixty years to further our understanding of the causes and mechanisms involved in the phenomenon of photoinhibition (Adir et al., 2003; Murata et al., 2007). Definitions of photoinhibition and photodamage have slight variations depending on the source, and are often used interchangeably, with the underlying consistency that they describe a decrease in PSII activity caused by light absorption. Photodamage is light-dependent, non-reversible damage to the photosynthetic apparatus that occurs under all light levels, but at low light levels repair processes are sufficient to keep up with rates of damage and the overall rate of photosynthesis is not affected

(Bouchard et al., 2006; Nishiyama et al., 2006; Murata et al., 2007). As light intensity increases, increased rates of photodamage can exceed repair capacity, then net damage occurs and photosynthetic rates can decrease (Lesser et al., 1994a; Heraud & Beardall 2000; Bouchard et al., 2006). In many cases, it is at this point that the process is referred to as photoinhibition, when the net negative effects of light stress can be detected (Murata et al., 2007). Photoinhibition can also be considered a form of PSII-down regulation: an active regulatory process involving reversible inactivation of PSII, reducing electron transport to protect the photosynthetic apparatus (Bouchard et al., 2006; Lohscheider et al., 2011). PSII down-regulation and a reduced electron transport in the thylakoids can also be achieved through non-photochemical quenching (NPQ). Thus, photodamage and photoinhibition are not always equivalent, and some forms of photoinhibition can be described as protective photoinactivation (Bouchard et al., 2006). Photodamage and photoinhibition are caused by both PAR and UVR, and while UV-B directly affects key proteins within PSII (e.g. D1), it has been suggested that the major cause of increased levels of photoinhibition is due to impairment of repair mechanisms by UV-B (Bouchard et al., 2006; Murata et al., 2007; Häder et al., 2015). This is also the case for other environmental stressors, such as temperature and nutrient deficiency, which also increase photoinhibition by slowing repair processes rather than increasing the rates of damage (Murata et al., 2007).

Photoprotection works to decrease the potential damage to phytoplankton cells from excess PAR and UVR by decreasing photodamage, increasing repair, or both. Short-term photoprotective mechanisms include alternate electron flow pathways, *de novo* synthesis of D1 proteins and photorepair, NPQ, state transitions, antioxidant enzyme activity, and vertical migration for motile and buoyant taxa. Extended or frequent exposure to high irradiance can lead to photoacclimation in some species, for example through upregulation of the short-term processes mentioned above, as well as the production of photoprotective carotenoids and UVR absorbing compounds, and adjustment of different cell pigment concentrations (MacIntyre et al., 2002; Moore et al., 2006; Brunet et al., 2011; Qin et al., 2015).

Alternate electron flow pathways include cyclic electron transport around PSI and the Mehler reaction, allowing the cell to utilize incoming excitation energy to generate ATP, without reduction of NADP⁺ or carbon fixation (Falkowski & Raven 2007). These processes already occur under light limiting conditions, and can be increased within seconds to minutes to help use excess excitation energy. State transitions enable the redistribution of a small amount of excitation energy between

photosystems to balance incoming energy in cyanobacteria and chlorophytes, reversibly and on short-time scales (5-10 minutes) (Falkowski & Raven 2007; Papageorgiou & Govindjee 2014; Kirilovsky 2015). NPQ via the xanthophyll pigments in eukaryotes and the orange carotenoid protein (OCP) in cyanobacteria both involve conversion of the xanthophylls or OCP to a form that dissipates energy as heat, reducing the amount of excitation going to the reaction centers. NPQ mechanisms can be initiated within 30 seconds to a few minutes due to increases in the proton gradient across the thylakoid membrane. State transitions and NPQ enable phytoplankton to adjust the functional absorption cross section of PSII, reducing the amount of incoming excitation energy and balancing electron flow through PSII and PSI (Brunet et al., 2011; Papageorgiou & Govindjee 2014; Kirilovsky 2015).

Photorepair of DNA by the enzyme photolyase is stimulated by UV-A, and involves the splitting of UV-B-induced cyclobutane pyrimidine dimers (CPDs) (Karentz et al., 1991; Häder et al., 2015). Because photodamage to PSII occurs at all levels of light exposure, photosynthetic organisms have a highly conserved, though metabolically expensive, light-dependent PSII repair cycle that replaces damaged components with newly synthesized D1 proteins (Bouchard et al., 2006). These repair processes generally take several hours, depending on the extent of the photodamage that occurred (Falkowski & Raven 2007). Phytoplankton also produce molecules and enzymes that are capable of scavenging and neutralizing ROS. Some of these antioxidants include α -tocopherol and non-photosynthetic carotenoids such as β -carotene. Antioxidant enzymes including superoxide dismutase, catalase and ascorbate peroxidase detoxify ROS into hydrogen peroxide, oxygen and water (Nishiyama et al., 2006). These enzymes are often present under regular growth conditions, and enhanced production can occur quickly under UVR exposure and ROS formation (Zeeshan & Prasad 2009; Waring et al., 2010).

Photoacclimation involves phenotypic responses to light availability at the organism level, and takes place on longer time scales from several hours to several days. Phytoplankton can acclimate to changes in light quantity and quality by adjusting the relative amounts of PSII and PSI or by adjusting the size of antenna complexes to balance the output of the two photosystems with respect to incoming light energy and cellular requirements (Moore et al., 2006; Falkowski & Raven 2007). Phytoplankton can increase the relative concentrations of photoprotective pigments, in particular non-photosynthetic carotenoids like zeaxanthin and β -carotene, and decrease photosynthetic pigment content in response to high light (Gao et al., 2007; Wulff et al., 2007; Guan & Gao 2008; Deblois et al., 2013; Qin et al.,

2015). Some phytoplankton, typically larger celled or colonial taxa, synthesize UVR absorbing compounds in response to both high PAR and UVR exposure, such as mycosporine-like amino acids (MAAs). MAAs absorb strongly in the UV-A region, acting as cellular sunscreens and antioxidants (Wulff et al., 2007; Laurion & Roy 2009; Roshan et al., 2015), and are commonly found in large diatoms, dinoflagellates and haptophytes (Marcoval et al., 2007; Halac et al., 2014) and some cyanobacteria (Sommaruga et al., 2009; Castenholz & Garcia-Pichel 2012).

1.4 Chlorophyll a fluorometry

Phytoplankton quantification and characterization are an important part of limnologic and oceanographic research, and there are a variety of methods to examine them, depending on the features of interest. Traditional methods such as Chl *a* extraction and microscopic examination can be time consuming, or require large sample volumes and storage. Estimates of pigment concentration can vary depending on the extraction solvents and treatments (Schagerl & Kuenzl 2007).

Furthermore, microscopic identification requires considerable expertise, and the confidence intervals around sample estimates can be considerable (Rott 1981; Lund et al., 1958; Vuorio et al., 2007). More recent methods of assessing taxonomic composition include pigment analysis by high performance liquid chromatography (HPLC) and genetic analysis to identify taxa using molecular markers, proteomics and gene sequencing (Campbell et al., 2003; Piquet et al., 2008; Simmons et al., 2016; Jeon et al., 2017) . While these techniques provide detailed and specific information on the composition of a given sample, they are time-consuming, sample preparation and protocols are highly sensitive and subject to error, and facilities with the necessary equipment may be limited.

Measurements of photosynthetic activity such as oxygen production or carbon assimilation require long incubation times and large volumes, are subject to bottle effects, and typically give results on the net effects of biological processes in the sample. Thus, methods of measuring phytoplankton biomass, composition and activity that provide rapid information with sufficient detail are extremely advantageous – and measurement of Chl *a* fluorescence has been explored and applied for these purposes.

Fluorescence is the re-emission of light energy as an electron returns to ground state from a singlet excited state, and occurs naturally in the environment when light is absorbed by Chl *a*. It is one of three competing pathways for the dissipation of absorbed excitation energy; the other two pathways are photochemistry and heat dissipation (Falkowski & Raven 2007). The earliest application of Chl *a* fluorescence measurements in aquatic environments was as a proxy for photosynthetic biomass

(Lorenzen 1966), and as technologies advanced and more complex instrumentation was used, more information could be gathered from this phenomenon. Variable fluorescence, for example, measures changes in emitted fluorescence intensity in response to different excitation light intensity and duration, providing information on energy conversion processes in PSII. There are different techniques and instrumentation used to examine variable fluorescence; including fast repetition rate (FRR) fluorometry and pulse amplitude modulated (PAM) fluorometry (Kromkamp & Forster 2003; Huot & Babin 2010), with the latter used in the present research. FRR fluorometry uses a series of rapid flashes, or flashlets, that produce a single reduction of the primary acceptor Q_A and is referred to as the 'single turnover' technique. PAM fluorometry uses a longer pulse of light, sufficient to close all PSII reaction centers and causing multiple turnovers (reducing all electron acceptors in the photosynthetic ETC). These two operational techniques provide different information and the derived variable fluorescence parameters are not directly comparable between the two (Kromkamp & Forster 2003; Cosgrove & Borowitzka 2010; Huot & Babin 2010).

PAM fluorometry can provide information on a variety of photosynthetic parameters including: the maximum (dark-adapted) and effective quantum yields of photochemistry (charge separation at PSII), photochemical and non-photochemical quenching, and rates of linear and cyclic electron flow around PSI (Schreiber et al., 1986; Falkowski & Raven 2007; Cosgrove & Borowitzka 2010). The maximum quantum yield of photochemistry measures the proportion of absorbed excitation energy that is used for photochemistry in PSII reaction centers following dark adaptation, such that NPQ is minimal. When all PSII reaction centers are oxidized and in the open state the majority of incoming excitation energy can be used for linear electron transport and minimal energy is released as Chl *a* fluorescence (minimum fluorescence, F_0). When all PSII reaction centers are reduced, or closed, excitation energy cannot be used for photochemistry, and more must be dissipated as fluorescence (maximum fluorescence, F_m). Thus, the quantum yield of photochemistry is equal to the ratio $F_v:F_m$, where variable fluorescence, $F_v = F_m - F_0$ (Genty et al., 1989; Maxwell & Johnson 2000; Falkowski & Raven 2007). Reduced $F_v:F_m$ can indicate decreased efficiency of photochemistry and linear electron transport, which can in turn affect overall photosynthesis (Genty et al., 1989; Maxwell & Johnson 2000). $F_v:F_m$ is inhibited by a variety of factors including nutrient limitation (Litchman et al., 2002; Shelly et al., 2002; Shelly et al., 2005) and photoinhibition due to excess PAR and UVR exposure (Heraud et al., 2005; Giordanino et al., 2011; Harrison & Smith 2011a), which is examined here.

Multi-wavelength, or spectral, fluorescence measures excitation and/or emission of fluorescence at multiple wavelengths to estimate taxonomic composition of phytoplankton, based on characteristic differences in antenna pigments (Yentsch & Yentsch 1979; Phinney & Yentsch 1985). There are a number of custom-designed instruments and protocols (Millie et al., 2002; Seppala & Olli 2008; Proctor & Roesler 2010; Chekalyuk & Hafez 2011), as well as commercially available fluorometers (Paresys et al., 2005; Aberle et al., 2006; Kahlert & McKie 2014) including FluoroProbe and Algae Online Analyzer (AOA) (FP; bbe Moldaenke GmbH, Kiel, Germany; (Beutler et al., 2002)), Phyto-PAM (Kolbowski & Schreiber 1995; Schreiber 1998), and recently Phyto-PAM-II (Heinz Walz GmbH, Effeltrich, Germany). As of the beginning of 2018 no published research was found using the Phyto-PAM-II. Fluoroprobe (FP) is a profiling fluorometer that discriminates up to four algal pigment groups (blues, greens, diatoms, cryptophytes) and CDOM ('yellow substance') based on sequential excitation with six light emitting diodes (LEDs) (380, 450, 525, 570, 590, 610 nm) (Beutler et al., 2002). Phyto-PAM is a bench top fluorometer that measures variable fluorescence using PAM and estimates Chl *a* concentrations, maximum quantum yield ($F_v:F_m$) and other F_v -related parameters for three pigment groups (blues, greens and browns) using excitation with four LEDs (470, 520, 645, 665 nm) (Schreiber 1998; Kolbowski & Schreiber 1995). Most multi-wavelength fluorometers discriminate pigment groups based on deconvolution of the sample spectrum using linear-unmixing and representative fluorescence excitation spectra, or reference spectra (RS), for each algal group. Reference spectra are created with one or more laboratory cultures of species from each group, or more recently, with natural community spectra that are dominated by a single pigment group (Schreiber 1998; Beutler et al., 2002; Harrison et al., 2016).

Multi-wavelength and variable fluorescence instruments provide estimates of taxonomic composition and photosynthetic electron transport processes quickly from small sample volumes (typically 5 mL or less). The potential to measure photosynthetic parameters and chlorophyll concentrations of multiple taxonomic groups quickly and easily has many applications, both in the laboratory and in the field, such as detection of algal bloom events, comparisons of sensitivity to different stressors among co-occurring groups, and high spatio-temporal sampling of algal composition and photophysiology. Some advantages of different fluorometric instruments include: small sample volumes required; flow-through system designs; minimal sample preparation (in many cases no chemical or reagent additions are needed); rapid measurement protocols; provides information on a variety of parameters and processes; potential post-calibration of algal group assignment; and while data interpretation requires an understanding of phytoplankton

photophysiology, sample handling can be performed by less experienced individuals. However, these fluorometers, like all the previously described methods of phytoplankton characterization, have methodological limitations and margins of error to be considered. The estimation accuracy of group-specific fluorescence parameters can be inconsistent due to physiological and instrumental sources of variability, including: differences in fluorescence excitation and emission properties among species within taxonomic groups; changes in relative pigment content in response to environmental conditions; and variable fluorescence yield in response to physiological cell condition and light exposure (Jakob et al., 2005; Falkowski & Raven 2007; Seppala & Olli 2008; MacIntyre et al., 2010). Individual reference or norm spectra cannot always provide robust group discrimination or estimation under dynamic field conditions or for complex communities. Quantifying the potential variability and uncertainty around estimates of pigment group abundance and variable fluorescence is essential for those collecting and reporting this type of data. While fluorescence results may be less precise compared to other techniques, the advantages described above still make it a valuable tool for aquatic research, and enable targeted sampling efforts if high resolution is required.

1.5 Research objectives

This thesis has two overarching focuses. The first of these was a comparative analysis of UVR effects and sensitivity to photoinhibition among freshwater phytoplankton pigment groups. In particular, a goal was to test the hypothesis that cyanobacteria exhibit higher levels of tolerance to sunlight stress compared to other algal groups – an opinion that is often included as a contributing factor to the dominance of bloom-forming cyanobacteria, but in fact does not have strong literature support. The second focus was an in-depth assessment of the discrimination capabilities and sources of uncertainty in multi-wavelength variable fluorescence measurements, specifically using Phyto-PAM. This area of inquiry evolved during the experimentation and analysis of the multi-wavelength fluorescence data associated with the first objectives.

The comparative UVR responses of freshwater phytoplankton were examined on the natural communities of Hamilton Harbour (Chapter 2), a meso-eutrophic embayment of Lake Ontario, that has been subject to heavy anthropogenic influences, and continues to experience cyanobacterial blooms (Watson et al., 2010), and on thirteen monoclonal freshwater phytoplankton cultures, including representatives from several taxonomic groups and each of the pigment groups distinguished by Phyto-PAM (Chapter 3). The maximum quantum yield of photochemistry ($F_v:F_m$) was used to assess sunlight sensitivity. All irradiance exposure treatments were conducted using the

same instrument under controlled settings, providing a close comparison between the responses of laboratory grown versus natural community organisms. The evaluation of irradiance sensitivity of the Hamilton Harbour assemblages incorporates the acclimation and light history characteristics from natural populations, demonstrating the sensitivity of different pigment groups in their natural state, from a system where bloom-forming cyanobacteria are known to occur, and examines the novel potential of Phyto-PAM to provide group-specific information for natural communities. The experiments with algal monocultures test variations in PSII sensitivity to PAR and UVR within and among major pigment groups under more controlled conditions, and demonstrate if culture results support inferences from field populations. These results will fill a knowledge gap for direct and controlled comparisons of sensitivity to photoinhibition in freshwater eukaryotic algae and cyanobacteria, a factor likely to play a role in succession and community composition in freshwater environments as PAR and UVR exposure change under climate warming conditions.

The potential sources of uncertainty in group classification using multi-wavelength fluorometry were examined by testing the variability of fluorescence excitation spectra within taxa and groups, and testing the potential for instrument error arising from variation in excitation spectra and mixtures of algal groups. The effects of taxonomic variation and light exposure on minimum and variable fluorescence excitation spectra (Phyto-PAM reference spectra) were examined using the thirteen phytoplankton cultures (Chapter 4), quantifying errors in parameter estimates associated with the observed variability. The group discrimination capabilities of the fluorometer were challenged by presenting it with simple mixtures of laboratory cultures at different levels of relative abundance, and following irradiance exposure, to quantify the range of uncertainty typical of parameter estimates (Chapter 5).

The Phyto-PAM fluorometer has been employed by a number of research groups with different experimental focuses. It has been used in more than twenty-five published studies in the last fourteen years, however the number of times its algal group discrimination functions are employed and reported appear to be much lower. Variations in fluorescence excitation (reference) spectra and uncertainty in group-specific biomass estimates have been demonstrated for the Fluoroprobe (Leboulanger et al., 2002; Kring et al., 2014; Escoffier et al., 2015; Harrison et al., 2015) and Algae Online Analyzer (MacIntyre et al., 2010; Goldman et al., 2013), but similar assessments are lacking for the Phyto-PAM. Furthermore, Phyto-PAM uses reference spectra for both F_0 and F_v to estimate both biomass/abundance as well as variable fluorescence parameters for each algal group, and

variations in variable fluorescence excitation spectra have not been as well characterized as those of minimal or background fluorescence. Improved understanding of the ranges and sources of variation in Phyto-PAM reference spectra, as well as quantifying levels of uncertainty in pigment-group estimates of abundance and variable fluorescence, are essential for researchers employing this, or similar, instruments. The results from these experiments will identify major sources of classification error and typical levels of estimate uncertainty, allowing for more informed use of multi-wavelength variable fluorescence in natural community sampling, and reporting of group-specific estimates in study reports.

Each of the four research chapters are written in the format of manuscripts with the intent to publish, with varying amounts of editing and revision support from Dr. Ralph Smith and Dr. Susan Watson as co-authors. Chapter 2, “Differential sensitivity of Photosystem II activity to ultraviolet radiation among phytoplankton pigment groups from natural communities” has been published: Beecraft et al., (2017) *Freshwater Biology*: 62(1): 72-86.

Chapter 2

Differential sensitivity of Photosystem II activity to ultraviolet radiation among phytoplankton pigment groups from natural communities

2.1 Summary

The effects of UV-B, UV-A and PAR on the photochemistry of phytoplankton from Hamilton Harbour, Lake Ontario, were measured to assess how well a multi-wavelength Pulse Amplitude Modulated fluorometer (Phyto-PAM) could discriminate among different pigment groups and to test whether bloom-forming cyanobacteria in this embayment have comparatively high resistance to sunlight stress. Estimates of abundance for the three groups (blues, greens and browns) identified by the Phyto-PAM generally agreed with microscope counts, but the maximum quantum efficiency of photochemistry ($F_v:F_m$) was usually quantified only for the dominant group. In acute exposure experiments, the average inhibition of $F_v:F_m$ by PAR, UV-A and UV-B was <10%, 30% and 60% respectively. More inhibition was observed in the cyanobacteria compared to the eukaryotic phytoplankton, due to higher rates of photosystem damage rather than lower rates of recovery based on the Kok model for photoinhibition. Both $F_v:F_m$ and photosynthetic carbon incorporation showed similar patterns of inhibition. Based on $F_v:F_m$ our results showed no evidence that cyanobacteria are more resistant to UVR stress compared to other groups, however their success as bloom-forming species suggests they must have other mechanisms to tolerate if not thrive under high irradiance conditions. These results demonstrate both the utility and limitations of the Phyto-PAM for the assessment of group-specific abundance and physiological responses in a natural community: general seasonal and inter-group variation can be captured, but improved resolution of less abundant groups would enhance its application.

2.2 Introduction

Selective inactivation of photosystem II (PSII) leads to photoinhibition of phytoplankton photosynthesis (Kok 1956), and is a mechanism that can protect the photosynthetic apparatus by decreasing electron transport through PSII (Anderson et al., 1997; Behrenfeld et al., 1998). However, photoinhibition also results in decreased quantum yield of photochemistry and can lead to lower rates of production and growth (Kok 1956; Heraud & Beardall 2000). Both photosynthetically active

radiation (PAR) and ultraviolet radiation (UVR) contribute to photoinhibition, but UVR is especially damaging and highly variable in aquatic environments (Harrison & Smith 2009; Häder et al., 2011). Irradiance sensitivity varies among phytoplankton taxa and with differences in environmental conditions, such as nutrient status and light history (Harrison & Smith 2009; Xenopoulos et al., 2009). Some cyanobacteria are able to tolerate high levels of sunlight stress (Sommaruga et al., 2009; Fragoso et al., 2014), which may confer a competitive advantage to these species, including some bloom-forming taxa, under these conditions (Xenopoulos et al., 2009; Wu et al., 2011; Paerl & Paul 2012). However, other cyanobacterial taxa exhibit relatively high sensitivity compared to many eukaryotic phytoplankton (Schwaderer et al., 2011), and even the more tolerant taxa suffer detrimental effects under high intensity UVR exposure (Castenholz & Garcia-Pichel 2012). To date, however, there is insufficient knowledge to predict how a given taxonomic entity, whether cyanobacterial or eukaryotic, will respond to sunlight stress in a particular habitat. New methods and more information are needed to assess the role of sunlight stress in phytoplankton ecology, including the particular case of bloom-forming cyanobacteria.

Analysis of the variable fluorescence of chlorophyll *a* (Chl *a*) enables rapid in situ measurement of photosynthetic light capture and utilization in eukaryotic algae and cyanobacteria, and the increased variety and utility of equipment available has made its use more prevalent (Huot & Babin 2010). Variable fluorescence using Pulse Amplitude Modulated (PAM) fluorometry measures minimal fluorescence (F_0) under low level light after dark acclimation, and maximal fluorescence (F_m) after excitation with a saturating pulse of light sufficient to transiently close all PSII reaction centers. The ratio of variable to maximal fluorescence gives the maximum quantum yield of photochemistry in the dark adapted state, $F_v:F_m$, where $F_v = F_m - F_0$ (Schreiber et al., 1986; Huot & Babin 2010). Decreases in $F_v:F_m$ are often indicative of photoinhibition and can be described effectively by simple models of first-order kinetics (Kok 1956; Heraud & Beardall 2000). The Kok model (1956) describes photoinhibition during light exposure as the product of competing processes of damage and repair, where damage is proportional to the concentration of the photosensitive component. Variable fluorescence thus provides a rapid and sensitive method for characterizing photoinhibition in phytoplankton populations and communities. However, photoinhibitory effects on photosynthetic production inferred from variable fluorescence may not correspond to results from more traditional ecological methods. $F_v:F_m$ can show considerable decreases while photosynthetic carbon fixation is relatively unimpaired (Behrenfeld et al., 1998; Gilbert et al., 2000), while in other cases it may correlate well with reductions in oxygen production and carbon fixation (Genty et al., 1989; Heraud

& Beardall 2000; Andreasson & Wängberg 2006). It remains desirable to supplement fluorescence measurements with oxygen or carbon flux measurements where possible.

Differences in fluorescence excitation spectra between 400-600 nm, derived from taxon-specific antennae pigments, can facilitate identification of the dominant algal groups present in a sample (Yentsch & Yentsch 1979; MacIntyre et al., 2010). This principle is used in commercially available PAM fluorometers, specifically the Phyto-PAM (Heinz Walz GmbH, Effeltrich, Germany), to assign $F_v:F_m$ values for up to three phytoplankton groups: blues (cyanobacteria), greens (chlorophytes), and browns (diatoms, dinoflagellates, chrysophytes and cryptophytes, collectively referred to as chromophytes) (Kolbowski & Schreiber 1995). Measures of group-specific abundance and variable fluorescence require calibration with an individual reference spectrum for each group, generally defined using monospecific laboratory cultures grown under standard conditions. In natural communities, variations in species composition and physiological condition within and between groups may cause observed spectra to differ from reference spectra, leading to uncertainty in group characterization by spectral fluorescence (Jakob et al., 2005; MacIntyre et al., 2010). To date there have been few published assessments of how such potential complications may affect interpretation of Phyto-PAM measurements of natural communities.

The objective of the current study was to assess the ability of the Phyto-PAM fluorometer to quantify algal group composition and maximum quantum yield ($F_v:F_m$) in natural phytoplankton communities of a meso-eutrophic system that experiences periodic blooms of colonial cyanobacteria. We hypothesized that Phyto-PAM would correctly detect relative group composition based on fluorescence and be able to assign group-specific $F_v:F_m$ for dominant groups, but that results would be more variable for less abundant groups. The second objective was to characterize the irradiance stress responses of community and group-specific quantum yield. It was hypothesized that UVR at simulated natural levels of exposure would cause higher levels of photoinhibition than PAR, that the photoinhibition kinetics of $F_v:F_m$ would follow the damage-recovery model of Kok (1956), and that cyanobacteria would be more resistant to photoinhibition compared to chromophyte and chlorophyte taxa. The third objective was to determine whether decreases in $F_v:F_m$ were indicative of decreases in photosynthetic carbon fixation for natural communities and individual pigment groups in our study system.

2.3 Methods

2.3.1 Sample collection and analyses

Field sampling was conducted at the central deep-water (ca. 22 m) station in Hamilton Harbour (Station 1001, 43°17.3'N; 79°50.4'W) from the Canada Center for Inland Waters (CCIW) Burlington, ON, once per month from April to September 2012 and September and October 2013. Hamilton Harbour is an embayment at the western end of Lake Ontario, subject to long-term heavy anthropogenic impacts, and regular occurrences of cyanobacterial blooms (Watson et al., 2010). Recent water quality assessments indicate it is meso-eutrophic, with long-term surface water (1 m) averages for total phosphorus of 31.6 ± 20.1 , 36.8 ± 12.6 and $30.8 \pm 9.1 \mu\text{g}\cdot\text{L}^{-1}$ and 7.6 ± 6.6 , 14.1 ± 8.6 , $8.9 \pm 14.4 \mu\text{g}\cdot\text{L}^{-1}$ for Chl *a* for spring (Mar-May), summer (Jun-Aug) and fall (Sep-Nov), respectively, and a summer average secchi depth of 2.1 ± 0.07 m (Hiriart-Baer et al., 2009). Temperature and radiometric profiles were taken using a Multichannel Cosine Irradiance Profiling Spectroradiometer (BIC-2104, Biospherical Instruments Inc., San Diego, CA); April and May profiles are missing due to technical complications, and supplemental data was provided by Dr. Veronique Hiriart-Baer (Environment and Climate Change Canada). Diffuse vertical attenuation coefficients (K_d) for PAR, 340, 320 and 305 nm were estimated from linear regression of the natural logarithm of irradiance vs. depth. Mean PAR in the surface mixed layer (SML) was calculated as:

$$(1) \quad \text{mean PAR} = E_0 (e^{-K_d \times Z_e} - 1) (-K_d \times Z_e)^{-1}$$

Where E_0 is PAR at depth zero, K_d is the attenuation coefficient for PAR, and Z_e is the depth of the mixed layer. Z_e was estimated from depth-temperature profiles using a thermocline criterion of $>\Delta 1 \text{ }^\circ\text{C}\cdot\text{m}^{-1}$. Lacking regular monitoring to define temporal trends of incident PAR across the sampling period, E_0 was estimated from the theoretical incident irradiance as calculated from date, latitude, and fixed atmospheric transmission constants (Fee 1990).

Whole water samples were collected mid-morning from 1m below surface using Niskin bottles, to capture phytoplankton from within the surface mixed layer with near-surface light history exposure. They were transported in coolers to an incubator where they were kept at *in situ* temperature and PAR of $80 \mu\text{mol}\cdot\text{m}^{-2}\cdot\text{s}^{-1}$ on a natural light/dark cycle until experiments were conducted the following day. Aliquots (100-250 mL) were filtered (47 mm Whatman GF/F glass fiber filters, nominal pore size 0.8 μm) and frozen for subsequent Chl *a* analysis (Parsons & Strickland 1963) using 90% acetone extraction at $-20 \text{ }^\circ\text{C}$ for 18-24 hrs., followed by pre- and post-acidification fluorescence

measurements using a Turner Fluorometer (Turner Designs 10-AU, Sunnyvale, CA). Samples were preserved with Lugol's iodine for microscopic examination by the Utermöhl technique for identification and quantification of the phytoplankton community. Biomass was calculated from average cell dimensions measured from samples applied to geometric shapes assigned to each cell (Brierly et al., 2007). Cells were identified to genus level when possible, and combined into classes for reporting biomass values.

2.3.2 Irradiance exposure experiments

Acute irradiance exposures were performed in triplicate in a solar simulator with a Xenon arc lamp (1 kW, Oriel Instruments, Irvine, CA), optical glass cut-off filters (Schott and Hoya optics) with nominal 50% transmission at 305, 340 and 420 nm, and neutral density filters (perforated nickel plates). This produced three spectral treatments: PAR only (>420 nm); PAR + UV-A (>340 nm); PAR + UV-A + UV-B (>305 nm), hereafter referred to as P, PA and PAB, respectively, at two intensities: 50% and 100%, for a total of six light treatments. The spectral irradiance incident on samples at 100% was measured using an LT-14 spectrometer (S/N: 09121132, Stellarnet Inc., Tampa FL USA) and is shown in Appendix Table A.1 and Figure A.1. Data for only the 100% intensity treatments are included in the current analysis, as they covered the range of responses exhibited. The photon flux density (PFD) of PAR was monitored throughout the experiments with a LiCor (Q15458) photometer. Samples were maintained at their original temperature ± 1 °C.

To begin experiments, subsamples were transferred to Pyrex beakers in the solar simulator. Experimental exposures were 90 minutes in duration, with 3 mL samples removed from each light treatment at 11 time points and transferred to a dark incubator maintained at original in situ temperature for ca. 20 to 30 minutes of dark acclimation, allowing relaxation of non-photochemical quenching (NPQ). Samples were measured in a quartz cuvette using the Saturation Pulse method with a Phyto-PAM fluorometer (S/N: PPAA0220) equipped with a System II emitter-detector unit (Phyto-ED, S/N EDEF0111), which includes an array with 4 wavelengths of measuring light, a red actinic light and a photomultiplier detector. Minimum dark adapted fluorescence (F_0) was measured using low frequency (ca. 25 Hz) modulated measuring light, followed by a pulse of saturating light (0.2 sec up to 2600 $\mu\text{mol quanta}\cdot\text{m}^2\cdot\text{sec}^{-1}$ at 655 nm) to measure maximal fluorescence (F_m), supporting calculation of maximum quantum yield of photochemistry in the dark-adapted state, or $F_v:F_m$ (where $F_v = F_m - F_0$) (Schreiber et al., 1986; Huot & Babin 2010). Corrections for dissolved fluorescence were made with 0.2 μm filtered sample water.

2.3.3 ¹⁴C-assimilation experiments

Triplicate irradiance exposure experiments on Sept. 19 and Oct. 2, 2013 samples provided comparisons of carbon uptake and Chl *a* fluorescence responses. Sample water inoculated with NaH¹⁴CO₃ to a concentration of 29.6 MBq·mL⁻¹ was incubated under the P, PA and PAB light treatments in 85 mL aliquots for 75 minutes, with parallel samples of un-inoculated sample water for Chl *a* fluorescence measures. Only the 100% intensity light treatments were used for these comparative measurements of irradiance effects on carbon assimilation and fluorescence. Due to the complexity of the manipulations, only initial and endpoint measurements were made for variable fluorescence (Phyto-PAM) and ¹⁴C incorporation.

Samples were size fractionated via low vacuum pressure (<100 mmHg) filtration through Nitex filters (30, 60, 100 μm) and Whatman GF/F filters to differentiate irradiance effects on different size classes, in particular larger colonial cyanobacteria. Unlabelled samples from the Nitex filters were re-suspended in filtered lake water and then dark-acclimated for 30 min at original *in situ* temperature. Triplicate subsamples from each size fraction were measured using the Phyto-PAM, including unfiltered samples to represent the whole community. ¹⁴C-labelled sample filters (duplicate) were acidified to remove inorganic tracer, followed by addition of 15 mL of EcoLume (MP Biomedicals LLC, Solon OH) scintillation cocktail. Activity was measured in 20 mL glass vials with a LS 6500 Multi-purpose Scintillation Counter (Beckman Coulter, USA) for 5 min. ¹⁴C incorporation by phytoplankton photosynthesis was corrected from dark bottle values, and normalized to the PAR-only (P) light treatment.

2.3.4 Phyto-PAM fluorescence parameters and Reference spectra

The Phyto-PAM returns fluorescence measurements and fluorescence-derived parameters for the four excitation diodes (470, 520, 645, 665 nm) and for three algal groups: blues (cyanobacteria), greens (chlorophytes), and browns (chromophytes). The algal group values are deconvoluted from the four diode signals, using linear unmixing based on one pre-selected reference spectrum for each of the three pigment groups. Two different combinations of reference spectra were used based on microscopic examination of the samples. Reference spectra measured for *Chlamydomonas reinhardtii* and *Asterionella formosa*, as representative of the green and brown signals, respectively, were used throughout. For the blue group, either *Dolichospermum* (syn. *Anabaena*) *lemmermannii* or *Microcystis aeruginosa* was used, depending on the predominant taxa present in the sample based on microscopic observations.

Group-specific $F_v:F_m$ estimates were accepted for subsequent analysis only when values were obtained for the majority of replicate measurements. The Phyto-PAM can give erratic estimates when a group is in low abundance, and its variable fluorescence is hard to resolve. In such cases, an appreciable fraction of attempted measurements will fail to return an $F_v:F_m$ value for the group concerned, and values that are returned can vary widely. A measurement frequency of 95% or higher was adopted as the criterion for accepting group-specific $F_v:F_m$ estimates, using all replicate time series measurements of algal group $F_v:F_m$ for a given sample date. The full ramifications of reference spectrum variability and other factors influencing the interpretation of group-specific results from the Phyto-PAM are the subject of Chapters 4 and 5.

2.3.5 Data and statistical analysis

Non-linear regression analysis was used to fit the kinetics of $F_v:F_m$ to the Kok (1956) model of photoinhibition:

$$(2) \quad \frac{P}{P_i} = \frac{r}{(r+k)} + \frac{k}{(k+r)} * e^{-(k+r)t}$$

Where t is time, P_i is the initial $F_v:F_m$ at time zero (prior to irradiance exposure), P is $F_v:F_m$ at time t , and k and r are rate constants for damage and recovery, respectively (Heraud & Beardall 2000). Statistical analyses were performed using Systat 10 (Systat Software, Inc., Chicago, IL).

2.4 Results

2.4.1 Environmental conditions

Light attenuation within the water column was relatively consistent among sampling dates for the UVR wavelengths measured (Table 2.1) with the depth of 1% surface irradiance ($Z_{1\%}$) averaging 0.6, 0.8 and 1.0 m for 305, 320 and 340 nm wavelengths, respectively. Transmission of PAR exhibited more seasonal variation (Table 2.1) with $Z_{1\%}$ ranging from 5.4 to 9.4 m. The lowest surface mixed layer water temperature of 9.4 °C was measured in April, increasing to a maximum of 24.2 °C in August, and then decreasing in the autumn of 2012. The mean irradiance throughout the surface mixed layer, affected by incident solar irradiance and mixing depth, was higher during the summer months of June and July, and lower in spring and early fall. It was unusually high in May 2012, likely due to low Chl a levels and the resulting reduction in light attenuation. Chl a concentration ranged from a low of 1.3 $\mu\text{g}\cdot\text{L}^{-1}$ in May 2012 to a high of 53.3 $\mu\text{g}\cdot\text{L}^{-1}$ in September 2012, the latter measured

during a peak in cyanobacterial biomass (e.g. $>40 \mu\text{g}\cdot\text{L}^{-1}$). The highest Chl *a* values were in August, September and October.

Table 2.1. Light, temperature and chlorophyll a (Chl *a*) at Station 1001, Hamilton Harbour (SML - surface mixed layer)

Sampling Date	1% Surface Irradiance Depths (m)				Mean Irradiance in SML (mol photons $\cdot\text{m}^{-2}\cdot\text{day}^{-1}$)	SML Temp ($^{\circ}\text{C}$)	Chl <i>a</i> conc ($\mu\text{g}\cdot\text{L}^{-1}$)
	PAR	340 nm	320 nm	305 nm			
18/04/2012	5.9*				3.87	9.4	10.9
23/05/2012	8.3				13.44	17.0	1.3
20/06/2012	5.7	1.0	0.8	0.6	8.24	21.5	11.2
11/07/2012	6.5	1.2	0.9	0.5	9.23	23.8	5.9
01/08/2012	4.6	1.2	0.9	0.6	6.8	24.2	16.0
13/09/2012	9.4	0.9	0.7	0.6	7.59	20.5	53.3
19/09/2013	5.4	1.0	0.8	0.6	4	17.6	43.0
02/10/2013	7.0	1.1	0.8	0.6	3.73	18.2	24.2

*Value calculated from May 10, 2012 profile data due to equipment problems on date of sample collection

2.4.2 Community composition and group discrimination

The dominant algal group identified by the Phyto-PAM in April, May and June 2012 was the browns (Table 2.2), consistent with microscopic identification indicating that a large majority of community biomass was cryptophytes, diatoms and dinoflagellates during that period. This corresponded well to the frequency of group-specific $F_v:F_m$ assignment, with the brown group above the 95% threshold in the first three sampling months, and other groups below (Table A.2). In July 2012 $F_v:F_m$ was resolved for both greens and browns with reliable frequency, and fluorescence proportions were slightly below 80% and 20%, respectively. This classification was again supported by microscopic examination which identified almost 70% of the sample biomass as chlorophytes and just over 30% as chromophytes, primarily dinoflagellates. For August 2012, Phyto-PAM indicated that green and brown groups were close to 20% each, with the blue group at 60% (Table 2.2). Filamentous cyanobacteria were the major contributors to biomass (ca. 70%), with smaller and approximately equal biomass of chlorophyte and chromophyte taxa. Only the blue group had $F_v:F_m$ estimates at a frequency above the 95% threshold (Table A.2). Despite the appreciable contributions of brown and green groups to fluorescence and biomass the Phyto-PAM was frequently unable to resolve their $F_v:F_m$ values in the August sample. In September 2012 the blue group was dominant in fluorescence and biomass (ca. 84%), in particular the colonial cyanobacteria *Microcystis*, with most of the

remaining fluorescence and biomass in the green group. $F_v:F_m$ was defined with high frequency (>95% threshold) for both blue and green groups, but not the brown group in the September sample. In September 2013, fluorescence and biomass measures both ranked browns as dominant, followed by blues and then greens (Table 2.2). $F_v:F_m$ was resolved with >95% frequency for the two more abundant groups (Table A.2). In October 2013 the fluorescence and biomass measures disagreed on the relative abundance of browns and greens, but both identified the browns as the most abundant group. $F_v:F_m$ was resolved with reliable frequency for both browns and blues. Due to the increased complexity of incorporating ^{14}C uptake experiments during the 2013 experiments, only initial and endpoint samples were taken, rather than a full times series. This decreased the overall number of fluorescence measures available for assessing the reliability of Phyto-PAM estimates of group abundance and $F_v:F_m$, and may contribute to the more variable group discrimination results.

Table 2.2. Algal group classification by fluorescence (Percentage of Ft) and microscopy (Biomass), and the identity of dominant classes (defined as >10% of total biomass) within each Phyto-PAM pigment group.

Sampling Date	Pigment Group	Group Ft Proportion	Biomass (mg·L ⁻¹)	Percentage of Total	Dominant Algal Classes (>10% of total biomass)
18/04/2012	Bl	0.0%	0.03	0.3%	Cryptophyceae, Bacillariophyceae
	Gr	3.3%	0.52	4.6%	
	Br	96.7%	10.76	95.1%	
	Total		11.31		
23/05/2012	Bl	0.0%	0.00	0.0%	Cryptophyceae
	Gr	26.5%	0.14	2.7%	
	Br	73.5%	5.22	97.3%	
	Total		5.36		
20/06/2012	Bl	6.0%	0.10	0.2%	Bacillariophyceae, Dinophyceae, Cryptophyceae
	Gr	14.0%	1.90	4.0%	
	Br	80.0%	45.86	95.8%	
	Total		47.85		
11/07/2012	Bl	1.9%	0.04	0.3%	Desmidiaceae, Chlorophyceae Dinophyceae
	Gr	79.2%	8.99	68.5%	
	Br	18.8%	4.10	31.2%	
	Total		13.13		
01/08/2012	Bl	57.6%	89.53	70.2%	Cyanophyceae (esp. <i>Dolichospermum</i>) Bacillariophyceae
	Gr	21.9%	25.06	15.4%	
	Br	20.5%	23.55	14.4%	
	Total		138.14		
13/09/2012	Bl	84.2%	82.98	83.7%	Cyanophyceae (esp. <i>Microcystis</i>)
	Gr	15.8%	24.88	12.0%	
	Br	0.0%	3.08	4.3%	
	Total		110.94		
20/09/2013	Bl	28.1%	33.62	33.7%	Cyanophyceae (esp. <i>Dolichospermum</i> , <i>Aphanizomenon</i>) Dinophyceae
	Gr	14.5%	19.96	20.0%	
	Br	57.4%	46.27	46.3%	
	Total		99.85		
03/10/2013	Bl	18.4%	10.32	15.5%	Dinophyceae (esp. <i>Gymnodinium</i>), Bacillariophyceae
	Gr	36.7%	6.26	9.4%	
	Br	44.9%	50.05	75.1%	
	Total		66.63		

2.4.3 Phytoplankton spectral responses and sensitivity

The initial (pre-exposure) $F_v:F_m$ for the blue group was lower than for the brown and green groups on the same or different dates when they were resolved (Table 2.3). Values for brown and green groups were high, usually close to or above 0.65. Averaged across all experiments (Figure 2.1), the largest decrease in quantum yield was in the full spectrum treatment (PAB), followed by PAR+UV-A (PA), and then the PAR-only treatment (P). Post-exposure $F_v:F_m$ response was assessed based on spectral treatment and algal group using two-way analysis of variance (ANOVA). There were significant differences within both spectral treatment and algal group ($F = 81.2$ and 16.2 , respectively, $p < 0.001$ for both), but no interactions between the two. Post-exposure $F_v:F_m$ of the blue group was significantly different from that of the brown group ($p = 0.005$), and all three spectral treatments had $F_v:F_m$ endpoints significantly different from each other ($p < 0.001$). Thus, within each spectral treatment the relative sensitivity among the three algal groups showed the same general relationship, with the blues showing the highest sensitivity, followed by greens and browns.

For all sampling dates, the P spectral treatment had little to no impact on $F_v:F_m$ (Figure 2.1, Table 2.3), with an average decrease of less than 10%. The strongest effects (Table 2.3) were measured for the green group in July (23%) and blue group in September 2012 and 2013 (16% and 18%, respectively). There was a wider range in response to the PA treatment, with decreases in $F_v:F_m$ (across dates and algal groups) between 30-35% from untreated values. $F_v:F_m$ in the PAB treatment was reduced by close to 60% on average. The blue group showed reductions of 48-88%, while the more resistant brown group had reductions of 23-73%. However, the browns that dominated in June and the greens that dominated in July exhibited relatively large decreases in $F_v:F_m$ (Table 2.3), emphasizing the potential for variation in response within groups and across dates. PAR intensity varied slightly among spectral treatments (Table A.1), but given the small differences and the relatively minor effect of PAR on relative $F_v:F_m$, it is unlikely to have significantly affected our results.

Table 2.3. Initial $F_v:F_m$ and post exposure relative $F_v:F_m$ (normalized to initial) of the algal group(s) resolved for each sampling date for treatments P (PAR only), PA (PAR + UV-A) and PAB (PAR + UV-A + UV-B). Values represent mean (\pm standard deviation).

Sample Date	Dominant Algal Group(s)	Initial $F_v:F_m$ (no exposure)	Post-exposure Relative $F_v:F_m$		
			P	PA	PAB
18/04/2012	Br	0.65 (\pm 0.01)	0.9 (\pm 0.16)	0.81 (\pm 0.02)	0.49 (\pm 0.1)
23/05/2012	Br	0.7 (\pm 0.03)	0.98 (\pm 0.03)	0.79 (\pm 0.04)	0.4 (\pm 0.06)
20/06/2012	Br	0.66 (\pm 0.03)	0.91 (\pm 0.02)	0.64 (\pm 0.05)	0.27 (\pm 0.09)
11/07/2012	Gr	0.59 (\pm 0.01)	0.77 (\pm 0.14)	0.52 (\pm 0.06)	0.32 (\pm 0)
	Br	0.51 (\pm 0.04)	1.07 (\pm 0.16)	1.08 (\pm 0.21)	0.77 (\pm 0.05)
01/08/2012	Bl	0.49 (\pm 0.06)	0.9 (\pm 0.17)	0.61 (\pm 0.14)	0.25 (\pm 0.15)
13/09/2012	Bl	0.38 (\pm 0.03)	0.84 (\pm 0.04)	0.37 (\pm 0.05)	0.12 (\pm 0.04)
	Gr	0.66 (\pm 0.03)	0.99 (\pm 0.1)	0.92 (\pm 0.06)	0.5 (\pm 0.05)
19/09/2013	Bl	0.51 (\pm 0.04)	0.82 (\pm 0.04)	0.54 (\pm 0.03)	0.33 (\pm 0.18)
	Br	0.64 (\pm 0.03)	0.93 (\pm 0.04)	0.63 (\pm 0.07)	0.49 (\pm 0.09)
02/10/2013	Bl	0.54 (\pm 0.05)	0.9 (\pm 0.08)	0.57 (\pm 0.05)	0.52 (\pm 0.08)
	Br	0.68 (\pm 0.06)	0.97 (\pm 0.05)	0.73 (\pm 0.08)	0.56 (\pm 0.02)

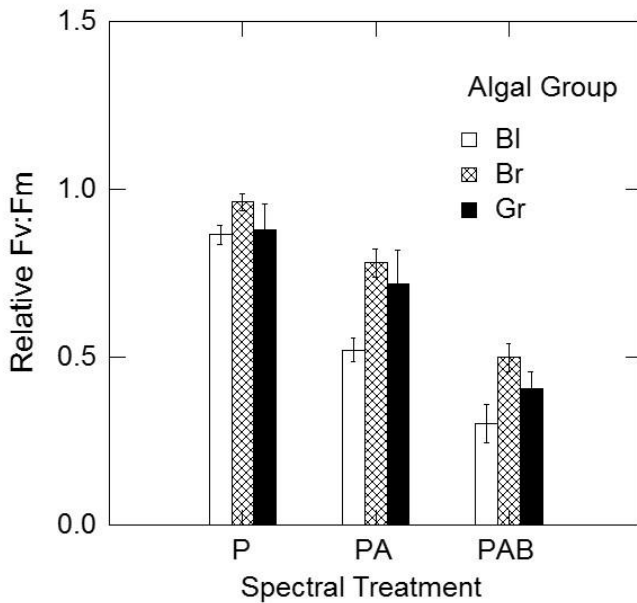


Figure 2.1. Relative $F_v:F_m$ (normalized to time 0 values) after 75 min irradiance exposure averaged across all sampling dates for each spectral treatment P (PAR only), PA (PAR + UV-A) and PAB (PAR + UV-A + UV-B) and algal group (BI - blues, Gr - greens, Br - browns). Error bars indicate standard deviation.

The Kok model of photoinhibition was applied to the change in relative quantum yield (i.e. $F_v:F_m$ normalized to pre-exposure $F_v:F_m$) over time and used to estimate rate constants of damage and repair (Equation 2) (Table 2.4). The model did not return significant (non-zero) parameter estimates for the irradiance exposure response of the brown group in July 2012 or September 2013. In these cases, and for the P spectral treatments generally, there was minimal decrease in relative quantum yield and thus little basis for parameter estimates.

Figure 2.2A and Figure 2.2B are examples of good and poor success in explaining the exposure response data with the Kok model. The green algal group measured in July Figure 2.2A showed strong model success (r^2 of 0.87 for PA and PAB treatments), representative of most groups and sampling dates (Table 2.4). The August sample (Figure 2.2B) contained a complex phytoplankton community and returned the lowest r^2 of all experiments (0.68 and 0.76 for PA and PAB treatments, respectively). The blues were dominant, but there was higher variability in $F_v:F_m$ among replicates, and group characterization by the Phyto-PAM was not as consistent as in other experiments.

Additional replicates were used to control variability, and while there was considerable scatter in the replicate time series, significant Kok model estimates were obtained (Table 2.4). Subjectively, the model appeared to describe the kinetics reasonably well, capturing the initial rapid decrease and subsequent deceleration in $F_v:F_m$ response. There were suggestions in some cases of more complicated kinetics (e.g. Figure 2.2B, treatments PA and PAB) but more complicated models were not attempted based on the data available.

Repair rates were generally higher for the PA than PAB treatment, while damage rates were generally higher for the PAB than PA treatment (Table 2.4). The highest damage rates were exhibited by the blue group, which dominated in the August and September 2012 experiments. The brown group showed a large range in both damage and repair rates across sampling dates, with rate constants for the green group falling within this range. There were significant linear relationships between damage rate and post-exposure $F_v:F_m$ for the PA and PAB spectral treatments (Figure 2.3B) but no significant relationships with repair rate (Figure 2.3A).

Table 2.4. Group-specific damage and repair rate constants (rate constant, 95% confidence interval) estimated by fitting the Kok model to $F_v:F_m$ exposure response kinetics.

Date	Algal Group	Spectral Treatment	Mean Corrected r^2	Repair Rate, r (min^{-1})	Damage Rate, k (min^{-1})
18/04/2012	Br	PA	0.94	0.028 (0.018 - 0.038)	0.007 (0.006 - 0.009)
		PAB	0.95	0.019 (0.012 - 0.025)	0.022 (0.018 - 0.026)
23/05/2012	Br	PA	0.74	0.078 (0.04 - 0.116)	0.02 (0.012 - 0.029)
		PAB	0.89	0.016 (0.008 - 0.024)	0.027 (0.02 - 0.034)
20/06/2012	Br	PA	0.92	0.041 (0.029 - 0.052)	0.024 (0.019 - 0.029)
		PAB	0.96	0.015 (0.01 - 0.02)	0.049 (0.041 - 0.056)
11/07/2012	Gr	PA	0.87	0.02 (0.01 - 0.031)	0.02 (0.014 - 0.025)
		PAB	0.87	0.021 (0.011 - 0.031)	0.041 (0.03 - 0.052)
01/08/2012	Bl	PA/PAB	n/a	n/a	n/a
		PA	0.68	0.032 (0.013 - 0.051)	0.028 (0.017 - 0.039)
13/09/2012	Bl	PAB	0.76	0.034 (0.018 - 0.05)	0.078 (0.056 - 0.101)
		PA	0.92	0.03 (0.021 - 0.04)	0.058 (0.047 - 0.07)
	Gr	PAB	0.97	0.018 (0.012 - 0.024)	0.115 (0.101 - 0.129)
		PA	n/a	n/a	n/a
		PAB	0.70	0.017 (-0.001 - 0.036)	0.014 (0.006 - 0.022)

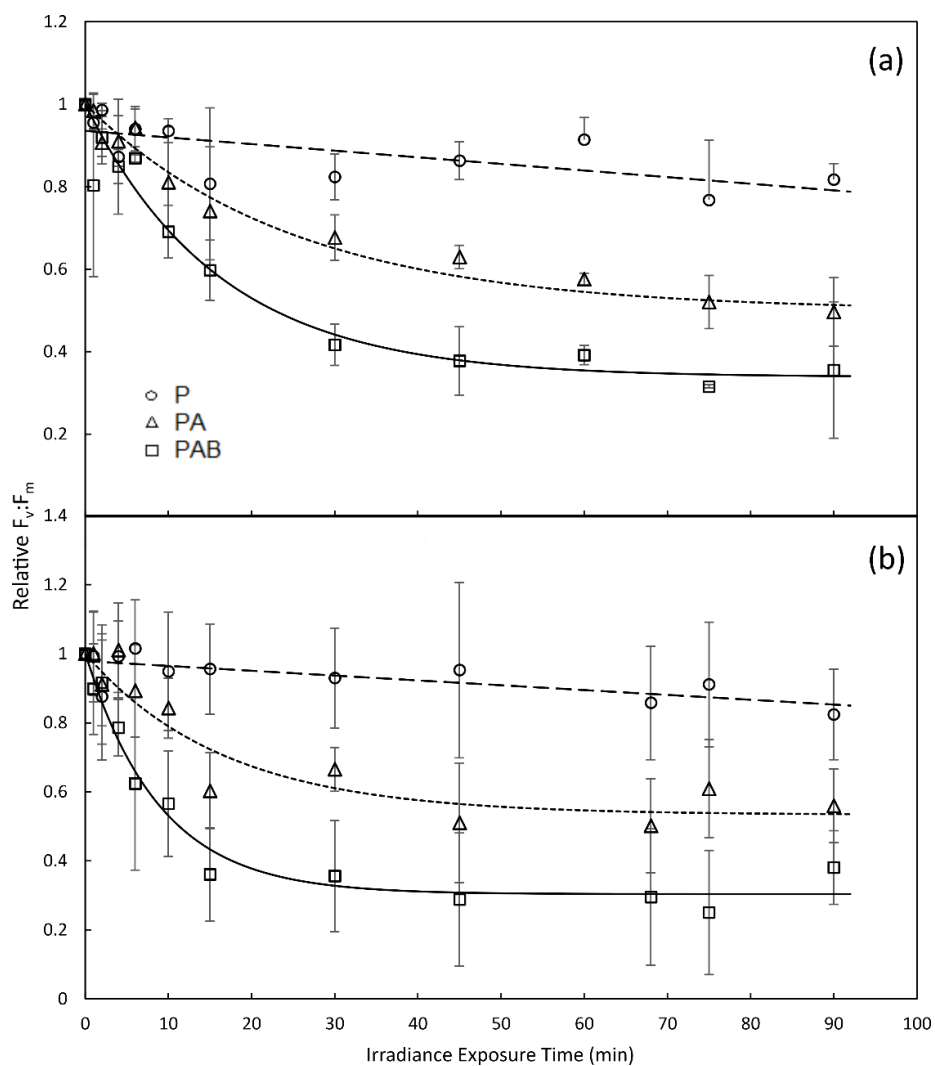


Figure 2.2. Kinetics of relative $F_v:F_m$ for the dominant algal group, where symbols represent average values and error bars indicate standard deviation, on (A) July 11, 2012 (green) and (B) August 1, 2012 (blue), with fitted values from the Kok model for treatments PA and PAB and a linear trend line for treatment P.

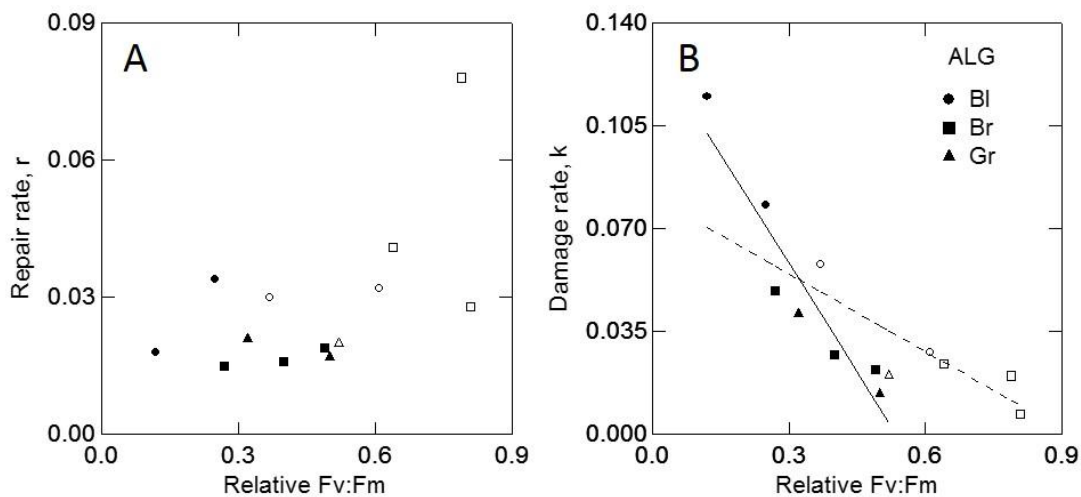


Figure 2.3. Rate constants of repair (A) and damage (B) compared to post-exposure relative $F_v:F_m$ for PA (open symbols) and PAB (shaded symbols) spectral treatments. Linear regression analyses yielded significant relationships between damage rate and relative $F_v:F_m$ (PA $r^2 = 0.724$, $p = 0.032$, dashed line; PAB $r^2 = 0.894$, $p = 0.001$, solid line).

Table 2.5. Phyto-PAM group-specific fluorescence (Ft) proportions as percentages (mean \pm standard deviation) separated by size class.

Sampling Date	Size Class	Group-specific Fluorescence (Ft) Proportion (as percentage)		
		Bl	Gr	Br
20/09/2013	Whole	28.1 (\pm 4.5)	14.5 (\pm 7)	57.4 (\pm 6.1)
	>30 μ m	50.3 (\pm 7.5)	37.5 (\pm 14.8)	12.2 (\pm 9.2)
	>60 μ m	64.7 (\pm 6.1)	26 (\pm 9)	9.3 (\pm 10.1)
	>100 μ m	79.6 (\pm 14.6)	19 (\pm 12.8)	1.4 (\pm 2.8)
03/10/2013	Whole	18.4 (\pm 3.3)	36.7 (\pm 10.1)	44.9 (\pm 9.8)
	>30 μ m	25.1 (\pm 7.6)	60.4 (\pm 15.3)	14.4 (\pm 13.2)
	>60 μ m	48.1 (\pm 12.4)	51.9 (\pm 12.4)	0 (\pm 0)
	>100 μ m	44.5 (\pm 31.2)	50 (\pm 28.6)	5.5 (\pm 15.8)

Table 2.6. Community (645 nm diode) $F_v:F_m$ and ^{14}C uptake spectral responses normalized to PAR-only (P) treatment (mean \pm standard deviation) for different size classes.

Size Class	Relative $F_v:F_m$ (645 nm)			Relative ^{14}C Uptake		
	P	PA	PAB	P	PA	PAB
Sampling date: 19/09/2013						
Whole	1.00 (\pm 0.07)	0.65 (\pm 0.15)	0.59 (\pm 0.07)	1.00 (\pm 0.17)	0.73 (\pm 0.15)	0.33 (\pm 0.06)
>30 μm	1.00 (\pm 0.07)	0.65 (\pm 0.11)	0.52 (\pm 0.13)	1.00 (\pm 0.16)	0.73 (\pm 0.11)	0.4 (\pm 0.09)
>60 μm	1.00 (\pm 0.2)	0.66 (\pm 0.21)	0.34 (\pm 0.14)	1.00 (\pm 0.11)	0.75 (\pm 0.21)	0.44 (\pm 0.09)
>100 μm	1.00 (\pm 0.27)	0.63 (\pm 0.35)	0.47 (\pm 0.2)	1.00 (\pm 0.46)	0.54 (\pm 0.31)	0.42 (\pm 0.22)
Sampling date: 02/10/2013						
Whole	1.00 (\pm 0.09)	0.62 (\pm 0.05)	0.53 (\pm 0.08)	1.00 (\pm 0.15)	0.79 (\pm 0.15)	0.39 (\pm 0.08)
>30 μm	1.00 (\pm 0.11)	0.66 (\pm 0.09)	0.55 (\pm 0.12)	1.00 (\pm 0.21)	0.84 (\pm 0.17)	0.49 (\pm 0.11)
>60 μm	1.00 (\pm 0.24)	0.59 (\pm 0.27)	0.54 (\pm 0.25)	1.00 (\pm 0.26)	0.81 (\pm 0.29)	0.39 (\pm 0.03)
>100 μm	1.00 (\pm 0.24)	0.59 (\pm 0.25)	0.41 (\pm 0.17)	1.00 (\pm 0.51)	0.72 (\pm 0.2)	0.39 (\pm 0.21)

Note: 645 nm diode $F_v:F_m$ measures were used because algal group $F_v:F_m$ values were not always reliably measured for different size classes/spectral treatments.

2.4.4 Irradiance responses of $F_v:F_m$ and ^{14}C uptake

Results for the two endpoints used to assess phytoplankton spectral exposure responses in 2013 (quantum yield of photochemistry and photosynthetic ^{14}C uptake) were normalized to the P treatment rather than pre-exposure values, because there is no equivalent to the pre-exposure $F_v:F_m$ when measuring ^{14}C uptake. As in 2012, the 2013 experiments showed little negative effect on $F_v:F_m$ in treatment P (Table 2.3). Normalizing to the P treatment should therefore capture most of the inhibitory effect, which was exerted mainly by UV-A and UV-B in our experiments. The $F_v:F_m$ values from the 645 nm diode were used because they provide a measure of community response (as does carbon uptake), and compare well to values for the dominant algal group (data not shown).

The Phyto-PAM showed differences in relative algal group composition among size classes as measured by fluorescence (Table 2.5). All three groups were present in both the September and October 2013 samples, with the brown group being dominant (Table 2.2). However, the blue group in September 2013 (ca. 80%) and both the blue and green group (ca. 45% and 50%, respectively) in October 2013 dominated the larger size classes (>30 μm). The PA and PAB treatments caused average decreases in $F_v:F_m$ of 35% and 50%, respectively, compared to the P treatment in the 2013 experiments (Table 2.6). ^{14}C uptake decreased less than $F_v:F_m$ in the PA treatment (26% on average), but decreased more than $F_v:F_m$ in the PAB treatment (averaging almost 60%). Two-way ANOVA was

used to compare the irradiance responses as defined by endpoint ($F_v:F_m$ and ^{14}C uptake) and size class for all spectral treatments. There was a significant difference in irradiance response based on endpoint for the October 2013 sample for both PA and PAB spectral treatments (PA $F = 6.347$, $p = 0.023$; PAB $F = 7.529$, $p = 0.014$), but not for the September sample. There was no effect due to size class or interactions of size class and end point in either of the 2013 experiments.

2.5 Discussion

2.5.1 Community composition and group discrimination

The meso-eutrophic embayment of Hamilton Harbour provided a biologically diverse sampling site for assessment with the Phyto-PAM. Monthly measures of Chl *a* concentration fell within the ranges reported from recent water quality assessments (Hiriart-Baer et al., 2009; Watson et al., 2010). The dominant algal groups identified each month were consistent with expected seasonal succession, and included many of the taxa typically found in the harbour (Watson et al., 2010). Spring and early summer samples consisted primarily of chromophyte taxa, chlorophyte taxa were dominant in mid-summer (July), and late summer and early fall saw increases in abundance of Cyanophyceae, including *Dolichospermum* and *Microcystis*. The dominant taxa within the chromophyte group varied across sampling dates, with significant proportions of Cryptophyceae and Bacillariophyceae in spring and early summer, while members of Dinophyceae dominated later in the season. The sparse sampling regime will have limited the capture of temporal and spatial dynamics, but did present a diverse and variable community with which to assess the ability of the Phyto-PAM to correctly discriminate among major pigment-based plankton groups.

There have been few published assessments of how well the Phyto-PAM can quantify pigment group abundance and resolve group-specific variable fluorescence in natural communities (Jakob et al., 2005; Schmitt-Jansen & Altenburger 2008; Zhang et al., 2008). Jakob et al. (2005) found good agreement between chlorophyll concentrations estimated by fluorescence and spectrophotometry in algal cultures. The natural communities they studied were diatom-dominated and, while the Phyto-PAM correctly identified the dominant pigment group and estimated chlorophyll concentration, there was no evidence of reliable identification of more than one group or resolution of group-specific $F_v:F_m$. Schmitt-Jansen & Altenburger (2008) found that the Phyto-PAM could identify the dominant pigment group in biofilms, but the accuracy of estimates for absolute chlorophyll concentrations and pigment group proportions were more variable. Zhang et al., (2008) measured $F_v:F_m$ of co-occurring

algal groups in a highly eutrophic freshwater system to assess diurnal changes in photoinhibition and differences in photochemical response among phytoplankton groups. However, it is not clear how consistently variable fluorescence metrics could be measured for multiple groups, or how this may relate to the relative abundance of the different pigment groups. In our study, the Phyto-PAM estimates of the proportion of Chl *a* fluorescence among pigment groups showed general agreement with biomass estimates based on microscopic analysis. Across all sampling dates fluorescence and biomass showed the same group as dominant, with some variation in relative group contribution. While not directly equivalent, fluorescence-derived Chl *a* and microscope-based biomass estimates are commonly expected to co-vary, and other spectral Chl *a* fluorometers have also demonstrated good agreement with microscope-estimated biomass (Seppala & Olli 2008; Catherine et al., 2012). Pigment group estimates by means of spectral fluorescence are vulnerable to errors and inaccuracies, resulting in part from the variability of reference spectra within pigment groups. The relative success of the Phyto-PAM in our application does not remove the need for care and verification of results in other applications.

The Phyto-PAM seeks not only to correctly estimate the relative composition of the community, but to further partition F_0 and F_m among groups in order to quantify group-specific $F_v:F_m$. The ability to resolve group-specific variable fluorescence and maximum quantum yield by the Phyto-PAM was more limited than its ability to quantify the relative abundance of pigment groups. For two of the sampling dates in 2012 (July and September) and both in 2013 (September and October) group-specific $F_v:F_m$ was reliably identified for two algal groups, based on the 95% frequency threshold applied here. For the remaining 2012 sampling dates $F_v:F_m$ was consistently assigned only for the dominant group, even though more groups were present. To our knowledge this is the first demonstration that a multi-wavelength PAM can accurately resolve $F_v:F_m$ for co-occurring groups in natural communities supported by independent analysis of community composition, but it also shows that the power to resolve less abundant groups was very limited in our application.

2.5.2 Phytoplankton spectral responses and UVR sensitivity

Pre-exposure $F_v:F_m$ for the brown and green groups was close to the empirical maximum quantum yield of 0.65 for eukaryotic phytoplankton under nutrient replete culture conditions (Kolber et al., 1988), suggesting they were not physiologically stressed prior to the experimental irradiance exposures. Pre-exposure $F_v:F_m$ for the cyanobacteria tended to be lower compared to the eukaryotes, a well-described feature resulting from differences in the major light harvesting complexes and

organization of the photosynthetic apparatus (phycobilisomes) (Campbell et al., 1998). Short-term irradiance exposure resulted in a decrease of $F_v:F_m$, with significant differences in endpoint among all spectral treatments. Spectral responses matched hypothesized results based on previous studies, with minimal decrease in $F_v:F_m$ from PAR (P treatment), more photoinhibition with UV-A added (PA), and often severe photoinhibition with UV-B added (PAB). Photoinactivation in PSII occurs even at low light intensities. However, under normal light conditions the efficient PSII repair process is faster than the rate of damage, preventing measurable effects of photoinhibition (Anderson et al., 1997). This may have been the case under the PAR only treatment for the majority of sampling dates, where minimal photoinhibitory effect was observed. Measurement of the maximum quantum yield of photochemistry ($F_v:F_m$) included a period of dark-adaptation, to ensure relaxation of non-photochemical fluorescence quenching. Low level light (PAR or UV-A) is required for appreciable repair of photodamaged PSII, and the effects of repair during dark-adaptation are typically minimal (Harrison & Smith 2013).

Algal groups differed in their responses to irradiance stress. The brown group was the most commonly observed across our sample dates, and its irradiance sensitivity ranged from minimal effect (July) to strongly photoinhibited (June); the responses of the green group fell within the range exhibited by the browns. The blue group showed strong sensitivity for all dates measured, and the highest levels of photoinhibition (August and September 2012) of any group or sample date. Only one or two groups were resolved on each date so a formal analysis of group-dependent vs. temporal variation was not possible. There was no supporting evidence for the hypothesis that the blue group (cyanobacteria) would show higher tolerance of UVR stress than the other groups, with average post-exposure $F_v:F_m$ significantly lower than the brown group. The two dates on which blues were resolved along with co-occurring groups showed blues to be the more sensitive. Similar experiments conducted on phytoplankton from inland lakes also found that cyanobacteria-dominated communities exhibited greater UVR sensitivity than chlorophyte and chromophyte-dominated communities (Harrison & Smith 2011a). Conversely, other studies describe the abilities of cyanobacteria to tolerate and even dominate surface waters under high irradiance conditions (Sommaruga et al., 2009; Wu et al., 2011; Paerl & Paul 2012) and have found cyanobacteria more resistant compared to eukaryotic phytoplankton (Xenopoulos et al., 2009). Chromophyte taxa were more prevalent in spring and early summer, while cyanobacteria were more prevalent in late summer and early fall, so seasonal differences in environmental factors affecting phytoplankton response to UVR, such as nutrient

availability, may have contributed to the observed differences in irradiance sensitivity at our study site.

Hamilton Harbour appears to be moving towards a more phosphorus limited condition in recent decades, with evidence of stronger phosphorus limitation during the summer (June to August) months (Hiriart-Baer et al., 2009). How this might affect our results is difficult to determine, as there are also periods where nitrogen limitation or light and mixing environment strongly influence phytoplankton taxa and biomass. Combined effects of nutrient stress and UVR on phytoplankton have presented varying outcomes in previous studies, from increased UVR sensitivity under phosphorus or nitrogen limitation (Shelly et al., 2002; Shelly et al., 2005), to greater UVR sensitivity at higher nutrient concentrations (Sobrino et al., 2009; Xenopoulos et al., 2009). If nutrient limitation was stronger in summer months in the present study, that period nonetheless showed a wide range of sensitivity to UVR. The relationship of $F_v:F_m$ to nitrogen and phosphorous limitation in phytoplankton has itself proven inconsistent and relatively weak (Kruskopf & Flynn 2006; Majarreis et al., 2014).

Variations in irradiance exposure over time (“light history”) could also contribute to the observed variations of UVR response in the present study, through both physiological acclimation and selection among taxa (Fouqueray et al., 2007; Laurion & Roy 2009). In Hamilton Harbour the attenuation coefficients for PAR and UVR showed little variation among sampling dates. Mean irradiance in the surface mixed layer showed more seasonal variation, but the between date variations did not display significant ($p < 0.05$) linear correlation with the severity of inhibition in $F_v:F_m$ or the values of repair and damage coefficients. Mean irradiance in the surface mixed layer was highest in May, June and July, and both the least and the most inhibition was observed for the brown group over that period. Our mean irradiance measurements may have failed to fully capture the variability of the light environment the phytoplankton were experiencing, but there was little evidence for a consistent influence of light history on phytoplankton responses during our study.

Group-specific differences in irradiance response are likely an important factor in community sensitivity, but difficult to generalize. There are some common characteristics at higher taxonomic levels (Andreasson & Wängberg 2006; Schwaderer et al., 2011) but much interspecific variation at lower taxonomic levels (Fouqueray et al., 2007; Harrison & Smith 2009; Sobrino et al., 2005). It is also unclear how well generalizations about group-specific utilization of PAR (e.g. Schwaderer *et al.*, 2011) can be translated to expectations for response to UVR (Harrison & Smith 2009). In the present study, dinoflagellates dominated the brown group on dates when it was less sensitive to UVR,

whereas diatoms and cryptophytes dominated when it was more sensitive, consistent with some evidence that freshwater diatoms and cryptophytes may be relatively sensitive to UVR (Harrison & Smith, 2009). For the blue group, sensitivity was greatest when *Microcystis* was abundant and less when filamentous genera (*Dolichospermum*, *Aphanizomenon*) were dominant. This may suggest that, at least in Hamilton Harbour, the strategies for success of *Microcystis* do not always include an intrinsically high resistance to UVR-dependent photoinhibition.

The Kok (1956) model proposes that photoinhibition represents a dynamic balance between damage and recovery, and that it follows simple first order kinetics. More complicated models can be necessary for exposure-response modelling of phytoplankton community responses in nature, but the Kok model has been successfully used to describe and compare irradiance responses of both phytoplankton cultures and natural communities (Shelly et al., 2002; Heraud et al., 2005; Fouqueray et al., 2007; Harrison & Smith 2011b). The density of observations in the current study was marginal for assessing the performance of the Kok model (or of alternates) but it appeared to fit the kinetics of $F_v:F_m$ reasonably well and explained a high percentage of the variation.

Damage and recovery coefficients in the model give some broad insight into strategies and mechanisms underlying the observed inhibition. For example, Harrison & Smith (2011a) showed that phytoplankton in one lake resisted inhibition by minimizing damage while those in a neighbouring lake depended more on elevated repair rates. In the present study, variation in the degree of inhibition suffered during our standardized exposures to UV-B and/or UV-A was significantly correlated with damage, but not repair, coefficients. This would suggest that mechanisms of resistance (e.g. photoprotective pigments, energy dissipation, etc.) were more important than mechanisms of repair (e.g. D1 protein replacement) in determining short-term vulnerability of Hamilton Harbour phytoplankton to UVR. The blue group in particular manifested relatively large damage coefficients, showing that the large colonial form of the dominant cyanobacteria did not bring the benefits of protection against UVR that might be expected (Wu et al., 2011; Sommaruga et al., 2009). Strategies affecting damage versus recovery vary at the species level (Harrison & Smith 2011b; Fouqueray et al., 2007) so further studies in additional lakes would be desirable to determine how general our observed pattern might be.

2.5.3 Significance of $F_v:F_m$ for photosynthetic C fixation

Variations of $F_v:F_m$ are not necessarily predictive of variations in photosynthetic C fixation (Behrenfeld et al., 1998; Gilbert et al., 2000), so the apparent sensitivity of cyanobacteria in the

present study, for example, may not translate into a corresponding vulnerability of photosynthetic C assimilation. However, our comparisons of $F_v:F_m$ and ^{14}C uptake indicated approximately proportional impacts of UVR on both. $F_v:F_m$ was more sensitive than ^{14}C uptake to the PA treatment and less to the PAB treatment, but both measures responded strongly to both treatments and in all size classes. All three algal groups were present during our comparative measurements, with the browns most abundant overall but with blues very important in the larger size classes. These results indicate that the observed sensitivity of $F_v:F_m$ to UVR stress corresponded to comparable reductions in photosynthetic carbon uptake, including for cyanobacteria. Our results were consistent with others that have found PSII quantum yield to be predictive of UVR impacts on carbon fixation (Sobrinho et al., 2005) or even to underestimate them (Andreasson & Wängberg 2006; Fragoso et al., 2014). It is therefore likely that the sensitivity of $F_v:F_m$ for the cyanobacterial populations in the present study indicated a relatively high vulnerability of carbon fixation processes to UV stress, and not merely the induction of a photo-protective strategy. The study by Zhang et al., (2008) on the summer phytoplankton of Lake Taihu also found cyanobacteria to show greater levels of photoinhibition based on $F_v:F_m$ compared to chlorophytes and chromophytes. Interestingly, cyanobacteria had higher levels of NPQ compared to the other groups, and showed no difference in growth rate, as estimated from chlorophyll fluorescence (Zhang et al., 2008). These varying results highlight the need for studies incorporating independent measures of photosynthesis and growth to determine the effects and mechanisms of irradiance on algal populations.

This study is among the first to rigorously evaluate the Phyto-PAM fluorometer and apply it to the assessment of group-specific physiological responses of natural communities to UVR, demonstrating both the utility and limitations of the Phyto-PAM in its current configuration. The results supported its usefulness in characterizing the relative abundance and physiological condition of cyanobacteria, when dominant, in comparison to other phytoplankton groups. This ability creates great potential for improving our predictive knowledge of the mechanisms that contribute to problem blooms. An increased ability to reliably resolve the variable fluorescence of sub-dominant or even rare groups would be desirable, particularly as it could then give a picture of potential problem populations when they are still small.

Resilience to UVR is widely held as one of the mechanisms enabling cyanobacterial dominance and bloom formation under the irradiance regimes associated with current and future climate change scenarios (Sommaruga et al., 2009; Paerl & Paul 2012), yet our results showed no evidence that

cyanobacteria are more resistant to UVR stress compared to other groups, even when sampled from a location where they do form blooms. However, their success as bloom-forming species suggests they must be able to tolerate if not thrive under high irradiance conditions. Future research is needed to elucidate this apparent paradox and evaluate adaptive UVR stress tolerance mechanisms of cyanobacteria, such as ROS scavengers and other physiological or behavioural (migratory) adaptations. Evaluation of variable fluorescence metrics and irradiance sensitivity during the different stages of bloom development could point to the importance of different response mechanisms under different conditions and as algal density increases. Such research would benefit from further development of spectral variable fluorescence methods to allow effective *in situ* measurements, which would better capture the spatial dynamics of distributions and physiology.

2.6 Acknowledgements

I thank Technical Operations staff at the Canada Centre for Inland Waters (Environment and Climate Change Canada, ECCC) for field sampling operational support. Thanks to Dr. Veronique Hiriart-Baer and Jacqui Milne (Watershed Hydrology and Ecology Research Division, ECCC) for provision of Station 1001 PAR profile data for May 10 and 23, 2012, as supplements for missing data due to equipment difficulties on the April and May sampling dates.

Chapter 3

Effects of solar radiation stress on Photosystem II efficiency in freshwater phytoplankton pigment groups

3.1 Summary

The effects of acute irradiation stress on the photosynthetic efficiency of 3 major freshwater phytoplankton pigment groups were evaluated for 13 laboratory culture strains and in mixed field populations from a meso-eutrophic embayment using spectrum-resolved variable fluorescence (Walz Phyto-PAM). UVR (UV-B and UV-A) induced photoinhibition in all taxa, with significant decreases in photochemical quantum efficiency ($F_v:F_m$), while responses to high PAR were smaller and often insignificant. Cyanobacteria were the least tolerant to PAR and UVR stress, while chlorophytes showed the greatest, and chromophytes variable, but generally intermediate, tolerance. Maximal fluorescence (F_m) decreased with irradiance exposures, indicative of non-photochemical quenching (NPQ), while minimum fluorescence (F_0) responses were variable among taxa and spectral treatments. Relative change in $F_v:F_m$ with irradiance exposure was well described by the Kok model of photoinhibition, and modeled damage rates were predictive of cumulative inhibition. Field populations of cyanobacteria and chromophytes showed greater resistance and lower damage rates than lab strains, but differences were insignificant due to large variations within each group. Notably, the field data were consistent with the laboratory culture results, showing cyanobacteria as generally more sensitive to acute UVR exposure than eukaryotic algae. Thus, the sunlight tolerance enabling some cyanobacteria to form surface blooms is not facilitated by maintenance of Photosystem II (PSII) efficiency.

3.2 Introduction

Exposure of phytoplankton to ultraviolet radiation (UVR) and strong blue light can cause primary photodamage to Photosystem II (PSII) at the oxygen-evolving complex, with light absorbed by photosynthetically active pigments contributing to the production of reactive oxygen species (ROS) and further PSII and cellular damage (Heraud & Beardall 2000; Bouchard et al., 2006; Nishiyama et al., 2006). Consequent impairment of photosynthetic carbon fixation and growth rates (e.g. (Litchman & Neale 2005) makes photoinhibition a significant factor in natural community dynamics (Xenopoulos et al., 2000; Xenopoulos et al., 2009). This is an important issue, because

phytoplankton will likely experience increased potential for photoinhibition due to elevated atmospheric UVR transmission and climate-driven changes in stratification (Häder et al., 2011; Williamson et al., 2014). Along with temperature and nutrients, differential susceptibilities to photoinhibition among taxa may play a role in the success of harmful algal blooms (Wulff et al., 2007; Sommaruga et al., 2009; Paerl & Paul 2012), yet the number of controlled comparisons remains small, and some of the currently held tenets on the role of light in competitive dominance have not been robustly tested. Our purpose here was to evaluate this by measuring the photo-sensitivity of three major phytoplankton pigment groups to extreme levels of photosynthetically active radiation (PAR) and UVR using both individual laboratory strains and mixed field populations from a meso-eutrophic embayment. In particular, we sought to evaluate the common impression that many cyanobacteria are resilient to harmful irradiation, enabling their dominance in eutrophic systems.

Phytoplankton exhibit a range in light preferences and tolerances, with different strategies of light utilization and photoacclimative mechanisms. Some cyanobacteria are reported to tolerate variable and high PAR and UVR (Xenopoulos et al., 2009; Fragoso et al., 2014), and for some larger colonial taxa their ability to form near-surface aggregations appears to require a high sunlight tolerance (Wulff et al., 2007; Sommaruga et al., 2009; Wu et al., 2011). On the other hand, many cyanobacteria are reported to require and tolerate minimal light, suggesting adaptation to low light environments (Schwaderer et al., 2011; Deblois et al., 2013). It is not clear whether such disparity represents diversity among different species or ecotypes (Six et al., 2009; Moore & Chisholm 1999), or a lack of standardized comparisons that include UVR as well as PAR. Chlorophytes, on the other hand, are generally reported with optimal growth at high light intensities and tolerance to UV-B (Herrmann et al., 1996; Montero et al., 2002a; Andreasson & Wängberg 2006; Schwaderer et al., 2011; Stamenkovic & Hanelt 2011; Deblois et al., 2013). Chromophytes encompass several taxonomic groups, including diatoms, dinoflagellates and chrysophytes, which represent a large diversity of accessory pigments and optimal light regimes. Diatoms tolerate a range of light intensities and often favour well mixed water columns, with high utilization efficiency at low light, high optimal light intensities for growth (Schwaderer et al., 2011; Deblois et al., 2013), and rapid photoacclimation mechanisms (Goss & Jakob 2010; Brunet et al., 2011). Dinoflagellates are often tolerant of high irradiance, while chrysophytes and cryptophytes tend to show sensitivity to UVR (Herrmann et al., 1996; Neale et al., 1998; Montero et al., 2002a; Litchman & Neale 2005; Xenopoulos et al., 2009).

Phytoplankton contain different accessory pigments that can transfer excitation energy to the photosynthetic reaction centres and/or provide photoprotection (Kirk 1994; MacIntyre et al., 2002; Brunet et al., 2011). Taxonomic groups exhibit similarities in accessory pigments (Falkowski & Raven 2007) and the differentiation of eukaryotic algae and cyanobacteria based on excitation and/or emission spectra is a well-established technique (Yentsch & Yentsch 1979; MacIntyre et al., 2010), using a variety of equipment and mathematical procedures. The Phyto-PAM fluorometer (Heinz Walz GmbH, 2003) is an example, using pulse amplitude modulation (PAM) and multiple wavebands of excitation light to distinguish three major pigment groups: greens (chlorophytes), blues (cyanobacteria), and browns (chromophytes) (Kolbowski & Schreiber 1995; Schreiber 1998).

Photoinhibition can be conveniently assessed using the maximum quantum yield of photochemistry ($F_v:F_m$), determined from the response of PSII chlorophyll *a* (Chl *a*) fluorescence to a saturating light pulse, allowing measurement of variable fluorescence: $F_v = F_m - F_0$ (Genty et al., 1989; Falkowski & Raven 2007). F_0 is the minimum fluorescence of dark-adapted cells when all PSII reaction centers are oxidised; F_m is maximum fluorescence measured after a saturating pulse of light reduces (closes) all reaction centers. Variations in F_0 and F_m under irradiance stress can provide insight into photoinhibition; for example, increases in F_0 can result from photo-oxidation, and be indicative of photodamage in the PSII reaction centers, while decreases in F_m can be caused by non-photochemical quenching (NPQ), which reduces excitation transfer to reaction centers (Demers et al., 1991; Herrmann et al., 1996; Maxwell & Johnson 2000). The contribution of such acclimation and damage processes to changes in photosynthetic yield metrics (i.e. carbon fixation, oxygen evolution, $F_v:F_m$) during irradiance exposure can be elucidated using models such as the Kok model of photoinhibition, which treats the inhibition kinetics of $F_v:F_m$ (or other photosynthesis metrics) as a dynamic balance between damage and repair processes (Kok & Businger 1956; Lesser et al., 1994b; Heraud & Beardall 2000; Shelly et al., 2002; Guan et al., 2011).

In theory, instruments like the Phyto-PAM enable assessments of phytoplankton pigment groups in natural communities (Jakob et al., 2005; Schmitt-Jansen & Altenburger 2008; Zhang et al., 2008; Beecraft et al., 2017), with a potential for insights into their photosynthetic physiology and light utilization under dynamic conditions. Laboratory studies are nonetheless still necessary to obtain controlled comparisons of traits among taxa and pigment groups. Many algal traits are maintained over time under controlled culture conditions (Xiong et al., 1999; Stamenkovic & Hanelt 2011), but they cannot be extrapolated uncritically to nature, as responses apparent in nature may arise from a

variety of environmental influences not occurring in culture, as well as taxon-specific traits. Our recent application of the Phyto-PAM in a meso-eutrophic embayment suggested that natural populations of large colonial cyanobacteria were more sensitive to solar UVR than co-occurring eukaryotic taxa (Beecraft et al., 2017), contrary to previously reported observations (Sommaruga et al., 2009; Xenopoulos et al., 2009; Wu et al., 2011; Paerl & Paul 2012). Experiments under more controlled conditions would help determine whether such results truly depict characteristic differences or whether they may reflect unrecognized environmental influences in nature, or even instrument errors in application to mixed communities.

The objectives of this study were to (1) determine how the response of maximum quantum yield of photochemistry ($F_v:F_m$) to UVR and elevated PAR vary within and among Phyto-PAM designated pigment groups, and (2) examine the utility of F_0 and F_m dynamics in explaining the cumulative inhibition responses. Based on previous evidence, we hypothesized that all taxa would exhibit photoinhibition when exposed to UVR, and that chlorophytes would show the most tolerance, while chromophyte and cyanobacterial taxa would show variable sensitivity. We used the Kok model to describe the kinetics of $F_v:F_m$ and determine varying contributions of repair and damage processes to group- and taxon-specific $F_v:F_m$ response. We further hypothesized that varying contributions of PSII damage and NPQ would be discernable from the kinetics of F_0 and F_m . Our third objective (3) was to compare the group-specific irradiance sensitivity of laboratory cultures with those from natural phytoplankton assemblages examined in the previous chapter, to assess the degree to which measured group-specific differences of UVR sensitivity in natural communities are reproduced by representative taxa under controlled *in vitro* conditions. We sought to provide a standardized comparison of acute sunlight, in particular UVR, sensitivity among a larger number of taxa and groups of freshwater phytoplankton than has previously been described, with complementary comparisons to natural populations.

3.3 Methods

3.3.1 Culture conditions

Clonal non-axenic microalgal and cyanobacterial cultures (Table 3.1) were obtained from the Canadian Phycological Culture Center (CPCC, University of Waterloo, Waterloo ON) and Dr. S. Watson at the Canadian Center for Inland Waters (CCIW, Burlington ON), Environment and Climate Change Canada. Representative taxa were chosen to capture some of the variation within the three

algal groups classified by the Phyto-PAM, and because of their common occurrence in a wide variety of freshwater environments. Batch monocultures were grown in 1L flasks of nutrient-replete WC (ed) media, modified by S.B. Watson from (Guillard & Lorenzen 1972) adjusted to pH 8.2-8.4 (Watson 1999). Cultures were incubated at 19 ± 2 °C at an illumination intensity of ca. 48 ± 4 $\mu\text{mol photons m}^{-2} \text{s}^{-1}$ from cool white fluorescent bulbs on a 16: 8 hr light: dark cycle, and mixed manually each day.

Growth was monitored by daily measurements of fluorescence and $F_v:F_m$ using a Phyto-PAM (S/N: PPAA0220, Walz GmbH, Effeltrich, Germany), supplemented by less frequent microscopic cell counts, to estimate growth phase. Irradiance exposure experiments were performed on samples from exponential phase cultures acclimated to the described growth conditions, and diluted with fresh media to reach cell densities for manufacturer-suggested gain settings when creating new reference spectra, approximately one hour prior to exposures to allow short term acclimation of cells.

Table 3.1 Phytoplankton species used in irradiance exposure experiments.

Taxon	Phyto-PAM Group	Algal Phylum
<i>Anabaena oscillarioides</i> ^a	Bl	Cyanophyta
<i>Dolichospermum</i> ^b <i>lemmermannii</i> LO08-01	Bl	Cyanophyta
<i>Microcystis aeruginosa</i> Kutz.em. Elenkin CPCC 299	Bl	Cyanophyta
<i>Synechococcus</i> sp. ^a	Bl	Cyanophyta
<i>Synechococcus rhodobaktron</i> NIVA 8	Br ^c	Cyanophyta
<i>Coelastrum cambricum</i> HH001-05	Gr	Chlorophyta
<i>Pediastrum simplex</i> Meyen CPCC 431	Gr	Chlorophyta
<i>Scenedesmus obliquus</i> EC-SW1	Gr	Chlorophyta
<i>Asterionella formosa</i> Hass CPCC 605	Br	Ochrophyta
<i>Fragilaria crotonensis</i> Kitton CPCC 269	Br	Ochrophyta
<i>Cryptomonas</i> sp. CPCC 336	Br	Cryptophyta
<i>Synura petersenii</i> Korshikov CPCC 495	Br	Ochrophyta
<i>Peridinium inconspicuum</i> UTEX LB 2255	Br	Dinophyta

^aStrain number not known

^bformerly named *Anabaena*

^c*Synechococcus rhodobaktron* is a phycoerythrin-rich cyanobacterium included as a member of the ‘blue’ group taxonomically, however it is recognised as predominantly ‘brown’ by the Phyto-PAM when using typical ‘blue’ reference spectra species. It is included with the Cyanobacteria throughout the present study.

3.3.2 Irradiance exposures experiments

Acute irradiance exposures were completed in triplicate in a solar simulator containing a Xenon arc lamp (1 kW, Oriel Instruments, Irvine, CA) and optical glass cut-off filters (Schott optical filters) with nominal 50% transmission at 305, 340 and 420 nm to produce three spectral treatments: PAR only (>420 nm); PAR + UV-A (>340 nm); and PAR + UV-A + UV-B (>305 nm), hereafter referred to as P, PA and PAB, respectively. The incident spectral irradiance was measured using an LT-14 spectrometer (S/N: 09121132, Stellarnet Inc., Tampa, FL) (Table 3.2, Figure 3.1). Photon flux density (PFD) was monitored using a LI-COR (Q15458) photometer (Li-COR Biosciences, Lincoln, NE) throughout experiments to ensure consistent exposures. Sample temperature was maintained at 19 ± 1 °C by a controlled water circulation system.

Subsamples (ca. 50 mL) of experimental batch cultures were transferred to 400 mL Pyrex beakers under dim light and placed in the incubation chambers. Exposures lasted 75 min, with 3 mL aliquots removed after mixing from each treatment at 11 time points (pre-exposure/ time zero samples taken from experimental batches at the start of exposures). Subsamples were dark acclimated at ambient temperature for ca. 30 min before measurement. Chl *a* fluorescence was measured using a Phyto-PAM equipped with a corresponding System II emitter-detector unit (Phyto-ED, S/N EDEF0111, Walz) containing an array with four wavelengths of measuring light and a red actinic light. Low intensity modulated measuring light with minimal actinic effect was used to measure F_0 , and then a saturating pulse (0.2 sec up to $2600 \mu\text{mol quanta}\cdot\text{m}^{-2}\cdot\text{sec}^{-1}$ at 655 nm) was applied to produce F_m . Corrections for background dissolved fluorescence were made with 0.2 μm filtered culture media. For each species, triplicate irradiance exposure experiments were performed on subsamples taken from the same batch culture.

The Phyto-PAM measures Chl *a* fluorescence and returns fluorescence-derived parameters for four excitation wavelengths (470, 520, 645, 665 nm) and three algal groups: blues (most cyanobacteria), greens (chlorophytes), and browns (diatoms, dinoflagellates, chrysophytes, cryptophytes). Algal group values are determined by deconvolution of the four diode signals using linear unmixing and one reference spectrum for each of the three pigment groups. The results for laboratory strains were obtained using only the reference spectrum previously determined for the selected taxon, to ensure that the Phyto-PAM would assign all measured signal to the correct algal group. The effects of reference spectrum variability and other factors influencing accuracy and interpretation of group-specific values from Phyto-PAM are examined in the subsequent chapters (4 and 5).

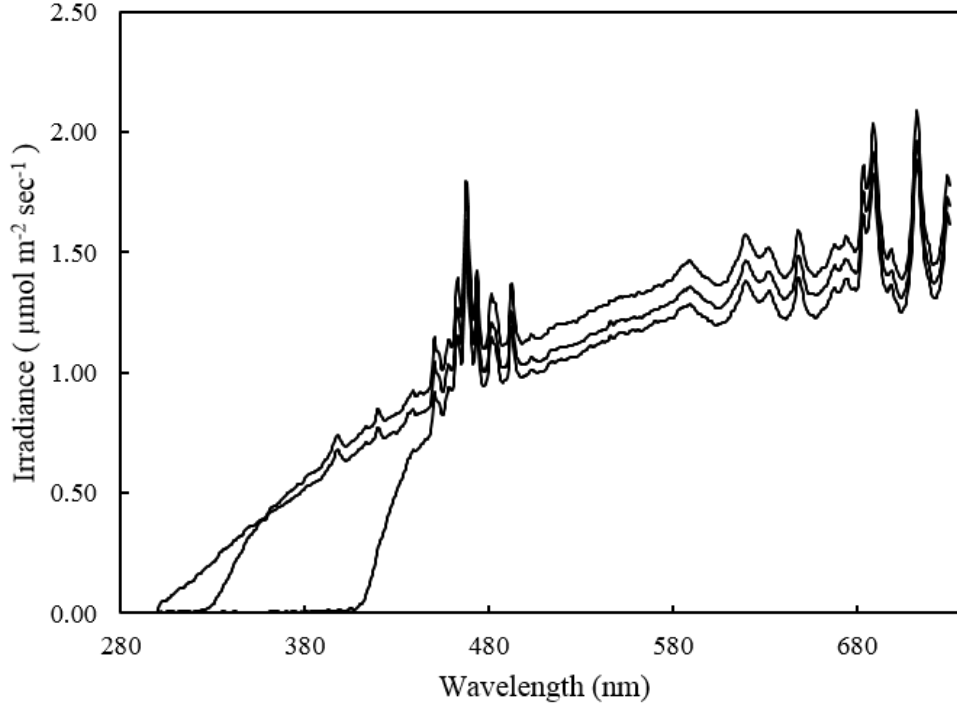


Figure 3.1 Spectral irradiance of experimental treatments P (PAR only), PA (PAR + UV-A) and PAB (PAR + UV-A + UV-B). Complete spectral irradiance data available electronically upon request.

Table 3.2 Broadband PFD for UV-B, UV-A and PAR in the three experimental spectral treatments.

Spectral Treatment	UV-B: 300-320 nm ($\mu\text{mol} \cdot \text{m}^{-2} \cdot \text{sec}^{-1}$)	UV-A: 320-400 nm ($\mu\text{mol} \cdot \text{m}^{-2} \cdot \text{sec}^{-1}$)	PAR: 400-700 nm ($\mu\text{mol} \cdot \text{m}^{-2} \cdot \text{sec}^{-1}$)
P (> 420 nm)	0.06	0.46	319.04
PA (> 340 nm)	0.12	29.80	384.11
PAB (> 305 nm)	1.70	32.23	356.01

3.3.3 Statistical analyses

The absolute fluorescence of F_0 and F_m over time were analyzed via polynomial regression, using a step function based on the Akaike information criterion (AIC) to select the regression model (first, second and third order) that best described each time series. These fitted models were compared

among spectral treatments, taxa and pigment groups. For each taxon and spectral treatment, the relative $F_v:F_m$ over time was fitted to the Kok model of photoinhibition (1956) using non-linear regression analysis and least-squares error minimization:

$$\frac{P}{P_i} = \frac{r}{(r+k)} + \frac{k}{(k+r)} * e^{-(k+r)t} \quad (1)$$

Where t is time, P_i is the initial $F_v:F_m$ at time zero (prior to irradiance exposure), P is $F_v:F_m$ at time t , and k and r are rate constants for damage and repair processes, respectively (Lesser et al., 1994b; Heraud & Beardall 2000).

The laboratory culture results were compared with those from similar irradiance exposure experiments performed on natural community (field) samples collected from a depth of 1m from April to September in Hamilton Harbour, a meso-eutrophic embayment of Lake Ontario, Canada. For the PA and PAB spectral treatments, the damage rate estimates for field samples were adjusted to account for the difference in total incident irradiance between culture and field experiments (multiplied by 0.45, for 450 vs. 1000 $\mu\text{mol m}^{-2} \text{sec}^{-1}$); damage rates could not be reliably estimated for the P treatment in field samples, as photoinhibition was minimal. The adjustment assumes that, all else being equal, damage rates should be directly proportional to the applied irradiance. The post-exposure relative $F_v:F_m$ was calculated for field samples using the adjusted damage rate constants, and these metrics were then compared to those obtained from the laboratory experiments (two sample t-test). These comparisons were made for the blue and brown groups only, as greens were rarely abundant enough in the natural community to provide reliable metrics. Statistical analyses were completed using Systat 10 (Systat Software, Inc., Chicago, IL) and R (R Core Team 2015).

3.4 Results

3.4.1 Cumulative inhibition of $F_v:F_m$ in acute exposure experiments

All three spectral treatments caused progressive decreases of $F_v:F_m$ in the laboratory strains, except for the chlorophytes *C. cambricum* and *S. obliquus* under the PAR-only treatment (Table 3.3). The full spectrum (PAB) treatment produced the greatest reductions in $F_v:F_m$, while the PAR-only treatment (P) elicited the smallest. The average relative sensitivity of the three algal groups was consistent across spectral treatments, with the blue group having the highest sensitivity to UVR, greens the least, and browns showing an intermediate, but highly variable response (Table 3.3, Figure B.2). Two-way analysis of variance (ANOVA) showed significant differences in post-exposure relative $F_v:F_m$ among spectral treatments and algal groups, but no interactive effect between the two. Based on post-hoc tests using Tukey's Honestly Significant difference (HSD) multiple comparisons of average post-exposure $F_v:F_m$, the blue group was significantly different from the brown and green groups ($p < 0.05$), while the latter two were not significantly different from each other. Post-exposure $F_v:F_m$ from P and PAB treatments differed ($p < 0.05$) for all three algal groups, but group responses to PA and PAB were generally similar, and differed only at $p < 0.10$ for the greens and browns. PAR intensity varied by up to 20% among spectral treatments (Table 3.2), but given the small differences and the relatively minor effect of PAR on relative $F_v:F_m$, it is unlikely to have significantly affected our results.

The three chlorophytes (green group) showed the greatest resistance to photoinhibition and the most within-group consistency in $F_v:F_m$ response (Figure 3.2). In contrast, the five taxa from the brown group, which included representatives from four different taxonomic groups, exhibited a broad range in responses. The synurophyte *Synura petersenii* was the most sensitive brown taxon with the largest decrease in $F_v:F_m$, while the cryptoflagellate *Cryptomonas* sp. and diatom *Fragilaria crotonensis* were more tolerant, with post-exposure $F_v:F_m$ values similar to those of the chlorophytes (Figure 3.2, Table 3.3). The five cyanobacteria tended to show the highest overall sensitivity to photoinhibition, with similar responses for *Microcystis aeruginosa*, *Dolichospermum lemmermannii* and *Synechococcus* sp., while *Anabaena oscillarioides* and *Synechococcus rhodobaktron* had significantly larger reductions in $F_v:F_m$ under all three spectral treatments (Figure 3.2, Table 3.3).

Table 3.3 Group-specific initial $F_v:F_m$ and post-exposure relative $F_v:F_m$ (normalized to initial) of phytoplankton taxa for spectral treatments P (PAR only), PA (PAR + UV-A), and PAB (PAR + UV-A + UV-B). Values are mean (\pm standard deviation). Algal Group refers to Phyto-PAM designated groups (Bl - blues, Gr - greens, Br - browns).

Taxon	Algal Group	Initial $F_v:F_m$ (no exposure)	Post-exposure Relative $F_v:F_m$		
			P	PA	PAB
<i>A. oscillarioides</i>	Bl	0.44 (\pm 0.03)	0.57 (\pm 0.06)	0.3 (\pm 0.02)	0.07 (\pm 0.01)
<i>D. lemmermannii</i>	Bl	0.39 (\pm 0.03)	0.85 (\pm 0.04)	0.67 (\pm 0.1)	0.31 (\pm 0.1)
<i>M. aeruginosa</i>	Bl	0.42 (\pm 0.01)	0.87 (\pm 0.01)	0.63 (\pm 0.04)	0.49 (\pm 0.04)
<i>Synechococcus</i> sp.	Bl	0.32 (\pm 0.01)	0.76 (\pm 0.03)	0.51 (\pm 0.08)	0.3 (\pm 0.05)
<i>S. rhodobaktron</i>	Bl	0.3 (\pm 0.01)	0.32 (\pm 0.06)	0.07 (\pm 0)	0.05 (\pm 0.02)
<i>C. cambricum</i>	Gr	0.69 (\pm 0.01)	1.01 (\pm 0.02)	0.9 (\pm 0.01)	0.83 (\pm 0.02)
<i>P. simplex</i>	Gr	0.59 (\pm 0.01)	0.94 (\pm 0.01)	0.82 (\pm 0.04)	0.65 (\pm 0.01)
<i>S. obliquus</i>	Gr	0.63 (\pm 0.03)	0.99 (\pm 0.04)	0.92 (\pm 0.03)	0.66 (\pm 0.06)
<i>A. formosa</i>	Br	0.56 (\pm 0.03)	0.82 (\pm 0.03)	0.62 (\pm 0.02)	0.55 (\pm 0.05)
<i>F. crotonensis</i>	Br	0.6 (\pm 0.02)	0.96 (\pm 0.02)	0.85 (\pm 0.04)	0.71 (\pm 0.05)
<i>Cryptomonas</i> sp.	Br	0.67 (\pm 0)	0.95 (\pm 0.01)	0.87 (\pm 0.03)	0.68 (\pm 0.02)
<i>S. petersenii</i>	Br	0.62 (\pm 0.01)	0.91 (\pm 0.02)	0.46 (\pm 0.15)	0.25 (\pm 0.05)
<i>P. inconspicuum</i>	Br	0.48 (\pm 0.02)	0.89 (\pm 0.05)	0.66 (\pm 0.04)	0.49 (\pm 0.02)

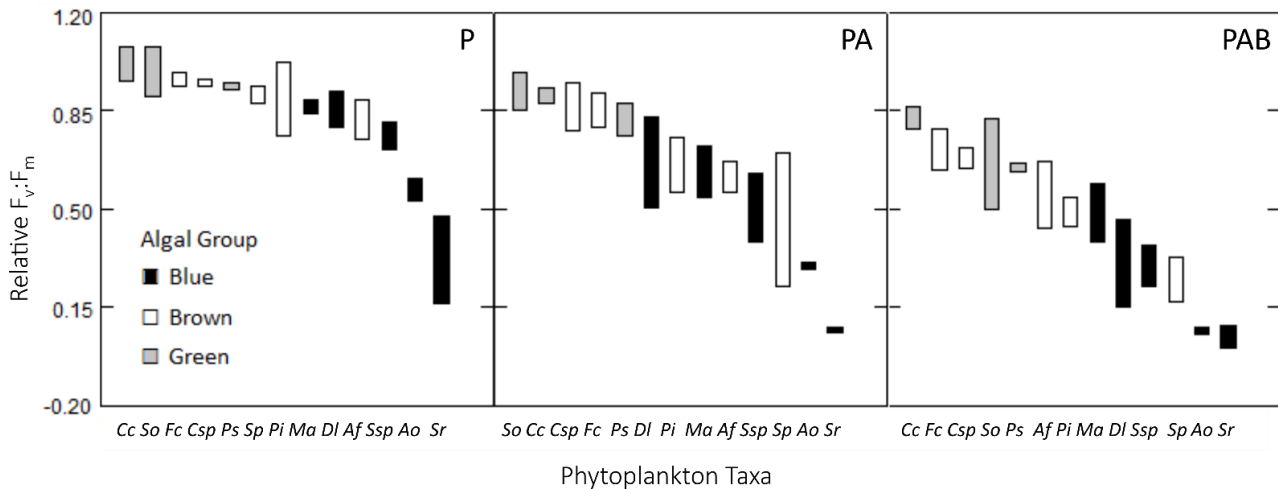


Figure 3.2 95% Confidence intervals for post-exposure (75 min) relative $F_v:F_m$ of experimental taxa, separated by spectral treatment P – PAR only (A), PA – PAR + UV-A (B), PAB – PAR + UV-A + UV-B (C), and algal group (Blue – black fill, Brown – no fill, Green – grey fill). Note: A. *oscillarioides* bar represents the range of values rather than the 95% confidence interval, as only 2 experimental replicates were used.

3.4.2 Kinetics of F_0 and F_m

The changes in minimal (F_0) and maximal (F_m) fluorescence over time for each taxon and spectral treatment were variable, with mostly non-linear responses (sample plots for three taxa in Figure 3.3). Polynomial regression analyses revealed significant relationships (first, second or third order, $p < 0.05$) for 71 out of 78 cases (Table B.4). The model of best fit was most often third order, with second and first order responses less common (3rd order = 48, 2nd order = 15, 1st order = 13). There was no apparent pattern in the polynomial order or incidence of significant versus non-significant relationships for either F_0 or F_m among pigment groups or spectral treatments. The fitted models were used to quantify the percent change of post-exposure (75 min endpoint) fluorescence relative to initial (Table 3.4). Changes in F_m were typically greater than in F_0 , with the exception of mean change for the PA and PAB treatments for the blue group, which were skewed by *S. rhodobaktron* (Table B.4). F_0 responses were variable with spectral treatment and across algal groups: the largest decreases generally occurred in the P treatment, followed by the PA and PAB treatments (Table 3.4), though only the brown group had reductions in F_0 across all taxa. *S. rhodobaktron* showed a unique trend among the taxa examined, with a large and sustained increase in both F_0 and F_m following irradiance

exposure (Figure 3.3A, B). The majority of taxa across all three pigment groups showed a decrease in F_m from initial values under all spectral treatments (i.e. negative values in Table 3.4, Figure 3.3D, F).

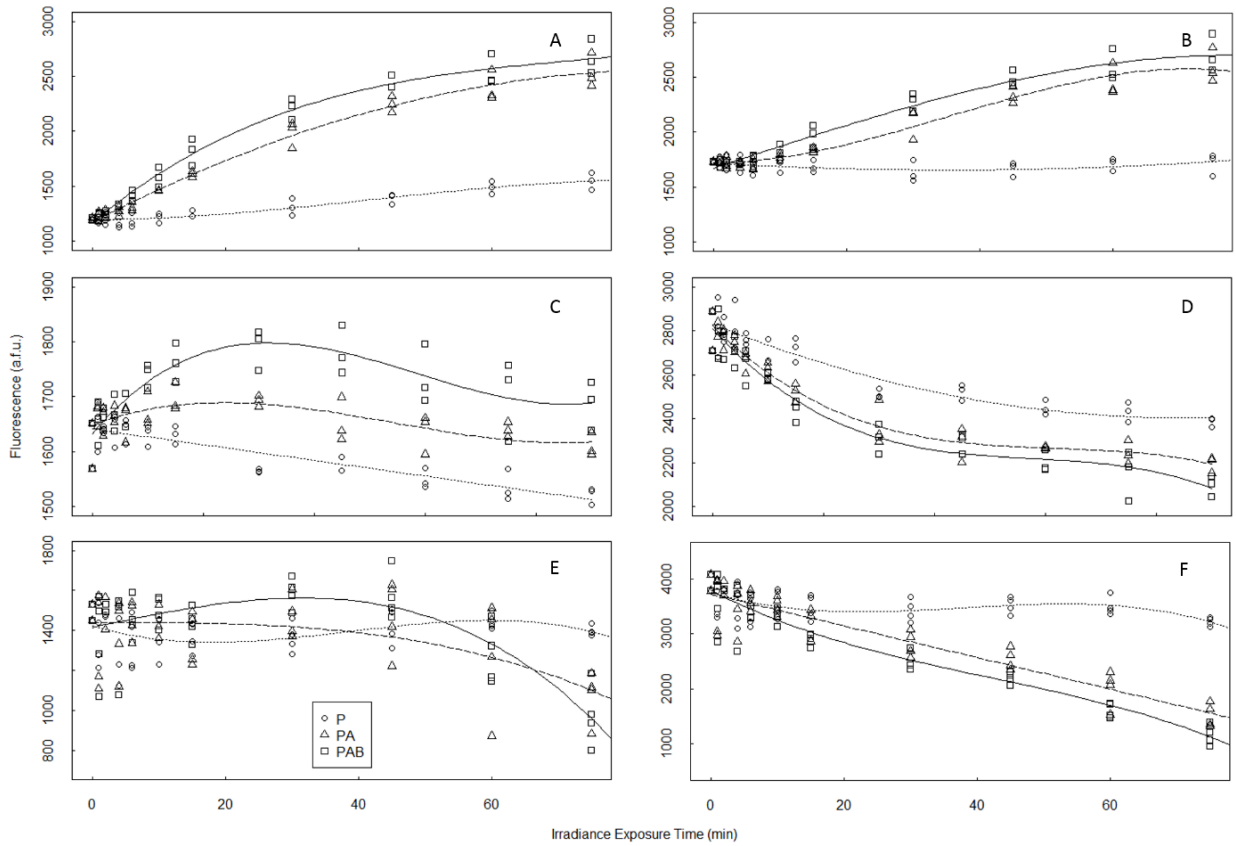


Figure 3.3 Minimum (F_0) and maximum (F_m) fluorescence over time for *Synechococcus rhodobaktron* (A. F_0 , B. F_m), *Microcystis aeruginosa* (C. F_0 , D. F_m), and *Synura petersenii*. (E. F_0 , F. F_m) with fitted polynomial regressions for each spectral treatment (P - dotted line, PA - dashed line, PAB - solid line).

Table 3.4 Percent change in minimal fluorescence (F_0) and maximum fluorescence (F_m) (endpoint relative to initial) during experimental irradiance exposures (P, PA, PAB) for each algal group.

		F_0			F_m		
		P	PA	PAB	P	PA	PAB
Blue	Mean	2.0	28.1	22.9	-11.4	-3.6	-12.1
	Median	-3.7	1.2	3.9	-12.3	-17.4	-24.9
Green	Mean	-30.8	-9.3	3.4	-33.4	-28.2	-29.4
	Median	-20.2	0.0	14.6	-23.5	-17.5	-23.9
Brown	Mean	-23.1	-28.3	-19.4	-31.5	-48.6	-47.7
	Median	-15.4	-23.5	-15.0	-23.6	-44.3	-40.7

3.4.3 Modeling kinetics and estimating repair and damage rates

Kok model estimates of repair and damage rates were used to evaluate which processes contributed to the observed $F_v:F_m$ following irradiance exposures. In one case the model could not converge on an estimate (*C. cambricum*, P treatment) and in several cases the estimates, predominantly repair rate constants, were not significantly different from zero (16 of 78 cases). These were generally for taxa and spectral treatments exhibiting minimal reductions in $F_v:F_m$, and thus displaying little variance for the model to describe. Examples of this are the green and tolerant brown taxa, where the large confidence intervals around damage and repair estimates preclude meaningful comparisons with other taxa and spectral treatments (Table B.5). Estimates of repair less than zero were adjusted to zero, as a negative rate is not biologically relevant. The model showed strong goodness of fit for species and spectral treatments exhibiting strong levels of photoinhibition, with >80% of the variation in $F_v:F_m$ for the PAB spectral treatment explained by the Kok model (Table 3.5, Figure 3.4).

Visual examination of residual plots was used to assess the applicability of the Kok model to the exposure response data (sample from each algal group and spectral treatment in Figure B.3). There were a few cases where residuals did not appear to be randomly distributed, for example Figure 3.4A and Figure B.3B show the relative $F_v:F_m$ of *D. lemmermannii* decreased faster than the Kok model estimates, reached a plateau and then began to increase slightly towards the end of the exposure period, suggesting some recovery that was not accounted for by this model. However, in the majority of cases the Kok model effectively captured the irradiance response of the algal taxa, and even in cases where some departure from the model was visible, the effects were minor.

Table 3.5 Kok model damage and repair rate constants and r/k ratio of relative $F_v:F_m$ exposure response kinetics for the PAB treatment. (complete results in Table B.5)

Taxon	Algal Group	Mean Corrected r^2	Repair Rate (min^{-1})	Damage Rate (min^{-1})	r/k
<i>A. oscillarioides</i>	Bl	0.931	0.02	0.109	0.18
<i>D. lemmermannii</i>	Bl	0.939	0.027	0.072	0.37
<i>M. aeruginosa</i>	Bl	0.983	0.03	0.033	0.91
<i>Synechococcus</i> sp.	Bl	0.984	0.027	0.061	0.44
<i>S. rhodobaktron</i>	Bl	0.992	0.004	0.084	0.05
<i>C. cambricum</i>	Gr	0.888	0.007	0.004	1.86
<i>P. simplex</i>	Gr	0.929	0.015	0.01	1.5
<i>S. obliquus</i>	Gr	0.946	0.012	0.008	1.5
<i>A. formosa</i>	Br	0.973	0.043	0.037	1.19
<i>F. crotonensis</i>	Br	0.826	0	0.004	0
<i>Cryptomonas</i> sp.	Br	0.976	0.03	0.015	2
<i>S. petersenii</i>	Br	0.981	0	0.015	0
<i>P. inconspicuum</i>	Br	0.931	0.019	0.022	0.86

Regression analyses indicated significant inverse relationships between damage rate constants and post-exposure $F_v:F_m$ for the PA and PAB spectral treatments, but none between repair rate constants and post-exposure $F_v:F_m$ (Figure 3.5). Damage rate constants increased with increasing short wavelength exposure (Table 3.6) with two exceptions (*A. oscillarioides* and *F. crotonensis*), which were not significantly different between spectral treatments (Table B.5), and were often higher for cyanobacteria compared to other taxa. For P treatments, model outcomes were not significantly different among the three pigment groups due to high within-group variability (Table 3.6, Table B.5).

The r/k ratio summarizes the simultaneous influence of repair and damage processes, and may correlate directly with ability to maintain high quantum yields under irradiance stress. The r/k ratios for the PAB treatment corresponded well to $F_v:F_m$ sensitivity among the phytoplankton examined (Table 3.3, Table 3.5), with the exception of *F. crotonensis* and *S. petersenii*. These two taxa showed very different sensitivities, reflecting differences in damage rate constants, but their low repair constants were not statistically distinguished from zero, making the r/k ratio uninformative. Cyanobacteria and chlorophyte taxa had r/k ratios <1 and ≥ 1.5 , respectively, with the ranking of r/k

matching closely that of post-exposure $F_v:F_m$. The r/k ratios for chromophytes, other than the two exception taxa, ranged from 0.86 to 1.19, again matching the species rank of post-exposure $F_v:F_m$.

Table 3.6 Average rate constants of damage and repair (\pm standard deviation) for each spectral treatment and pigment group.

Algal Group	Spectral Treatment	Repair Rate (min^{-1})	Damage Rate (min^{-1})
Blue	P	0.089 (\pm 0.099)	0.032 (\pm 0.046)
	PA	0.036 (\pm 0.026)	0.049 (\pm 0.02)
	PAB	0.022 (\pm 0.011)	0.072 (\pm 0.028)
Green	P	0.16 (\pm 0.181)	0.011 (\pm 0.013)
	PA	0.03 (\pm 0.026)	0.005 (\pm 0.004)
	PAB	0.011 (\pm 0.004)	0.007 (\pm 0.003)
Brown	P	0.172 (\pm 0.335)	0.006 (\pm 0.007)
	PA	0.034 (\pm 0.031)	0.012 (\pm 0.008)
	PAB	0.018 (\pm 0.019)	0.019 (\pm 0.012)

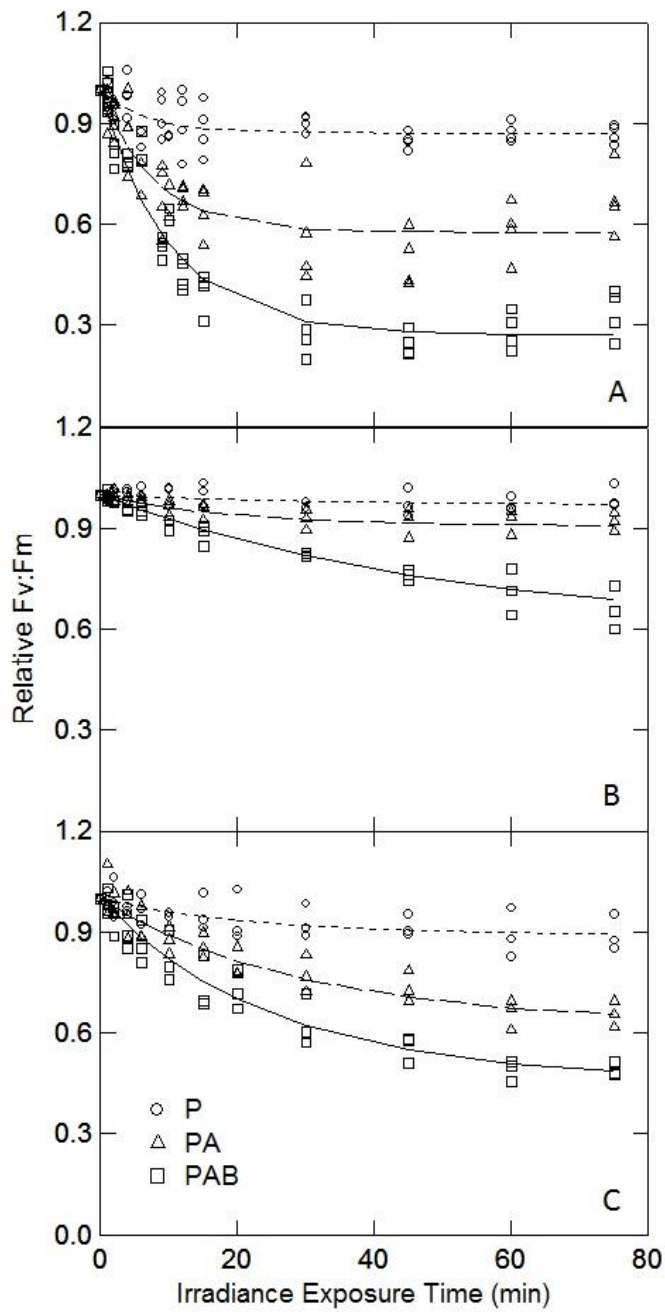


Figure 3.4 Kinetics of relative $F_v:F_m$ for (A) *Dolichospermum lemmermannii*, (B) *Scenedesmus obliquus*, and (C) *Peridinium inconspicuum* with fitted Kok model values for each spectral treatment (P, PA, PAB).

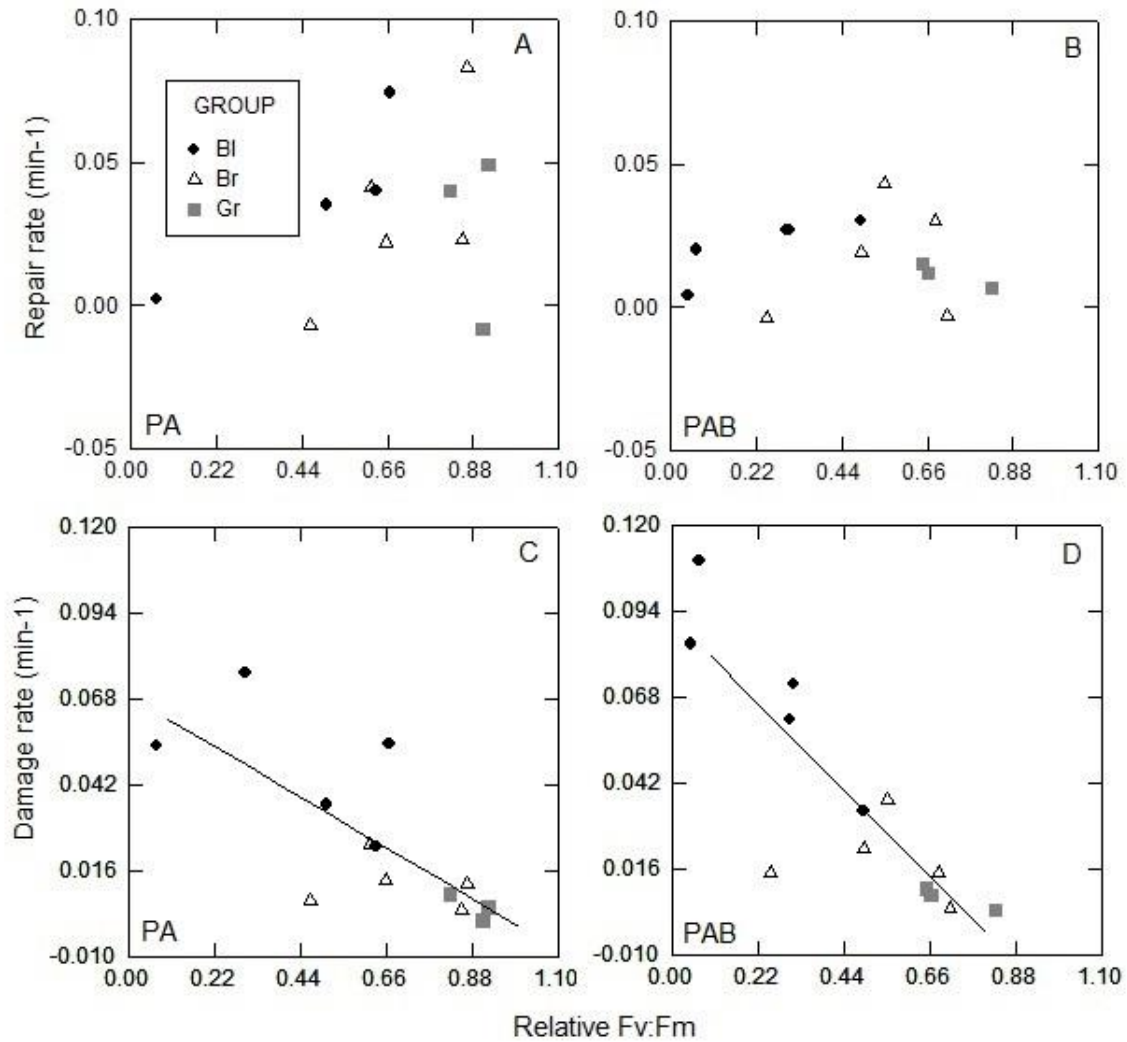


Figure 3.5 Repair (upper panel) and damage (lower panel) rate constants for culture strains compared to post-exposure relative $F_v:F_m$ for PA (A,C) and PAB (B,D) spectral treatments. Linear regression analyses yielded significant relationships between damage rate and relative $F_v:F_m$ for PA and PAB (PA $r^2 = 0.561$, $p = 0.003$, dashed line; PAB $r^2 = 0.748$, $p < 0.003$, solid line). Relationships between repair rate and relative $F_v:F_m$ were non-significant ($p > 0.2$).

Table 3.7 Comparison of irradiance response metrics ($F_v:F_m$ and Kok model coefficients) between laboratory monocultures (“Culture”), Hamilton Harbour field assemblages (“Field”1), and field results adjusted for comparison to the lower-irradiance laboratory experiments (“Adjusted Field”, see Methods). Values are pigment-group averages (95% confidence interval, or range in cases where n=2, indicated by ²).

Parameter	Spectral Treatment	Culture	Field	Adjusted Field
		Blue		
Pre-exposure $F_v:F_m$		0.376 (0.302 - 0.45)	0.483 (0.37 - 0.596)	
Post-exposure relative $F_v:F_m$	P	0.674 (0.388 - 0.961)	0.864 (0.8 - 0.929)	
	PA	0.434 (0.124 - 0.744)	0.521 (0.358 - 0.684)	0.635 (0.542 - 0.727) ²
	PAB	0.242 (0.013 - 0.472)	0.302 (0.035 - 0.569)	0.378 (0.262 - 0.495) ²
Repair Rate	PA	0.036 (0.004 - 0.068)	0.031 (0.03 - 0.032) ²	
	PAB	0.022 (0.009 - 0.035)	0.026 (0.018 - 1.143) ²	
Damage Rate	PA	0.049 (0.024 - 0.074)	0.043 (0.028 - 0.058) ²	0.019 (0.013 - 0.026) ²
	PAB	0.072 (0.037 - 0.107)	0.097 (0.078 - 0.115) ²	0.043 (0.035 - 0.052) ²
Green				
Pre-exposure $F_v:F_m$		0.637 (0.516 - 0.758)	0.623 (0.591 - 0.655) ²	
Post-exposure relative $F_v:F_m$	P	0.982 (0.885 - 1.078)	0.88 (0.768 - 0.992) ²	
	PA	0.881 (0.749 - 1.013)	0.718 (0.52 - 0.915) ²	0.725 (n/a)
	PAB	0.712 (0.468 - 0.956)	0.407 (0.315 - 0.499) ²	0.667 (0.557 - 0.777) ²
Repair Rate	PA	0.03 (-0.035 - 0.094)	0.02 (n/a)	
	PAB	0.011 (0.001 - 0.022)	0.019 (0.017 - 0.021) ²	
Damage Rate	PA	0.005 (-0.005 - 0.015)	0.02 (n/a)	0.009 (n/a)
	PAB	0.007 (-0.001 - 0.015)	0.028 (0.014 - 0.041) ²	0.012 (0.006 - 0.018) ²
Brown				
Pre-exposure $F_v:F_m$		0.585 (0.497 - 0.673)	0.642 (0.571 - 0.712)	
Post-exposure relative $F_v:F_m$	P	0.907 (0.836 - 0.978)	0.961 (0.897 - 1.025)	
	PA	0.691 (0.481 - 0.901)	0.78 (0.607 - 0.953)	0.867 (0.802 - 0.932)
	PAB	0.537 (0.308 - 0.765)	0.499 (0.323 - 0.674)	0.586 (0.449 - 0.724)
Repair Rate	PA	0.034 (-0.005 - 0.073)	0.049 (-0.015 - 0.113)	
	PAB	0.018 (-0.005 - 0.042)	0.017 (0.011 - 0.022)	
Damage Rate	PA	0.012 (0.003 - 0.021)	0.017 (-0.005 - 0.039)	0.008 (-0.002 - 0.018)
	PAB	0.019 (0.004 - 0.033)	0.033 (-0.003 - 0.068)	0.015 (-0.001 - 0.031)

3.4.4 Comparisons between laboratory and natural populations

Experiments on field populations from Hamilton Harbour revealed relatively small changes in photosynthetic yield in response to treatment P and larger responses to PA and PAB, similar to laboratory cultures (Table 3.7). Despite the approximately 2.2 times higher irradiance in the field population experiments, post-exposure relative $F_v:F_m$ and damage rates from PA and PAB were similar to those for laboratory culture experiments. Average repair rates showed little systematic difference between field and laboratory populations. When adjusted for the difference in experimental exposure irradiance, field populations had lower damage rates and higher post-exposure relative $F_v:F_m$ than laboratory cultures, with the exception of chlorophytes (Table 3.7). Under PA and PAB, both laboratory and field populations of chlorophytes showed low damage rate constants and high resistance. There were no significant ($p < 0.05$) differences between laboratory cultures and field populations in damage rate constants and post-exposure $F_v:F_m$, most likely due to the small sample numbers and within-group variance. Laboratory versus field measures of damage rate constants for the blue group under PA treatment and post-exposure $F_v:F_m$ for the brown group under PAB were marginally significant ($p < 0.10$). Furthermore, laboratory and field populations showed the same relative rankings for damage rates and photosynthetic yield (cyanobacteria-chromophytes-chlorophytes).

3.5 Discussion

While there is ample research describing the photoinhibitory effects of UVR and excess PAR on marine and freshwater phytoplankton, direct comparisons of different taxonomic groups under identical and controlled conditions are limited (Herrmann et al., 1996; Montero et al., 2002a; Montero et al., 2002b; Litchman & Neale 2005). To our knowledge, the current study is the first to use multiple cultured freshwater phytoplankton taxa to achieve replicated comparisons of sunlight sensitivity among three major pigment groups, with results that both support and contradict common group-specific descriptions. All cultures were growing exponentially when tested, and had $F_v:F_m$ values near the accepted empirical maxima of 0.65 for eukaryotic algae (Kolber et al., 1988) and 0.4 for cyanobacteria (Campbell et al., 1998). The results supported our expectation that acute irradiance exposure effects would increase with the addition of shorter wavebands (i.e., $PAB > PA > P$) (Cullen et al., 1992; Harrison & Smith 2009). Higher photoinhibition due to UVR was consistent across the three pigment groups and six microalgal classes examined, despite the taxonomic diversity and variations in photoacclimation strategies of the different groups.

Our post-exposure relative quantum yield ($F_v:F_m$) measurements represent the proportion of lost potential photosynthetic efficiency from short-term exposure to intense light and photoinhibition. On this time scale (75 min), post-exposure $F_v:F_m$ for the blue group was significantly more sensitive than the green or brown groups, and the brown group was more sensitive than the green, but with considerable interspecific variability. As a group, the chlorophytes (albeit only three in number) were consistently the most tolerant to PAR and UVR exposure, with decreases in $F_v:F_m$ of 17 to 35% under the full spectrum treatment (PAB). The published literature reports a range in the UVR and/or PAR tolerance of different chlorophyte strains and species (Xiong et al., 1999): with some marine picoplanktonic chlorophytes showing high sensitivity to UVR and photoinhibition (Sobrino et al., 2005; Six et al., 2009); while other studies comparing UV-B sensitivity of marine species from the Chlorophyceae (and related groups, i.e. Prasinophyceae) with chromophyte taxa found the former more resistant (Herrmann et al., 1996; Montero et al., 2002a; Andreasson & Wängberg 2006). The results of the present study demonstrate high PAR and UVR tolerance in freshwater chlorophyte taxa, supporting the prevailing view that chlorophytes are typically adapted to high light environments (Schwaderer et al., 2011; Deblois et al., 2013).

Considering the enormous phylogenetic and ecological diversity within the brown pigment group, i.e. chromophytes and cryptophytes, it is expected they would show a range in tolerance both in lab and field populations. Consistent with this, the five taxa representing the brown group exhibited variable irradiance sensitivity, particularly in response to UVR. *F. crotonensis* and *Cryptomonas* were relatively tolerant (29-32% reduction in $F_v:F_m$ under PAB), while other chromophyte taxa showed moderate (*A. formosa*, 45%; *P. inconspicuum* 51%) to large (*S. petersenii*, 75%) reductions in $F_v:F_m$. Of the subgroups, the diatoms are commonly associated with variable PAR environments, such as vertically-mixed water columns, and many can maintain high photosynthetic efficiency at low light levels while responding rapidly to high irradiance (Wagner et al., 2006; Schwaderer et al., 2011; Deblois et al., 2013), often utilizing NPQ via the xanthophyll cycle (Dimier et al., 2007; Laurion & Roy 2009). Even within the diatoms, however, the sensitivity to PAR and UVR can be variable, as exemplified here and in previous studies (Montero et al., 2002b; Dimier et al., 2007; Fouqueray et al., 2007). In contrast, chrysophycean flagellates tend to demonstrate high sensitivity to PAR and UVR both in cultures: *S. petersenii* in the present study, *Ochromonas danica* (Herrmann et al., 1996), and in comparison to co-occurring taxa in lake communities (Xenopoulos & Frost 2003; Doyle et al., 2005).

The cryptomonads and dinoflagellates, which are somewhat better-studied than the chrysophycean flagellates, show variable sensitivities to PAR and UVR and can be found in a range of light environments. For example, in a study of UVR effects on $F_v:F_m$ in marine phytoplankton, *Cryptomonas* sp. exhibited a higher tolerance, and the dinoflagellate *Amphidinium* sp. much less (Montero et al., 2002b), similar to the relative sensitivity of *Cryptomonas* sp. and *P. inconspicuum* seen here. In contrast, other studies demonstrated higher UVR sensitivity in *Cryptomonas* and *Rhodomonas* compared to marine taxa from different groups (Montero et al., 2002a; Litchman & Neale 2005). Dinoflagellates also vary in UVR sensitivity (Demers et al., 1991; Laurion & Roy 2009), some showing high sensitivity to photoinhibition, and others a measure of UVR tolerance afforded by the capacity to synthesize UV-absorbing compounds and xanthophyll cycle pigments (Demers et al., 1991; Litchman et al., 2002; Marcoval et al., 2007).

Our *in vitro* experiments showed that as a group, cyanobacteria were most sensitive to irradiance, with all five strains showing large decreases in $F_v:F_m$ under each spectral treatment. They also exhibited appreciable within-group variation, with three strains having similar responses ($F_v:F_m$ decreases of 51 to 70% under treatment PAB) and the other two (*A. oscillarioides* and *S. rhodobaktron*) much larger ones (93 to 95% under PAB). Similar variance has been reported by other studies; for example, marine picocyanobacteria had a greater sensitivity to PAR and UVR and lower photoacclimation potential compared to eukaryotic picoplankton (Kulk et al., 2011; Neale et al., 2014), while other studies have demonstrated sensitivity of cyanobacteria to UVR, with species-specific responses among cultured strains and taxa (Zeeshan & Prasad 2009; Giordanino et al., 2011; Fragoso et al., 2014). The apparent differences in tolerance among the cyanobacteria studied here may be related to differences in their typical habitats and associated capacities for photoacclimation and mitigation of light stress. The three more tolerant cyanobacteria (*M. aeruginosa*, *D. lemmermannii*, *Synechococcus* sp.) are members of the pelagic and surface mixed layer phytoplankton (Callieri et al., 2014; Fragoso et al., 2014), with *Microcystis* notorious for its surface blooms (Wu et al., 2011; Qin et al., 2015). *Microcystis* and other surface bloom forming taxa contain carotenoids, such as zeaxanthin, which provide photoprotection by heat dissipation and antioxidant activity, and they have the ability to synthesize UV-absorbing compounds such as mycosporine-like amino acids (MAAs) (Sommaruga et al., 2009; Qin et al., 2015). *Synechococcus* is unicellular, picoplanktonic, and a polyphyletic genus with numerous strains having varying habitat preferences and irradiance sensitivities (Willame et al., 2006; Lohscheider et al., 2011; Neale et al., 2014). Studies using PC-rich cyanobacteria strains (of which our *Synechococcus* sp. is an example) have

demonstrated UVR sensitivity but also effective repair capacity via synthesis of the D1 protein (Fragoso et al., 2014). While specific habitat information is limited for the two more sensitive species in this study, taxa similar to *A. oscillarioides* tend to be benthic (Willame et al., 2006), and PE-rich cyanobacteria (e.g. *S. rhodobaktron*) are more commonly located deeper in the water column and exhibit greater sensitivity to high PAR and UVR compared to PC-rich strains (Lohscheider et al., 2011; Selmeczy et al., 2016). In addition, phycobilinprotein content has been shown to decrease with high PAR and UVR exposure, with PE more sensitive compared to PC (MacIntyre et al., 2010; Lohscheider et al., 2011; Kannaujiya & Sinha 2015), which may contribute to the dramatic response of *S. rhodobaktron*. Overall, our results agree with the suggested acclimation and adaptation of cyanobacteria to low light environments, based on observations of their high efficiency of light utilization as well as high susceptibility to photoinhibition (Schwaderer et al., 2011; Deblois et al., 2013).

We examined the changes in F_0 and F_m over time to gain insight into the relative contributions of reaction center damage (increasing F_0) and NPQ (decreasing F_m) to changes in $F_v:F_m$. Previous studies have observed decreasing F_m indicative of NPQ in marine diatoms (Fouqueray et al., 2007), and a marine chlorophyte (*Dunaliella salina*) and chrysophyte (*Ochromonas danica*) (Herrmann et al., 1996), while F_0 responses varied among species. In the present study, high PAR and UVR reduced F_m for all taxa examined (with the exception of *S. rhodobaktron*), with notably strong responses in the chromophyte taxa, suggesting particularly effective NPQ mechanisms. F_0 typically had smaller changes between initial and post-exposure values compared to F_m , with varying responses among taxa and groups. *S. rhodobaktron* showed a distinct and dramatic response to UVR and PAR, with substantial increases in F_0 and smaller increases in F_m . Our results provided greater temporal resolution of the response kinetics, demonstrating the second and third order changes in fluorescence on acute time scales, as well as a broader sampling of taxonomic groups, compared with previously published studies. However, our results of F_0 and F_m dynamics did not show clear trends predictive of the cumulative photoinhibition responses.

Previous studies have applied the Kok model to photosynthetic metrics under inhibitory light exposures and have reported damage and repair rate constants in a similar range to those found in the current study (Shelly et al., 2002; Heraud et al., 2005; Harrison & Smith 2011b). The modelled responses for the taxa examined suggested that differences in acute photoinhibition among pigment groups was driven by differences in damage processes. Average repair rate constants varied among

algal groups and across spectral treatments, and were not predictive of the endpoint sensitivity for the current light exposures. Damage processes are the same across species, while the forms of photoacclimation vary in mechanism and response time (Dimier et al., 2007; Laurion & Roy 2009; Brunet et al., 2011), which may explain why damage rates were predictive of observed sensitivity here. With the exceptions of *F. crotonensis* and *P. simplex*, damage rates increased under short wavelength light stress for all experimental taxa, consistent with earlier studies (Heraud & Beardall 2000; Guan et al., 2011; Harrison & Smith 2011a; Wong et al., 2015). Furthermore, we observed a consistent group-specific response in average damage rate constants across spectral treatments which were highest for cyanobacteria, intermediate for chromophytes, and lowest for chlorophytes. However, there were differences among species within a group, as has been also observed even for strains of the same species (Wong et al., 2015).

The r/k ratio provides a summary parameter which can be used to compare irradiance sensitivity based on the combined outcome of damage and repair processes (Fouqueray et al., 2007; Guan et al., 2011); however, we were unable to quantify repair rate constants in all cases, illustrating a limitation of the r/k index. Overall, however, these ratios corresponded well with the post-exposure $F_v:F_m$ values for the full spectrum (PAB treatment), indicating chlorophytes as most tolerant ($r/k > 1$) and cyanobacteria as most sensitive ($r/k < 1$). The range of r/k ratios seen here was similar to that reported for marine diatoms (Fouqueray et al., 2007; Guan et al., 2011), with ratios greater than 1 for the tolerant species but closer to zero for more sensitive taxa.

Prediction of solar radiation effects in nature from laboratory studies is complicated by environmental factors (e.g. temperature and nutrients) and photoacclimation processes, which can alter susceptibility to photoinhibition on a species-specific basis (Doyle et al., 2005; Marcoval et al., 2007; Halac et al., 2013; Halac et al., 2014). Using a consistent experimental irradiance exposure protocol, our data suggest that field populations have higher average tolerance to UVR than laboratory strains, supporting previous evidence that exposure to high levels of PAR and UVR can lead to photoacclimation and diminished sensitivity to UVR (Moore et al., 2006; Ragni et al., 2008; Harrison & Smith 2011b). In addition, the relative UVR sensitivity among the three pigment groups from laboratory experiments was consistent with what we observed for the natural communities of Hamilton Harbour. Cyanobacterial-dominated populations in the harbour samples showed the highest sensitivity to UVR, while chlorophyte populations showed the least and chromophyte populations were intermediate. It is of particular significance that the high sensitivity of the natural and lab

populations of cyanobacteria studied here differs markedly from the high PAR and UVR tolerance often attributed to this group (Paerl & Kellar 1979; Xenopoulos et al., 2000; van Donk et al., 2001; Wulff et al., 2007; Sommaruga et al., 2009; Xenopoulos et al., 2009; Paerl & Paul 2012), and is not an artifact of the culture conditions or taxon selection. Tolerance to sunlight stress may still be an important attribute of some bloom-forming cyanobacteria, but is not mediated by an innate PSII resistance to acute irradiance stress. They may rely on enhanced recovery capacity at low light intensity (Giordanino et al., 2011), resistance over longer exposure periods (Gao et al., 2007), or compensation through other mechanisms.

Future studies should aim to further understand how changes in the quantum yield of photochemistry correspond to overall photosynthetic efficiency and growth, if this differs among major groups, and if the comparative group sensitivity observed in the present study occurs in other systems. These experiments could incorporate measurement of variable fluorescence dynamics with other photosynthetic metrics under light stress on natural communities and recently isolated phytoplankton strains. Studies could assess the relative effectiveness of different photoacclimative and photoprotective mechanisms of cyanobacteria compared to other eukaryotic algae. C^{14} uptake experiments and the use of chemical inhibitors or spontaneous/knockout mutants could identify how reaction processes are affected for different steps of the light reactions and Calvin Benson cycle by irradiance stress (Lavaud et al., 2012; Mann et al., 2014; Schuurmans et al., 2015). The results may elucidate the underlying mechanisms for the apparent paradox of highly sensitive quantum yield of PSII to UVR exposure with the ability of many species of cyanobacteria to form near-surface blooms.

Chapter 4

Quantifying the challenges of taxon- and irradiance-dependent variability for multi-wavelength PAM fluorometry: patterns in excitation spectra and consequences for pigment group estimation

4.1 Summary

The application of multi-wavelength Chl *a* fluorometers to assess phytoplankton health and pigment-group composition is impeded by poor characterization of the variability in excitation spectra within taxa and groups. The present study characterized fluorescence excitation spectra (FES), referred to Reference Spectra (RS), for 13 monoalgal cultures representative of the three pigment groups characterized by the Phyto-PAM. We examined the effects of taxonomic and light history variation on background (F_0) and variable (F_v) FES, and response spectra following acute irradiance stress for freshwater phytoplankton. Short-term UVR exposure had minor effect on response spectra shape, such that classification of algal groups would not likely be affected. In comparison, taxonomic variation in RS shape was greater compared to light history effects, in particular for F_v RS, resulting in the potential misclassification of algal group $F_v:F_m$ by the instrument. F_0 RS were distinct between pigment groups, but some F_v spectra were not. Errors in F_0 and $F_v:F_m$ estimates were within 10% of true values on average, when a variety of RS combinations were applied to uni-algal cultures, but ranged up to 23-27%. The majority of F_0 (ca. 90%) was assigned to the correct group on average, but up to 20% of fluorescence was mis-attributed in some trials. $F_v:F_m$ was regularly estimated for the correct group, but could also be simultaneously estimated for the incorrect groups at a frequency of 1 to 30% on average, but for 100% of measurements in some RS trials. While group-specific estimates were often robust, the scope for classification and quantification errors in F_0 and $F_v:F_m$ were large, emphasizing the importance of replicate sample measurements and secondary taxonomic identification.

4.2 Introduction

The natural fluorescence emitted from Photosystem II (PSII) chlorophyll *a* (Chl *a*) with light exposure allows for the measurement of photosynthetic organisms across a range of spatio-temporal scales, and has become an indispensable tool of aquatic research (Lorenzen 1966; Phinney & Yentsch 1985; Schreiber et al., 1986). The increasing variety and sensitivity of commercially available

instruments using active Chl *a* fluorometry provides rapid measurement of phytoplankton biomass, physiology and composition. Multi-wavelength fluorometers enable automated identification of major pigment groups, providing a coarse taxonomic description of the community, which would otherwise require more expensive and time-consuming analyses such as high-performance liquid chromatography (HPLC) for pigment quantification or microscopic identification. Monitoring changes in species composition in relation to environmental conditions is important from both research and management perspectives, providing rapid biomass and composition data, as well as identifying the presence of harmful and/or nuisance algae. However, variations in Chl *a* fluorescence excitation spectra (FES) and intensity due to factors such as taxonomy, stress and light history complicate the interpretation of fluorescence data, highlighting the need to account for these factors (Leboulanger et al., 2002; Jakob et al., 2005; MacIntyre et al., 2010; Goldman et al., 2013; Kring et al., 2014; Escoffier et al., 2015).

Multi-wavelength (or spectral) fluorometry measures fluorescence using multiple excitation and/or emission wavelengths to identify major phytoplankton groups based on characteristic differences in dominant antenna pigments among taxonomic groups (Yentsch & Yentsch 1979). There are a number of custom-designed instruments and protocols (Millie et al., 2002; Seppala & Olli 2008; Proctor & Roesler 2010; Chekalyuk & Hafez 2011), as well as commercially available fluorometers (Paresys et al., 2005; Aberle et al., 2006; Kahlert & McKie 2014) including FluoroProbe (FP) and Algae Online Analyzer (AOA) (bbe Moldaenke GmbH, Kiel, Germany (Beutler et al., 2002)), Phyto-PAM (Kolbowski & Schreiber 1995; Schreiber 1998), and recently Phyto-PAM II (Heinz Walz GmbH, Effeltrich, Germany), which typically use a small number (three to six) of excitation wavelengths and a single emission wavelength to target Chl *a* fluorescence excited by different light-harvesting pigments. The Phyto-PAM is the focus of the present study; it measures variable fluorescence (F_v) using pulse amplitude modulation (PAM) and estimates Chl *a* concentrations, maximum quantum yield of photochemistry ($F_v:F_m$) and other F_v parameters for three major pigment groups (blues, greens and browns), using four wavebands of excitation light (Kolbowski & Schreiber 1995; Schreiber 1998).

Pigment group discrimination via multi-wavelength fluorescence is typically achieved by comparing the response spectrum of an unknown sample to representative FES/RS for each algal group, and estimating the relative signal contribution from each group via iterative statistical methods such as least-squares fitting (also referred to as linear un-mixing) (MacIntyre et al., 2010). The

representative FES are generally measured from uni-algal culture(s) of species from each pigment group (Schreiber 1998; Beutler et al., 2002), or increasingly, from a natural community sample that is dominated by one algal group (Jakob et al., 2005; Alexander et al., 2012). The inherent variability in the FES of phytoplankton is a challenge for algal group identification using multi-wavelength fluorometry.

FES vary within algal pigment groups due to differences in the types and relative amounts of light-harvesting pigments of different taxa affiliated with each group, for example phycocyanin (PC) vs. phycoerythrin (PE), types of xanthophylls, and antenna:Chl *a* ratios (Alexander et al., 2012; Kring et al., 2014; Escoffier et al., 2015). Fluorescence yield can vary as a result of light exposure, nutrient stress, and cell/colony size (Kruskopf & Flynn 2006; Falkowski & Raven 2007; MacIntyre et al., 2010). Changes in light intensity due to diel fluctuations, cloud passage, vertical mixing, and other factors which induce the short- or long-term photoacclimation abilities of phytoplankton affect excitation transfer from antenna pigments to reaction centers, and thus may also affect FES. Because of this, automated characterization of phytoplankton community composition in the field, and the application and reporting of multi-wavelength fluorescence data, is still developing. There are studies demonstrating the potential variation of FES for FP (Catherine et al., 2012; Kring et al., 2014; Harrison et al., 2016) and other spectral fluorescence techniques (Gaevsky et al., 2005; Jakob et al., 2005; MacIntyre et al., 2010; Goldman et al., 2013). Variations in the spectra of variable fluorescence, used to make and apportion estimates of quantum yield $F_v:F_m$ have not received similar examination, but should be equally important in applications of multi-wavelength PAM fluorometry. To our knowledge, there has been no published assessment of the variability in Phyto-PAM FES and the potential effects on algal group classification.

The first objective of the present study was to determine how within-group variation in 4-point FES (as measured by Phyto-PAM) compared to among-group variation, and if this may challenge the accuracy of pigment group discrimination. The second objective was to quantify the extent of group misclassifications, if any, for algal monocultures of freshwater phytoplankton resulting from the observed variations in FES. The third objective was to determine the potential of solar irradiance (both visible and ultraviolet) to alter taxon-specific spectra and produce uncertainties in parameter estimates and assignment. To address these objectives, we analyzed reference and response FES of algal monocultures to determine the bases and extents of classification uncertainty under controlled

conditions, and demonstrating the potential challenges that may be encountered in more complex environments.

4.3 Methods

4.3.1 Phytoplankton cultures and irradiance exposure conditions

Thirteen monoclonal freshwater phytoplankton cultures (Table 4.1) were obtained from the Watershed Hydrology and Ecology Research Division (WHERD), Canadian Center for Inland Waters (CCIW, Burlington ON) and the Canadian Phycological Culture Center (CPCC, University of Waterloo, Waterloo ON). Species from the three algal pigment groups identified by the Phyto-PAM were selected as illustrative examples of potential variation within each of the three groups and because of their presence in natural communities of the Laurentian Great Lakes and regional freshwater environments. Culture conditions were as described in Chapter 3.

Table 4.1 Experimental Freshwater Phytoplankton Taxa

Taxon	Phyto-PAM Group	Algal Phylum	RS applied (cases)
<i>Anabaena oscillaroides</i> ¹	Bl	Cyanophyta	6
<i>Dolichospermum</i> ² <i>lemmermannii</i> LO08-01	Bl	Cyanophyta	6
<i>Microcystis aeruginosa</i> Kutz.em. Elenkin CPCC 299	Bl	Cyanophyta	7
<i>Synechococcus</i> sp. ¹	Bl	Cyanophyta	7
<i>Synechococcus rhodobaktron</i> NIVA 8	Br ³	Cyanophyta	7
<i>Coelastrum cambricum</i> HH001-05	Gr	Chlorophyta	6
<i>Pediastrum simplex</i> Meyen CPCC 431	Gr	Chlorophyta	5
<i>Scenedesmus obliquus</i> EC-SW1	Gr	Chlorophyta	7
<i>Asterionella formosa</i> Hass CPCC 605	Br	Ochrophyta	8
<i>Fragilaria crotonensis</i> Kitton CPCC 269	Br	Ochrophyta	10
<i>Cryptomonas</i> sp. CPCC 336	Br	Cryptophyta	10
<i>Synura petersenii</i> Korshikov CPCC 495	Br	Ochrophyta	8
<i>Peridinium inconspicuum</i> UTEX LB 2255	Br	Dinophyta	7

¹Strain number unknown

² Formerly named *Anabaena*

³ *Synechococcus rhodobaktron* is a phycoerythrin-rich cyanobacterium included as a member of the ‘blue’ group taxonomically, however it is recognised as predominantly ‘brown’ by the Phyto-PAM when using typical ‘blue’ reference spectra species. It is included with the cyanobacteria/blue group throughout the present study.

Triplicate subsamples (50 mL) of monocultures in exponential phase were exposed to short-term (75 minutes) irradiance treatments in a solar simulator containing a Xenon arc lamp (1 kW, Oriel Instruments, Irvine, CA) light source and optical glass cut-off filters (Schott optical filters) to produce three light treatments: PAR only (>420 nm); PAR + UVA (>340 nm); and PAR + UVA + UVB (>305 nm), referred to as P, PA and PAB, respectively. Details of the irradiance exposure experiments are as described in Chapter 3.

4.3.2 Chl *a* variable fluorescence measurements

Chl *a* fluorescence of replicate pre-exposure (time 0) and post-exposure (75 min) samples were measured using a Phyto-PAM fluorometer (S/N: PPAA0220, Walz GmbH, Effeltrich, Germany) with an attached System II emitter-detector unit (Phyto-ED, S/N EDEF0111, Walz GmbH) and the corresponding software Phyto-WIN (Walz GmbH). Correction for background fluorescence was measured using 0.2 μm filtered culture media. Minimum fluorescence (F_0) of a dark adapted sample was assessed with the Phyto-ED unit by applying low frequency (ca. 25 Hz) LED-pulses at a width of 12 μsec , resulting in little to no actinic effect. Maximum fluorescence (F_m) was measured with a saturating pulse of light from actinic LEDs (0.2 sec up to 2600 $\mu\text{mol quanta}\cdot\text{m}^{-2}\cdot\text{sec}^{-1}$ at 655 nm), sufficient to close all reaction centers. Phyto-PAM returns F_v , equal to $(F_m - F_0)$, and the maximum quantum yield of photochemistry ($F_v:F_m$), the efficiency with which absorbed excitation energy is utilized for photosynthetic electron transfer (Genty et al., 1989; Maxwell & Johnson 2000).

4.3.3 Statistical analyses

The replicate FES, measured as absolute fluorescence in instrument units, were normalized to the diode (wavelength) of maximum excitation, the same as with Phyto-PAM/Phyto-WIN Reference Spectra (RS) (e.g. Table C.6). These normalized spectra are termed ‘response spectra’ to distinguish them from the RS defined for each taxon by Phyto-PAM protocol and used for linear un-mixing analysis. For the evaluation of results, each case (N) is a single combination of experimental taxon presented and RS scenario used (Table 4.2, Table C.7), with 100-120 readings for each case. The averages and frequencies of parameter measurement for each case were used to calculate the summary statistics shown, such that the minimum and maximum values are averages of multiple measurements from one case. The cases used were not exhaustive, but provide an informative sampling of the potential inconsistencies in algal fluorescence parameters than can result from variable/incorrect RS application.

Two-way analysis of variance (ANOVA) was used to test for effects of irradiance and taxon on F_0 and F_v response spectra. Non-metric multidimensional scaling (NMDS) analysis was used to visualize these differences, with hierarchical cluster analysis used to quantify the similarities among groups. NMDS and cluster analyses were also performed on a library of 57 RS of F_0 and F_v (Table C.6) to assess variation within and among pigment groups. Some library RS are for the same species, in some cases different strains/isolates, but in all cases were independently grown and measured, and present slightly different RS. Data analyses were performed using R version 3.2.2 statistical environment (R Development Core Team, 2015), including the vegan package (Oksanen et al., 2016) for NMDS and cluster analyses, and Systat 10 (Systat Software, Inc., Chicago, IL).

4.3.4 Reference Spectra selection

Phyto-PAM excitation light is produced by an array of measuring light LEDs (light emitting diodes) with peaks at 470, 520, 645 and 665 nm and actinic light LEDs with a peak at 655 nm (Walz 2003). The measuring light pulses are applied alternately at high frequency, producing near-simultaneous measurement of Chl *a* fluorescence excited by four wavelengths. The Phyto-PAM measures emitted Chl *a* fluorescence and returns metrics for the four excitation wavelengths and derived fluorescence metrics for three algal pigment groups: blues (cyanobacteria), greens (chlorophytes and related taxa), and browns (diatoms, dinoflagellates, chrysophytes, cryptophytes). The Phyto-PAM is not equipped to simultaneously detect PC-rich and PE-rich cyanobacteria. When typical RS are used, a PE-rich cyanobacterium will appear as a mixture of predominantly brown, with some blue algae. However, if it is known that a sample will contain a significant contribution of PE-rich cyanobacteria a corresponding RS can be created (measured from culture) and selected. Algal group estimates are calculated in Phyto-WIN by deconvolution of the four diode signals, using selected RS via linear unmixing. The user can specify that one, two or all three of the algal groups be estimated, with one RS selected for each group. If it is known that a given sample contains predominantly or only one group, the user can select only that RS, forcing Phyto-PAM to attribute all fluorescence signal to that group and increasing estimation accuracy (Walz, 2003). This approach was used in the current study to obtain the ‘true’ fluorescence values for each culture/taxon. F_0 , F_v and $F_v:F_m$ metrics are reported and analyzed, with F_0 considered proportional to Chl *a* concentration and indicative of group-specific biomass (McClellan et al., 2008).

Table 4.2 Scenarios to assess uncertainty in Phyto-PAM estimates of group-specific fluorescence arising from variability of reference spectra (RS), illustrated with *Asterionella formosa* as the taxon presented to the instrument.

Scenario	Group(s) selected	Algal Group	Taxa selected for Reference Spectra
Base case (Correct RS)	X	Blue	<i>D. lemmermannii</i>
		Green	<i>P. simplex</i>
		Brown	<i>A. formosa</i>
1 Uni-algal mismatch	X	Blue	<i>D. lemmermannii</i>
		Green	<i>P. simplex</i>
		Brown	<i>F. crotonensis</i>
2 Multi-algal match	X	Blue	<i>D. lemmermannii</i>
	X	Green	<i>P. simplex</i>
	X	Brown	<i>A. formosa</i>
3 Multi-algal mismatch	X	Blue	<i>D. lemmermannii</i>
	X	Green	<i>P. simplex</i>
	X	Brown	<i>F. crotonensis</i>

Each Phyto-PAM RS for a given taxon is defined as two (F or F_0 and F_v) 4-point fluorescence spectra from the 4 excitation diodes, normalized to the highest diode for a given sample, measured with a particular instrument. RS were created for thirteen experimental taxa using the protocol specified by Walz: measured on cultures in exponential growth phase, diluted with media such that colour was not visible with the naked eye (Phyto-PAM Gain setting of approximately 11), and after adaptation (ca. 30 min) to low level light on the laboratory bench top. Additional RS, measured using the same instrument at CCIW, were included in the comparison (S. Watson, unpubl. data) (Table C.6, referred to as ‘library’ RS).

Three different scenarios (Table 4.2) were examined to illustrate how the variability of RS can produce uncertainty in quantification and assignment of F_0 and F_v among groups. The scenarios provided an escalating degree of challenge to the instrument. Scenario 1, termed uni-algal mismatch, specified estimates for one group only, matching the group to which the test taxon belonged (e.g. blue when a cyanobacterial taxon was presented), but using a RS derived from a different member of that group. In this scenario, there can be no confusion over the identity of the group, but the values for F_0 and F_v may be affected. Scenario 2, termed multi-algal match, allowed multiple (up to three) groups

to be estimated when a single taxon was presented, using the group RS derived from the taxon presented. In this case, there is scope for error in the assignment of F_0 and F_v among groups, and for variations in the estimated magnitude of F_0 and F_v . Scenario 3, termed multi-algal mismatch, allowed multiple groups to be estimated when a single taxon was presented, and used a RS derived from a different member of that group (as in Scenario 1). All results were compared to the base case in which instrument choice is constrained to the correct group and the RS used is for the taxon actually presented; these were considered the true values for F_0 and F_v .

4.4 Results and Discussion

4.4.1 Taxonomic variation of Reference Spectra

Phyto-PAM RS reflect differences in pigment composition and excitation spectra among groups but are additionally weighted by light intensity of the excitation diodes, which varies among wavelengths and individual instruments. RS therefore can vary among instruments and have a different shape than the underlying excitation spectra.

For the blue group F_0 spectra were consistently highest at 645 nm, while F_v spectra were maximal at 645 nm, or occasionally 665 nm for some strains (Figure 4.1, Table C.6). This corresponds to the dominant light harvesting complexes of many freshwater cyanobacteria, the blue phycobiliproteins, PC and allophycocyanin (APC), with absorption peaks near 620 nm and 655 nm, respectively (Kirk 1994; Rastogi et al., 2015). The exceptions were PE-rich cyanobacteria, such as *Synechococcus rhodobaktron* (referred to as special-case blues in Figure 4.1), which had maximal F_0 and F_v at 520 nm, due to their high content of PE, which has absorption maxima between 545-575 nm (Kirk 1994; Rastogi et al., 2015). While the Phyto-PAM does not have an excitation diode targeted for excitation of PE, it still absorbs effectively at 520 nm.

Fluorescence excitation for green taxa was highest at 645 nm for F_0 and 645 or 665 nm for F_v . Chlorophytes use Chl *a* and *b* with absorption peaks in the blue and red portions of the visible spectrum, corresponding to higher excitation by the 470 and 645 nm diodes, respectively (Figure 4.1, Figure 4.2). Small differences in RS shape among green taxa may be due to differences in the relative amounts of Chl *a* and *b*, contributions from carotenoids, or differences in self-shading or back-scattering due to differences in colonial versus unicellular growth forms (Schagerl & Donabaum 2003; Graham et al., 2016).

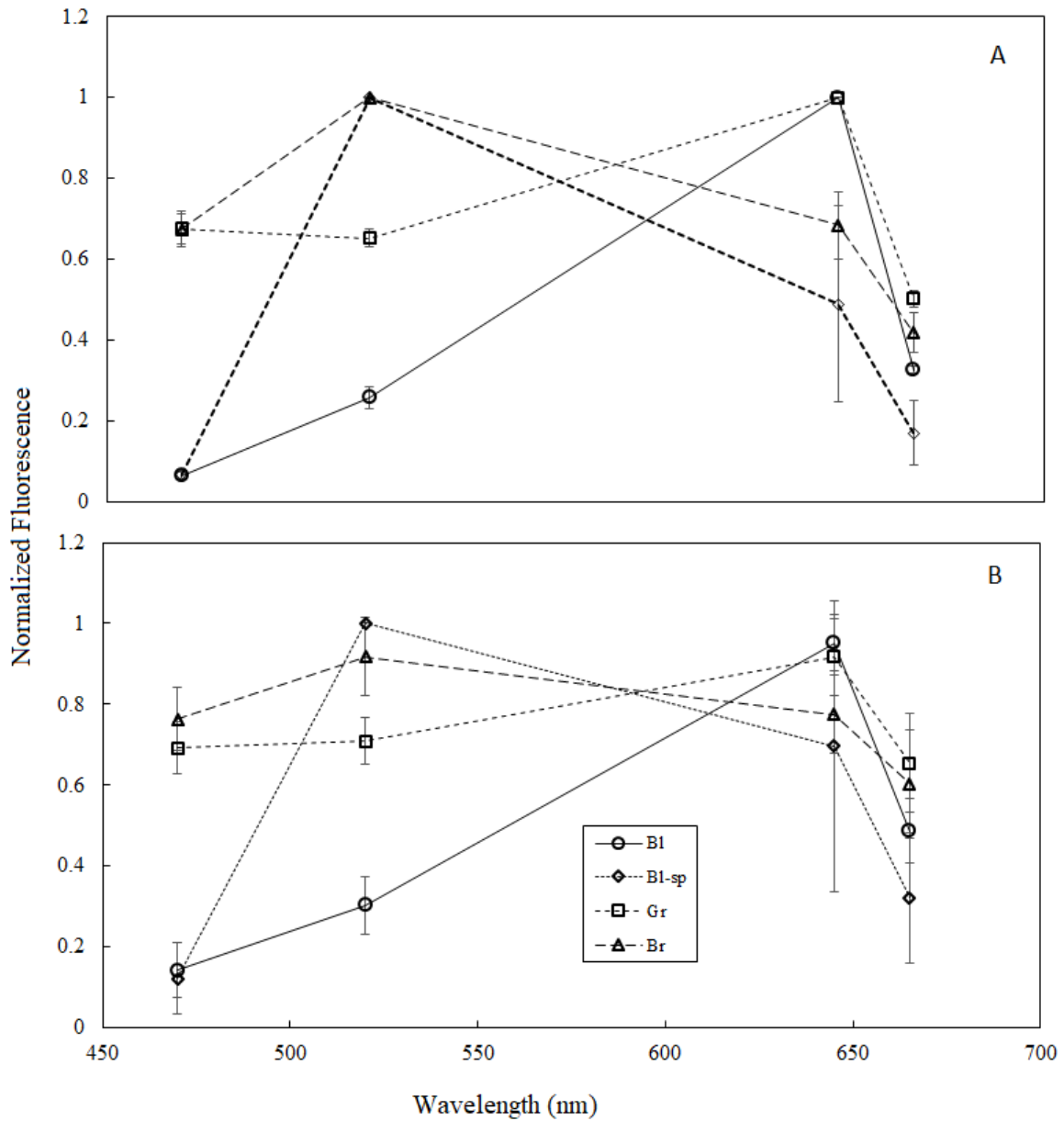


Figure 4.1 Average Reference Spectra (RS) for each algal group (Bl – blues, N = 28, circles and solid line; Bl-sp – special case blues (PE-rich taxa), N = 4, diamonds and dotted line; Gr – greens, N = 13, squares and short-dashed line; Br – browns, N = 12, triangles and dashed line) with error bars representing 95% confidence intervals. (A) F₀ RS, (B) F_v RS.

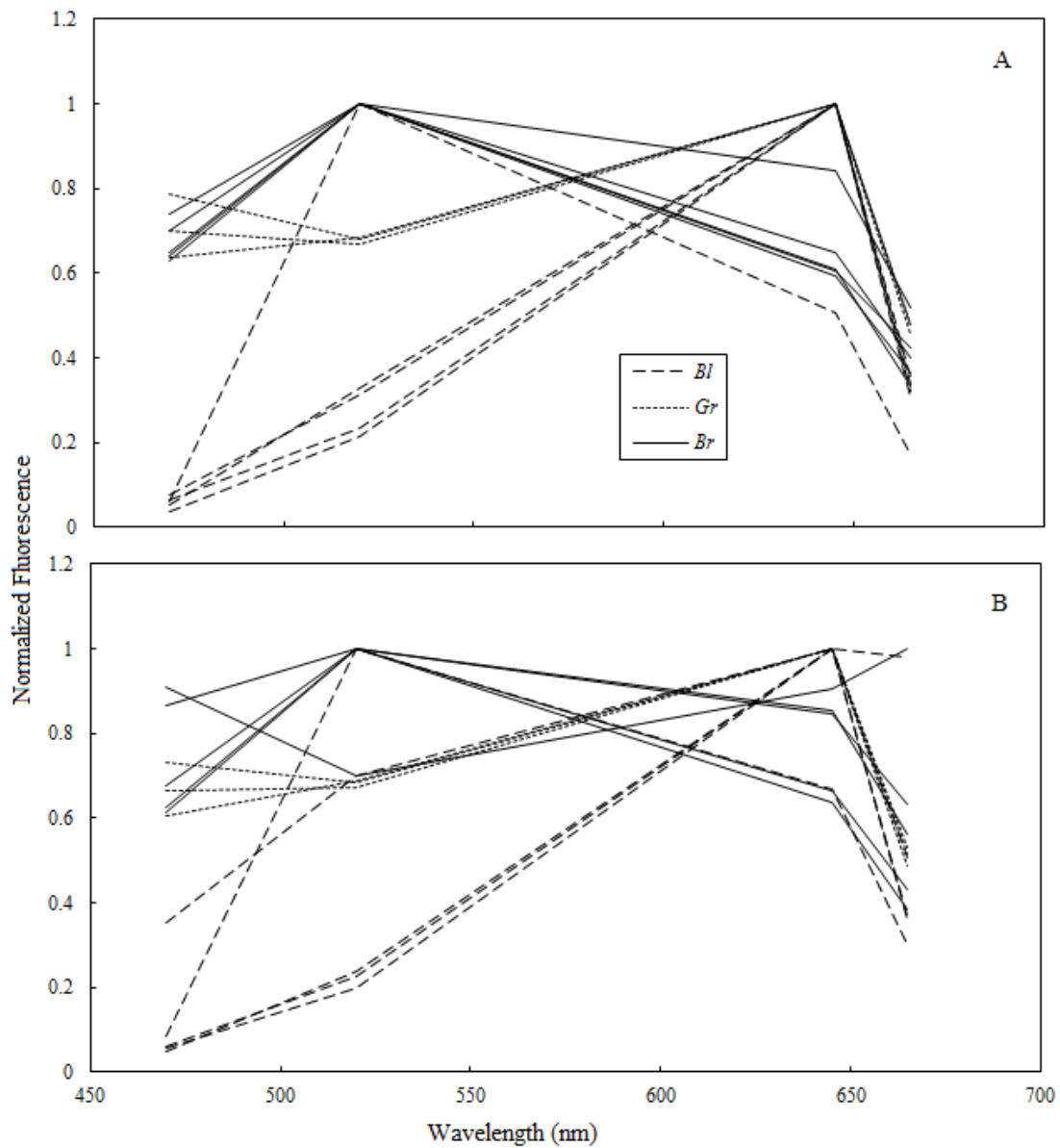


Figure 4.2 Minimum, F_0 (A) and variable, F_v (B) fluorescence RS for 13 monoculture experimental taxa, with line type distinguishing algal group: dashed line – blue, short-dashed line – green, solid line – brown. Note: *S. rhodobaktron* is included with the blue group here, though it does not exhibit the typical blue RS shape.

F₀ spectra of the brown group were maximal at 520 nm; however, the wavelength of maximum excitation for F_v was more variable, with RS normalizing to 520, 645 or 665 nm for different taxa. The brown pigment group encompasses more taxonomic diversity than the other groups, and in the context of Phyto-PAM, includes both chromophytes and cryptophytes. These taxa use Chl *a*, *c*, various xanthophylls, and PE in the case of cryptophytes. Xanthophylls have absorption maxima in the range 510-525 nm (Kirk 1994), corresponding to the 520 nm diode. Differences in spectral shape among brown/chromophyte taxa are likely caused by different light-harvesting xanthophylls (including fucoxanthin, peridinin, violaxanthin) and carotenoids, and differences in the relative contribution of those pigments to reaction center excitation (Kirk 1994; MacIntyre et al., 2010; Richardson et al., 2010).

Average pigment group spectra for F₀ showed less within-group variability (i.e., smaller confidence intervals) than for F_v, and the blue (PC-rich) and green groups had greater within-group similarity compared to the brown and special-case (PE-rich) blue groups (Figure 4.1). Figure 4.2 shows F₀ and F_v RS for the subset of experimental taxa used in the irradiance exposures. RS shapes were different between F₀ and F_v in all taxa, with smaller (*D. lemmermannii*, *M. aeruginosa*, three chlorophyte taxa, *P. inconspicuum*) or larger (*Cryptomonas* sp., *S. petersenii*) amounts of variation. In fact, the normalizing diode and thus spectrum shape of *Cryptomonas* sp. changed between F₀ and F_v (Figure 4.2, Table C.6). RS also showed variation even for the same species: 57 RS were included in the examination of taxonomic variation in RS, which included 32 different species. Multiple RS created from different strains/variants of the same species consistently produced different RS. In most cases these differences were quite small, such that RS had the same shape and normalizing diode, but in other cases the normalizing diode varied (e.g. *Coelastrum* spp., *Fragilaria crotonensis* –Table C.6). Small differences in RS that fall in the range of within-group variation should not alter pigment group assignment, but larger variations in RS that increase the similarity to another pigment group create the potential for misclassification.

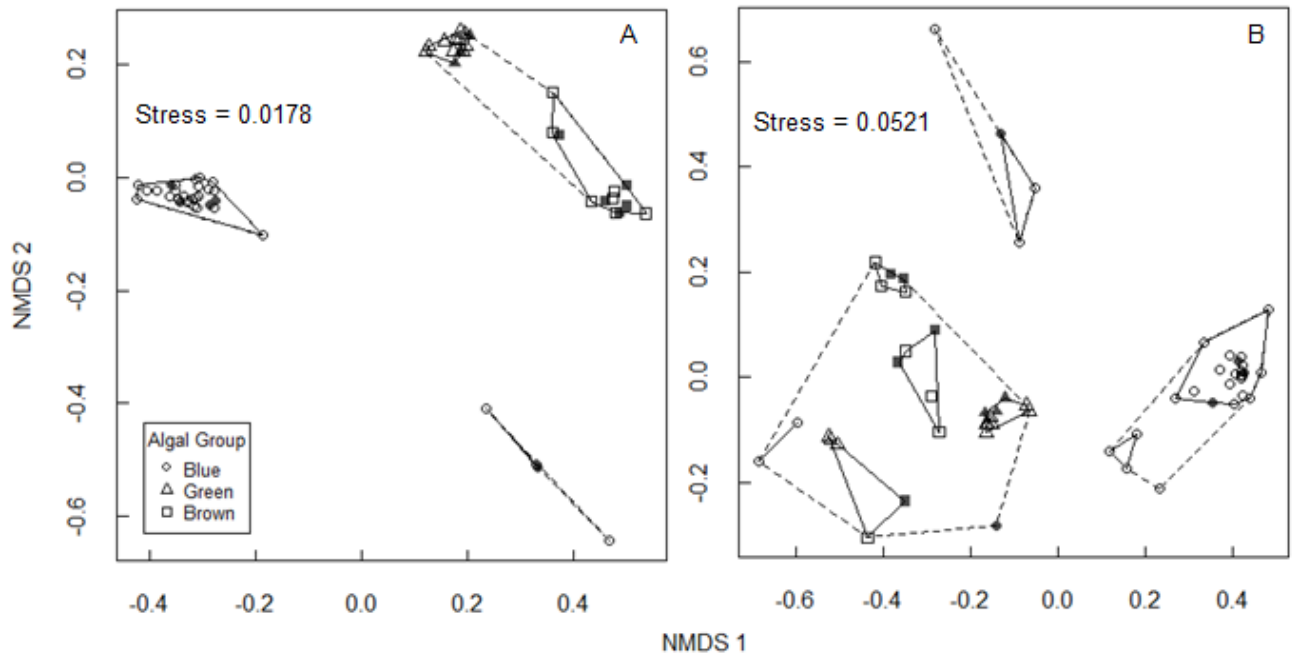


Figure 4.3 NMDS ordination of Phyto-PAM minimum, F_0 (A) and variable, F_v (B) fluorescence Reference Spectra (RS) for freshwater phytoplankton taxa. Solid symbols: RS of 13 experimental taxa, open symbols: remaining library RS (both created using the same Phyto-PAM fluorometer). Stress type 1. Groupings indicated are from hierarchical cluster analysis, with solid lines indicating groups with 90% similarity, and dashed lines around groups with 80% similarity.

NMDS ordination of F_0 RS (Figure 4.3A) showed four distinct clusters, corresponding to four pigment groups: blues (left), greens (top), browns (right), and PE-rich blues (bottom right). The type 1 stress parameter fell within the ‘excellent’ range (0.00-0.025), producing a solution of very good fit with only a slight distortion from representing the data in a two-dimensional plot (Kruskal 1964; Wickelmaier 2003). The F_0 RS of PC-rich cyanobacteria and chlorophytes were each tightly grouped and shared 90% or higher similarity based on hierarchical clustering. Chromophyte F_0 RS also shared 90% similarity, although some taxa (Fr.cr, Sy.pe, Sp; Table C.6) appeared as outliers from the main group, falling between the brown and green clusters. Chromophyte and chlorophyte F_0 RS grouped together at 80% similarity, aligning with their similar spectra shape compared to PC-rich cyanobacteria (Figure 4.1, Figure 4.2). The F_0 RS of the PE-rich cyanobacteria grouped together at

80% similarity, and plotted outside the triangle formed by the other three pigment groups, below and between the clusters of the blue and brown groups (Figure 4.3A). Similar pigment-group divisions were identified via ordination of spectral data from the Algae Online Analyzer (AOA) (MacIntyre et al., 2010). Applying cluster analysis and ordination to the spectra of different taxa presented four spectrally-distinct pigment groups, distinguishable using multi-wavelength excitation of fluorescence, despite Phyto-PAM not having a diode targeted to PE. However, these four groups would not be simultaneously identified by Phyto-PAM using its un-mixing algorithm, which can solve for at most three pigment groups with the 4-point spectra.

The ordination of F_v RS did not produce the clearly defined groups observed with F_0 RS (Figure 4.3B). The stress parameter was classified as good to fair (>0.05) (Wickelmaier 2003), indicating a weaker, but still acceptable, fit compared to the previous ordination. The brown and green groups did not form distinct clusters; and the brown taxa in particular were highly scattered. Most of the chlorophyte RS clustered together and were grouped at 90% similarity, with the exception of two strains/local variants of *Coelastrum*, which were grouped at 90% similarity with two brown taxa (*Cryptomonas* and *Synura*). Different subsets of chromophyte taxa were grouped together at 90% similarity, but did not all form a distinct cluster. As with the F_0 RS ordination, the chromophyte and chlorophyte F_v RS were grouped together at 80% similarity. The majority of the cyanobacteria F_v RS plotted in the same region at 80% and 90% similarity, though three cyanobacterial taxa were grouped with the greens and browns at 80% similarity (Ao, An.cr, Pl.sp.3, Table C.6). F_v RS of PE-rich cyanobacteria plotted outside the region of the other three groups and were grouped at 80%, and in some cases 90%, similarity.

In this assessment, light history effects and their contribution to species-specific differences in RS should be minimal because all cultures were preconditioned to the same low level light prior to fluorescence measurement. The variability between F_0 and F_v spectra suggests differences in the contribution of antenna pigments to reaction center fluorescence between the two measurements. Non-PSII fluorescence may occur from disconnected antenna pigments, such as phycobiliproteins or chlorophylls, which would enhance F_0 excitation compared to F_v at the respective wavelengths (Campbell et al., 1998).

4.4.2 Effects of Reference Spectra selection on algal group assignment in monocultures

Table 4.3 Offset in Algal F_0 and $F_v:F_m$ estimates (as percentage of true values) using different Reference Spectra (RS) scenarios, with minimum and maximum parameters summarizing relative offsets, and mean values summarizing absolute offsets.

Algal Group	Summary Statistic	Scenario 1		Scenario 2		Scenario 3	
		Uni-Algal Mismatch	Multi-algal Match	Multi-Algal Mismatch			
		ΔF_0	$\Delta F_v:F_m$	ΔF_0	$\Delta F_v:F_m$	ΔF_0	$\Delta F_v:F_m$
Blue	N	12	12	13	13	12	11
	Min	-10.48	-7.45	0.00	-1.61	-5.07	-12.62
	Max	26.86	9.94	2.42	2.92	37.10	11.92
	Abs Mean	5.83	4.32	0.92	0.71	9.36	6.81
Green	N	4	4	7	6	7	7
	Min	-0.40	-0.14	2.61	-1.59	0.56	-8.31
	Max	1.16	0.09	3.48	-1.02	23.14	0.09
	Abs Mean	0.63	0.08	3.06	1.22	10.94	3.59
Brown	N	11	11	10	10	23	23
	Min	-1.50	-1.89	-1.33	-38.95	-1.50	-5.43
	Max	3.96	3.84	9.02	0.00	21.06	25.61
	Abs Mean	1.32	1.05	2.33	7.48	5.91	2.75

The first step in assessing the consequences of within-group RS variability was to measure the impacts on F_0 and $F_v:F_m$ estimates when group assignment was constrained to the correct algal group for the taxon presented, but a RS for a different taxon in the same group was used: scenario 1, uni-algal mismatch (Table 4.2). RS scenarios were applied to measurements on experimental taxa; these correspond to the shaded symbols of the NMDS ordination in Figure 4.3 and the first thirteen taxa in Table C.6 (5 blue, including 1 PE-rich taxon, 3 green, 5 brown). While these taxa do not represent the most extreme outlier points for each pigment group, they provide an estimate of the potential variability within each group. Absolute average offsets of F_0 and $F_v:F_m$ were lowest for the green and brown groups (> 1.5% of true values), and higher for the blue group (> 6% of true values) (Table 4.3). The range in offsets presented the same pattern among pigment groups, with the highest offsets of 26.86% for the blue group (*S. rhodobaktron* applying *M. aeruginosa* RS). Natural phytoplankton assemblages can often be dominated by a single pigment group, such as during bloom events, but

there may be multiple species from the same group, and users may not have RS for the dominant taxon. These offsets demonstrate both the range and typical level of error that could occur when estimating abundance and photochemical efficiency for an algal population dominated by a taxon/taxa other than the RS taxon. However, natural phytoplankton assemblages are often comprised of representatives from more than one pigment group – addressed in scenarios 2 and 3.

In scenario 2, multi-algal match, a correct RS was used for the taxon presented but the instrument's linear un-mixing algorithm must now assign the measured fluorescence to the correct group. In this scenario, the average offsets for F_0 and $F_v:F_m$ were less than 3% of true values for all groups, with the exception of $F_v:F_m$ for the brown group (Table 4.3). Offsets ranged as high as 9% of true values for F_0 and -38.95% for $F_v:F_m$ (*Cryptomonas* sp. applying RS using: *M. aeruginosa*, *C. cambricum*, *Cryptomonas* sp.). Application of the correct RS for the presented taxon produced reasonably accurate results, even when there was potential to assign the fluorescence signal to other groups. However, the magnitude of offsets in brown estimates increased compared to scenario 1, due to a small number of cases. Scenario 3 introduced additional potential for error because the taxon presented was not represented by its own RS, but by the RS for another taxon from the same group. With this scenario, cases from each of the pigment groups demonstrated offsets >10% for F_0 and/or $F_v:F_m$. Average offsets were <11% for F_0 and <7% for $F_v:F_m$ (Table 4.3). The maximum offset for F_0 was shown by the blue group: 37.1% of the true value (*S. rhodobaktron* applying RS using: *D. lemmermannii* and *Cryptomonas* sp.), and for $F_v:F_m$ the maximum offset was shown by the brown group: 25.61% (*S. petersenii* applying RS using: *M. aeruginosa*, *C. cambricum*, *Cryptomonas* sp.).

With multi-algal RS combinations (scenarios 2 and 3) there was the potential for Phyto-PAM to incorrectly quantify F_0 and $F_v:F_m$ of the correct group, and to attribute fluorescence to an algal group that was not actually present. The latter may be of greater concern than small errors in parameter quantification for the correct group. In scenario 2, with the correct RS for the taxon presented, 97-98% of the F_0 signal was identified correctly (Table 4.4), with mis-assigned signal averaging only 0.31 to 2.84% of total F_0 signal. At most, 9.34% of the F_0 signal was assigned to an incorrect algal group (for *Cryptomonas* applying RS using: *M. aeruginosa*, *C. cambricum*, *Cryptomonas* sp.). In scenario 3, when a RS from a different taxon within the same group was used other than the one presented, the scope for, and incidence of, mis-assignment was greater. Correctly assigned algal F_0 averaged 89 to 95% of total signal. However, there were cases when up to 20% of F_0 was misclassified for taxa from all three groups: *M. aeruginosa* identified as 16% brown (RS using: *D.*

lemmermannii, *C. cambricum*, *Cryptomonas* sp.); *C. cambricum* identified as 19% brown and 4% blue (RS using: *D. lemmermannii*, *C. reinhardtii*, *A. formosa*); and *S. petersenii* identified as 20% blue (RS using: *A. oscillarioides*, *P. simplex*, *P. inconspicuum*).

Table 4.4 Algal F₀ proportions estimated for each algal group in Reference Spectra (RS) scenarios 2 and 3. Proportions were calculated from replicate measurements for a given case, N, and summary statistics were calculated for all cases for a given algal group.

Algal Group	Summary Statistic	(2) Multi-Algal Match			(3) Multi-Algal Mismatch		
		Bl	Gr	Br	Bl	Gr	Br
Blue	N	13	11	13	12	11	12
	Min	96.58	0.00	0.00	83.76	0.00	0.00
	Max	100.00	2.91	2.25	100.00	1.23	16.24
	Median	99.23	0.00	0.46	99.39	0.00	0.00
	Mean	98.65	0.94	0.55	95.32	0.11	4.58
Green	N	7	7	7	7	7	7
	Min	0.00	96.41	2.35	0.00	76.08	0.00
	Max	0.97	97.27	3.39	7.54	100.00	19.50
	Median	0.20	96.68	2.73	0.00	88.06	11.94
	Mean	0.32	96.84	2.84	1.71	89.09	9.21
Brown	N	10	10	10	23	23	23
	Min	0.00	0.00	90.41	0.00	0.00	80.14
	Max	0.74	9.34	100.00	19.86	2.44	100.00
	Median	0.28	0.00	99.41	0.51	0.00	99.49
	Mean	0.31	1.89	97.80	5.21	0.21	94.58

When the correct RS for the taxon presented was used (scenario 2), F_v:F_m was consistently estimated for the correct group when presented with a blue or green taxon, but not when it was a brown (Table 4.5). Brown group F_v:F_m was not consistently measured for *Cryptomonas* sp. or *S. petersenii* monocultures, and was often misattributed to the green group, in particular for *Cryptomonas* sp. This may be due to the difference in F_v RS shape seen in these two species – with 645 nm as the normalizing diode rather than the typical 520nm, changing the shape of the F_v RS to appear more like a typical green species. On average, brown F_v:F_m was estimated only 81% of the time when a brown taxon was presented. In the unusual case of *Cryptomonas*, brown F_v:F_m was reported only 12% of the time. With scenario 2, F_v:F_m was rarely estimated for a group not present,

indicated by the low mean and median frequencies (< 2%), with the exception of green $F_v:F_m$ estimated for brown taxa (Table 4.5).

Table 4.5 Frequency of $F_v:F_m$ estimation for each algal group in Reference Spectra (RS) scenarios 2 and 3. Frequencies were calculated from replicate measurements for a given case, N, and summary statistics were calculated for all cases for a given algal group.

Algal Group	Summary Statistic	(2) Multi-Algal Match			(3) Multi-Algal Mismatch		
		Bl	Gr	Br	Bl	Gr	Br
Blue	N	13	11	13	12	11	12
	Min	100.00	0.00	0.00	82.57	0.00	0.00
	Max	100.00	14.85	3.96	100.00	17.43	99.36
	Median	100.00	0.00	0.00	100.00	0.00	0.00
	Mean	100.00	1.35	0.38	98.55	1.58	19.16
Green	N	7	7	7	7	7	7
	Min	0.00	100.00	0.75	0.00	100.00	0.00
	Max	0.00	100.00	3.06	98.98	100.00	100.00
	Median	0.00	100.00	1.00	0.00	100.00	0.75
	Mean	0.00	100.00	1.48	14.14	100.00	14.83
Brown	N	9	9	9	23	23	23
	Min	0.00	0.00	12.00	0.00	0.00	74.81
	Max	1.00	89.00	100.00	100.00	25.19	100.00
	Median	0.00	0.00	100.00	0.00	0.00	100.00
	Mean	0.39	19.44	80.78	29.92	1.23	98.69

The occurrence of incorrect $F_v:F_m$ assignment was higher using scenario 3 compared to 2. $F_v:F_m$ was consistently reported for the correct group when the taxon presented was green (mean = 100%), but not when it was a blue or brown (mean ca. 98%) (Table 4.5). Brown $F_v:F_m$ were measured more consistently for our two ‘problem’ brown taxa, *Cryptomonas* and *S. petersenii*, when RS from different brown taxa were used, likely for the same reason that green $F_v:F_m$ estimates were common under scenario 2. Using brown RS with consistent F_0 and F_v spectra shape would be more likely to return correctly (brown) assigned $F_v:F_m$ estimates. $F_v:F_m$ estimation for algal groups not present was more common under scenario 3 compared to scenario 2, occurring from 1 to 30% of the time on average (Table 4.5), but for up to almost 100% of measurements for some cases (taxon-RS combinations) in each pigment group.

A total of 81 different RS scenarios were applied to thirteen experimental taxa (24 uni-algal and 57 multi-algal scenarios) to assess variability in algal F_0 and $F_v:F_m$ estimation using different Phyto-PAM RS settings. In general, blue taxa were effectively discriminated from the other two algal groups, consistent with the large spatial separation of the blue group in the ordination plots. However, their estimation accuracy (offsets) were sensitive to taxon-specific RS variations. The Phyto-PAM showed higher incidence and magnitude of classification errors when presented with brown taxa, the group with the highest level of scatter in both F_0 and F_v spectra as visualized via ordination. Group classification of green taxa appeared sensitive to taxon-specific RS differences, despite a strong grouping in ordination space. These multi-algal scenario results show that, even given the correct RS for the taxon presented (scenario 2), within-group variability (and between group similarity) in RS can produce mis-assignments of $F_v:F_m$ at a frequency that could, at the least, be confusing and potentially quite misleading – a problem that is amplified when RS do not match the taxon presented (scenario 3). These results highlight the challenges likely to be encountered when sampling natural communities, where it is not feasible to have independent taxonomic classification for a high number of samples, multiple taxa are present in each pigment group, and a user may not have RS available for the dominant taxa. It also illustrates the importance of replicate measurements to inform the user when an estimate may be questionable, and to provide certainty in fluorescence estimates. Spectral fluorometry is a tool that may prove useful for improving detection of algal groups that form nuisance and/or harmful blooms, but incorrect assignment of abundance and quantum yield measurements to groups that are not present may limit this application, or at least complicate its implementation.

4.4.3 Effects of PAR and UVR on fluorescence excitation spectra

High PAR and UVR exposure causes photoinhibition in algal cells, primarily through damage to PSII components including the oxygen evolving complex and the D1 protein (Bouchard et al., 2006; Nishiyama et al., 2006). The experimental taxa tested showed significant levels of photoinhibition following irradiance exposure, in particular under the PAB treatment (PAR + UV-A + UV-B), indicated by reduced quantum yields ($F_v:F_m$) (Chapter 3, Table 3.3). Acute irradiance exposure may change the quantification and group assignments of F_0 and F_v by the Phyto-PAM if it changes the shape of the RS, and changes the shape for a given taxon to become more similar to a different pigment group. This could occur, for example, if photoacclimation responses alter the relative transfer of excitation energy from antenna pigments to reaction center chlorophylls, or if damaged vs. undamaged reaction centers are supplied differentially by antenna pigments.

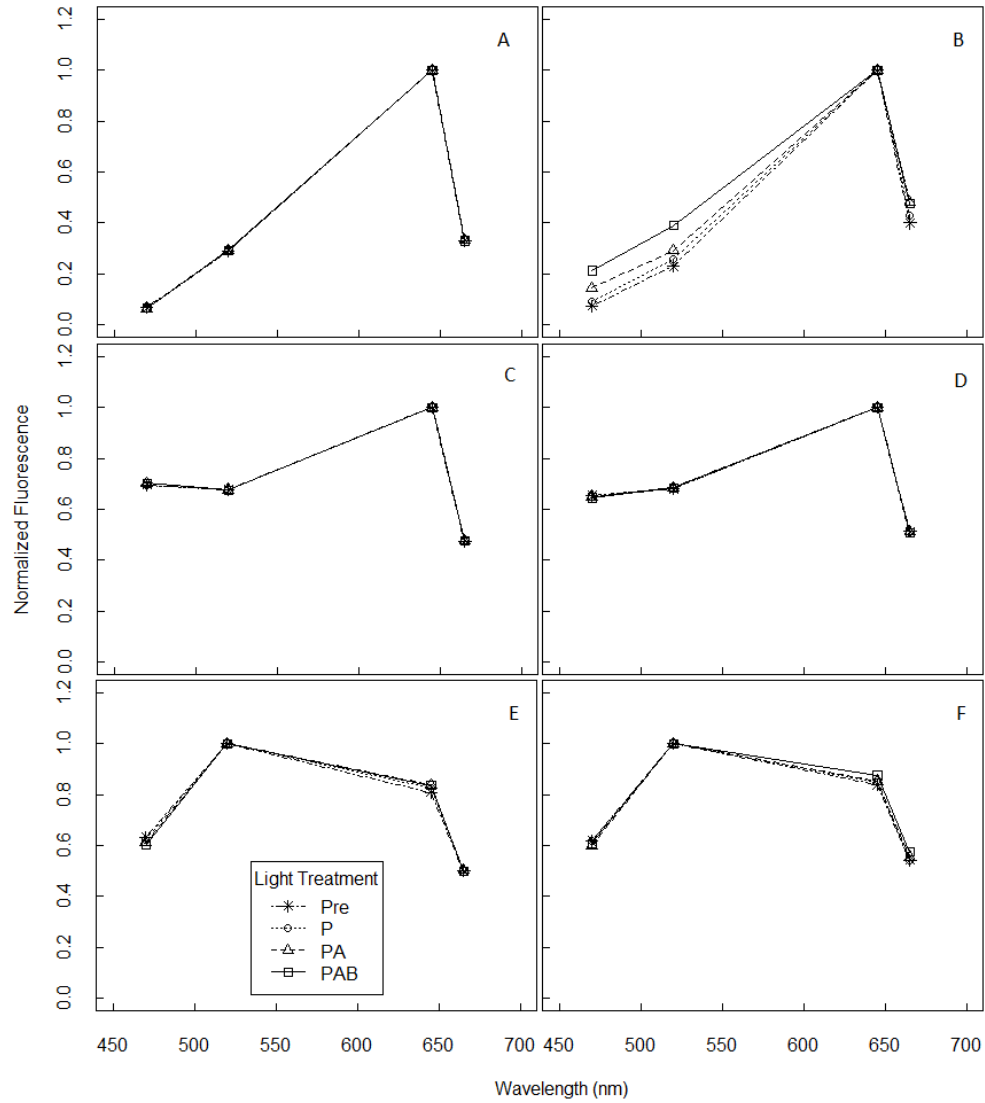


Figure 4.4 Normalized response spectra from different light treatments (Pre-exposure, P – PAR only, PA – PAR + UV-A, PAB – PAR + UV-A + UV-B) for F_0 (A, C, E) and F_v (B, D, F) for *A. oscillarioides* (A, B), *P. simplex* (C, D) and *S. petersenii* (E,F).

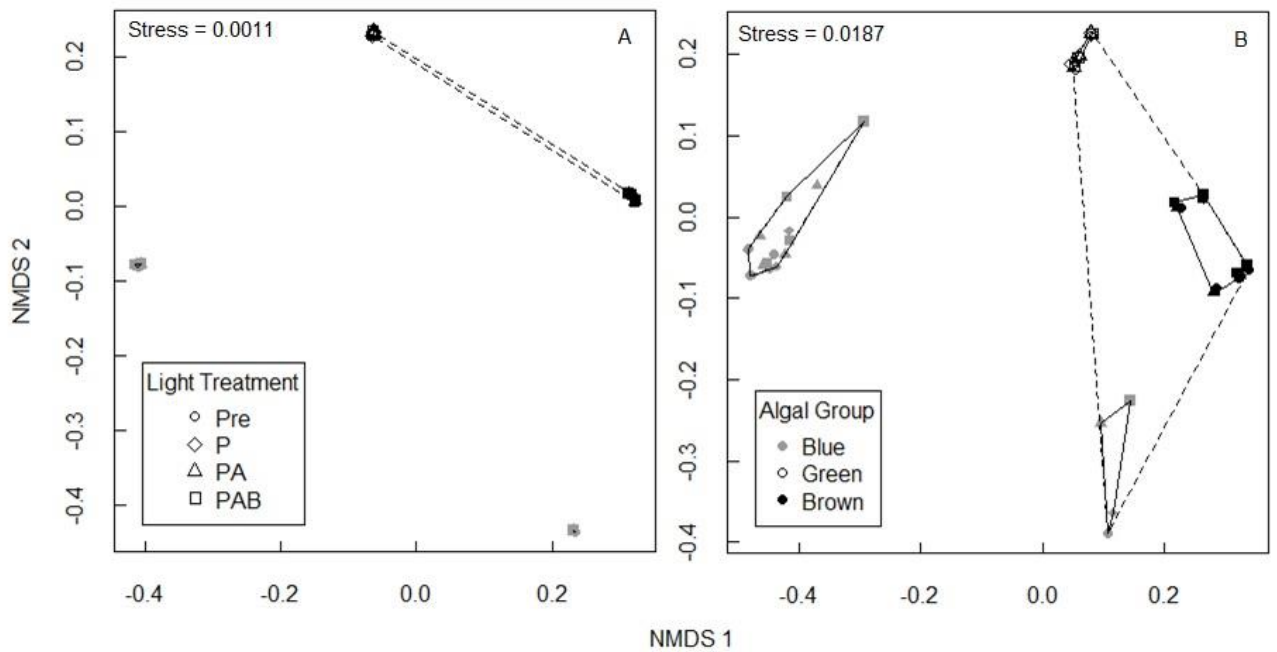


Figure 4.5 NMDS ordination of response spectra for F_0 (A) and F_v (B) of 13 experimental taxa (distinguished by Phyto-PAM pigment group: blue, green, brown) following different light exposure treatments (Pre-exposure, P – PAR only, PA – PAR + UV-A, PAB – PAR + UV-A + UV-B). Stress type 1. Groupings indicated are from hierarchical cluster analysis, with solid lines indicating groups with 90% similarity, and dashed lines around groups with 80% similarity.

The effects of light treatment on response spectra shape appeared to be small (Figure 4.4); *A. oscillarioides* F_v (Figure 4.4B) showed visible changes in shape, as did *S. rhodobaktron* (not shown), while the responses of *P. simplex* and *S. petersenii* (Figure 4.4, C-F) were typical of most experimental taxa. The NMDS ordination of F_0 response spectra (Figure 4.5) showed four distinct apices/clusters, consistent with the pigment groups observed in the taxonomic NMDS plot, and with the stress parameter within the ‘excellent’ range (0.00-0.025) (Wickelmaier 2003). The F_0 response spectra from different light treatments were essentially super-imposed (Figure 4.4, Figure 4.5A), such that the 90% similarity groupings could not be seen on the ordination plot, and suggesting little to no change in relative spectra shape. However, despite the visual similarity, changes to F_0 spectra shape were significant ($p < 0.05$) for nine of the thirteen taxa (Table 4.6). A significant interaction term from

the two-way ANOVA indicates the effects of light treatment on fluorescence intensity were different among the four excitation diodes – resulting in a change in spectra shape.

F_v response spectra showed more variation compared to F_0 (Figure 4.5B), with an ordination stress parameter an order of magnitude higher, though still categorized as ‘excellent’. The same four clusters corresponding to blue, special-case blue, green and brown pigment groups were distinguished, with each of the four groups shared 90% similarity, and the greens, browns and special-case blues were grouped together at 80% similarity. Some of the points representing post-exposure response spectra of blue and brown taxa moved away from their pre-exposure and respective algal group cluster, and towards the ‘green’ cluster, and post-exposure *S. rhodobaktron* spectra moved closer to the triangle formed by the other three algal groups, with the largest differences from the treatments including UVR. This may indicate the potential for partial misclassification of F_v to the green group following high light exposure. F_v spectra shape varied significantly with light exposure for nine of the thirteen taxa, though not all the same taxa as for F_0 (Table 4.6).

Two-way ANOVA confirmed that among-diode differences in fluorescence excitation were significant (Table C.8), which is both expected and the premise of pigment group discrimination by multi-wavelength fluorometry. F_0 response spectra varied significantly ($p < 0.05$) with light treatment for seven taxa, and for eight taxa when F_v ($p < 0.03$) was compared (Table C.8). All pigment groups included taxa with response spectra that changed compared to pre-exposure, and those that did not. Response spectra of the cyanobacterial taxa were the most consistently affected by light exposure, including significant change in the F_v spectra of all five taxa. Thus, the risk for inaccurate classification and quantification of fluorescence for this group may be higher following high light exposure. There were two taxa (*S. obliquus*, *A. formosa*) where neither F_0 nor F_v exhibited significant interaction effects, suggesting the shape of the 4-point excitation spectra of these species were not affected by high PAR and UVR, and light stress should not affect algal group classification of F_0 or $F_v:F_m$.

Changes in response spectra due to light treatment suggests the relative amount of energy being transferred to PSII Chl *a* from antenna pigments was affected by acute PAR and UVR exposure, and that these changes persisted over a thirty minute period of dark adaptation. These types of changes may be associated with rapid acclimation responses to excess light energy, such as state transitions, xanthophyll cycle activity and non-photochemical quenching (NPQ) by carotenoids (Goss & Jakob

2010; Brunet et al., 2011; Kirilovsky 2015), which may remain activated during the subsequent dark acclimation following exposure. Excitation transfer by antenna pigments is often adjustable, and these processes act to redirect the flow of excitation energy away from PSII when the electron transport chain and plastoquinone pool are completely reduced, in an attempt to minimize photodamage (Bouchard et al., 2006; Brunet et al., 2011; Kirilovsky 2015). These photoacclimation responses could result in a reduced fluorescence yield following excitation of accessory pigments at specific wavelengths, causing species that are identified by these accessory pigments to appear more like species without them, namely the chlorophytes. These types of mechanisms acting on acute time scales are likely the same between PAR and UVR exposures, but at higher levels for the latter. This agrees with the spatial distribution of F_v response spectra in the NMDS ordination (Figure 4.5). Photoacclimation to high irradiance (PAR) levels of longer time periods produce changes in relative antenna pigment content, reducing the amounts of accessory pigments relative to Chl *a*, and causing brown and blue taxa to be partially misidentified as green (MacIntyre et al., 2010), however these changes reflect longer response times compared to the acute exposures used here, and did not include UVR wavelengths.

Table 4.6 Interaction probabilities between diode and light treatment for minimum (F_0) and variable (F_v) fluorescence response spectra for each taxon from 2-way ANOVA.

Taxon	F_0	F_v
<i>A. oscillarioides</i>	0.760	0.010
<i>D. lemmermannii</i>	0.000	0.002
<i>M. aeruginosa</i>	0.000	0.000
<i>Synechococcus</i> sp.	0.000	0.000
<i>S. rhodobaktron</i>	0.000	0.003
<i>C. cambricum</i>	0.002	0.001
<i>P. simplex</i>	0.044	0.835
<i>S. obliquus</i>	0.103	0.354
<i>A. formosa</i>	0.625	0.844
<i>F. crotonensis</i>	0.000	0.274
<i>Cryptomonas</i> sp.	0.000	0.000
<i>S. petersenii</i>	0.000	0.000
<i>P. inconspicuum</i>	0.528	0.038

The results of both the ANOVA and NMDS analysis indicate there is the potential for misclassification of F_v signal, and therefore $F_v:F_m$, among algal groups by the Phyto-PAM following acute UVR exposure, though the misclassified fraction would typically not dominate the signal. If the changes in relative diode fluorescence for a given species produce a response spectrum more similar to another (incorrect) group, then $F_v:F_m$ could be misattributed and/or partially attributed to the wrong algal group for nine of the thirteen experimental species. However, while light treatment effects on spectra shape were often significant, the magnitude of the effects were small, in particular when compared to that of taxonomic variability. The extent of misclassification of algal group F_0 and $F_v:F_m$ due to short-duration light exposure should not exceed that observed in the RS scenarios summarized previously.

4.5 Conclusions and recommendations

Observations and recommendations from the present study are consistent with those from other researchers using multi-wavelength fluorometers. Discrete samples and independent taxonomic analyses are necessary to ground-truth algal group estimation by multi-wavelength fluorometers such as Phyto-PAM, Fluoroprobe and AOA, and application of taxon-specific RS often improve parameter estimates (Gaevsky et al., 2005; Jakob et al., 2005; Schmitt-Jansen & Altenburger 2008; Kring et al., 2014; Escoffier et al., 2015; Echenique-Subiabre et al., 2016). Variation in fluorescence excitation spectra for biomass estimation has been assessed in a number of studies, but uncertainty in variable fluorescence excitation spectra for the group-specific estimation of photochemical quantum yield has not. While we examined a number of taxa, more insight could be gained by applying similar methods to include multiple representatives from different taxonomic groups (e.g. cryptophytes, dinoflagellates), and bloom-forming strains that may be of particular interest in certain systems. Our data suggest that users can expect quantification errors for F_0 and $F_v:F_m$ within 10% of true values on average, but which can range to almost 30% of true values. On average, 10% or less of F_0 was attributed to a group not present, while $F_v:F_m$ was assigned incorrectly up to 30% of the time on average. In particular, fluorescence attributed to non-dominant algal groups or those at low Chl *a* concentrations, and associated $F_v:F_m$ estimates, should be interpreted with caution, and independent analysis of community composition is encouraged to verify these estimates (Schmitt-Jansen & Altenburger 2008; Kring et al., 2014; Escoffier et al., 2015). Additionally, replicate measurements are highly recommended, to provide users with certainty in estimates that are highly reproducible, and identify those that may be suspect. With these considerations in mind, researchers can report more

algal group estimates from multi-wavelength fluorescence, along with typical ranges of uncertainty, as part of phytoplankton research studies.

Chapter 5

Quantifying the challenges of taxon- and irradiance-dependent variability for multi-wavelength PAM fluorometry in phytoplankton mixtures

5.1 Summary

Algal group discrimination using multi-wavelength fluorometry is based on chlorophyll *a* (Chl *a*) fluorescence excitation spectra that are group-specific and assumed to be invariant with fluctuating environmental factors such as irradiance. However, appreciable within-group and environmentally-related variation in these spectra generate poorly quantified uncertainty when working with mixed populations typical of most natural communities. Using mixtures of laboratory cultures, a commercially available multi-wavelength PAM fluorometer (Phyto-PAM) was shown to produce group-specific estimates of minimal fluorescence (F_0), a proxy for biomass, that were largely robust even when reference excitation spectra (RS) not specific to the taxa present were applied: 74% and 61% of estimates within 10% of true values across ten binary and two ternary mixtures, respectively. $F_v:F_m$ estimates describing photophysiological health were often within 10% of true values for the dominant taxon in a given mixture, but error levels increased significantly when taxa were present at low levels of relative abundance, with less than 50% of estimates within 10% of true values. Photoacclimative and photoinhibitory responses to PAR and UVR stress affected relative F_0 attributed to different groups, with increased estimates for cyanobacteria and decreased estimates for chromophyte abundance. $F_v:F_m$ estimates were not significantly affected by irradiance exposure, in particular relative to the effects of taxonomic variation in RS. F_0 estimates are generally reliable with a 5 to 10% margin of error, though errors can increase with high light exposure. $F_v:F_m$ estimates show greater uncertainty compared to F_0 and we recommend disregarding estimates for algal groups present at less than 10% relative abundance, and interpreting with caution $F_v:F_m$ estimates for groups present between 10 and 25% relative abundance.

5.2 Introduction

The abundance and taxonomic composition of phytoplankton in a given water body are important for both ecological and water quality monitoring, including early detection and measurement of algal bloom events and assessments of primary productivity. *In vivo* chlorophyll *a* (Chl *a*) fluorescence,

originating primarily from Photosystem II (PSII) in photosynthetic organisms, has become a standard tool for the quantification of Chl *a* as a proxy for phytoplankton biomass. Beyond quantification, changes in the magnitude of PSII fluorescence provide information on the photophysiological state of cells, including photochemical and non-photochemical quenching (NPQ) processes (Schreiber et al., 1986; Maxwell & Johnson 2000). Measurement of Chl *a* fluorescence excitation and/or emission at multiple wavelengths can be used to characterize the taxonomic composition of phytoplankton samples, based on characteristic differences in antenna pigment complexes among major groups (Yentsch & Yentsch 1979; Yentsch & Phinney 1985; Kolbowski & Schreiber 1995; MacIntyre et al., 2010). A variety of portable and bench top fluorometers have been developed using different combinations of measuring chambers, excitation and emission wavelengths, light intensities and durations to measure different parameters from Chl *a* fluorescence. Among these, the Phyto-PAM (Walz GmbH, Effeltrich, Germany) is a bench-top fluorometer that utilizes multi-wavelength excitation to differentiate and measure phytoplankton from three major pigment groups, and applies Pulse Amplitude Modulated (PAM) measures of variable fluorescence to assess the efficiency of light utilization for photosynthesis (Kolbowski & Schreiber 1995).

While multi-wavelength fluorometers are commonly used in oceanographic and limnologic surveys community composition estimates are not frequently reported. This may be due to demonstrated uncertainty in Chl *a* estimates of different pigment groups resulting from intra-group variability in excitation spectra, natural community complexity and differences in abundance, and physiological variation in Chl *a* fluorescence due to nutrient status and light history (Jakob et al., 2005; Aberle et al., 2006; MacIntyre et al., 2010). Multi-wavelength fluorometers discriminate pigment groups based on representative fluorescence excitation spectra, or reference spectra (RS), for each algal group. Species within pigment groups can have different amounts and types of antenna pigments, and the same species can have different RS shape and/or intensity depending on growth stage, light acclimation, or environmental stress conditions (Gregor et al., 2005; Brunet et al., 2011).

Short-term photoprotective responses can alter the transfer of excitation energy from antenna pigments to photosynthetic reaction centers, resulting in fluorescence quenching (Brunet et al., 2011; Papageorgiou & Govindjee 2014). These quenching responses reduce Chl *a* fluorescence intensity, decreasing estimates of Chl *a* biomass and algal abundance. Furthermore, the type and extent of photoprotective responses vary among taxa, with the potential to change both the intensity and shape of fluorescence excitation spectra. Thus, there is considerable scope for quantification and

classification error, and the time and effort required for validation and/or correction of measurements can be significant. Microscopic analysis provides a more detailed assessment of community composition, but the time and expertise required make it impractical for high sample numbers. Independent measures of Chl *a* concentration using standard extraction methods are often completed in parallel. However, a more detailed pigment analysis that provides comparable information on taxonomic composition, such as high performance liquid chromatography (HPLC), is expensive and time consuming. Therefore, there is a growing consensus that spectral fluorescence is a valuable adjunct when measuring phytoplankton communities (Leboulanger et al., 2002; Gregor et al., 2005; Schmitt-Jansen & Altenburger 2008; Seppala & Olli 2008; Kring et al., 2014), but robust evaluations of the accuracy of the measures are needed to validate these data.

Studies employing the submersible multi-wavelength bbe Moldaenke Fluoroprobe (Beutler et al., 2002) have demonstrated its ability to measure Chl *a* for multiple pigment groups (up to four), with varying accuracy in quantification depending on community complexity, abundance levels, environmental conditions, and the specific taxa present (Leboulanger et al., 2002; Gregor et al., 2005; Rolland et al., 2010; Kring et al., 2014; Escoffier et al., 2015). Jakob et al. (2005) assessed the effects of light history and Chl-specific fluorescence on algal group Chl *a* estimation by Phyto-PAM in laboratory cultures and two diatom-dominated rivers. Their results showed strong correlation between extracted and fluorescence-based Chl *a* when species-specific RS with corresponding light history were applied. Schmitt-Jansen and Altenburger (2008) used Phyto-PAM to measure biofilms, comparing algal group estimates to HPLC analysis of taxonomic marker pigments. To the best of our knowledge, while Phyto-PAM is used in comparative studies and on natural communities (Van der Grinten et al., 2004; van der Grinten et al., 2005; McClellan et al., 2008; Zhang et al., 2008; Zhang et al., 2011) there has been no systematic quantification of uncertainties arising from the known departures of real communities from the assumptions of the multi-wavelength discrimination approach.

To address this issue, the present study aimed to provide a quantitative assessment of uncertainty in estimates of minimum fluorescence (F_0), which can be used as a proxy for biomass, and $F_v:F_m$, the quantum yield of photochemistry, which provides information on the photosynthetic efficiency and relative photophysiological status of phytoplankton. Our objectives were to determine the effects on accuracy of F_0 and $F_v:F_m$ estimation by the Phyto-PAM caused by (1) within-group RS variation, (2) low relative pigment-group contribution, and (3) photoprotective and photoinhibitory effects induced

by PAR and UVR exposure, and (4) if these factors make the measurement of some taxa or pigment-groups more error-prone compared to others. When taxa are present in equal abundance and matching RS are applied, instrument error should be minimal and departures from expected values should be at a minimum. We hypothesize the factors manipulated in our experiments: non-matching RS, increasing mixture complexity (binary vs. ternary), varying relative abundance, and photoacclimation responses, may challenge the accuracy of Phyto-PAM group assignment and quantification. Furthermore, the extent of classification errors may be greater in taxonomic groups with large variation in antennae pigments, such as cyanobacteria and chromophytes. The results of this study will provide Phyto-PAM users with measures of certainty in their data, and thus aid in the interpretation and reporting of abundance and variable fluorescence estimates for different pigment groups. They will also indicate thresholds and conditions under which estimates may be unreliable, with the potential to extrapolate to other multi-wavelength fluorometers.

5.3 Methods

5.3.1 Growth conditions and experimental design

Clonal non-axenic microalgal and cyanobacterial cultures (Table D.9) representative of the three algal groups classified by the Phyto-PAM were obtained from the Canadian Phycological Culture Centre (CPCC, University of Waterloo, Waterloo ON) and from Dr. S. Watson at the Canadian Center for Inland Waters (CCIW, Burlington ON), Environment and Climate Change Canada. Batch monocultures were grown in nutrient replete WC (ed) media (modified by S.B. Watson from (Guillard & Lorenzen 1972)), adjusted to pH 8.2-8.4, and incubated at 19 ± 2 °C at an illumination intensity of ca. 48 ± 4 $\mu\text{mol photons}\cdot\text{m}^{-2}\cdot\text{sec}^{-1}$ from cool white fluorescent bulbs on a 16: 8hr light: dark cycle, and mixed manually each day. Though WC media is not a typical media for some taxonomic groups (e.g. cyanobacteria), it was used here to avoid potential confounding factors due to mixing of medias when experimental mixtures were created. Growth was monitored by measurements of Chl *a* fluorescence using Phyto-PAM and experiments were performed on cultures in exponential growth phase.

Two types of experiments were conducted to test our hypotheses: measurements on mixtures with different levels of relative taxon abundance and on mixtures with equal levels of abundance following short-duration light treatments. Just prior to the experiments, cultures were diluted with fresh media to reach manufacturer recommended gain settings for creating new Reference Spectra with Phyto-

PAM, which also avoided short-term shading effects and is more comparable to environmental samples. Binary and ternary mixtures (Table 5.1) were made based on average fluorescence measurements of pure cultures, with mixture volumes calculated based on taxon contribution to total fluorescence signal, i.e. a 50:50 mixture represents one where each taxon contributes 50% of the Chl *a* fluorescence signal. Each pigment group was represented by only one taxon in a given experimental mixture. For objectives 1-3 multiple mixtures were created with taxa at different levels of relative contribution: in binary mixtures 100:0, 90:10, 75:25, 50:50, and vice versa; in ternary mixtures 100:0:0, 80:10:10, 50:25:25, 33:33:33, and vice versa for each taxon/algal group. For the irradiance exposure experiments one mixture with equal fluorescence contribution from each taxon was made: 50:50 (binary) and 33:33:33 (ternary). Extracted Chl *a* concentrations of experimental mixtures ranged from 5.3 to 51.5 µg/L, with average and median concentrations of 22.8 and 22.5 µg/L, respectively.

Table 5.1 Experimental binary (A-J) and ternary (K, L) mixtures of freshwater phytoplankton.

Mixture Code	Blue	Green	Brown
A	<i>Microcystis aeruginosa</i>	<i>Coelastrum cambricum</i>	
B	<i>Microcystis aeruginosa</i>	<i>Pediastrum simplex</i>	
C	<i>Synechococcus rhodobaktron</i>	<i>Pediastrum simplex</i>	
D	<i>Dolichospermum lemmermannii</i>		<i>Asterionella formosa</i>
E	<i>Microcystis aeruginosa</i>		<i>Asterionella formosa</i>
F	<i>Microcystis aeruginosa</i>		<i>Cryptomonas sp.</i>
G	<i>Synechococcus rhodobaktron</i>		<i>Fragilaria crotonensis</i>
H		<i>Coelastrum cambricum</i>	<i>Asterionella formosa</i>
I		<i>Coelastrum cambricum</i>	<i>Cryptomonas sp.</i>
J		<i>Pediastrum simplex</i>	<i>Fragilaria crotonensis</i>
K	<i>Dolichospermum lemmermannii</i>	<i>Pediastrum simplex</i>	<i>Fragilaria crotonensis</i>
L	<i>Microcystis aeruginosa</i>	<i>Coelastrum cambricum</i>	<i>Synura petersennii</i>

Triplicate irradiance exposure experiments were performed in triplicate in a solar simulator with a Xenon arc lamp light source (1 kW, Oriel Instruments, Irvine, C) and optical glass cut-off filters (Schott optical filters) with nominal 50% transmission at 420, 340, and 305 nm to produce three light treatments: PAR only (P), PAR + UVA (PA), and PAR + UVA + UVB (PAB), respectively. The photon flux density (PFD) was monitored throughout experiments to maintain consistent light

intensity using a LI-COR (Q15458) photometer (Li-COR Biosciences, Lincoln, NE) and water temperature was maintained at growth temperatures (19 ± 1 °C) by a controlled water circulation system. Subsamples (50 mL) of the experimental mixtures were transferred to 250 mL Pyrex beakers and placed in the solar simulator. Light treatments were 75 min in duration, with 3 mL subsamples removed from each treatment at four time-points. High intensity PAR and UVR are known to produce photo-responses in phytoplankton. However, the mechanisms and extent of responses may vary among species, potentially affecting estimates of algal group abundance and quantum yield of photochemistry due to changes in excitation spectra and fluorescence intensity.

5.3.2 Chlorophyll fluorescence measurements

All subsamples were dark acclimated at ambient temperature for ca. 30 min prior to fluorescence measurement to allow for relaxation of NPQ processes. Chl *a* fluorescence was measured using a Phyto-PAM fluorometer (S/N: PPAA0220) equipped with a corresponding System II emitter-detector unit (Phyto-ED, S/N EDEF0111, Walz) and Phyto-WIN computer software and interface (Walz 2003). The Phyto-ED unit contains an array of measuring light LEDs (light emitting diodes) with peaks at 470, 520, 645 and 665 nm, which are applied alternating at high frequency, and red actinic lights peaking at 655 nm. Low intensity modulated measuring light (ca. 25 Hz frequency with a width of 12 μ sec) with minimal actinic effect was used to measure F_0 , and a saturating pulse (0.2 sec up to $2600 \mu\text{mol quanta}\cdot\text{m}^{-2}\cdot\text{sec}^{-1}$ at 655 nm) was applied to measure maximum fluorescence (F_m). $F_v:F_m$ is the quantum yield of photochemistry, where variable fluorescence F_v is equal to $(F_m - F_0)$. Background corrections for dissolved fluorescence were made with 0.2 μm filtered culture media.

Phyto-PAM measures emitted Chl *a* fluorescence and returns fluorescence metrics for the four measuring light LEDs and derives fluorescence metrics for three algal pigment groups: blues (cyanobacteria), greens (chlorophytes and related taxa), and browns (diatoms, dinoflagellates, chrysophytes, cryptophytes). Algal group fluorescence parameters are estimated based on the deconvolution of the four diode fluorescence signals using linear un-mixing and a single RS for each algal group. The user can select which algal groups are to be estimated, and the species' RS to be used for those groups. For example, if it is known a sample contains only one species the user can select only the corresponding algal group, using the RS for that species. This forces Phyto-PAM to attribute all measured fluorescence to the correct group, increasing accuracy and reliability of results (Walz, 2003).

Chl *a* fluorescence measures were analyzed using the ‘matching’ RS (i.e. using RS for taxon present in the mixture). Additional RS scenarios (Table D.10) were applied to assess Phyto-PAM discrimination and quantification under conditions more typical of field settings – when the exact species composition of communities may not be known, and creation of new RS may not be feasible. RS combinations were created contingent on culture and instrument availability. Testing all possible RS combinations would be unrealistic, and those selected covered a wide sampling range of potential RS scenarios.

5.3.3 Testing effects of taxon abundance and irradiance exposure on estimates of F_0 and $F_v:F_m$

Phyto-PAM F_0 and $F_v:F_m$ estimates were averaged from replicate (3 or 4) measurements. Estimated algal F_0 proportions at different levels of taxon contribution in mixtures were expressed as percentage of total F_0 signal and compared to true proportions. Estimated $F_v:F_m$ at different levels of taxon contribution were compared to true $F_v:F_m$ ($F_v:F_m$ of pure culture measured with the matching mixture RS) and expressed as percent difference from true values (i.e. $\text{offset} = (\text{estimated} - \text{true}) / \text{true} * 100$). Signed relative differences across mixtures and RS scenarios often balance out, giving smaller means and medians, when in fact the scope for error is larger. Therefore, absolute values were used in summary statistics. The effects of algal group, RS selection and taxon contribution level on absolute offset from true values were compared using analysis of variance (ANOVA, $p < 0.05$) for F_0 and $F_v:F_m$. Log transformation was used to ensure homogeneity of variance.

Acute irradiance exposure treatments were sufficient to cause photoinhibition (reduction in $F_v:F_m$) for the taxa and light intensities used. Post-exposure F_0 were compared to pre-exposure proportions and among algal groups (ANOVA). To assess the combined effects of PAR and UVR exposure and mixtures on $F_v:F_m$ estimation pre-exposure and relative post-exposure $F_v:F_m$ (end-point $F_v:F_m$ normalized to pre-exposure values) from mixture experiments were compared (2-way ANOVA) with results from previously conducted monoculture experiments using the same methodology (Chapter 3). $\Delta F_v:F_m$ was calculated from absolute pre-exposure $F_v:F_m$ (Pre) and post-exposure (P, PA, PAB) relative $F_v:F_m$ values from monoculture and binary/ternary mixture experiments (Table S6 and S7, respectively), and expressed as a percentage of monoculture values. Statistical analyses for both F_0 and $F_v:F_m$ from irradiance exposures were performed on arc-sine transformed data when necessary to ensure normality (MacDonald 2014). Statistical analyses were performed using Systat 10 (Systat

Software, Inc., Chicago, IL) and R version 3.4.2 statistical environment (R Core Team 2017), including the ‘car’ (Fox & Weisberg 2011) and ‘agricolae’ (de Mendiburu 2017) packages.

5.4 Results

Table 5.2 Differences (expressed as percentage) of estimated F_0 proportions from true values in binary mixtures using matching and non-matching Reference Spectra (RS). Different superscript letters (^{A, B}) indicate groups (contribution levels) that are significantly different ($p < 0.05$).

Parameter	True Proportion	Matching RS				Non-matching RS			
		Bl	Gr	Br	All	Bl	Gr	Br	All
Mean (absolute)	0	0.8	3.1	0.0	1.2 ^B	0.1	1.6	1.2	1.0
	10	2.3	6.6	4.0	4.2 ^A	13.7	13.3	6.1	11.0
	25	1.3	5.4	3.7	3.4 ^{AB}	7.3	10.0	7.0	8.1
	50	2.9	3.8	3.6	3.4 ^{AB}	4.7	6.8	7.5	6.4
	75	3.5	3.5	3.2	3.4 ^{AB}	10.7	7.0	8.4	8.6
	90	4.5	3.8	4.1	4.2 ^A	15.9	10.0	7.3	10.9
	100	0.7	0.8	2.1	1.2 ^B	10.5	4.9	4.5	6.5
	Average	2.3 ^B	3.9 ^A	2.9 ^{AB}		9	7.7	6	
Maximum (absolute)	0	3.8	7.3	0.0	7.3	0.2	20.5	8.6	20.5
	10	4.4	10.0	8.3	10.0	19.1	32.6	10.0	32.6
	25	3.1	11.5	6.3	11.5	14.4	24.7	20.3	24.7
	50	5.6	10.8	10.8	10.8	9.8	29.0	29.0	29.0
	75	9.1	6.3	11.5	11.5	24.1	31.4	25.0	31.4
	90	10.0	8.3	10.0	10.0	29.8	35.2	21.2	35.2
	100	4.6	3.8	7.3	7.3	29.1	20.8	15.7	29.1
N		7	6	7	20	19	22	21	62
Percentage of cases within 10% of expected		98.0	95.2	98.0	97.1	67.6	74.0	80.1	74.0

When measuring two taxa at equal levels of abundance using the matching RS the average absolute offsets of F_0 were small for all groups (<4%) (Table 5.2), and relative error in $F_v:F_m$ estimation averaged 7.6% of true values (Table 5.3). These conditions (equal taxon contribution and matching RS) should produce the lowest amount of instrument error in F_0 and $F_v:F_m$ estimation, though some may still occur, providing an upper limit for the contribution of allelopathic effects to errors in group-specific Chl fluorescence estimates. Larger departures from true values under conditions of varying

relative abundance, irradiance exposure, or RS selection can be attributed mainly to instrument error in algal group assignment of fluorescence.

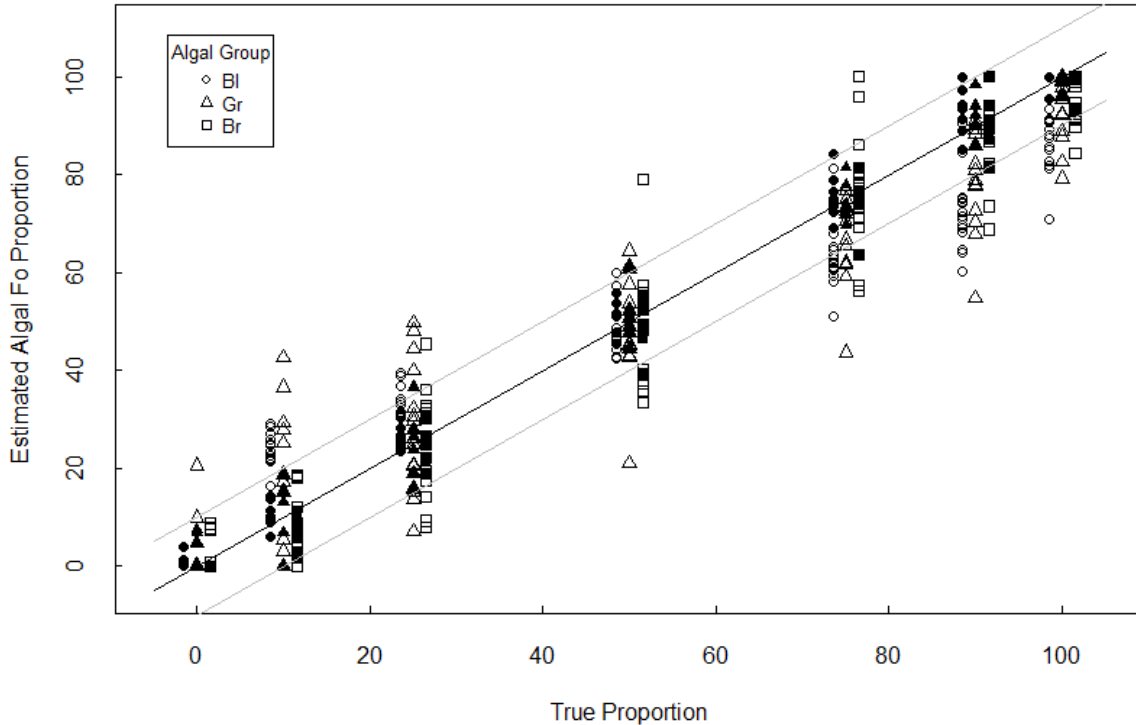


Figure 5.1 Estimated algal F_0 (as percentage of total F_0 signal) compared to true proportions at different contribution levels in binary mixtures. 1:1 line is shown in black, and 1:1 $\pm 10\%$ lines are shown in gray. Solid symbols are matching Reference Spectra (RS) scenarios, open symbols are non-matching RS scenarios.

Algal F_0 estimates in binary mixtures were very close to true proportions across contribution levels when matching RS were used (Figure 5.1), with average offsets $<7\%$ of true values and maximum offsets up to 11.5% (Table 5.2). Indeed, relative algal F_0 was often within 5% of true values (Table D.11) for most taxa examined, and 95-98% of measurements were within 10% of true proportions for all three algal groups (Table 5.2, Figure 5.1). We can measure estimation error at all levels of contribution for F_0 , as Phyto-PAM can assign fluorescence to two (binary) or three (ternary) groups even when presented with a pure culture (100% contribution). While offsets were significantly different between the 0:100 and 10:90 mixtures ($p < 0.05$), the magnitude of difference among taxon

contribution levels was minor. Absolute offsets in F_0 varied among algal groups ($p < 0.05$), with blue F_0 estimates more accurate compared to green and brown estimates. Even the PE-rich *S. rhodobaktron*, with a RS atypical of cyanobacteria, was accurately estimated in mixtures when the correct RS was applied (Table D.11). Classification of algal F_0 remained robust when alternate/non-matching RS scenarios were applied to binary mixture data, though the error range increased (Figure 5.1, Table 5.2). Average F_0 offsets were $< 14\%$ of total signal, with maximal offsets up to 35%. Estimated F_0 proportions were within 10% of true proportions in 68, 74 and 80% of cases for the blue, green and brown group, respectively. All three factors (RS selection, algal group, and contribution level) had significant interaction effects on F_0 estimation accuracy in binary mixtures (Table 5.4).

Table 5.3 Relative differences (expressed as percentage) of Estimated $F_v:F_m$ from True Values in Binary Mixtures using matching and non-matching RS. Different superscript letters (^{A,B}) indicate groups (contribution levels) that are significantly different ($p < 0.05$).

Parameter	True Proportion	Matching RS				Non-matching RS			
		Bl	Gr	Br	All	Bl	Gr	Br	All
Mean (absolute)	10	61.5	42.7	32.6	45.7 ^A	78.6	64.8	49.9	64.0
	25	36.7	21.6	5.6	21.3 ^B	35.7	25.4	14.7	24.9
	50	11.2	4.5	6.7	7.6 ^B	12.3	5.0	11.9	9.6
	75	10.6	2.7	19.9	11.5 ^B	7.2	3.7	19.6	10.2
	90	10.8	2.6	14.4	9.6 ^B	13.1	3.6	15.3	10.5
	100	--	--	--	--	4.0	0.5	17.4	7.3
	Average	26.2 ^A	14.8 ^A	15.8 ^A		29.4	20.5	22.3	
Maximum (absolute)	10	100.0	100.0	65.3	100.0	100.0	100.0	100.0	100.0
	25	100.0	76.8	13.0	100.0	100.0	100.0	100.0	100.0
	50	37.3	8.7	19.1	37.3	100.0	12.6	100.0	100.0
	75	46.2	7.1	100.0	100.0	19.8	8.1	100.0	100.0
	90	47.6	7.3	83.7	83.7	100.0	7.3	100.0	100.0
	100	--	--	--	--	19.3	6.9	100.0	100.0
N	N	7	6	7	20	19	22	21	62
Percentage of cases within 10% of expected		69.0	77.8	69.0	71.7	55.3	74.2	60.3	63.7

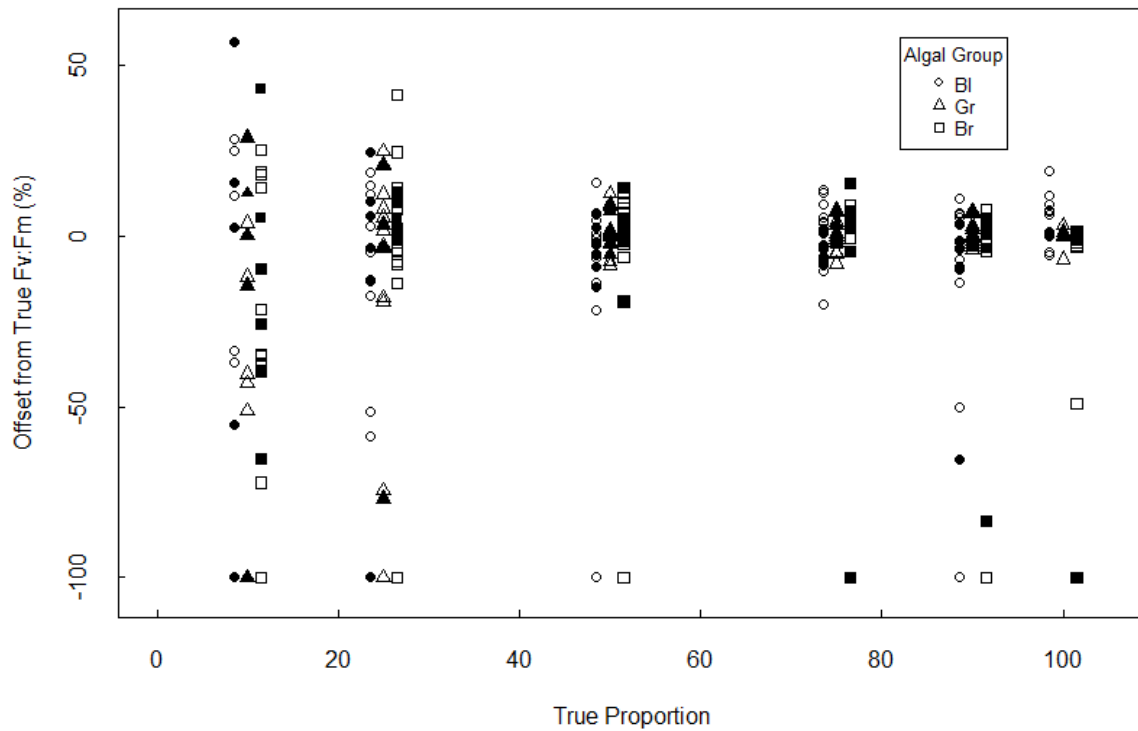


Figure 5.2 Relative offset between observed algal $F_v:F_m$ compared to true $F_v:F_m$ (expressed as percentage of true $F_v:F_m$) in binary mixtures at different contribution levels. Solid symbols are matching RS scenarios; open symbols are non-matching RS scenarios.

Quantification errors were larger for $F_v:F_m$ compared to F_0 (Figure 5.2), with significantly higher offsets from true values at low taxon contribution levels (e.g. 10%, $p < 0.05$), and no significant difference among algal groups (Table 5.3). Another way to view the effect of contribution level on estimating accuracy of $F_v:F_m$ is to compare the frequency of significant errors as contribution level changes, and we see an increasing number of cases where $F_v:F_m$ was significantly different from pure culture as contribution level decreased (Table D.12). $F_v:F_m$ offsets averaged 7.6% of pure culture values at 50% contribution levels but 45.7% at 10% contribution levels, with maximum offsets up to 100% (i.e. no $F_v:F_m$ estimated for a group), even when matching RS were applied (Table 5.3). Maximum offsets were high in particular for the brown group even at high contribution levels, due to incorrect $F_v:F_m$ assignment of *Cryptomonas* sp. in mixture I (Table 5.3, Table D.12). Estimated $F_v:F_m$ were within 10% of expected values in 69% of cases for the blue and brown groups, and 78% of cases

for the green group. Accuracy in $F_v:F_m$ estimates decreased when non-matching RS were applied: offsets ranged from 7.3% of true values in pure cultures (100% contribution level) to 64% at 10% contribution level, with multiple cases where $F_v:F_m$ was not estimated (Table 5.3, Figure 5.2). $F_v:F_m$ estimates were within 10% of true values for 55, 74 and 60% of cases for the blue, green and brown taxa, respectively. Taxon contribution level and the algal group measured had significant interaction effects on the accuracy of $F_v:F_m$ measurements in the binary mixtures examined, but the effects of RS selection were not significant (Table 5.4).

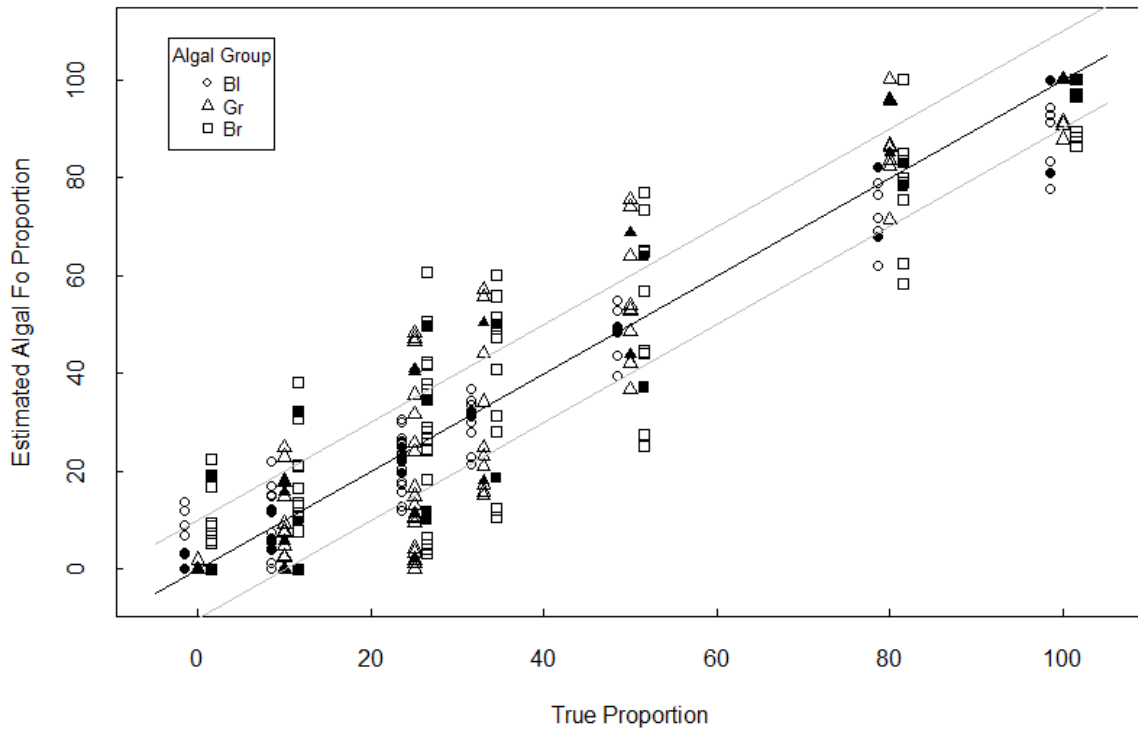


Figure 5.3 Estimated Algal F_0 (as percentage of total F_0 signal) compared to True proportions at different contribution levels in ternary mixtures. 1:1 line is shown in black, and 1:1 $\pm 10\%$ lines are shown in gray. Solid symbols are matching RS scenarios, open symbols are non-matching RS scenarios.

Phyto-PAM continued to correctly discriminate algal group fluorescence when challenged with more complex ternary mixtures, but often with a larger margin of error than in binary mixtures (Figure 5.3, Table 5.5). When the matching RS were used, average offsets from true proportions in F_0 estimates ranged from 1.8% at 0% contribution (i.e. cases when F_0 was estimated for groups not present) to 11.7% (at 25% contribution), and these two contribution levels had F_0 offsets significantly different from each other (Table 5.5). The blue taxa examined had significantly lower F_0 offsets compared to the green and brown taxa ($p < 0.05$). 100% of blue and 75% of brown and green F_0 estimates were within 10% of expected values when matching RS were used. When non-matching RS scenarios were applied the average offsets from true proportions showed a small increase, while the range increased to a larger extent, with maximum offsets as high as 35.6% of total signal. Estimated F_0 proportions in ternary mixtures were within 10% of true proportions 80, 55 and 47.5% for the blue, green and brown groups, respectively (Table 5.5). The algal group of the taxon examined and its relative contribution level had significant interaction effects on F_0 estimates, while the RS selection did not (Table 5.4).

Table 5.4 Main and interaction effects of RS selection (RS), algal group (AG) and taxon contribution level (TC) on estimation errors of F_0 and $F_v:F_m$ in binary and ternary mixtures.

		Binary (N = 574)			Ternary (N = 360)		
		Df	F-statistic	Probability	Df	F-statistic	Probability
F_0	RS (match or mismatch)	1	61.396	0.000	1	2.641	0.105
	Algal Group (AG)	2	4.321	0.014	2	16.057	0.000
	Species Contribution (TC)	6	47.884	0.000	6	33.331	0.000
	RS:AG	2	4.950	0.007	2	0.873	0.419
	RS: TC	6	3.611	0.002	6	0.340	0.915
	AG: TC	12	2.400	0.005	12	6.379	0.000
		Binary (N = 493)			Ternary (N = 282)		
		Df	F-statistic	Probability	Df	F-statistic	Probability
$F_v:F_m$	RS (match or mismatch)	1	0.205	0.651	1	9.353	0.002
	Algal Group (AG)	2	4.619	0.010	2	1.684	0.188
	Species Contribution (TC)	5	56.374	0.000	5	30.681	0.000
	RS:AG	2	1.491	0.226	2	2.256	0.107
	RS: TC	4	0.322	0.863	4	0.416	0.797
	AG: TC	10	2.357	0.010	10	1.100	0.363

Table 5.5 Differences (expressed as percentage) of estimated F_0 proportions from true values in ternary mixtures using matching and non-matching RS. Different superscript letters (^{A,B}) indicate groups (contribution levels) that are significantly different ($p > 0.05$)

Parameter	True Proportion	Matching RS				N / group	Non-matching RS				N / group
		Bl	Gr	Br	All		Bl	Gr	Br	All	
Mean (absolute)	0	0.8	0.0	4.8	1.8 ^B	4	2.6	0.1	6.3	3.0	20
	10	3.9	6.9	10.6	7.1 ^{AB}	4	6.1	8.2	11.4	8.6	20
	25	2.7	16.9	15.5	11.7 ^A	4	5.1	16.2	14.8	12.0	20
	33	1.3	16.1	15.6	11 ^{AB}	2	3.9	14.0	15.6	11.2	10
	50	1.1	12.5	13.4	9 ^{AB}	2	4.1	10.4	16.1	10.2	10
	80	7.1	10.3	2.3	6.6 ^{AB}	2	7.7	11.5	9.8	9.7	10
	100	9.6	0.0	1.5	3.7 ^{AB}	2	10.2	3.0	4.6	6.0	10
	Average	3.8 ^B	9 ^A	9.1 ^A			5.7	9	11.2		
Maximum (absolute)	0	3.0	0.0	19.2	19.2	4	13.7	1.9	22.4	22.4	20
	10	5.7	10.0	22.1	22.1	4	11.8	14.8	28.0	28.0	20
	25	5.4	22.9	24.5	24.5	4	13.2	25.0	35.6	35.6	20
	33	1.8	17.2	16.8	17.2	2	11.7	24.0	27.0	27.0	10
	50	1.6	18.6	13.8	18.6	2	10.6	25.5	26.8	26.8	10
	80	12.1	15.7	2.8	15.7	2	18.0	20.0	21.7	21.7	10
	100	19.2	0.0	3.0	19.2	2	22.4	12.3	13.7	22.4	10
Percentage of cases within 10% of expected		100.0	75.0	75.0	83.3		80.0	55.0	47.5	60.8	

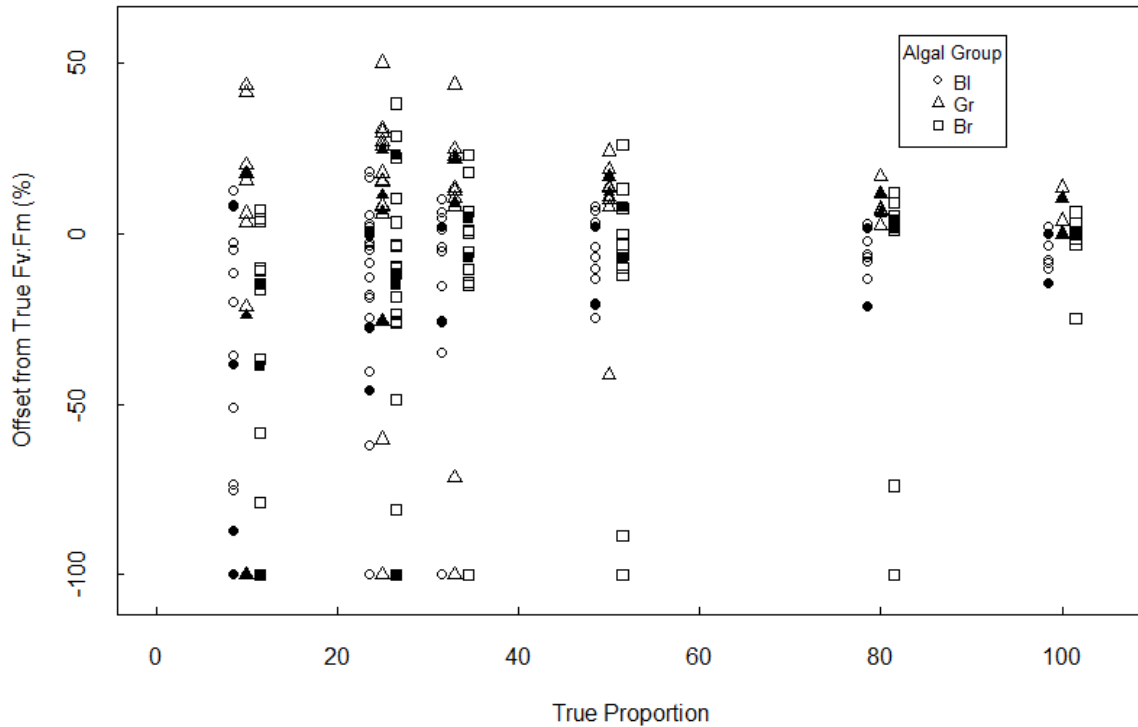


Figure 5.4 Relative offset between observed algal $F_v:F_m$ compared to true $F_v:F_m$ (expressed as percentage of true $F_v:F_m$) in ternary mixtures at different contribution levels. Solid symbols are matching RS scenarios, open symbols are non-matching RS scenarios.

Departures of estimated $F_v:F_m$ from pure culture values displayed similar trends in binary and ternary mixtures when matching RS were used, with significantly higher offsets at low contribution levels (Table 5.6, Figure 5.4), and no significant differences in $F_v:F_m$ error among algal groups. Even with the matching RS, there were cases when $F_v:F_m$ was not estimated for taxa present at 10 and 25% contribution (maximum offsets of 100%). Estimates were within 10% of true values in 57% of cases for the blue and green groups, and 43% of cases for the brown group. Errors increased when non-matching RS were applied, in particular the frequency at which $F_v:F_m$ was not estimated for a group present at 33% or lower relative contribution, for all three algal groups (Table 5.6, Figure 5.4). $F_v:F_m$ estimates with non-matching RS were within 10% of expected values in 44, 24 and 43% of cases for the blue, green and brown groups, respectively. RS scenario and taxon contribution level significantly affected the accuracy of $F_v:F_m$ estimates in ternary mixtures, with no interaction effects (Table 5.4).

Table 5.6 Relative differences (expressed as percentage) of estimated $F_v:F_m$ from true values in ternary mixtures using matching and non-matching RS. Different superscript letters (^{A,B}) indicate groups (contribution levels) that are significantly different ($p < 0.05$).

Parameter	True Proportion	Matching RS				N / group	Non-matching RS				N / group
		Bl	Gr	Br	All		Bl	Gr	Br	All	
Mean (absolute)	10	57.9	34.5	63.4	51.9 ^A	4	64.8	64.3	57.8	62.3	20
	25	13.4	13.7	37.3	21.4 ^{AB}	4	26.2	47.3	28.9	34.1	20
	33	7.5	11.3	5.5	8.1 ^B	2	20.7	32.9	19.4	24.4	10
	50	4.5	9.1	7.0	6.8 ^B	2	10.6	17.1	26.7	18.1	10
	80	4.7	3.7	2.1	3.5 ^B	2	8.6	8.4	20.9	12.6	10
	100	--	--	--	--	2	7.4	4.9	4.2	5.5	10
	Average	17.6 ^A	14.4 ^A	23.1 ^A			26.2	34.0	30.7		
Maximum (absolute)	10	100.0	100.0	100.0	100.0	4	100.0	100.0	100.0	100.0	20
	25	36.9	25.6	100.0	100.0	4	100.0	100.0	100.0	100.0	20
	33	13.0	21.4	7.2	21.4	2	100.0	100.0	100.0	100.0	10
	50	6.7	12.0	7.1	12.0	2	24.5	41.4	100.0	100.0	10
	80	7.6	6.0	3.0	7.6	2	21.1	16.8	100.0	100.0	10
	100	--	--	--	--	2	14.7	13.7	25.0	25.0	10
Percentage of cases within 10% of expected		57.1	57.1	42.9	52.4	42	43.8	23.8	42.5	36.7	240

Table 5.7 Relative offset in F_0 estimates (compared to pre-exposure proportions) following acute irradiance exposure (P – PAR only, PA – PAR + UVA, PAB – PAR + UVA + UVB) in mixtures. Mixture codes and taxa correspond to experimental mixtures in Table 5.1. Symbols indicate (γ) significant light treatment effects (1-way ANOVA, $p < 0.05$), and (β) light treatments producing algal proportions significantly different from pre-exposure values (Tukey HSD, $p < 0.05$). Taxon 1 of each mixture is shown, taxon 2 offsets are complementary.

Mixture Code	Taxon/ Taxa	Relative F_0 offset		
		P	PA	PAB
A	<i>MaCc</i>	14.2	13.3	14.3
B	<i>MaPs</i> γ	1.1	-2.1	-2.7
C	<i>SrPs</i> γ	8 β	12.9 β	15.6 β
D	<i>DIAf</i> γ	30.2 β	28.4 β	30.8 β
E	<i>MaAf</i> γ	26.4 β	27.7 β	31.2 β
F	<i>MaCsp</i> γ	11.4 β	13.4 β	13.6 β
G	<i>SrFc</i> γ	9.1 β	17.8 β	16.2 β
H	<i>CcAf</i> γ	2.2	4.4 β	4.9 β
I	<i>CcCsp</i> γ	32.1 β	21.8 β	24.1 β
J	<i>PsFc</i>	-1.2	1.2	3.8
K	<i>Dl</i> γ	7.6 β	6.9 β	5.2
	<i>Ps</i> γ	-12.6 β	-11.8 β	-10
	<i>Fc</i> γ	5	4.9	4.8
L	<i>Ma</i>	2.2	3.3	6.3
	<i>Cc</i>	4.1	3.7	3.2
	<i>Sp</i>	-6.3	-7	-9.5

Short term irradiance exposure caused a significant change in relative F_0 attributed to each algal group in eight of the ten binary mixtures and one of the two ternary mixtures (1-way ANOVA, $p < 0.05$) (Table 5.7). F_0 offsets from pre-exposure proportions ranged from 1.1 to 32.1% of total F_0 signal. In the majority of cases all three spectral treatments (P, PA, and PAB) had significantly different estimated F_0 proportions compared to pre-exposure values, and while there was some difference between post-exposure treatments, these were generally small compared to the differences from pre-exposure values. Change in F_0 following light exposure varied among algal groups (2-way ANOVA, $p < 0.05$), with no interaction from the spectral treatments (Table 5.8). Post-exposure F_0 offsets differed among all three algal groups in binary mixtures, and among the blue and brown groups in ternary mixtures. The changes in estimated F_0 proportions resulted from changes in

fluorescence intensity attributed to each group. In the binary mixtures, estimated blue F_0 increased with PAR and UVR exposure by 14-17% on average, while estimated brown F_0 decreased by 16-18% (Table 5.8). Estimated green F_0 following light exposure increased in some cases and decreased in others, producing a small average change, though absolute changes indicate the scope for error was as high as 9-10% of the total F_0 signal. In ternary mixtures, post-exposure blue F_0 increased on average, while green and brown F_0 tended to decrease relative to pre-exposure proportions.

All phytoplankton taxa demonstrated photoinhibition due to the high intensity PAR and UVR treatments, with observed post-exposure $F_v:F_m$ reduced from pre-exposure values and the largest decreases resulting from the full spectrum (PAB) treatment. High light exposure and measurement in mixtures significantly affected post-exposure $F_v:F_m$ estimates for 14 of 20 taxa in binary mixtures (Table 5.9) and 4 of 6 taxa in ternary mixtures (Table 5.10). The magnitude of difference in binary mixtures was <7% of pure culture $F_v:F_m$ values, but was much larger in $F_v:F_m$ estimates from ternary mixtures, ranging as high as -76.4% of pure culture observed $F_v:F_m$.

Table 5.8 Signed and absolute average change in post-exposure F_0 proportions compared to pre-exposure values for each algal group in binary and ternary mixtures. Different superscript letters (^{A,B,C}) indicate algal groups that are significantly different ($p < 0.05$).

	Algal Group	ΔF_0			Absolute ΔF_0		
		P	PA	PAB	P	PA	PAB
Binary	Bl ^A	14.3	15.9	17.0	14.3	16.5	17.8
	Gr ^B	1.6	0.5	0.8	9.8	9.3	10.8
	Br ^C	-15.7	-16.4	-17.7	16.1	16.4	17.7
Ternary	Bl ^A	4.9	5.1	5.8	4.9	8.4	5.7
	Gr ^{AB}	-4.3	-4.1	-3.4	5.1	7.8	6.0
	Br ^B	-0.7	-1.1	-2.4	5.8	6.6	7.2

Table 5.9 Relative difference in observed $F_v:F_m$ between monoculture and binary mixture (expressed as percentage of monoculture values) following irradiance exposures, with interaction effect (IE) p-values for suspension type and light treatment (2-way ANOVA).

Mixture Code	Taxon	Taxon 1				IE p-value	Taxon 2				IE p-value
		Pre	P	PA	PAB		Pre	P	PA	PAB	
A	<i>MaCc</i>	-1.1	-0.7	-1.9	-4.1	0.000	-0.2	-0.4	0.1	0.4	0.045
B	<i>MaPs</i>	0	0.1	0.6	0	0.427	-0.1	0	-0.5	-0.6	0.189
C	<i>SrPs</i>	-1.2	0	7.2	6.3	0.107	0.8	0	0	-0.8	0.000
D	<i>DIAf</i>	-1.5	-0.4	0.1	-0.9	0.533	0.4	1.8	0.9	0.8	0.047
E	<i>MaAf</i>	-3.4	0.3	0.1	-0.9	0.000	0.7	2.4	3.1	3.4	0.001
F	<i>MaCsp</i>	0.2	-4	-3.5	-3.6	0.000	0	-0.5	-0.9	-0.2	0.001
G	<i>SrFc</i>	-0.8	4.7	5	12	0.000	0	-0.3	-0.9	-1	0.153
H	<i>CcAf</i>	-0.5	-1	-0.8	-1	0.002	1.5	1	1.8	0.2	0.204
I	<i>CcCsp</i>	1.3	-1.9	-1.3	-1.8	0.000	-3.3	4.3	1.8	2.2	0.001
J	<i>PsFc</i>	0.4	-0.1	-0.5	-1	0.000	-0.2	-0.8	-0.9	-0.5	0.023

Table 5.10 Relative difference in observed $F_v:F_m$ between monoculture and ternary mixture (expressed as percentage of monoculture values) following irradiance exposures, with interaction effect (IE) p-values for suspension type and light treatment.

Taxa	Algal Group	Pre	P	PA	PAB	IE p-value
<i>D.lemm</i> /	Bl	18.7	-1.6	-35.7	-9.5	0.004
<i>P.simp</i> /	Gr	22.5	20.4	28.0	36.1	0.000
<i>F.croto</i>	Br	-17.7	-3.4	-13.4	-18.6	0.508
<i>M.aeru</i> /	Bl	-13.5	-13.3	-42.3	-76.4	0.001
<i>C.camb</i> /	Gr	-2.4	-8.0	-2.1	-2.9	0.000
<i>S.peter</i>	Br	-5.1	-16.4	-2.5	-41.0	0.860

5.5 Discussion

Our purpose was to investigate instrument-based sources of uncertainty in group-specific estimates of F_0 and $F_v:F_m$ using the Phyto-PAM, but we also recognize that mixing taxa together can result in physiological changes, such as effects of allelopathy. Allelopathy can include direct and indirect biochemical interactions, producing stimulatory or inhibitory effects from secondary metabolites produced by an organism (Legrand et al., 2003), in this case algae. The magnitude of measured offsets in F_0 and $F_v:F_m$ in equal part binary mixtures and using matching RS (derived from the same taxa) provides a reasonable estimate for the maximum extent of allelopathic effects on the chlorophyll fluorescence estimates. Under these conditions, where instrument variability should have been minimal, F_0 offsets averaged 3.4% of total signal, and $F_v:F_m$ offsets averaged 7.6% of true values. Comparisons of algal $F_v:F_m$ in pure culture and equal part mixtures prior to irradiance exposure experiments yielded similar results, with an average absolute offset of 7.3%. We cannot determine to what extent these differences are due to allelopathic effects among phytoplankton taxa, differences in fluorescence signal assignment by the Phyto-PAM, or both. Studies have demonstrated allelopathic effects in a variety of phytoplankton, which are species and even strain specific (Legrand et al., 2003; Barreiro & Vasconcelos 2014). Identifying allelopathic effects on growth and photosynthetic parameters with certainty is challenging, and algal sensitivity varies with exposure time and the parameters and methods used (Hilt et al., 2012; Wang et al., 2016). We must consider allelopathic effects as a potential contributor to the measured changes in Chl *a* fluorescence estimates, but the larger departures from true values discussed subsequently can be more confidently attributed to instrument error resulting from relative abundance, irradiance exposure, or RS selection.

Phyto-PAM estimates of pigment-group abundance based on relative algal F_0 were robust in the ten binary mixtures examined, in particular when matching RS were applied, with more than 95% of cases within 10% of expected values. As might be expected with increasing sample complexity, the average estimation accuracy of algal F_0 decreased when a third taxon was added to the mixtures, with 83% of cases within 10% of expected. Both taxon contribution level and algal group significantly affected offsets from true proportions, however the magnitude of offsets among the groups was small. There were cases where algal F_0 was not estimated for a group that was present, typically when this group was at low relative contribution, which was observed by Kring et al. (2014) for species at low abundance in mixtures measured using Fluoroprobe.

Our results show similar margins of variation to comparisons of group-specific Chl *a* concentration measured using Phyto-PAM (Jakob et al., 2005) and Fluoroprobe (Kring et al., 2014; Escoffier et al., 2015). Phyto-PAM Chl *a* estimates of freshwater microalgal cultures using species-specific RS had maximum differences from extracted Chl *a* concentrations of 5% (Jakob et al., 2005). Total and group-specific Chl *a* estimates measured using Fluoroprobe were within 12 and 13% of expected values, respectively, in mixture experiments by Escoffier et al. (2015), and Kring et al. (2014) found that algal group Chl *a* was correctly classified in 90% of cases, although the range of error could be very large. These and other studies (Leboulanger et al., 2002; Schmitt-Jansen & Altenburger 2008; Houliez et al., 2012) note the importance and improved fluorescence-estimation accuracy of species-specific RS. The same was observed in the present study, as application of alternate RS scenarios produced larger average and maximum offsets in F_0 estimation.

One taxon assessed that presented a problem for the Phyto-PAM, and could be indicative of potential challenges when measuring natural communities, was *Cryptomonas*. In the binary mixture with a cyanobacterium (*M. aeruginosa*) F_0 estimates for both groups were close to true values. However, in the binary mixture with a chlorophyte (*C. cambricum*) algal F_0 estimates showed large offsets from true proportions, though the majority of F_0 was still attributed to the correct group. Of the nine taxa presented to the instrument in different combinations, *Cryptomonas* sp. was the only taxon where the majority of $F_v:F_m$ estimates were attributed to an incorrect group, with no values assigned to the correct group, when the correct RS was applied. *Cryptomonas* sp. F_0 and F_v RS had very different shapes with different normalizing diodes, such that the F_0 RS was more typical of brown taxa (normalized to 520 nm diode), while the F_v RS was more similar to green taxa (normalized to 665 nm). For the other cultures examined F_0 and F_v RS had a consistent shape, with only small changes in relative fluorescence at each diode. Estimation errors in F_0 and $F_v:F_m$ likely resulted from differences in RS shape of *Cryptomonas* sp., that made it more similar to the shape of green spectra. Examination of F_0 and F_v spectra for cases with dramatic changes in shape may indicate RS that should not be used for variable fluorescence discrimination.

We applied a large number of alternative RS scenarios to examine the scope for classification and quantification errors when measuring natural communities, where the use of matching RS may not be practical. Across a range of taxa and contribution levels, algal group F_0 was often reliable and reasonably close to expected values, but the potential range of error was also large, with under- or over-estimations as large as 35% of the total F_0 signal. Additionally, there is the potential for Phyto-

PAM, and other multi-wavelength fluorometers, to assign fluorescence signal for group(s) not present, which occurred in 30% of cases for F_0 . While very low proportions of fluorescence attributed to an absent group are not critical (for example less than 10%), depending on the application, higher amounts become more problematic. Without independent analysis, users cannot know with certainty if a given group is present or not, and at low relative abundance even a method such as microscopic identification of taxa is not always reliable (Vuorio et al., 2007). In 7-10% of cases examined in our study, the Phyto-PAM assigned more than 10% of the total F_0 signal to a group that was not present. These situations present challenges for early detection of bloom-forming taxa for example, or for monitoring of spatio-temporal changes in relative group abundance, both of which are desirable applications for multi-wavelength fluorometry.

The Phyto-PAM assigned variable fluorescence and estimated $F_v:F_m$ for the correct algal group(s) in the majority of cases in both binary and ternary mixtures. However, the accuracy of these estimates showed considerable variation, with taxon contribution level significantly affecting $F_v:F_m$ offset from true values. At lower levels of relative abundance, such as 10% and 25% taxon contribution, estimates were often significantly different from true values. $F_v:F_m$ varied by as much as 40% from true values, or was not estimated at all in a few cases, even when matching RS were applied. The inability of Phyto-PAM to accurately estimate algal $F_v:F_m$ at lower abundance is supported by other studies using spectrofluorometers, that have noted larger margins of error in fluorescence estimates when a given pigment group is present at relatively low abundance (Gaevsky et al., 2005; Seppala & Olli 2008; Kring et al., 2014; Escoffier et al., 2015). However, to the best of our knowledge, the present study represents the first in-depth evaluation of group-specific $F_v:F_m$ estimation using multi-wavelength fluorometry.

As with F_0 , algal $F_v:F_m$ was also estimated for algal groups not presented to the instrument. In some cases, these values were uncharacteristically high, such that a user could identify that a potential misclassification of F_v signal may have occurred. In other cases, the $F_v:F_m$ estimates were realistic values, either typical of healthy cells or those under stress with a reduced quantum yield, making them much more challenging for a user to detect as incorrect. Failure of the Phyto-PAM to measure the presence (F_0) and/or variable fluorescence ($F_v:F_m$) of a pigment group that is present, or estimation for an algal group not present (i.e. false positives and negatives), are both of particular concern, and can be particularly misleading when describing the composition and/or photosynthetic activity of a phytoplankton community.

High intensity PAR and UVR exposure are known to cause photoinhibition, manifested as a decrease in $F_v:F_m$ (Cullen & Neale 1997; Bouchard et al., 2005; Murata et al., 2007), and this was seen for the phytoplankton taxa examined. Changes in $F_v:F_m$ due to high light conditions can result from processes that reduce F_m , increase F_0 , or both (Murata et al., 2007), and irradiance effects have the potential to change both the shape and intensity of phytoplankton excitation spectra. There were significant changes in algal F_0 and in the relative proportions of F_0 attributed to each algal group between pre-exposure and post-exposure measurements. This was more apparent in binary compared to ternary mixtures, in part because of the respective taxon proportions, and perhaps due to the lower number of ternary combinations assessed. Estimated algal F_0 proportions following PAR and UVR exposure changed from pre-exposure values by 9 to 18% in binary and 4 to 8% in ternary mixtures on average. The offsets from pre-exposure estimates varied among algal groups, but were not significantly different among the three spectral treatments. High light exposure and photoinhibition affect chlorophyll-specific fluorescence (Kiefer 1973; Jakob et al., 2005; Falkowski & Raven 2007), and these effects can vary among taxa (MacIntyre et al., 2010; Escoffier et al., 2015), creating the potential for opposing changes in fluorescence intensity in different pigment groups.

Estimated post-exposure blue F_0 proportions were consistently higher compared to pre-exposure values in both binary and ternary mixtures. Post-exposure brown F_0 proportions were consistently lower in binary and variable in ternary mixtures, while green F_0 proportions showed smaller increases or decreases in different mixtures. Increases in blue F_0 following high light treatments may be caused by photoprotective mechanisms of cyanobacteria, including decoupling of phycobilisomes (PBS) from PSII, state transitions and orange carotenoid protein NPQ (Kirilovsky 2015; Acuna et al., 2016). This decoupling can increase the amount of uncoupled PBS fluorescence contributing to F_0 , which would be maximal at the same LED excitation wavelength (645 nm and 665 nm) as Chl *a* fluorescence due to PBS absorption when the antennae are linked to the reaction centers, increasing estimated blue F_0 (Campbell et al., 1998). Alternatively, cyanobacterial taxa tended to show the highest susceptibility to photoinhibition, and the increased blue F_0 estimates may be due to increased F_0 intensity due to photodamage of PSII reaction centers. Photoprotective mechanisms in brown taxa, particularly diatoms, involve highly effective NPQ via xanthophyll (diadinoxanthin-diatoxanthin) cycling, which reduces the excitation energy transferred from antenna pigments to the reaction centers (Goss & Jakob 2010). The xanthophyll pigments remove excess excitation energy via thermal decay, and do not produce any non-PSII fluorescence emission contributing to F_0 . Therefore, Chl *a* fluorescence excited by the 520 nm LED would decrease, as well as overall fluorescence emission

from brown algal cells due to effective NPQ, reducing brown F_0 contribution. Photoprotection in chlorophyte taxa is typically via state transitions and NPQ via the xanthophyll (violaxanthin-antheraxanthin-zeaxanthin) cycle (Brunet et al., 2011; Papageorgiou & Govindjee 2014). However, because the major antenna pigments in chlorophytes are Chl *a* and *b*, with similar excitation spectra to the reaction center pigments, decreased excitation transfer from antenna pigments in response to high light does not change the wavelengths that excite the highest fluorescence. Therefore, the relative contributions estimated for green F_0 may show minimal variations, with changes in fluorescence intensity due to photophysiological changes. These results clearly demonstrate the potential for the immediate light conditions at the time of sampling or measurement, such as near-surface exposure under high light conditions, to alter the apparent contributions of different algal groups to total fluorescence, and thus group-specific Chl *a* estimates.

All taxa exhibited reduced post-exposure $F_v:F_m$, with the largest reductions resulting from the full spectrum treatment (PAB), followed by treatments PA, and P, respectively, consistent with expected responses (Heraud & Beardall 2000; Murata et al., 2007; Harrison & Smith 2011a). The differences in sensitivity of $F_v:F_m$ to the experimental light treatments between monocultures and ternary mixtures were large, with post-exposure observed $F_v:F_m$ varying as much as 76% from monoculture values. However, the differences between binary and monoculture $F_v:F_m$ responses were quite small, not more than 7% and typically less than 5%, similar to $F_v:F_m$ offsets observed independent of irradiance exposure. The significant interaction effects seen between light treatment and suspension type for a number of taxa, and the larger magnitude in variation in ternary compared to binary mixtures, suggest the accuracy of algal $F_v:F_m$ estimates is affected (reduced) when measured in mixed assemblages, consistent with our results from measurements on different levels of relative taxon abundance.

The aim of the present study was to provide widely applicable ranges of certainty for group-specific fluorescence parameters from multi-wavelength fluorometry, specifically Phyto-PAM. Our data indicate that pigment-group estimates of fluorescence derived from Phyto-PAM or similar multi-wavelength fluorometers generally allow robust estimates of F_0 , with a 5 to 10% margin of error in abundance estimates, which is consistent across a range of relative taxonomic contribution levels. We recommend, however, that estimates of F_0 for algal groups present at 10% or less of the relative abundance are interpreted with caution, and should be validated via independent analysis. In contrast, estimates of $F_v:F_m$ for algal groups are much more uncertain: those for taxa present at 10% relative

abundance should be disregarded, even if the presence of the respective group has been confirmed by alternate analysis, due to the high variability and scope for error. Estimates for groups present at 10 to 25% relative abundance should be interpreted with caution, in particular for variable fluorescence. In fact, we would recommend when measuring mixed samples/communities only $F_v:F_m$ estimates for a group comprising 50% or more of a sample are reported, although these may still have a large margin of error. Additionally, the Chl *a* concentrations used here are typical of meso- to eutrophic systems, and the uncertainty in fluorescence estimates observed at low relative contribution here may be greater when examining low Chl *a* samples or oligotrophic systems.

The need for independent characterization of phytoplankton taxa present in different samples remains (Schmitt-Jansen & Altenburger 2008; Seppala & Olli 2008; Rolland et al., 2010; Escoffier et al., 2015), and can be valuable in selecting species-specific RS that can be applied to raw fluorescence data post-measurement. Application of matching RS whenever possible will usually increase the reliability of group-specific estimates (Jakob et al., 2005; Schmitt-Jansen & Altenburger 2008; Houliez et al., 2012; Kring et al., 2014). However, RS are instrument-specific, such that libraries of species-specific RS must be independently developed in most cases – a considerable obstacle for the use of multi-wavelength fluorometers. Users should be aware of species with fluorescence excitation spectra atypical of a given pigment group, as their measurement or application as RS can produce incorrect and misleading results. We did not examine the scope of error resulting from mixtures of different taxa from the same pigment group, however we expect the range of uncertainty in these cases would not be greater than observed with the application of non-matching RS to a single taxon. Replicate sample measurements are extremely valuable for identifying questionable algal group estimates, as sample reproducibility is high under most conditions and cases of inconsistent classification can indicate non-reliable measurements where Phyto-PAM discrimination is challenged. The value of multi-wavelength fluorescence is not diminished by the inherent challenges and multiple sources of variability in pigment-group identification, as evidenced by the range of instruments available and the many research programs utilizing them, and we hope the presented results allow increased reporting and group-specific estimates from multi-wavelength fluorescence surveys.

Chapter 6

Conclusions and future outlook

The effects of climate warming on phytoplankton have been, and remain, an area of concern for scientific researchers and environmental managers, with numerous interacting factors to be considered. In freshwater systems cyanobacterial blooms are a continuing challenge, anticipated to increase with climate warming effects and anthropogenic nutrient inputs, and high PAR and UVR tolerance are often described as a contributing factor enabling surface bloom formation. The first focus of this thesis was a comparative analysis of irradiance stress responses among freshwater phytoplankton pigment groups, measured using the quantum yield of photochemistry ($F_v:F_m$) by the multi-wavelength pulse amplitude modulated fluorometer Phyto-PAM.

Photoinhibition, measured as decreases in $F_v:F_m$, resulted from acute exposure to UVR in the natural assemblages of Hamilton Harbour (Table 2.3, Figure 2.1) and algal monocultures (Table 3.3 Figure 3.2). Relative pigment-group sensitivity to light stress was consistent between field and laboratory phytoplankton, with the blue group showing larger decreases in $F_v:F_m$ compared to the green and brown groups. This result contradicted our hypothesis that cyanobacteria would be more resistant to sunlight stress compared to other taxa – an interesting outcome that was strengthened by the consistent result from natural communities and laboratory cultures. This suggests that the high UVR sensitivity of the cultures was not an artefact of culture growth conditions, or of being in culture for extended periods of time. It also suggests that natural cyanobacteria populations with previous exposure, and potential photoacclimation, to natural sunlight are still susceptible to photoinhibition.

Damage rates estimated from the Kok model of photoinhibition were predictive of end-point levels of photoinhibition from the acute irradiance exposures examined here (Figure 2.3, Figure 3.5), with the highest damage rates estimated for the cyanobacteria-dominated communities and cultures, while their repair rates were similar to eukaryotic taxa. The variety of response mechanisms (repair, photoacclimation, photoprotection) to irradiance stress employed by different phytoplankton can act on a range of time scales (minutes, hours, days) (Papageorgiou & Govindjee 2014). Repair rates may be more predictive of sunlight tolerance over longer time periods, and a number of phytoplankton taxa may rely upon recovery processes occurring after damaging light exposure to repair damaged cellular components.

Maximum fluorescence (F_m) decreased with irradiance exposure for the majority of culture taxa examined, indicative of NPQ processes. However, the dynamics of minimum (F_0) fluorescence and F_m generally were not predictive of the relative end-point $F_v:F_m$ among taxa. F_0 and F_m responses to light stress have been described for a small number of taxa (Herrmann et al., 1996; Xiong et al., 1999; Fouqueray et al., 2007) with similar results to those observed here: decreases in F_m indicating NPQ following light exposure, but variable F_0 responses. Based on my results, I did not find the F_0 and F_m dynamics helpful in assessing the relative contributions of reaction center damage and NPQ mechanisms to observed cumulative inhibition, and would not recommend them for future focus.

Despite our results demonstrating high sensitivity to photoinhibition in cyanobacteria, they must be able to tolerate, if not thrive, under high sunlight conditions in order to form and persist as surface blooms, and this tolerance is not facilitated by maintaining high levels of Photosystem II (PSII) efficiency under light exposure. There are a number of photoacclimative and photoprotective responses employed by cyanobacteria to tolerate high light, including production of sunscreen/UVR-absorbing compounds, photoprotective carotenoids, colony formation, mucilage production, vertical migration, protein repair, and antioxidant molecules/enzymes (Wulff et al., 2007; Wu et al., 2011; Paerl & Paul 2012; Fragoso et al., 2014; Roshan et al., 2015). However, there are also observations supporting sunlight sensitivity of cyanobacteria (Kulk et al., 2011; Neale et al., 2014) and their adaptation to low light environments (Schwaderer et al., 2011; Carey et al., 2012; Xiao et al., 2017). The experiments conducted in this thesis measure the acute response of variable fluorescence to high PAR and UVR exposure; responses to longer exposures, or exposures followed by recovery periods in darkness or low light were not examined – but have been elsewhere (Hader et al., 2000; Sobrino et al., 2005; Harrison & Smith 2011b; Qin et al., 2015), and may yield a different outcome with respect to comparative light tolerance among groups. Furthermore, photoinhibition can also be considered a form of PSII down-regulation: an active regulatory process involving reversible inactivation of PSII (Hader et al., 2000; Bouchard et al., 2006; Lohscheider et al., 2011). This causes a reduction in the population of functional reaction centers, but not necessarily a decrease in the light saturated rates of photosynthesis. As the number of functional PSII reaction centers decreases, the rate of reduction and electron transport in the remaining reaction centers can increase to compensate (Falkowski & Raven 2007). Parallel measurements showed decreases in both variable fluorescence and ^{14}C uptake following UVR exposure (Table 2.6), demonstrating inhibition of both photochemistry and photosynthesis, but perhaps not to the same extent. The natural community samples used in these comparisons (^{14}C and $F_v:F_m$) contained taxa from all three pigment groups, with the largest

contributions from the brown group (Table 2.2). Additional experiments measuring variable fluorescence and carbon uptake on high density cyanobacterial blooms would have been very interesting. Future work could examine the carbon incorporation and variable fluorescence responses of different phytoplankton cultures to similar irradiance exposure experiments to those conducted here, to test if the relationship between photoinhibition measured by variable fluorescence vs. carbon incorporation is consistent among taxa and pigment/taxonomic groups.

What processes or mechanisms enable cyanobacteria to thrive under high light conditions near the surface, despite the apparent sensitivity of PSII to photoinhibition? Are they more efficient at certain photoprotective or recovery mechanisms compared to other taxa, that were not captured in the present experiments? Or are they in fact highly sensitive to photoinhibition, as observed here, but are such strong competitors in other ways (for example, nutrient uptake and luxury storage, carbon concentrating mechanisms, buoyancy control and shading of co-occurring taxa) that they maintain the ability to dominate the phytoplankton under conditions supporting bloom-formation? These questions offer future directions for research. Subsequent work could measure different parameters (variable fluorescence metrics including $F_v:F_m$ and NPQ, growth rate, colony size, carbon assimilation, nutrient content) to compare irradiance sensitivity, photoacclimation, photosynthetic rate, etc. during the stages of bloom development and/or on samples of algal blooms from different freshwater systems, determining the importance of different processes/mechanisms under different conditions and for different taxa. In addition, the activity and relative importance of different sunlight responses over longer time periods could be compared among and within taxonomic groups. Experiments could target the extent of vertical migration of cyanobacteria relative to other motile and non-motile eukaryotic phytoplankton in response to light stress, and how this affects sensitivity to UVR. Multi-wavelength and variable fluorescence instruments could be particularly informative in targeting some of these sampling and experimentation efforts. However, use of multi-wavelength fluorescence for the early detection of bloom formation requires further work and most likely should involve alternative measurement techniques, given our estimates of the uncertainty around Phyto-PAM-based estimates for groups present at low relative abundance.

The ability for fast and simple measurements of phytoplankton abundance, composition and photophysiology is an extremely valuable tool enabled by chlorophyll fluorescence technology, and which has become commonly used in aquatic research. Nevertheless, variability in fluorescence signals due to taxonomic and environmental factors produce uncertainty in parameter estimates,

which present a continuing challenge for the use and reporting of fluorometric data. The second focus of this thesis was an assessment of the potential variability of pigment-group discrimination and quantification by the Phyto-PAM fluorometer. This included several aspects: estimation accuracy for natural communities; taxonomic and light history variations in minimum (F_0) and variable (F_v) fluorescence excitation spectra (FES), also termed Reference spectra (RS); estimation errors in F_0 and $F_v:F_m$ for uni-algal cultures under different RS scenarios; and estimation errors for binary and ternary mixtures at different levels of relative contribution and following acute light exposures.

Acute UVR exposure did not have large effects on the shape of the Phyto-PAM 4-point FES (Figure 4.4, Figure 4.5), indicating that group classification should not be affected by short-term light exposure. Acute exposures did, however, affect the relative intensity of FES, altering quantification accuracy following high light exposure, with increased estimates of abundance for the blue group and decreased estimates for the brown group (Table 5.8), consistent with the respective effects of NPQ in these groups. The intensity of chlorophyll fluorescence is known to change with light history, both due to light exposure directly before sample measurement, and growth intensity, and the potential effects on pigment-group quantification using chlorophyll fluorescence have been demonstrated (Jakob et al., 2005; MacIntyre et al., 2010; Chekalyuk & Hafez 2011; Escoffier et al., 2015). Taxonomic variation in RS was greater compared to light history effects, in particular for the variable fluorescence (F_v) RS, such that F_v could be partially misclassified among pigment groups. F_0 and $F_v:F_m$ estimates were within 10% of true values on average when a variety of different RS combinations were applied to algal monocultures (Table 4.3) – providing a baseline for potential errors in group assignment for natural communities, when using species-specific RS is often not practical.

Errors in pigment-group quantification due to light history can be minimized with sufficient dark- or low-adaptation of samples prior to measurement. On the other hand, measurements of photophysiological parameters indicative of the current state of light acclimation and electron transport require rapid measurements after removal from the natural light environment. In either case, researchers must be aware of the light conditions at the time of sampling, and take light history into account when assessing fluorescence results (i.e. taken at different dates/times, depths, etc.). A broader examination (i.e. more species from multiple taxonomic/pigment groups) of the effects of growth irradiance on chlorophyll-specific fluorescence and Phyto-PAM pigment-group estimates could be undertaken. However, even with knowledge of the range and typical levels of uncertainty

resulting from differences in growth light intensity on RS and chlorophyll estimates, the challenge of accounting for this when employing multi-wavelength fluorescence to field measurements would remain.

The Phyto-PAM was able to reliably classify and estimate both F_0 and $F_v:F_m$ for the dominant algal group present in a sample, as seen in estimates of pigment group composition for Hamilton Harbour samples compared to microscopic identification (Table 2.2), and in estimates of pigment group composition in mixtures of laboratory cultures at different levels of known contribution (Table 5.2, Table 5.5). Estimates of abundance (F_0) in mixtures were often within 10% of true values across a range of contribution levels and RS scenarios (Figure 5.1, Figure 5.3), but as sample complexity increased (i.e. ternary vs. binary mixtures), error levels increased. $F_v:F_m$ estimates were only reliable for groups at high relative abundance, and the scope for error was significant at low contribution levels and depending on the RS used (Table 4.5, Figure 5.2, Table 5.4). Based on these results, F_0 estimates are generally reliable with a 10% margin of error, which can increase with light exposure. I would recommend $F_v:F_m$ estimates for algal groups present at less than 10% relative abundance be disregarded, and those for groups present below 25% relative abundance, are interpreted with caution. The chlorophyll *a* concentrations of the mixtures used in these assessments were characteristic of mesotrophic to eutrophic systems. The margins of error for low phytoplankton abundance typical of oligotrophic waters may vary from those observed here, and could bear examination as part of future studies.

The variation between the F_0 and F_v RS of a given taxon and among taxa within a pigment groups presents a significant challenge to the accurate classification and estimation of group-specific $F_v:F_m$. F_0 and F_v spectra for the same taxa ranged from near identical, to slightly different values but with the same normalizing diode and the same general shape, to different normalizing diodes and thus different spectra shape (Table C.6). Small differences in RS values that do not change the spectra shape should not affect group discrimination, but differences in normalizing diode and that change the spectra shape create the potential for misclassification. It is not clear which processes may be causing the observed differences in relative fluorescence intensity among the different excitation diodes between F_0 and F_v spectra, and this could be an interesting question for future inquiry. However, even if one could determine the causes for these differences in spectra shape, it does not alter the challenge this variability presents for group classification. My recommendation is to examine the shapes of the F_0 and F_v spectra for Reference Spectra taxa, and avoid using RS where F_0 and F_v have different

shapes, unless one is measuring a pure culture of that taxon, and the Phyto-PAM is restricted to assigning all fluorescence signal to one algal group. Thus, when sampling natural communities, depending on the dominant taxa present within each pigment group and the researchers' prior knowledge of the system, it could be better to choose RS representative of the average shape for a given group.

The use of species-specific RS to improve estimation accuracy by multi-wavelength fluorescence is consistently suggested; both by researchers using these instruments and by the manufacturers (Leboulanger et al., 2002; Schmitt-Jansen & Altenburger 2008; Houliez et al., 2012; Kring et al., 2014; Escoffier et al., 2015). However, as previously described, this may not always be the best strategy. Furthermore, due to differences in LED intensity across diodes and instruments, RS are specific to a given instrument. The effort of creating a library of RS for multiple species can be considerable (isolation, culturing, etc.), and often impractical when conducting large scale surveys of natural systems. It could be extremely advantageous if there were a way to use RS on different Phyto-PAM instruments, perhaps with some type instrument calibration factors for LED intensity that could be applied to ratios of diode-specific fluorescence. This could allow researchers to contribute RS to a shared database, providing a larger selection of species-specific RS, as well as a more comprehensive data set for analyzing central tendencies and variations of pigment-group excitation spectra. Alternative solutions that will likely become more common are the implementation of molecular and genetic techniques, such as large scale or targeted genomics and proteomics studies to complement spectrofluorometric and/or chemotaxonomic approaches (Campbell et al., 2003; Piquet et al., 2008; Jeon et al., 2017).

The new Phyto-PAM-II chlorophyll fluorometer has five wavelengths of measuring light (440, 480, 540, 590, 625 nm) compared to four in Phyto-PAM, with actinic light from the same five LEDs plus white light, compared to 655 nm in Phyto-PAM, enabling the discrimination of a fourth pigment group and a wider suite of photophysiological parameters (Walz, Effeltrich, Germany). To the best of my knowledge there are no published studies using the Phyto-PAM-II at this time. The additional LEDs should improve pigment-group classification abilities, in particular with the ability to measure a fourth PE-rich group, similar to Fluoroprobe and Algae Online Analyzer. However, it is likely that some of the underlying uncertainties in parameter estimates that have been quantified here (Chapter 4 and 5), and by other researchers (MacIntyre et al., 2010; Goldman et al., 2013; Kring et al., 2014; Escoffier et al., 2015) will remain.

Variation in antenna pigments within pigment groups due to taxonomic and environmental differences are an unavoidable challenge of multi-wavelength fluorometry – one that I do not think can be completely accounted for even with further advances in instrumentation. The advantages of classifying phytoplankton communities at a coarser level, i.e. major pigment groups, compared to microscopic identification or HPLC for example, remains an extremely valuable tool despite this challenge. It enables fast and efficient measurements for high spatio-temporal sampling that would not otherwise be possible, providing large amounts of data to characterize aquatic systems, and effective targeting of sites or regions where more detailed measurements are required. I hope the results from this thesis quantifying uncertainty in pigment group estimates will allow for increased reporting of multi-wavelength fluorometric data, specifically Phyto-PAM, with margins of error that enable useful reporting and comparisons of group abundance, as well as indications when estimates should be disregarded or confirmed with secondary analysis.

Bibliography

- Aberle, N., Beutler, M., Moldaenke, C., and Wiltshire, K.H. 2006. 'Spectral fingerprinting' for specific algal groups on sediments in situ: a new sensor. *Archiv Fur Hydrobiologie*. **167**(1-4): 575-592. doi: 10.1127/0003-9136/2006/0167-0575.
- Acuna, A.M., Snellenburg, J.J., Gwizdala, M., Kirilovsky, D., van Grondelle, R., and van Stokkum, I.H.M. 2016. Resolving the contribution of the uncoupled phycobilisomes to cyanobacterial pulse-amplitude modulated (PAM) fluorometry signals. *Photosynthesis Res.* **127**(1): 91-102. doi: 10.1007/s11120-015-0141-x.
- Adir, N., Zer, H., Shochat, S., and Ohad, I. 2003. Photoinhibition - a historical perspective. *Photosynthesis Res.* **76**(1-3): 343-370. doi: 10.1023/A:1024969518145.
- Alexander, R., Gikuma-Njuru, P., and Imberger, J. 2012. Identifying spatial structure in phytoplankton communities using multi-wavelength fluorescence spectral data and principal component analysis. *Limnology and Oceanography-Methods*. **10**: 402-415. doi: 10.4319/lom.2012.10.402.
- Anderson, J.M., Park, Y.I., and Chow, W.S. 1997. Photoinactivation and photoprotection of photosystem II in nature. *Physiol. Plantarum*. **100**(2): 214-223. doi: 10.1034/j.1399-3054.1997.1000202.x.
- Andreasson, K.I.M., and Wängberg, S. 2006. Biological weighting functions as a tool for evaluating two ways to measure UVB radiation inhibition on photosynthesis. *J. Photochem. Photobiol. B.* **84**(2): 111-118. doi: 10.1016/j.jphotobiol.2006.02.004.

Armstrong, G., and Hearst, J. 1996. Carotenoids .2. Genetics and molecular biology of carotenoid pigment biosynthesis. *Faseb Journal*. **10**(2): 228-237.

Austin, J., and Colman, S. 2008. A century of temperature variability in Lake Superior. *Limnol. Oceanogr.* **53**(6): 2724-2730. doi: 10.4319/lo.2008.53.6.2724.

Barreiro, A., and Vasconcelos, V.M. 2014. Interactions between allelopathic properties and growth kinetics in four freshwater phytoplankton species studied by model simulations. *Aquat. Ecol.* **48**(2): 191-205. doi: 10.1007/s10452-014-9475-2.

Beardall, J., Stojkovic, S., and Gao, K. 2014. Interactive effects of nutrient supply and other environmental factors on the sensitivity of marine primary producers to ultraviolet radiation: implications for the impacts of global change. *Aquatic Biology*. **22**: 5-23. doi: 10.3354/ab00582.

Beecraft, L., Watson, S.B., and Smith, R.E.H. 2017. Multi-wavelength Pulse Amplitude Modulated fluorometry (Phyto-PAM) reveals differential effects of ultraviolet radiation on the photosynthetic physiology of phytoplankton pigment groups. *Freshwat. Biol.* **62**(1): 72-86. doi: 10.1111/fwb.12850.

Behrenfeld, M.J., Prasil, O., Kolber, Z.S., Babin, M., and Falkowski, P.G. 1998. Compensatory changes in Photosystem II electron turnover rates protect photosynthesis from photoinhibition. *Photosynthesis Res.* **58**(3): 259-268. doi: 10.1023/A:1006138630573.

Beutler, M., Wiltshire, K.H., Meyer, B., Moldaenke, C., Luring, C., Meyerhofer, M., Hansen, U.P., and Dau, H. 2002. A fluorometric method for the differentiation of algal populations in vivo and in situ. *Photosynthesis Res.* **72**(1): 39-53. doi: 10.1023/A:1016026607048.

Bouchard, J., Campbell, D., and Roy, S. 2005. Effects of UV-B radiation on the D1 protein repair cycle of natural phytoplankton communities from three latitudes (Canada, Brazil, and Argentina). *J. Phycol.* **41**(2): 273-286. doi: 10.1111/j.1529-8817.2005.04126.x.

Bouchard, J., Roy, S., and Campbell, D.A. 2006. UVB effects on the photosystem II-D1 protein of phytoplankton and natural phytoplankton communities. *Photochem. Photobiol.* **82**(4): 936-951. doi: 10.1562/2005-08-31-IR-666.

Brierly, B., Carvalho, L., Davis, S., and Krokowski, J. 2007. Guidance on the quantitative analysis of phytoplankton in freshwater samples. NERC Open Research Archive.

Brunet, C., Johnsen, G., Lavaud, J., and Roy, S. 2011. Pigments and photoacclimation processes. *In* *Phytoplankton pigments: Characterization, chemotaxonomy and applications in oceanography*. Edited by.

Cabrerizo, M.J., Carrillo, P., Villafane, V.E., and Helbling, E.W. 2014. Current and predicted global change impacts of UVR, temperature and nutrient inputs on photosynthesis and respiration of key marine phytoplankton groups. *J. Exp. Mar. Biol. Ecol.* **461**: 371-380. doi: 10.1016/j.jembe.2014.08.022.

Callieri, C., Bertoni, R., Contesini, M., and Bertoni, F. 2014. Lake Level Fluctuations Boost Toxic Cyanobacterial "Oligotrophic Blooms". *Plos One.* **9**(10): e109526. doi: 10.1371/journal.pone.0109526.

Campbell, D., Hurry, V., Clarke, A.K., Gustafsson, P., and Oquist, G. 1998. Chlorophyll fluorescence analysis of cyanobacterial photosynthesis and acclimation. *Microbiol Mol Biol Rev.* **62**(3): 667-683.

Campbell, D., Cockshutt, A., and Porankiewicz-Asplund, J. 2003. Analysing photosynthetic complexes in uncharacterized species or mixed microalgal communities using global antibodies. *Physiol. Plantarum*. **119**(3): 322-327. doi: 10.1034/j.1399-3054.2003.00175.x.

Carey, C.C., Ibelings, B.W., Hoffmann, E.P., Hamilton, D.P., and Brookes, J.D. 2012. Eco-physiological adaptations that favour freshwater cyanobacteria in a changing climate. *Water Res.* **46**(5): 1394-1407. doi: 10.1016/j.watres.2011.12.016.

Castenholz, R.W., and Garcia-Pichel, F. 2012. Cyanobacterial responses to UV radiation. *In Ecology of cyanobacteria their diversity in space and time. Edited by edited by Brian A. Whitton.* Dordrecht ;London : Springer, 2012, pp. 481-499.

Catherine, A., Escoffier, N., Belhocine, A., Nasri, A.B., Hamlaoui, S., Yepremian, C., Bernard, C., and Troussellier, M. 2012. On the use of the FluoroProbe (R), a phytoplankton quantification method based on fluorescence excitation spectra for large-scale surveys of lakes and reservoirs. *Water Res.* **46**(6): 1771-1784. doi: 10.1016/j.watres.2011.12.056.

Chekalyuk, A., and Hafez, M. 2011. Photo-physiological variability in phytoplankton chlorophyll fluorescence and assessment of chlorophyll concentration. *Optics Express*. **19**(23): 22643-22658. doi: 10.1364/OE.19.022643.

Cosgrove, J., and Borowitzka, M. 2010. Chlorophyll fluorescence terminology: An introduction. *In Chlorophyll a fluorescence in aquatic sciences methods and applications. Edited by D.J. Suggett, O. Prášil and M.A. Borowitzka.* Springer, New York. pp. 1-17.

Cullen, J.J., and Neale, P.J. 1997. Effect of UV on short-term photosynthesis of natural phytoplankton. *Photochem. Photobiol.* **65**(2): 264-266. doi: 10.1111/j.1751-1097.1997.tb08557.x.

Cullen, J.J., Neale, P.J., and Lesser, M.P. 1992. Biological Weighting Function for the Inhibition of Phytoplankton Photosynthesis by Ultraviolet-Radiation. *Science*. **258**(5082): 646-650. doi: 10.1126/science.258.5082.646.

de Mendiburu, F. 2017. *Agricolae*: Statistical procedures for agricultural research. R package version 1.2-8, <https://CRAN.R-project.org/package=agricolae>.

Deblois, C.P., Marchand, A., and Juneau, P. 2013. Comparison of Photoacclimation in Twelve Freshwater Photoautotrophs (Chlorophyte, Bacillariophyte, Cryptophyte and Cyanophyte) Isolated from a Natural Community. *Plos One*. **8**(3): e57139. doi: 10.1371/journal.pone.0057139.

Demers, S., Roy, S., Gagnon, R., and Vignault, C. 1991. Rapid Light-Induced-Changes in Cell Fluorescence and in Xanthophyll-Cycle Pigments of *Alexandrium-Excavatum* (Dinophyceae) and *Thalassiosira-Pseudonana* (Bacillariophyceae) - a Photo-Protection Mechanism. *Mar. Ecol. Prog. Ser.* **76**(2): 185-193. doi: 10.3354/meps076185.

Dimier, C., Corato, F., Tramontano, F., and Brunet, C. 2007. Photoprotection and xanthophyll-cycle activity in three marine diatoms. *J. Phycol.* **43**(5): 937-947. doi: 10.1111/j.1529-8817.2007.00381.x.

Doyle, S.A., Saros, J.E., and Williamson, C.E. 2005. Interactive effects of temperature and nutrient limitation on the response of alpine phytoplankton growth to ultraviolet radiation. *Limnol. Oceanogr.* **50**(5): 1362-1367.

Echenique-Subiabre, I., Dalle, C., Duval, C., Heath, M.W., Coute, A., Wood, S.A., Humbert, J., and Quiblier, C. 2016. Application of a spectrofluorimetric tool (bbe BenthosTorch) for monitoring potentially toxic benthic cyanobacteria in rivers. *Water Res.* **101**: 341-350. doi: 10.1016/j.watres.2016.05.081.

- Escoffier, N., Bernard, C., Hamlaoui, S., Groleau, A., and Catherine, A. 2015. Quantifying phytoplankton communities using spectral fluorescence: the effects of species composition and physiological state. *J. Plankton Res.* **37**(1): 233-247. doi: 10.1093/plankt/fbu085.
- Falkowski, P.G., and Raven, J.A. 2007. *Aquatic photosynthesis*, 2nd edition. Princeton University Press, Princeton, New Jersey.
- Fee, E.J. 1990. Computer programs for calculating *in situ* phytoplankton photosynthesis. 1740, Can. Tech. Rep. Fish. Aquat. Sci.
- Fouqueray, M., Mouget, J., Morant-Manceau, A., and Tremblin, G. 2007. Dynamics of short-term acclimation to UV radiation in marine diatoms. *J. Photochem. Photobiol. B.* **89**(1): 1-8. doi: 10.1016/j.jphotobiol.2007.07.004.
- Fox, J., and Weisberg, S. 2011. *An {R} companion to applied regression*, second edition. Thousand Oaks CA, URL: <http://socserv.socsci.mcmaster.ca/jfox/Books/Companion>.
- Fragoso, G.M., Neale, P.J., Kana, T.M., and Pritchard, A.L. 2014. Kinetics of Photosynthetic Response to Ultraviolet and Photosynthetically Active Radiation in *Synechococcus* WH8102 (Cyanobacteria). *Photochem. Photobiol.* **90**(3): 522-532. doi: 10.1111/php.12202.
- Gaevsky, N., Kolmakov, V., Anishchenko, O., and Gorbaneva, T. 2005. Using DCMU-fluorescence method for the identification of dominant phytoplankton groups. *J. Appl. Phycol.* **17**(6): 483-494. doi: 10.1007/s10811-005-2903-x.

Gao, K., Yu, H., and Brown, M.T. 2007. Solar PAR and UV radiation affects the physiology and morphology of the cyanobacterium *Anabaena* sp PCC 7120. *J. Photochem. Photobiol. B-Biol.* **89**(2-3): 117-124. doi: 10.1016/j.jphotobiol.2007.09.006.

Genty, B., Briantais, J.M., and Baker, N.R. 1989. The relationship between the quantum yield of photosynthetic electron-transport and quenching of chlorophyll fluorescence. *Biochim. Biophys. Acta.* **990**(1): 87-92.

Gilbert, M., Domin, A., Becker, A., and Wilhelm, C. 2000. Estimation of primary productivity by chlorophyll a in vivo fluorescence in freshwater phytoplankton. *Photosynthetica.* **38**(1): 111-126. doi: 10.1023/A:1026708327185.

Giordanino, V.M.F., Sebastian, S.M., Villafane, V.E., and Helbling, W.E. 2011. Influence of temperature and UVR on photosynthesis and morphology of four species of cyanobacteria. *J. Photochem. Photobiol. B.* **103**(1): 68-77. doi: 10.1016/j.jphotobiol.2011.01.013.

Goldman, E.A., Smith, E.M., and Richardson, T.L. 2013. Estimation of chromophoric dissolved organic matter (CDOM) and photosynthetic activity of estuarine phytoplankton using a multiple-fixed-wavelength spectral fluorometer. *Water Res.* **47**(4): 1616-1630. doi: 10.1016/j.watres.2012.12.023.

Goss, R., and Jakob, T. 2010. Regulation and function of xanthophyll cycle-dependent photoprotection in algae. *Photosynth. Res.* **106**(1-2): 103-122.

Graham, L.E., Graham, J.M., Wilcox, L.W., and Cook, M.E. 2016. *Algae* 3rd edition. LJLM Press, LLC, www.ljlmpress.com.

Gregor, J., Geris, R., Marsalek, B., Hetesa, J., and Marvan, P. 2005. In situ quantification of phytoplankton in reservoirs using a submersible spectrofluorometer. *Hydrobiologia*. **548**: 141-151. doi: 10.1007/s10750-005-4268-1.

Guan, W., and Gao, K. 2008. Light histories influence the impacts of solar ultraviolet radiation on photosynthesis and growth in a marine diatom, *Skeletonema costatum*. *J. Photochem. Photobiol. B*. **91**(2-3): 151-156. doi: 10.1016/j.jphotobiol.2008.03.004.

Guan, W., Li, P., Jian, J.B., Wang, J.Y., and Lu, S.H. 2011. Effects of solar ultraviolet radiation on photochemical efficiency of *Chaetoceros curvisetus* (Bacillariophyceae). *Acta Physiologiae Plantarum*. **33**(3): 979-986. doi: 10.1007/s11738-010-0630-7.

Guillard, R.R., and Lorenzen, C. 1972. Yellow-Green Algae with Chlorophyllide C. *J. Phycol.* **8**(1): 10-14. doi: 10.1111/j.0022-3646.1972.00010.x.

Hader, D.P., Porst, M., and Lebert, M. 2000. On site photosynthetic performance of Atlantic green algae. *J. Photochem. Photobiol. B*. **57**(2-3): 159-168. doi: 10.1016/S1011-1344(00)00093-2.

Häder, D.P., Helbling, W.E., Williamson, C.E., and Worrest, R.C. 2011. Effects of UV radiation on aquatic ecosystems and interactions with climate change. *Photochem. Photobiol. Sci.* **10**(2): 242-260. doi: 10.1039/c0pp90036b.

Häder, D.P., Williamson, C.E., Wangberg, S., Rautio, M., Rose, K.C., Gao, K., Walter Helbling, E., Sinha, R.P., and Worrest, R. 2015. Effects of UV radiation on aquatic ecosystems and interactions with other environmental factors. *Photochemical & Photobiological Sciences*. **14**(1): 108-126. doi: 10.1039/c4pp90035a.

Halac, S.R., Villafane, V.E., Goncalves, R.J., and Helbling, W.E. 2014. Photochemical responses of three marine phytoplankton species exposed to ultraviolet radiation and increased temperature: Role of photoprotective mechanisms. *J. Photochem. Photobiol. B.* **141**: 217-227. doi: 10.1016/j.jphotobiol.2014.09.022.

Halac, S.R., Guendulain-Garcia, S.D., Villafane, V.E., Walter Helbling, E., and Banaszak, A.T. 2013. Responses of tropical plankton communities from the Mexican Caribbean to solar ultraviolet radiation exposure and increased temperature. *J. Exp. Mar. Biol. Ecol.* **445**: 99-107. doi: 10.1016/j.jembe.2013.04.011.

Harrison, J.W., and Smith, R.E.H. 2013. Effects of nutrients and irradiance on PSII variable fluorescence of lake phytoplankton assemblages. *Aquat. Sci.* **75**(3): 399-411. doi: 10.1007/s00027-012-0285-0.

Harrison, J.W., and Smith, R.E.H. 2011a. The spectral sensitivity of phytoplankton communities to ultraviolet radiation-induced photoinhibition differs among clear and humic temperate lakes. *Limnol. Oceanogr.* **56**(6): 2115-2126. doi: 10.4319/lo.2011.56.6.2115.

Harrison, J.W., and Smith, R.E.H. 2011b. Deep chlorophyll maxima and UVR acclimation by epilimnetic phytoplankton. *Freshwat. Biol.* **56**(5): 980-992. doi: 10.1111/j.1365-2427.2010.02541.x.

Harrison, J.W., and Smith, R.E.H. 2009. Effects of ultraviolet radiation on the productivity and composition of freshwater phytoplankton communities. *Photochem. Photobiol. Sci.* **8**(9): 1218-1232. doi: 10.1039/b902604e.

Harrison, J.W., Silsbe, G.M., and Smith, R.E.H. 2015. Photophysiology and its response to visible and ultraviolet radiation in freshwater phytoplankton from contrasting light regimes. *J. Plankton Res.* **37**(2): 472-488. doi: 10.1093/plankt/fbv003.

Harrison, J.W., Howell, E.T., Watson, S.B., and Smith, R.E.H. 2016. Improved estimates of phytoplankton community composition based on in situ spectral fluorescence: use of ordination and field-derived norm spectra for the bbe FluoroProbe. *Can. J. Fish. Aquat. Sci.* **73**(10): 1472-1482. doi: 10.1139/cjfas-2015-0360.

He, Y.Y., and Hader, D.P. 2002. Involvement of reactive oxygen species in the UV-B damage to the cyanobacterium *Anabaena* sp. *J. Photochem. Photobiol. B.* **66**(1): 73-80. doi: 10.1016/S1011-1344(01)00278-0.

Helbling, W.E., and Zagarese, H.E. 2003. UV effect on aquatic organisms and ecosystems. The Royal Society of Chemistry, Springer, Cambridge, UK.

Heraud, P., and Beardall, J. 2000. Changes in chlorophyll fluorescence during exposure of *Dunaliella tertiolecta* to UV radiation indicate a dynamic interaction between damage and repair processes. *Photosynth. Res.* **63**: 123-134.

Heraud, P., Roberts, S., Shelly, K., and Beardall, J. 2005. Interactions between UV-B exposure and phosphorus nutrition. II. Effects on rates of damage and repair. *J. Phycol.* **41**(6): 1212-1218. doi: 10.1111/j.1529-8817.2005.00149.x.

Herrmann, H., Hader, D., Kofferlein, M., Seidlitz, H., and Ghetti, F. 1996. Effects of UV radiation on photosynthesis of phytoplankton exposed to solar simulator light. *J. Photochem. Photobiol. B.* **34**(1): 21-28. doi: 10.1016/1011-1344(95)07245-4.

Hilt, S., Beutler, E., and Bauer, N. 2012. Comparison of Methods to Detect Allelopathic Effects of Submerged Macrophytes on Green Algae. *J. Phycol.* **48**(1): 40-44. doi: 10.1111/j.1529-8817.2011.01106.x.

Hiriart-Baer, V.P., Milne, J., and Charlton, M.N. 2009. Water quality trends in Hamilton Harbour: Two decades of change in nutrients and chlorophyll a. *J. Great Lakes Res.* **35**(2): 293-301. doi: 10.1016/j.jglr.2008.12.007.

Houliez, E., Lizon, F., Thyssen, M., Artigas, L.F., and Schmitt, F.G. 2012. Spectral fluorometric characterization of Haptophyte dynamics using the FluoroProbe: an application in the eastern English Channel for monitoring *Phaeocystis globosa*. *J. Plankton Res.* **34**(2): 136-151. doi: 10.1093/plankt/fbr091.

Huot, Y., and Babin, M. 2010. Overview of fluorescence protocols: Theory, basic concepts, and practice. *In Chlorophyll a fluorescence in aquatic sciences methods and applications. Edited by David J. Suggett, Ondrej Prášil, Michael A. Borowitzka, editors.* Dordrecht ;New York : Springer, c2010, pp. 31.

Jakob, T., Schreiber, U., Kirchesch, V., Langner, U., and Wilhelm, C. 2005. Estimation of chlorophyll content and daily primary production of the major algal groups by means of multiwavelength-excitation PAM chlorophyll fluorometry: performance and methodological limits. *Photosynth Res.* **83**(3): 343-361. doi: 10.1007/s11120-005-1329-2.

Jeon, S., Lim, J., Lee, H., Shin, S., Kang, N.K., Park, Y., Oh, H., Jeong, W., Jeong, B., and Chang, Y.K. 2017. Current status and perspectives of genome editing technology for microalgae. *Biotechnology for Biofuels.* **10**: 267. doi: 10.1186/s13068-017-0957-z.

Kahlert, M., and McKie, B.G. 2014. Comparing new and conventional methods to estimate benthic algal biomass and composition in freshwaters. *Environmental Science-Processes & Impacts*. **16**(11): 2627-2634. doi: 10.1039/c4em00326h.

Kalff, J. 2002. *Limnology*. Prentice Hall, Upper Saddle River, NJ.

Kannaujiya, V.K., and Sinha, R.P. 2015. Impacts of varying light regimes on phycobiliproteins of *Nostoc* sp HKAR-2 and *Nostoc* sp HKAR-11 isolated from diverse habitats. *Protoplasma*. **252**(6): 1551-1561. doi: 10.1007/s00709-015-0786-5.

Karentz, D., Cleaver, J., and Mitchell, D. 1991. Cell-Survival Characteristics and Molecular Responses of Antarctic Phytoplankton to Ultraviolet-B Radiation. *J. Phycol.* **27**(3): 326-341. doi: 10.1111/j.0022-3646.1991.00326.x.

Kiefer, D. 1973. Fluorescence Properties of Natural Phytoplankton Populations. *Mar. Biol.* **22**(3): 263-269. doi: 10.1007/BF00389180.

Kirilovsky, D. 2015. Modulating energy arriving at photochemical reaction centers: orange carotenoid protein-related photoprotection and state transitions. *Photosynthesis Res.* **126**(1): 3-17. doi: 10.1007/s11120-014-0031-7.

Kirk, J.T.O. 1994. *Light and photosynthesis in aquatic ecosystems*. Cambridge University Press, Cambridge.

Kok, B. 1956. On the inhibition of photosynthesis by intense light. *Biochim. Biophys. Acta.* **21**(2): 234-244. doi: 10.1016/0006-3002(56)90003-8.

Kok, B., and Businger, J.A. 1956. Kinetics of Photosynthesis and Photo-Inhibition. *Nature*. **177**(4499): 135-136. doi: 10.1038/177135a0.

Kolber, Z., Zehr, J., and Falkowski, P. 1988. Effects of growth irradiance and nitrogen limitation on photosynthetic energy-conversion in photosystem-II. *Plant Physiol.* **88**(3): 923-929. doi: 10.1104/pp.88.3.923.

Kolbowski, J., and Schreiber, U. 1995. Computer-controlled phytoplankton analyzer based on a 4-wavelengths PAM chlorophyll fluorometer.

Kring, S.A., Figary, S.E., Boyer, G.L., Watson, S.B., and Twiss, M.R. 2014. Rapid in situ measures of phytoplankton communities using the bbe FluoroProbe: evaluation of spectral calibration, instrument intercompatibility, and performance range. *Can. J. Fish. Aquat. Sci.* **71**(7): 1087-1095. doi: 10.1139/cjfas-2013-0599.

Kromkamp, J., and Forster, R. 2003. The use of variable fluorescence measurements in aquatic ecosystems: differences between multiple and single turnover measuring protocols and suggested terminology. *Eur. J. Phycol.* **38**(2): 103-112. doi: 10.1080/0967026031000094094.

Kruskal, J. 1964. Multidimensional-Scaling by Optimizing Goodness of Fit to a Nonmetric Hypothesis. *Psychometrika*. **29**(1): 1-27. doi: 10.1007/BF02289565.

Kruskopf, M., and Flynn, K.J. 2006. Chlorophyll content and fluorescence responses cannot be used to gauge reliably phytoplankton biomass, nutrient status or growth rate. *New Phytol.* **169**(3): 525-536. doi: 10.1111/j.1469-8137.2005.01601.x.

Kulk, G., van de Poll, W.H., Visser, R.J.W., and Buma, A.G.J. 2011. Distinct differences in photoacclimation potential between prokaryotic and eukaryotic oceanic phytoplankton. *J. Exp. Mar. Biol. Ecol.* **398**(1-2): 63-72. doi: 10.1016/j.jembe.2010.12.011.

Laurion, I., and Roy, S. 2009. Growth and photoprotection in three dinoflagellates (including two strains of *Alexandrium tamarense*) and one diatom exposed to four weeks of natural and enhanced ultraviolet-B radiation. *J. Phycol.* **45**(1): 16-33. doi: 10.1111/j.1529-8817.2008.00618.x.

Lavaud, J., Materna, A.C., Sturm, S., Vugrinec, S., and Kroth, P.G. 2012. Silencing of the Violaxanthin De-Epoxidase Gene in the Diatom *Phaeodactylum tricornutum* Reduces Diatoxanthin Synthesis and Non-Photochemical Quenching. *Plos One.* **7**(5): e36806. doi: 10.1371/journal.pone.0036806.

Leboulanger, C., Dorigo, U., Jacquet, S., Le Berre, B., Paolini, G., and Humbert, J. 2002. Application of a submersible spectrofluorometer for rapid monitoring of freshwater cyanobacterial blooms: a case study. *Aquat. Microb. Ecol.* **30**(1): 83-89. doi: 10.3354/ame030083.

Legrand, C., Rengefors, K., Fistarol, G., and Graneli, E. 2003. Allelopathy in phytoplankton - biochemical, ecological and evolutionary aspects. *Phycologia.* **42**(4): 406-419. doi: 10.2216/i0031-8884-42-4-406.1.

Lesser, M.P., Cullen, J.J., and Neale, P.J. 1994a. Carbon Uptake in a Marine Diatom during Acute Exposure to Ultraviolet-B Radiation - Relative Importance of Damage and Repair. *J. Phycol.* **30**(2): 183-192. doi: 10.1111/j.0022-3646.1994.00183.x.

Lesser, M.P., Cullen, J.J., and Neale, P.J. 1994b. Carbon Uptake in a Marine Diatom during Acute Exposure to Ultraviolet-B Radiation - Relative Importance of Damage and Repair. *J. Phycol.* **30**(2): 183-192. doi: 10.1111/j.0022-3646.1994.00183.x.

Litchman, E., and Neale, P. 2005. UV effects on photosynthesis, growth and acclimation of an estuarine diatom and cryptomonad. *Mar. Ecol. Prog. Ser.* **300**: 53-62. doi: 10.3354/meps300053.

Litchman, E., Neale, P., and Banaszak, A. 2002. Increased sensitivity to ultraviolet radiation in nitrogen-limited dinoflagellates: Photoprotection and repair. *Limnol. Oceanogr.* **47**(1): 86-94.

Lohscheider, J.N., Strittmatter, M., Kuepper, H., and Adamska, I. 2011. Vertical Distribution of Epibenthic Freshwater Cyanobacterial *Synechococcus* spp. Strains Depends on Their Ability for Photoprotection. *Plos One.* **6**(5): e20134. doi: 10.1371/journal.pone.0020134.

Lorenzen, C. 1966. A method for the continuous measurement of in vivo chlorophyll concentration. *Deep-Sea Research.* **13**: 223-227.

Lund, J.W.G., Kipling, C., and Le Cren, E.D. 1958. The inverted microscope method of estimating algal numbers and the statistical basis of estimations by counting. *Hydrobiologia.* **11**(2): 143-170.

MacDonald, J.H. 2014. Handbook of biological statistics. Sparky House Publishing, Baltimore, Maryland.

MacIntyre, H.L., Lawrenz, E., and Richardson, T.L. 2010. Taxonomic discrimination of phytoplankton by spectral fluorescence. *In Chlorophyll a fluorescence in aquatic sciences methods and applications. Edited by David J. Suggett, Ondrej Prášil, Michael A. Borowitzka, editors.* Dordrecht ;New York : Springer, c2010, pp. 129-169.

MacIntyre, H.L., Kana, T.M., Anning, T., and Geider, R.J. 2002. Photoacclimation of photosynthesis irradiance response curves and photosynthetic pigments in microalgae and cyanobacteria. *J. Phycol.* **38**(1): 17-38. doi: 10.1046/j.1529-8817.2002.00094.x.

Madronich, S., Wagner, M., and Groth, P. 2011. Influence of Tropospheric Ozone Control on Exposure to Ultraviolet Radiation at the Surface. *Environ. Sci. Technol.* **45**(16): 6919-6923. doi: 10.1021/es200701q.

Majarreis, J.M., Watson, S.B., and Smith, R.E.H. 2014. Nutrient status and its assessment by pulse amplitude modulated (PAM) fluorometry of phytoplankton at sites in Lakes Erie and Ontario. *Can. J. Fish. Aquat. Sci.* **71**(12): 1840-1851. doi: 10.1139/cjfas-2014-0017.

Mann, M., Hoppenz, P., Jakob, T., Weisheit, W., Mittag, M., Wilhelm, C., and Goss, R. 2014. Unusual features of the high light acclimation of *Chromera velia*. *Photosynth. Res.* **122**(2): 159-169. doi: 10.1007/s11120-014-0019-3.

Marcovall, M.A., Villafane, V.E., and Helbling, E.W. 2007. Interactive effects of ultraviolet radiation and nutrient addition on growth and photosynthesis performance of four species of marine phytoplankton. *J. Photochem. Photobiol. B.* **89**(2-3): 78-87. doi: 10.1016/j.jphotobiol.2007.09.004.

Maxwell, K., and Johnson, G.N. 2000. Chlorophyll fluorescence - a practical guide. *J. Exp. Bot.* **51**(345): 659-668. doi: 10.1093/jexbot/51.345.659.

McClellan, K., Altenburger, R., and Schmitt-Jansen, M. 2008. Pollution-induced community tolerance as a measure of species interaction in toxicity assessment. *J. Appl. Ecol.* **45**(5): 1514-1522. doi: 10.1111/j.1365-2664.2008.01525.x.

McKenzie, R.L., Aucamp, P.J., Bais, A.F., Bjoern, L.O., Ilyas, M., and Madronich, S. 2011. Ozone depletion and climate change: impacts on UV radiation. *Photochemical & Photobiological Sciences*. **10**(2): 182-198. doi: 10.1039/c0pp90034f.

Millie, D., Schofield, O., Kirkpatrick, G., Johnsen, G., and Evens, T. 2002. Using absorbance and fluorescence spectra to discriminate microalgae. *Eur. J. Phycol.* **37**(3): 313-322. doi: 10.1017/S0967026202003700.

Montero, O., Klisch, M., Hader, D., and Lubian, L. 2002a. Comparative sensitivity of seven marine microalgae to cumulative exposure to ultraviolet-B radiation with daily increasing doses. *Bot. Mar.* **45**(4): 305-315. doi: 10.1515/BOT.2002.030.

Montero, O., Sobrino, C., Pares, G., and Lubian, L. 2002b. Photoinhibition and recovery after selective short-term exposure to solar radiation of five chlorophyll c-containing marine microalgae. *Cienc. Mar.* **28**(3): 223-236.

Moore, C.M., Suggett, D., Hickman, A., Kim, Y., Tweddle, J., Sharples, J., Geider, R., and Holligan, P. 2006. Phytoplankton photoacclimation and photoadaptation in response to environmental gradients in a shelf sea. *Limnol. Oceanogr.* **51**(2): 936-949. doi: 10.4319/lo.2006.51.2.0936.

Moore, L.R., and Chisholm, S. 1999. Photophysiology of the marine cyanobacterium *Prochlorococcus*: Ecotypic differences among cultured isolates. *Limnol. Oceanogr.* **44**(3): 628-638. doi: 10.4319/lo.1999.44.3.0628.

Murata, N., Takahashi, S., Nishiyama, Y., and Allakhverdiev, S.I. 2007. Photoinhibition of photosystem II under environmental stress. *Biochim. Biophys. Acta Bioenerg.* **1767**(6): 414-421. doi: 10.1016/j.bbabi.2006.11.019.

Neale, P.J., Pritchard, A.L., and Ihnacik, R. 2014. UV effects on the primary productivity of picophytoplankton: biological weighting functions and exposure response curves of *Synechococcus*. *Biogeosciences*. **11**(10): 2883-2895. doi: 10.5194/bg-11-2883-2014.

Neale, P.J., Davis, R.F., and Cullen, J.J. 1998. Interactive effects of ozone depletion and vertical mixing on photosynthesis of Antarctic phytoplankton. *Nature*. **392**(6676): 585-589.

Nishiyama, Y., Allakhverdiev, S.I., and Murata, N. 2006. A new paradigm for the action of reactive oxygen species in the photoinhibition of photosystem II. *Biochim. Biophys. Acta. Bioenerg.* **1757**(7): 742-749. doi: 10.1016/j.bbabi.2006.05.013.

Obertegger, U., Camin, F., Guella, G., and Flaim, G. 2011. Adaptation of a Psychrophilic Freshwater Dinoflagellate to Ultraviolet Radiation. *J. Phycol.* **47**(4): 811-820. doi: 10.1111/j.1529-8817.2011.01025.x.

Oksanen, J., F., Blanchet, G., Friendly, M., Kindt, R., Legendre, P., McGlinn, D., Minchin, P.R., O'Hara, R.B., Simpson, G.L., Solymos, P., Stevens, M.H., H., Szoecs, E., and Wagner, H. 2016. *Vegan: Community ecology package*. R package version 2.4-1. R Foundation for Statistical Computing, Vienna, Austria.

O'Reilly, C.M., Sharma, S., Gray, D.K., Hampton, S.E., Read, J.S., Rowley, R.J., Schneider, P., Lenters, J.D., McIntyre, P.B., Kraemer, B.M., Weyhenmeyer, G.A., Straile, D., Dong, B., Adrian, R., Allan, M.G., Anneville, O., Arvola, L., Austin, J., Bailey, J.L., Baron, J.S., Brookes, J.D., de Eyto, E., Dokulil, M.T., Hamilton, D.P., Havens, K., Hetherington, A.L., Higgins, S.N., Hook, S., Izmet'eva, L.R., Joehnk, K.D., Kangur, K., Kasprzak, P., Kumagai, M., Kuusisto, E., Leshkevich, G., Livingstone, D.M., MacIntyre, S., May, L., Melack, J.M., Mueller-Navarra, D.C., Naumenko, M.,

Noges, P., Noges, T., North, R.P., Plisnier, P., Rigosi, A., Rimmer, A., Rogora, M., Rudstam, L.G., Rusak, J.A., Salmaso, N., Samal, N.R., Schindler, D.E., Schladow, S.G., Schmid, M., Schmidt, S.R., Silow, E., Soylu, M.E., Teubner, K., Verburg, P., Voutilainen, A., Watkinson, A., Williamson, C.E., and Zhang, G. 2015. Rapid and highly variable warming of lake surface waters around the globe. *Geophys. Res. Lett.* **42**(24): 10773-10781. doi: 10.1002/2015GL066235.

Paerl, H.W., and Otten, T.G. 2013. Harmful Cyanobacterial Blooms: Causes, Consequences, and Controls. *Microb. Ecol.* **65**(4): 995-1010. doi: 10.1007/s00248-012-0159-y.

Paerl, H.W., and Paul, V.J. 2012. Climate change: Links to global expansion of harmful cyanobacteria. *Water Res.* **46**(5): 1349-1363. doi: 10.1016/j.watres.2011.08.002.

Paerl, H.W., and Kellar, P.E. 1979. Nitrogen-Fixing *Anabaena* - Physiological Adaptations Instrumental in Maintaining Surface Blooms. *Science.* **204**(4393): 620-622. doi: 10.1126/science.204.4393.620.

Papageorgiou, G.C., and Govindjee. 2014. The non-photochemical quenching of the electronically excited state of chlorophyll a in plants: Definitions, timelines, viewpoints, open questions. *In* Non-photochemical quenching and energy dissipation in plants, algae and cyanobacteria. *Edited by* B. Demmig-Adams, G. Garab, W. Adams III and Govindjee. Springer, pp. 1-33.

Paresys, G., Rigart, C., Rousseau, B., Wong, A., Fan, F., Barbier, J., and Lavaud, J. 2005. Quantitative and qualitative evaluation of phytoplankton communities by trichromatic chlorophyll fluorescence excitation with special focus on cyanobacteria. *Water Res.* **39**(5): 911-921. doi: 10.1016/j.watres.2004.12.005.

Parsons, T.R., and Strickland, J.D.H. 1963. Discussion of spectrophotometric determination of marine-plant pigments, with revised equations for ascertaining chlorophylls and carotenoids. *J. Mar. Res.* **21**(3): 155-163.

Phinney, D., and Yentsch, C. 1985. A Novel Phytoplankton Chlorophyll Technique - Toward Automated-Analysis. *J. Plankton Res.* **7**(5): 633-642. doi: 10.1093/plankt/7.5.633.

Piquet, A.M.-., Bolhuis, H., Davidson, A.T., Thomson, P.G., and Buma, A.G.J. 2008. Diversity and dynamics of Antarctic marine microbial eukaryotes under manipulated environmental UV radiation. *FEMS Microbiol. Ecol.* **66**(2): 352-366. doi: 10.1111/j.1574-6941.2008.00588.x.

Proctor, C.W., and Roesler, C.S. 2010. New insights on obtaining phytoplankton concentration and composition from in situ multispectral Chlorophyll fluorescence. *Limnology and Oceanography-Methods.* **8**: 695-708. doi: 10.4319/lom.2010.8.695.

Qin, H., Li, S., and Li, D. 2015. Differential responses of different phenotypes of *Microcystis* (Cyanophyceae) to UV-B radiation. *Phycologia.* **54**(2): 118-129. doi: 10.2216/PH14-93.1.

R Core Team. 2017. R: A language and environment for statistical computing. R Foundation for Statistical Computing, Vienna, Austria.

R Core Team. 2015. R: A language and environment for statistical computing. R Foundation for Statistical Computing, Vienna, Austria.

Rabinowitch, E., and Govindjee. 1970. Photosynthesis. John Wiley & Sons, Inc.,

Ragni, M., Airs, R.L., Leonardos, N., and Geider, R.J. 2008. Photoinhibition of PSII in *Emiliana huxleyi* (Haptophyta) under high light stress: The roles of photoacclimation, photoprotection, and photorepair. *J. Phycol.* **44**(3): 670-683. doi: 10.1111/j.1529-8817.2008.00524.x.

Rastogi, R.P., Sonani, R.R., and Madamwar, D. 2015. Effects of PAR and UV Radiation on the Structural and Functional Integrity of Phycocyanin, Phycoerythrin and Allophycocyanin Isolated from the Marine Cyanobacterium *Lyngbya* sp A09DM. *Photochem. Photobiol.* **91**(4): 837-844. doi: 10.1111/php.12449.

Richardson, T.L., Lawrenz, E., Pinckney, J.L., Guajardo, R.C., Walker, E.A., Paerl, H.W., and MacIntyre, H.L. 2010. Spectral fluorometric characterization of phytoplankton community composition using the Algae Online Analyser (R). *Water Res.* **44**(8): 2461-2472. doi: 10.1016/j.watres.2010.01.012.

Richter, P.R., Häder, D., Goncalves, R.J., Marcoval, M.A., Villafane, V.E., and Helbling, E.W. 2007. Vertical migration and motility responses in three marine phytoplankton species exposed to solar radiation. *Photochem. Photobiol.* **83**(4): 810-817. doi: 10.1111/j.1751-1097.2007.00076.x.

Rolland, A., Rimet, F., and Jacquet, S. 2010. A 2-year survey of phytoplankton in the Marne Reservoir (France): A case study to validate the use of an in situ spectrofluorometer by comparison with algal taxonomy and chlorophyll a measurements. *Knowledge and Management of Aquatic Ecosystems*.(398): 02. doi: 10.1051/kmae/2010023.

Roshan, S.K., Farhangi, M., Emtiazjoo, M., and Rabbani, M. 2015. Effects of solar radiation on pigmentation and induction of a mycosporine-like amino acid in two cyanobacteria, *Anabaena* sp and *Nostoc* sp ISC26. *Eur. J. Phycol.* **50**(2): 173-181. doi: 10.1080/09670262.2015.1021384.

- Rott, E. 1981. Some Results from Phytoplankton Counting Intercalibrations. *Schweizerische Zeitschrift Fur Hydrologie-Swiss Journal of Hydrology*. **43**(1): 34-62. doi: 10.1007/BF02502471.
- Schagerl, M., and Donabaum, K. 2003. Patterns of major photosynthetic pigments in freshwater algae. 1. Cyanoprokaryota, Rhodophyta and Cryptophyta. *Annales De Limnologie-International Journal of Limnology*. **39**(1): 35-47. doi: 10.1051/limn/2003003.
- Schagerl, M., Pichler, C., and Donabaum, K. 2003. Patterns of major photosynthetic pigments in freshwater algae. 2. Dinophyta, Euglenophyta, Chlorophyceae and Charales. *Annales De Limnologie-International Journal of Limnology*. **39**(1): 49-62. doi: 10.1051/limn/2003005.
- Schagerl, M., and Kuenzl, G. 2007. Chlorophyll a extraction from freshwater algae - a reevaluation. *Biologia*. **62**(3): 270-275. doi: 10.2478/s11756-007-0048-x.
- Schmitt-Jansen, M., and Altenburger, R. 2008. Community-level microalgal toxicity assessment by multiwavelength-excitation PAM fluorometry. *Aquatic Toxicology*. **86**(1): 49-58. doi: 10.1016/j.aquatox.2007.10.001.
- Schreiber, U. 1998. Chlorophyll fluorescence: New instruments for special applications.
- Schreiber, U., Schliwa, U., and Bilger, W. 1986. Continuous recording of photochemical and nonphotochemical chlorophyll fluorescence quenching with a new type of modulation fluorometer. *Photosynthesis Res*. **10**(1-2): 51-62. doi: 10.1007/BF00024185.
- Schuermans, R.M., van Alphen, P., Schuermans, J.M., Matthijs, H.C.P., and Hellingwerf, K.J. 2015. Comparison of the Photosynthetic Yield of Cyanobacteria and Green Algae: Different Methods Give Different Answers. *Plos One*. **10**(9): e0139061. doi: 10.1371/journal.pone.0139061.

Schwaderer, A.S., Yoshiyama, K., de Tezanos Pinto, P., Swenson, N.G., Klausmeier, C.A., and Litchman, E. 2011. Eco-evolutionary differences in light utilization traits and distributions of freshwater phytoplankton. *Limnol. Oceanogr.* **56**(2): 589-598. doi: 10.4319/lo.2011.56.2.0589.

Scott, C.E., Saros, J.E., Williamson, C.E., Salm, C.R., Peters, S.C., and Mitchell, D.L. 2009. Effects of nutrients and dissolved organic matter on the response of phytoplankton to ultraviolet radiation: experimental comparison in spring versus summer. *Hydrobiologia.* **619**: 155-166. doi: 10.1007/s10750-008-9608-5.

Selmeczy, G.B., Tapolczai, K., Casper, P., Krienitz, L., and Padisak, J. 2016. Spatial- and niche segregation of DCM-forming cyanobacteria in Lake Stechlin (Germany). *Hydrobiologia.* **764**(1): 229-240. doi: 10.1007/s10750-015-2282-5.

Seppala, J., and Olli, K. 2008. Multivariate analysis of phytoplankton spectral in vivo fluorescence: estimation of phytoplankton biomass during a mesocosm study in the Baltic Sea. *Mar. Ecol. Prog. Ser.* **370**: 69-85. doi: 10.3354/meps07647.

Shelly, K., Heraud, P., and Beardall, J. 2002. Nitrogen limitation in *Dunaliella tertiolecta* (Chlorophyceae) leads to increased susceptibility to damage by ultraviolet-B radiation but also increased repair capacity. *J. Phycol.* **38**(4): 713-720. doi: 10.1046/j.1529-8817.2002.01147.x.

Shelly, K., Roberts, S., Heraud, P., and Beardall, J. 2005. Interactions between UV-B exposure and phosphorus nutrition. I. Effects on growth, phosphate uptake, and chlorophyll fluorescence. *J. Phycol.* **41**(6): 1204-1211. doi: 10.1111/j.1529-8817.2005.00148.x.

Simmons, L.J., Sandgren, C.D., and Berges, J.A. 2016. Problems and pitfalls in using HPLC pigment analysis to distinguish Lake Michigan phytoplankton taxa. *J. Great Lakes Res.* **42**(2): 397-404. doi: 10.1016/j.jglr.2015.12.006.

Six, C., Sherrard, R., Lionard, M., Roy, S., and Campbell, D.A. 2009. Photosystem II and Pigment Dynamics among Ecotypes of the Green Alga *Ostreococcus*. *Plant Physiol.* **151**(1): 379-390. doi: 10.1104/pp.109.140566.

Sobrinho, C., Neale, P.J., and Lubian, L.M. 2005. Interaction of UV radiation and inorganic carbon supply in the inhibition of photosynthesis: Spectral and temporal responses of two marine picoplankton. *Photochem. Photobiol.* **81**(2): 384-393. doi: 10.1562/2004-08-27-RA-295.1.

Sobrinho, C., Neale, P.J., Phillips-Kress, J.D., Moeller, R.E., and Porter, J.A. 2009. Elevated CO₂ increases sensitivity to ultraviolet radiation in lacustrine phytoplankton assemblages. *Limnol. Oceanogr.* **54**(6): 2448-2459. doi: 10.4319/lo.2009.54.6_part_2.2448.

Sommaruga, R., Chen, Y., and Liu, Z. 2009. Multiple strategies of bloom-forming *Microcystis* to minimize damage by solar ultraviolet radiation in surface waters. *Microb. Ecol.* **57**(4): 667-674. doi: 10.1007/s00248-008-9425-4.

Sommer, U., Adrian, R., Domis, L.D.S., Elser, J.J., Gaedke, U., Ibelings, B., Jeppesen, E., Lurling, M., Molinero, J.C., Mooij, W.M., van Donk, E., and Winder, M. 2012. Beyond the Plankton Ecology Group (PEG) Model: Mechanisms Driving Plankton Succession. *Annual Review of Ecology, Evolution, and Systematics*, Vol 43. **43**: 429-448. doi: 10.1146/annurev-ecolsys-110411-160251.

Stamenkovic, M., and Hanelt, D. 2011. Growth and photosynthetic characteristics of several *Cosmarium* strains (Zygnematophyceae, Streptophyta) isolated from various geographic regions

under a constant light-temperature regime. *Aquat. Ecol.* **45**(4): 455-472. doi: 10.1007/s10452-011-9367-7.

Van der Grinten, E., Simis, S., Barranguet, C., and Admiraal, W. 2004. Dominance of diatoms over cyanobacterial species in nitrogen-limited biofilms. *Archiv Fur Hydrobiologie.* **161**(1): 99-112. doi: 10.1127/0003-9136/2004/0161-0099.

van der Grinten, E., Janssen, A., de Mutsert, K., Barranguet, C., and Admiraal, W. 2005. Temperature- and light-dependent performance of the cyanobacterium *Leptolyngbya foveolarum* and the diatom *Nitzschia perminuta* in mixed biofilms. *Hydrobiologia.* **548**: 267-278. doi: 10.1007/s10750-005-5324-6.

van Donk, E., Faafeng, B., de Lange, H., and Hessen, D. 2001. Differential sensitivity to natural ultraviolet radiation among phytoplankton species in Arctic lakes (Spitsbergen, Norway). *Plant Ecol.* **154**(1-2): 247-259. doi: 10.1023/A:1012978328768.

Vuorio, K., Lepistöe, L., and Holopainen, A. 2007. Intercalibrations of freshwater phytoplankton analyses. *Boreal Environ. Res.* **12**(5): 561-569.

Wagner, H., Jakob, T., and Wilhelm, C. 2006. Balancing the energy flow from captured light to biomass under fluctuating light conditions. *New Phytol.* **169**(1): 95-108. doi: 10.1111/j.1469-81.7.2005.01550.x.

Wang, R., Hua, M., Yu, Y., Zhang, M., Xian, Q., and Yin, D. 2016. Evaluating the effects of allelochemical ferulic acid on *Microcystis aeruginosa* by pulse-amplitude-modulated (PAM) fluorometry and flow cytometry. *Chemosphere.* **147**: 264-271. doi: 10.1016/j.chemosphere.2015.12.109.

Waring, J., Klenell, M., Bechtold, U., Underwood, G.J.C., and Baker, N.R. 2010. Light-Induced Responses of Oxygen Photoreduction, Reactive Oxygen Species Production and Scavenging in Two Diatom Species. *J. Phycol.* **46**(6): 1206-1217. doi: 10.1111/j.1529-8817.2010.00919.x.

Watson, S.B., Milne, J., Yang, R., and Hiriart-Baer, V. 2010. Recent and long term patterns in water quality and cyanobacterial beach impairment in Hamilton Harbour. Environment Canada, Aquatic Ecosystem Management Research, Hamilton Harbour Remedial Action Plan, Report. **2010 season:** 102-119.

Whittington, J., Sherman, B., Green, D., and Oliver, R. 2000. Growth of *Ceratium hirundinella* in a subtropical Australian reservoir: the role of vertical migration. *J. Plankton Res.* **22**(6): 1025-1045. doi: 10.1093/plankt/22.6.1025.

Wickelmaier, F. 2003. An introduction to MDS.

Wilhelm, C., Becker, A., Toepel, J., Vieler, A., and Rautenberger, R. 2004. Photophysiology and primary production of phytoplankton in freshwater. *Physiol. Plantarum.* **120**(3): 347-357. doi: 10.1111/j.0031-9317.2004.00267.x.

Willame, R., Boutte, C., Grubisic, S., Wilmotte, A., Komarek, J., and Hoffmann, L. 2006. Morphological and molecular characterization of planktonic cyanobacteria from Belgium and Luxembourg. *J. Phycol.* **42**(6): 1312-1332. doi: 10.1111/j.1529-8817.2006.00284.x.

Williamson, C.E., Saros, J.E., Vincent, W.F., and Smol, J.P. 2009. Lakes and reservoirs as sentinels, integrators, and regulators of climate change. *Limnol. Oceanogr.* **54**(6): 2273-2282. doi: 10.4319/lo.2009.54.6_part_2.2273.

Williamson, C.E., Zepp, R.G., Lucas, R.M., Madronich, S., Austin, A.T., Ballare, C.L., Norval, M., Sulzberger, B., Bais, A.F., McKenzie, R.L., Robinson, S.A., Häder, D., Paul, N.D., and Bornman, J.F. 2014. Solar ultraviolet radiation in a changing climate. *Nature Climate Change*. **4**(6): 434-441. doi: 10.1038/NCLIMATE2225.

Wong, C., Teoh, M., Phang, S., Lim, P., and Beardall, J. 2015. Interactive Effects of Temperature and UV Radiation on Photosynthesis of *Chlorella* Strains from Polar, Temperate and Tropical Environments: Differential Impacts on Damage and Repair. *Plos One*. **10**(10): e0139469. doi: 10.1371/journal.pone.0139469.

Wu, X., Kong, F., and Zhang, M. 2011. Photoinhibition of colonial and unicellular *Microcystis* cells in a summer bloom in Lake Taihu. *Limnology*. **12**(1): 55-61. doi: 10.1007/s10201-010-0321-5.

Wu, H., Cockshutt, A.M., McCarthy, A., and Campbell, D.A. 2011. Distinctive Photosystem II Photoinactivation and Protein Dynamics in Marine Diatoms. *Plant Physiol*. **156**(4): 2184-2195. doi: 10.1104/pp.111.178772.

Wulff, A., Mohlin, M., and Sundback, K. 2007. Intraspecific variation in the response of the cyanobacterium *Nodularia spumigena* to moderate UV-B radiation. *Harmful Algae*. **6**(3): 388-399. doi: 10.1016/j.hal.2006.11.003.

Xenopoulos, M.A., and Frost, P.C. 2003. UV radiation, phosphorus, and their combined effects on the taxonomic composition of phytoplankton in a boreal lake. *J. Phycol.* **39**(2): 291-302.

Xenopoulos, M.A., Prairie, Y.T., and Bird, D.F. 2000. Influence of ultraviolet-B radiation, stratospheric ozone variability, and thermal stratification on the phytoplankton biomass dynamics in a mesohumic lake. *Can. J. Fish. Aquat. Sci.* **57**(3): 600-609. doi: 10.1139/cjfas-57-3-600.

- Xenopoulos, M.A., Leavitt, P.R., and Schindler, D.W. 2009. Ecosystem-level regulation of boreal lake phytoplankton by ultraviolet radiation. *Can. J. Fish. Aquat. Sci.* **66**(11): 2002-2010. doi: 10.1139/F09-119.
- Xiao, M., Willis, A., and Burford, M.A. 2017. Differences in cyanobacterial strain responses to light and temperature reflect species plasticity. *Harmful Algae.* **62**: 84-93. doi: 10.1016/j.hal.2016.12.008.
- Xiong, F., Nedbal, L., and Neori, A. 1999. Assessment of UV-B sensitivity of photosynthetic apparatus among microalgae: Short-term laboratory screening versus long-term outdoor exposure. *J. Plant Physiol.* **155**(1): 54-62.
- Yentsch, C., and Phinney, D. 1985. Spectral Fluorescence - an Ataxonomic Tool for Studying the Structure of Phytoplankton Populations. *J. Plankton Res.* **7**(5): 617-632. doi: 10.1093/plankt/7.5.617.
- Yentsch, C., and Yentsch, C. 1979. Fluorescence spectral signatures - characterization of phytoplankton populations by the use of excitation and emission-spectra. *J. Mar. Res.* **37**(3): 471-483.
- Zeeshan, M., and Prasad, S.M. 2009. Differential response of growth, photosynthesis, antioxidant enzymes and lipid peroxidation to UV-B radiation in three cyanobacteria. *S. Afr. J. Bot.* **75**(3): 466-474. doi: 10.1016/j.sajb.2009.03.003.
- Zhang, M., Kong, F., Wu, X., and Xing, P. 2008. Different photochemical responses of phytoplankters from the large shallow Taihu Lake of subtropical China in relation to light and mixing. *Hydrobiologia.* **603**: 267-278. doi: 10.1007/s10750-008-9277-4.

Zhang, M., Shi, X., Yu, Y., and Kong, F. 2011. The Acclimative Changes in Photochemistry After Colony Formation of the Cyanobacteria *Microcystis aeruginosa*. *J. Phycol.* **47**(3): 524-532. doi: 10.1111/j.1529-8817.2011.00987.x.

Zhang, Y., Liu, X., Osburn, C.L., Wang, M., Qin, B., and Zhou, Y. 2013. Photobleaching Response of Different Sources of Chromophoric Dissolved Organic Matter Exposed to Natural Solar Radiation Using Absorption and Excitation-Emission Matrix Spectra. *Plos One.* **8**(10): e77515. doi: 10.1371/journal.pone.0077515.

Appendix A

Chapter 2 Supplementary Tables and Figures

Table A.1 Broadband photon flux density (PFD) for UV-B, UV-A and PAR in 100% intensity experimental spectral treatments. (Complete radiometric data used to calculate waveband PFD available electronically.)

Spectral Treatment	UV-B (300-320 nm)	UV-A (320-400 nm)	PAR (400-700 nm)
$\mu\text{mol} \cdot \text{m}^{-2} \cdot \text{sec}^{-1}$			
P (> 420 nm)	0.17	1.20	766.44
PA (> 340 nm)	0.35	73.26	923.44
PAB (> 305 nm)	4.35	78.86	854.33
$\text{W} \cdot \text{m}^{-2}$			
P (> 420 nm)	0.07	0.42	166.62
PA (> 340 nm)	0.14	25.53	200.75
PAB (> 305 nm)	1.76	27.48	185.72

Table A.2 Frequency of group-specific $F_v:F_m$ measurement for each experiment date, where frequencies <95% (grey text) were considered unreliable and not analyzed further (groups >95% shown in black text).

Sampling Date	Pre-exposure (T_0)			Pre+Post-exposure		
	Bl	Gr	Br	Bl	Gr	Br
18/04/2012	0.0%	0.0%	100.0%	0.0%	0.0%	100.0%
23/05/2012	0.0%	0.0%	100.0%	0.0%	4.8%	100.0%
20/06/2012	33.3%	8.3%	100.0%	21.3%	2.8%	99.5%
11/07/2012	7.7%	100.0%	92.3%	13.3%	96.7%	97.6%
01/08/2012	100.0%	33.3%	71.4%	98.9%	27.6%	76.9%
13/09/2012	100.0%	100.0%	0.0%	97.6%	99.5%	0.0%
19/09/2013	100.0%	0.0%	100.0%	96.4%	5.4%	100.0%
02/10/2013	100.0%	0.0%	100.0%	95.0%	10.0%	100.0%

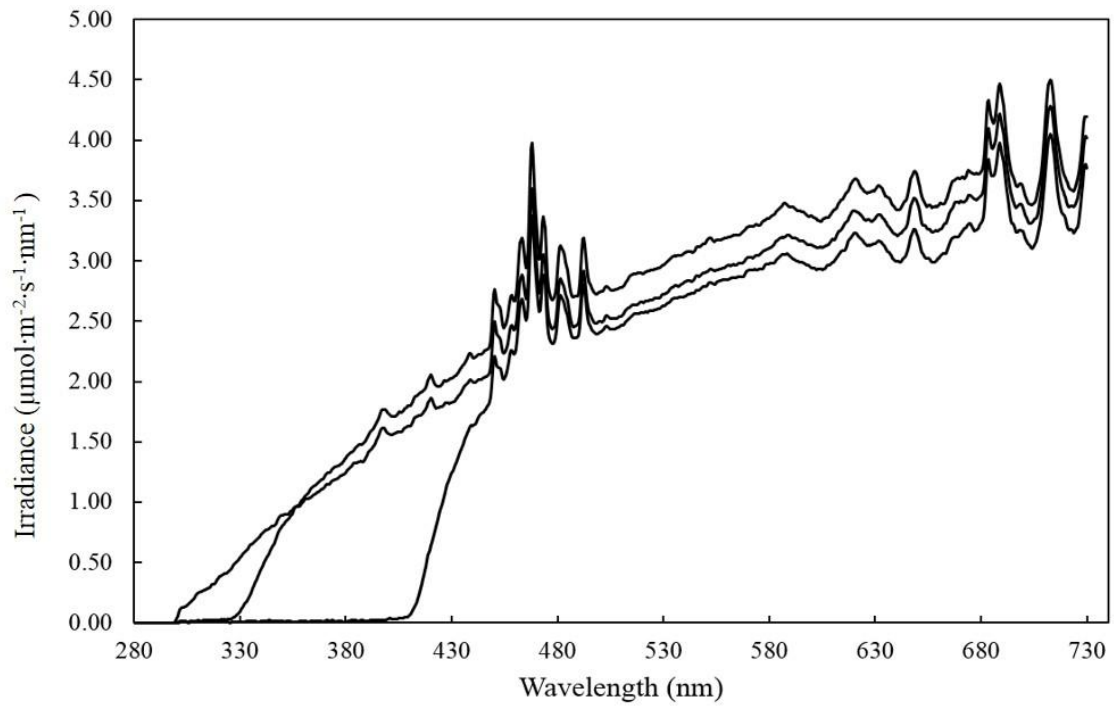


Figure A.1 Spectral irradiance of 100% intensity experimental treatments (PAB – PAR + UV-A + UV-B, PA – PAR + UVA-A, and P – PAR only).

Appendix B

Chapter 3 Supplementary Tables and Figures

Table B.3 Broadband photon flux density (PFD) for UV-B, UV-A and PAR in experimental spectral treatments. (Complete radiometric data used to calculate waveband PFD available electronically.)

Spectral Treatment	UV-B (300-320 nm)	UV-A (320-400 nm)	PAR (400-700 nm)
$\mu\text{mol} \cdot \text{m}^{-2} \cdot \text{sec}^{-1}$			
P (> 420 nm)	0.06	0.46	319.04
PA (> 340 nm)	0.12	29.80	384.11
PAB (> 305 nm)	1.70	32.23	356.01
$\text{W} \cdot \text{m}^{-2}$			
P (> 420 nm)	0.02	0.15	67.70
PA (> 340 nm)	0.05	9.57	83.14
PAB (> 305 nm)	0.63	10.51	76.93

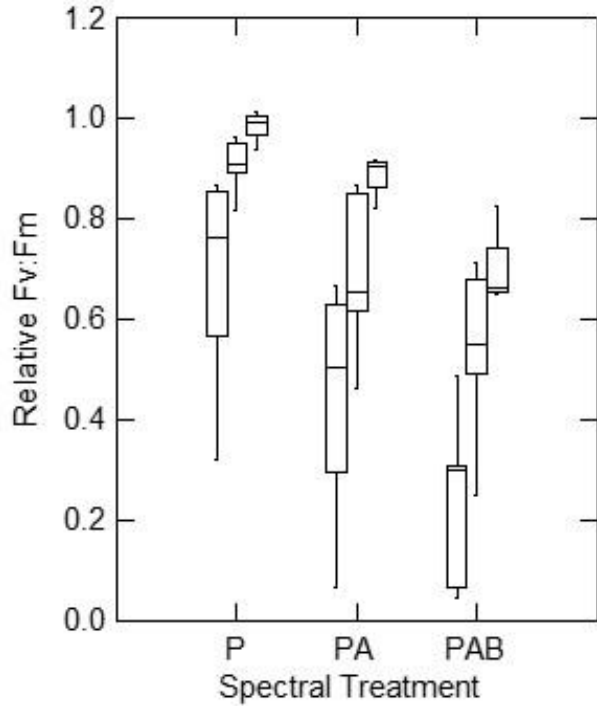


Figure B.2 Box plot (Tukey) of relative $F_v:F_m$ (normalized to initial) after 75 min irradiance exposure for all taxa in each spectral treatment (P – PAR only, PA – PAR + UV-A, PAB – PAR + UV-A + UV-B) and algal group, left to right: blues, browns, greens. Boxes represent the median within the first and third quartiles, whiskers represent the lowest and highest points within 1.5 times the first and third quartiles, respectively, with outliers (asterisks) falling beyond this range (outliers not present).

Table B.4 Polynomial regression analysis results of minimal fluorescence (F_0) and maximal fluorescence (F_m) during experimental irradiance exposures (P – PAR only, PA – PAR + UV-A, PAB – PAR + UV-A + UV-B) for all taxa examined, and percent change between endpoint and initial (normalized to endpoint) and percent change between initial and point of maximum change (normalized to point of maximum change).

Taxon	Parameter	Spectral Treatment	Polynom. Order	Adjusted r^2	p-value	Endpoint - Initial (%)	Maximum - Initial (%)
<i>Anabaena oscillarioides</i>	F_0	P	1	0.13	0.048	-10.5	-10.5
		PA	3	0.58	0.000	32.1	32.1
		PAB	3	0.17	0.084	9.6	11.3
	F_m	P	2	0.57	0.000	-23.3	-24.0
		PA	3	0.76	0.000	-9.2	-41.4
		PAB	2	0.65	0.000	-28.8	-36.1
<i>Dolichospermum lemmeramannii</i>	F_0	P	3	0.31	0.000	1.4	-17.0
		PA	3	0.36	0.000	-7.2	-23.9
		PAB	3	0.61	0.000	-24.6	-25.6
	F_m	P	3	0.48	0.000	-7.6	-23.1
		PA	3	0.67	0.000	-20.3	-38.9
		PAB	2	0.87	0.000	-45.8	-46.8
<i>Microcystis aeruginosa</i>	F_0	P	1	0.75	0.000	-6.5	-6.5
		PA	3	0.32	0.001	-1.6	2.5
		PAB	3	0.64	0.000	3.9	10.1
	F_m	P	2	0.87	0.000	-14.8	-14.8
		PA	3	0.95	0.000	-20.3	-20.3
		PAB	3	0.93	0.000	-22.4	-22.4
<i>Synechococcus</i> sp.	F_0	P	2	0.17	0.003	-3.7	-3.7
		PA	3	0.57	0.000	1.2	5.6
		PAB	3	0.73	0.000	-1.4	7.3
	F_m	P	3	0.83	0.000	-12.3	-12.7
		PA	3	0.95	0.000	-17.4	-17.4
		PAB	3	0.97	0.000	-24.9	-24.9
<i>Synechococcus rhodobaktron</i>	F_0	P	3	0.86	0.000	29.3	29.3
		PA	2	0.98	0.000	116.0	116.0
		PAB	3	0.98	0.000	127.1	127.1
	F_m	P	2	0.07	0.131	0.8	-3.7
		PA	3	0.94	0.000	49.2	49.6
		PAB	3	0.95	0.000	61.2	61.2
<i>Coelastrum cambricum</i>	F_0	P	2	0.92	0.000	-68.6	-68.6
		PA	1	0.82	0.000	-34.8	-34.8

		PAB	2	0.80	0.000	-30.6	-30.6
		P	3	0.90	0.000	-68.3	-68.3
	F _m	PA	1	0.89	0.000	-52.3	-52.3
		PAB	2	0.92	0.000	-51.8	-51.8
<i>Pediastrum simplex</i>		P	3	0.14	0.017	-3.6	-5.4
	F ₀	PA	3	0.17	0.014	7.1	9.0
		PAB	3	0.75	0.000	26.2	26.2
		P	2	0.43	0.000	-8.5	-11.0
	F _m	PA	1	0.42	0.000	-14.9	-14.9
		PAB	3	0.51	0.000	-12.6	-14.0
<i>Scenedesmus obliquus</i>		P	1	0.20	0.005	-20.2	-20.2
	F ₀	PA		na	na	0.0	0.0
		PAB	3	0.12	0.027	14.6	14.6
		P	1	0.15	0.015	-23.5	-23.5
	F _m	PA	1	0.10	0.045	-17.5	-17.5
		PAB	2	0.30	0.002	-23.9	-26.8
<i>Asterionella formosa</i>		P	3	0.55	0.000	-15.4	-50.9
	F ₀	PA	3	0.18	0.025	-17.9	-35.8
		PAB	2	0.07	0.123	-15.0	-28.1
		P	3	0.65	0.000	-31.1	-57.8
	F _m	PA	3	0.51	0.000	-39.8	-58.4
		PAB	3	0.38	0.000	-40.7	-60.6
<i>Fragilaria crotonensis</i>		P	2	0.11	0.017	-22.7	-22.7
	F ₀	PA	1	0.19	0.002	-32.9	-32.9
		PAB	3	0.00	0.403	-1.2	-19.6
		P	1	0.14	0.008	-23.6	-23.6
	F _m	PA	1	0.36	0.000	-44.3	-44.3
		PAB	1	0.09	0.027	-27.4	-27.4
<i>Cryptomonas sp.</i>		P	3	0.93	0.000	-75.3	-75.3
	F ₀	PA	3	0.95	0.000	-78.2	-78.2
		PAB	3	0.85	0.000	-60.1	-63.2
		P	3	0.93	0.000	-77.0	-77.0
	F _m	PA	3	0.94	0.000	-82.7	-82.7
		PAB	3	0.88	0.000	-76.0	-78.1
<i>Synura petersenii</i>		P	3	0.02	0.279	-2.1	-5.8
	F ₀	PA	3	0.30	0.000	-23.5	-23.5
		PAB	3	0.58	0.000	-32.1	-32.1
		P	3	0.24	0.004	-14.3	-14.3
	F _m	PA	1	0.86	0.000	-58.0	-58.0
		PAB	3	0.91	0.000	-70.3	-70.3

		P		na	na	0.0	0.0
<i>Peridinium inconspicuum</i>	F ₀	PA	2	0.24	0.001	11.2	11.2
		PAB	3	0.58	0.000	11.4	16.4
		P	3	0.25	0.006	-11.2	-11.2
	F _m	PA	3	0.65	0.000	-18.0	-19.2
		PAB	3	0.79	0.000	-24.0	-24.0

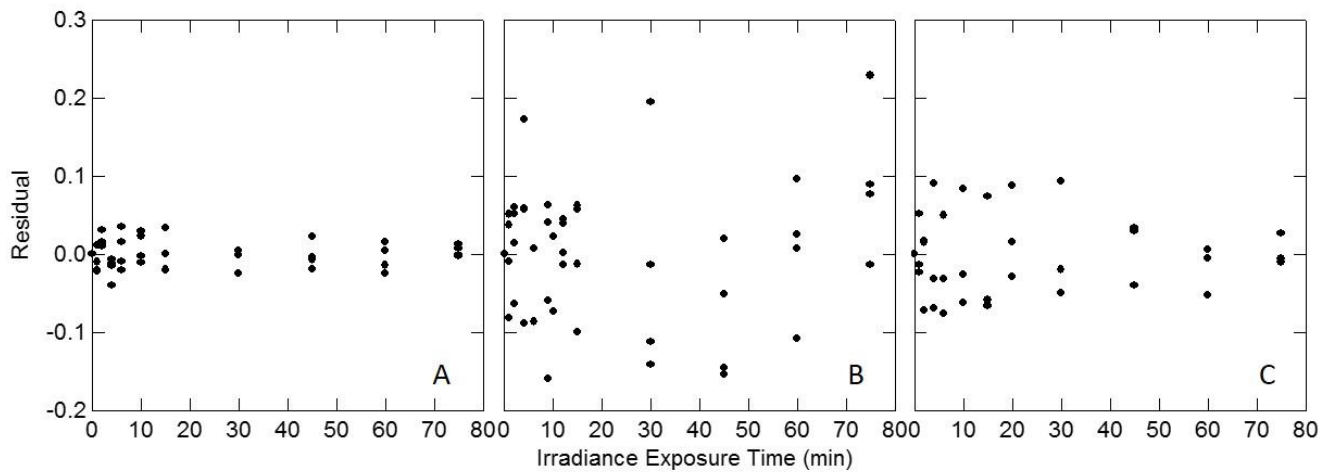


Figure B.3 Sample residual plots from Kok model non-linear regression analysis for (A) *P. simplex* treatment P, (B) *D. lemmermannii* treatment PA, (C) *P. inconspicuum* treatment PAB

Table B.5 Damage and repair rate constants (rate constants, 95% confidence interval) estimated by fitting the Kok model to relative $F_v:F_m$ exposure response kinetics, for all taxa and spectral treatments (P, PA, PAB).

Species	Spectral Treatment	Mean Corrected r^2	Repair Rate (min^{-1})	Damage Rate (min^{-1})
<i>Anabaena oscillarioides</i>	P	0.606	0.243 (0.064 - 0.423)	0.113 (0.04 - 0.186)
	PA	0.891	0.029 (0.014 - 0.043)	0.076 (0.056 - 0.095)
	PAB	0.931	0.02 (0.009 - 0.032)	0.109 (0.086 - 0.133)
<i>Dolichospermum lemmermannii</i>	P	0.418	0.132 (0.04 - 0.225)	0.02 (0.008 - 0.031)
	PA	0.765	0.074 (0.045 - 0.104)	0.054 (0.039 - 0.07)
	PAB	0.939	0.027 (0.019 - 0.034)	0.072 (0.062 - 0.081)
<i>Microcystis aeruginosa</i>	P	0.904	0.042 (0.029 - 0.054)	0.007 (0.005 - 0.009)
	PA	0.962	0.04 (0.032 - 0.048)	0.023 (0.02 - 0.027)
	PAB	0.983	0.03 (0.026 - 0.035)	0.033 (0.03 - 0.037)
<i>Synechococcus sp.</i>	P	0.877	0.029 (0.017 - 0.04)	0.01 (0.008 - 0.013)
	PA	0.966	0.035 (0.029 - 0.041)	0.036 (0.032 - 0.04)
	PAB	0.984	0.027 (0.024 - 0.031)	0.061 (0.056 - 0.065)
<i>Synechococcus rhodobaktron</i>	P	0.965	0 (-0.012 - -0.002)	0.01 (0.008 - 0.012)
	PA	0.989	0.002 (0 - 0.005)	0.054 (0.05 - 0.058)
	PAB	0.992	0.004 (0.001 - 0.006)	0.084 (0.078 - 0.089)
<i>Coelastrum cambricum</i>	P	n/a	n/a (-)	n/a (-)
	PA	0.796	0 (-0.027 - 0.011)	0.001 (0 - 0.002)
	PAB	0.888	0.007 (-0.006 - 0.019)	0.004 (0.002 - 0.005)
<i>Pediastrum simplex</i>	P	0.615	0.288 (0.143 - 0.434)	0.02 (0.011 - 0.029)
	PA	0.837	0.04 (0.024 - 0.055)	0.009 (0.006 - 0.011)
	PAB	0.929	0.015 (0.008 - 0.022)	0.01 (0.008 - 0.012)
<i>Scenedesmus obliquus</i>	P	0.144	0.032 (-0.083 - 0.148)	0.001 (-0.001 - 0.003)

	PA	0.694	0.049 (0.015 - 0.083)	0.005 (0.002 - 0.007)
	PAB	0.946	0.012 (0.004 - 0.019)	0.008 (0.007 - 0.01)
<i>Asterionella formosa</i>	P	0.739	0.027 (0.005 - 0.05)	0.006 (0.003 - 0.008)
	PA	0.914	0.041 (0.028 - 0.054)	0.024 (0.018 - 0.029)
	PAB	0.973	0.043 (0.036 - 0.05)	0.037 (0.032 - 0.041)
<i>Fragilaria crotonensis</i>	P	0.06	0.771 (-1.572 - 3.114)	0.018 (-0.033 - 0.068)
	PA	0.464	0.023 (-0.004 - 0.051)	0.004 (0.002 - 0.007)
	PAB	0.826	0 (-0.015 - 0.008)	0.004 (0.003 - 0.006)
<i>Cryptophyta sp.</i>	P	0.025	0.021 (-0.016 - 0.059)	0.001 (0 - 0.002)
	PA	0.818	0.083 (0.054 - 0.112)	0.012 (0.009 - 0.016)
	PAB	0.976	0.03 (0.025 - 0.036)	0.015 (0.013 - 0.017)
<i>Synura petersenii</i>	P	0.758	0 (-0.017 - 0.012)	0.001 (0.001 - 0.002)
	PA	0.9	0 (-0.014 - 0)	0.007 (0.005 - 0.009)
	PAB	0.981	0 (-0.007 - -0.002)	0.015 (0.013 - 0.016)
<i>Peridinium inconspicuum</i>	P	0.439	0.041 (-0.002 - 0.084)	0.005 (0.001 - 0.008)
	PA	0.886	0.022 (0.011 - 0.033)	0.013 (0.01 - 0.016)
	PAB	0.931	0.019 (0.011 - 0.026)	0.022 (0.018 - 0.026)

Appendix C

Chapter 4 Supplementary Tables and Figures

Table C.6 Phyto-PAM minimum (F_0) and variable (F_v) fluorescence Reference Spectra.

Taxon	Use	Taxon Code	F_0 (Minimum Fluorescence)				F_v (Variable fluorescence)			
			470 nm	520 nm	645 nm	665 nm	470 nm	520 nm	645 nm	665 nm
<i>Anabaena oscillarioides</i>	Expt	Ao	0.054	0.329	1.000	0.355	0.355	0.701	1.000	0.980
<i>Dolichospermum lemmermannii</i>	Expt	Dl	0.039	0.215	1.000	0.339	0.061	0.226	1.000	0.506
<i>Microcystis aeruginosa</i>	Expt	Ma	0.078	0.315	1.000	0.321	0.049	0.237	1.000	0.359
<i>Synechococcus</i> sp	Expt	Ssp	0.065	0.233	1.000	0.305	0.057	0.200	1.000	0.370
<i>Synechococcus rhodobaktron</i>	Expt	Sr	0.060	1.000	0.508	0.170	0.086	1.000	0.669	0.304
<i>Coelastrum cambricum</i>	Expt	Cc	0.636	0.683	1.000	0.454	0.607	0.689	1.000	0.485
<i>Pediastrum simplex</i>	Expt	Ps	0.700	0.669	1.000	0.474	0.666	0.674	1.000	0.516
<i>Scenedesmus obliquus</i>	Expt	So	0.787	0.681	1.000	0.481	0.730	0.684	1.000	0.532
<i>Asterionella formosa</i>	Expt	Af	0.699	1.000	0.605	0.425	0.865	1.000	0.847	0.633
<i>Fragilaria crotonensis</i>	Expt	Fc	0.648	1.000	0.594	0.363	0.627	1.000	0.666	0.433
<i>Cryptomonas</i> sp	Expt	Csp	0.639	1.000	0.648	0.399	0.909	0.699	0.906	1.000
<i>Synura petersenii</i>	Expt	Sp	0.631	1.000	0.842	0.518	0.612	1.000	0.854	0.564
<i>Peridinium inconspicuum</i>	Expt	Pi	0.740	1.000	0.611	0.333	0.678	1.000	0.638	0.383
<i>Dolichospermum lemmermannii</i>	Lib	Do.le1	0.042	0.220	1.000	0.314	0.461	0.188	1.000	0.364
<i>Dolichospermum lemmermannii</i>	Lib	Do.le2	0.062	0.498	1.000	0.310	0.039	0.353	1.000	0.382
<i>Anabaena flos-aquae</i>	Lib	An.fa	0.044	0.219	1.000	0.342	0.060	0.216	1.000	0.432
<i>Anabaena oscillarioides</i>	Lib	An.os	0.063	0.277	1.000	0.339	0.057	0.217	1.000	0.396
<i>Anabaena smithii</i>	Lib	An.sm	0.044	0.172	1.000	0.321	0.051	0.182	1.000	0.465
<i>Dolichospermum crassum</i>	Lib	An.cr	0.097	0.243	1.000	0.350	0.676	0.801	0.221	1.000
<i>Aphanizomenon flos-aquae</i>	Lib	Ap.fl1	0.040	0.154	1.000	0.307	0.053	0.148	1.000	0.419
<i>Aphanizomenon flos-aquae</i>	Lib	Ap.fl2	0.031	0.139	1.000	0.310	0.207	0.368	1.000	0.687

<i>Pseudoanabaena</i> sp	Lib	Ps.sp	0.080	1.000	0.665	0.221	0.104	1.000	0.840	0.339
<i>Synechococcus</i> ARC11	Lib	Sy.sp1	0.031	0.168	1.000	0.270	0.058	0.163	1.000	0.342
<i>Synechococcus</i> ARC21	Lib	Sy.sp2	0.065	1.000	0.291	0.101	0.091	1.000	0.388	0.199
<i>Synechococcus</i> sp	Lib	Sy.sp3	0.062	0.227	1.000	0.312	0.060	0.199	1.000	0.381
<i>Synechococcus rhodobaktron</i>	Lib	Sy.rh	0.068	1.000	0.494	0.189	0.205	1.000	0.888	0.446
<i>Microcystis aeruginosa</i>	Lib	Mi.ae1	0.081	0.331	1.000	0.316	0.064	0.257	1.000	0.359
<i>Microcystis aeruginosa</i>	Lib	Mi.ae2	0.095	0.309	1.000	0.344	0.068	0.260	1.000	0.408
<i>Microcystis flos-aquae</i>	Lib	Mi.fl1	0.096	0.288	1.000	0.342	0.109	0.326	1.000	0.527
<i>Microcystis flos-aquae</i>	Lib	Mi.fl2	0.098	0.288	1.000	0.366	0.044	0.215	1.000	0.378
<i>Microcystis ichthyoblabe</i>	Lib	Mi.ic	0.094	0.249	1.000	0.363	0.079	0.211	1.000	0.342
<i>Microcystis viridis</i>	Lib	Mi.vi	0.085	0.260	1.000	0.347	0.056	0.202	1.000	0.380
<i>Planktothrix</i> isolate (LErie)	Lib	Pl.sp1	0.061	0.237	1.000	0.326	0.046	0.202	1.000	0.391
<i>Planktothrix</i> isolate (LErie)	Lib	Pl.sp2	0.064	0.280	1.000	0.308	0.049	0.216	1.000	0.361
<i>Planktothrix</i> isolate (LErie)	Lib	Pl.sp3	0.063	0.266	1.000	0.323	0.643	0.840	0.430	1.000
<i>Planktothrix</i> isolate (LErie)	Lib	Pl.sp4	0.075	0.268	1.000	0.325	0.168	0.385	1.000	0.613
<i>Planktothrix</i> isolate (LErie)	Lib	Pl.sp5	0.062	0.291	1.000	0.310	0.203	0.462	1.000	0.654
<i>Planktothrix</i> isolate (LErie)	Lib	Pl.sp6	0.053	0.219	1.000	0.331	0.049	0.262	1.000	0.197
<i>Planktothrix</i> isolate (LErie)	Lib	Pl.sp7	0.063	0.258	1.000	0.318	0.084	0.286	1.000	0.495
<i>Planktothrix</i> isolate GLSM	Lib	Pl.sp8	0.060	0.260	1.000	0.310	0.058	0.164	1.000	0.422
<i>Chlamydomonas reinhardtii</i>	Lib	Ch.r1	0.631	0.617	1.000	0.529	0.638	0.685	1.000	0.615
<i>Chlamydomonas reinhardtii</i>	Lib	Ch.r2	0.694	0.687	1.000	0.481	0.844	0.852	0.626	1.000
<i>Chlamydomonas reinhardtii</i>	Lib	Ch.r3	0.729	0.667	1.000	0.542	0.674	0.681	1.000	0.595
<i>Coelastrum</i> sp	Lib	Co.sp1	0.650	0.657	1.000	0.495	0.912	0.902	0.695	1.000
<i>Coelastrum</i> sp	Lib	Co.sp2	0.720	0.681	1.000	0.492	0.821	0.854	0.608	1.000
<i>Coelastrum cambricum</i>	Lib	Co.ca1	0.615	0.562	1.000	0.478	0.592	0.572	1.000	0.485
<i>Coelastrum cambricum</i>	Lib	Co.ca2	0.664	0.650	1.000	0.543	0.638	0.664	1.000	0.599
<i>Pediastrum simplex</i>	Lib	Pe.si1	0.547	0.613	1.000	0.477	0.542	0.625	1.000	0.501
<i>Pediastrum simplex</i>	Lib	Pe.si2	0.684	0.661	1.000	0.530	0.656	0.672	1.000	0.573
<i>Scenedesmus obliquus</i>	Lib	Sc.ob	0.719	0.643	1.000	0.551	0.683	0.661	1.000	0.614

<i>Asterionella formosa</i>	Lib	As.fo	0.695	1.000	0.514	0.354	0.651	1.000	0.548	0.403
<i>Diatoma elongatum</i>	Lib	Di.el	0.599	1.000	0.688	0.405	0.822	0.827	1.000	0.693
<i>Fragilaria crotonensis</i>	Lib	Fr.cr	0.814	1.000	0.942	0.542	0.831	0.956	1.000	0.648
<i>Fragilaria crotonensis</i>	Lib	Fr.cr2	0.638	1.000	0.626	0.414	0.611	1.000	0.675	0.492
<i>Cryptomonas</i> sp	Lib	Cr.sp	0.630	1.000	0.601	0.375	0.833	1.000	0.840	0.578
<i>Peridinium inconspicuum</i>	Lib	Pe.in	0.761	1.000	0.670	0.346	0.759	1.000	0.643	0.404
<i>Synura petersenii</i>	Lib	Sy.pe	0.586	1.000	0.858	0.545	0.955	0.536	0.680	1.000

Table C.7 Reference Spectra (RS) scenarios applied to each experimental taxon.

Taxon (presented to instrument)	Scenario Type	# of Groups Selected	Reference Spectra Taxa Selected		
			Blue	Green	Brown
<i>Anabaena oscillarioides</i>	MIS	1	D. lemmermannii	--	--
	MIS	1	M. aeruginosa	--	--
	MA	3	A. oscillarioides	P. simplex	F. crotonensis
	MIS	3	D. lemmermannii	C. reinhardtii	A. formosa
	MA	3	A. oscillarioides	S. obliquus	Cryptomonas sp
	MIS	3	Synechococcus sp	C. cambricum	Cryptomonas sp
<i>Dolichospermum lemmermannii</i>	MIS	1	M. aeruginosa	--	--
	MA	3	D. lemmermannii	C. reinhardtii	A. formosa
	MA	3	D. lemmermannii	C. cambricum	Cryptomonas sp.
	MIS	3	M. aeruginosa	C. reinhardtii	A. formosa
	MIS	3	M. aeruginosa	C. cambricum	F. crotonensis
	MIS	3	A. oscillarioides	P. simplex	P. inconspicuum
<i>Microcystis aeruginosa</i>	MIS	1	D. lemmermannii	--	--
	MA	3	M. aeruginosa	C. reinhardtii	A. formosa
	MA	3	A. oscillarioides	P. simplex	F. crotonensis
	MA	3	M. aeruginosa	C. cambricum	Cryptomonas sp.
	MIS	3	D. lemmermannii	C. reinhardtii	A. formosa
	MIS	3	D. lemmermannii	C. cambricum	Cryptomonas sp.
<i>Synechococcus sp</i>	MIS	3	A. oscillarioides	P. simplex	P. inconspicuum
	MIS	1	D. lemmermannii	--	--
	MIS	1	M. aeruginosa	--	--
	MA	3	Synechococcus sp	P. simplex	A. formosa
	MA	3	Synechococcus sp	C. cambricum	Cryptomonas sp.
	MIS	3	M. aeruginosa	C. reinhardtii	A. formosa
	MIS	3	D. lemmermannii	S. obliquus	A. formosa
MIS	3	A. oscillarioides	P. simplex	P. inconspicuum	
<i>Synechococcus rhodobaktron</i>	MIS	1	M. aeruginosa	--	--
	MIS	1	--	--	F. crotonensis
	MA	2	M. aeruginosa	--	S. rhodobaktron
	MA	2	S. rhodobaktron	--	F. crotonensis
	MA	3	D. lemmermannii	C. cambricum	S. rhodobaktron
	MA	3	S. rhodobaktron	C. cambricum	F. crotonensis
	MIS	2	D. lemmermannii	--	Cryptomonas sp.
<i>Coelastrum cambricum</i>	MIS	1	--	S. obliquus	--
	MIS	1	--	P. simplex	--
	MA	3	D. lemmermannii	C. cambricum	A. formosa

	MA	3	M. aeruginosa	C. cambricum	F. crotonensis
	MIS	3	D. lemmermannii	C. reinhardtii	A. formosa
	MIS	3	D. lemmermannii	P. simplex	F. crotonensis
<i>Pediastrum simplex</i>	MIS	1	--	C. cambricum	--
	MA	3	M. aeruginosa	P. simplex	F. crotonensis
	MA	3	D. lemmermannii	P. simplex	F. crotonensis
	MIS	3	D. lemmermannii	C. reinhardtii	A. formosa
	MIS	3	M. aeruginosa	C. cambricum	F. crotonensis
<i>Scenedesmus obliquus</i>	MIS	1	--	C. cambricum	--
	MA	3	D. lemmermannii	S. obliquus	A. formosa
	MA	3	M. aeruginosa	S. obliquus	A. formosa
	MA	3	D. lemmermannii	S. obliquus	F. crotonensis
	MIS	3	M. aeruginosa	C. cambricum	A. formosa
	MIS	3	D. lemmermannii	C. reinhardtii	A. formosa
	MIS	3	D. lemmermannii	P. simplex	F. crotonensis
<i>Asterionella formosa</i>	MIS	1	--	--	F. crotonensis
	MA	3	D. lemmermannii	C. reinhardtii	A. formosa
	MA	3	M. aeruginosa	C. reinhardtii	A. formosa
	MIS	3	M. aeruginosa	C. cambricum	F. crotonensis
	MIS	3	M. aeruginosa	C. cambricum	S. petersenii
	MIS	3	D. lemmermannii	C. cambricum	Cryptomonas sp.
	MIS	3	Synechococcus sp	S. obliquus	P. inconspicuum
	MIS	3	A. oscillarioides	P. simplex	P. inconspicuum
<i>Fragilaria crotonensis</i>	MIS	1	--	--	A. formosa
	MIS	1	--	--	S. petersenii
	MA	3	M. aeruginosa	C. cambricum	F. crotonensis
	MA	3	D. lemmermannii	S. obliquus	F. crotonensis
	MIS	3	M. aeruginosa	C. reinhardtii	A. formosa
	MIS	3	M. aeruginosa	C. cambricum	A. formosa
	MIS	3	D. lemmermannii	P. simplex	S. petersenii
	MIS	3	M. aeruginosa	C. cambricum	Cryptomonas sp.
	MIS	3	Synechococcus sp	S. obliquus	P. inconspicuum
	MIS	3	A. oscillarioides	P. simplex	P. inconspicuum
<i>Cryptomonas sp</i>	MIS	1	--	--	A. formosa
	MIS	1	--	--	S. petersenii
	MIS	1	--	--	F. crotonensis
	MA	3	D. lemmermannii	C. cambricum	Cryptomonas sp.
	MA	3	M. aeruginosa	C. cambricum	Cryptomonas sp.
	MIS	3	D. lemmermannii	C. reinhardtii	A. formosa
	MIS	3	M. aeruginosa	C. cambricum	A. formosa

	MIS	3	M. aeruginosa	C. cambricum	S. petersenii
	MIS	3	Synechococcus sp	S. obliquus	P. inconspicuum
	MIS	3	A. oscillarioides	P. simplex	P. inconspicuum
<i>Synura petersenii</i>	MIS	1	--	--	A. formosa
	MA	3	D. lemmermannii	P. simplex	S. petersenii
	MA	3	M. aeruginosa	C. cambricum	S. petersenii
	MIS	3	M. aeruginosa	C. cambricum	F. crotonensis
	MIS	3	M. aeruginosa	C. cambricum	Cryptomonas sp.
	MIS	3	M. aeruginosa	C. reinhardtii	A. formosa
	MIS	3	Synechococcus sp	S. obliquus	P. inconspicuum
	MIS	3	A. oscillarioides	P. simplex	P. inconspicuum
<i>Peridinium inconspicuum</i>	MIS	1	--	--	F. crotonensis
	MIS	1	--	--	S. petersenii
	MIS	1	--	--	Cryptomonas sp.
	MA	3	D. lemmermannii	C. cambricum	P. inconspicuum
	MA	3	M. aeruginosa	S. obliquus	P. inconspicuum
	MIS	3	D. lemmermannii	C. cambricum	S. petersenii
	MIS	3	A. oscillarioides	P. simplex	F. crotonensis

Table C.8 Effect of excitation wavelength (Exc LED: 470, 520, 645, 665 nm) and light treatment (LightTr: Pre-exposure and post-exposure P, PA, PAB) on normalized minimum (F_0) and variable (F_v) fluorescence for each taxon, based on two-way ANOVA.

Taxon	ANOVA Factor	p-value	
		F_0	F_v
<i>Anabaena oscillarioides</i>	LightTr	0.839	0.000
	Exc LED	0.000	0.000
	Interaction	0.760	0.010
<i>Dolichospermum lemmermannii</i>	LightTr	0.000	0.000
	Exc LED	0.000	0.000
	Interaction	0.000	0.002
<i>Microcystis aeruginosa</i>	LightTr	0.000	0.000
	Exc LED	0.000	0.000
	Interaction	0.000	0.000
<i>Synechococcus sp</i>	LightTr	0.000	0.000
	Exc LED	0.000	0.000
	Interaction	0.000	0.000

<i>Synechococcus rhodobaktron</i>	LightTr	0.000	0.000
	Exc LED	0.000	0.000
	Interaction	0.000	0.003
<i>Coelastrum cambricum</i>	LightTr	0.000	0.109
	Exc LED	0.000	0.000
	Interaction	0.002	0.001
<i>Pediastrum simplex</i>	LightTr	0.076	0.508
	Exc LED	0.000	0.000
	Interaction	0.044	0.835
<i>Scenedesmus obliquus</i>	LightTr	0.146	0.029
	Exc LED	0.000	0.000
	Interaction	0.103	0.354
<i>Asterionella formosa</i>	LightTr	0.233	0.262
	Exc LED	0.000	0.000
	Interaction	0.625	0.844
<i>Fragilaria crotonensis</i>	LightTr	0.000	0.652
	Exc LED	0.000	0.000
	Interaction	0.000	0.274
<i>Cryptomonas</i> sp	LightTr	0.000	0.000
	Exc LED	0.000	0.000
	Interaction	0.000	0.000
<i>Synura petersenii</i>	LightTr	0.215	0.000
	Exc LED	0.000	0.000
	Interaction	0.000	0.000
<i>Peridinium inconspicuum</i>	LightTr	0.435	0.899
	Exc LED	0.000	0.000
	Interaction	0.528	0.038

Appendix D

Chapter 5 Supplementary Tables and Figures

Table D.9 Phytoplankton Taxa used in Binary and Ternary Experimental Mixtures

Taxon	Phyto-PAM Group	Algal Phylum
<i>Dolichospermum lemmermannii</i> LO08-01	Bl	Cyanophyta
<i>Microcystis aeruginosa</i> Kutz.em. Elenkin CPCC 299	Bl	Cyanophyta
<i>Synechococcus rhodobaktron</i> NIVA 8	Bl ^a	Cyanophyta
<i>Coelastrum cambricum</i> HH001-05	Gr	Chlorophyta
<i>Pediastrum simplex</i> Meyen CPCC 431	Gr	Chlorophyta
<i>Asterionella formosa</i> Hass CPCC 605	Br	Ochrophyta
<i>Fragilaria crotonensis</i> Kitton CPCC 269	Br	Ochrophyta
<i>Cryptomonas</i> sp. CPCC 336	Br	Cryptophyta
<i>Synura petersenii</i> Korshikov CPCC 495	Br	Ochrophyta

^a *Synechococcus rhodobaktron* is a phycoerythrin-rich Cyanobacteria, it is included as a member of the ‘blue’ group taxonomically, however it is classified as predominantly ‘brown’ by the Phyto-PAM when using typical ‘blue’ reference spectra taxa. It will be included with the Cyanobacteria throughout the present study.

Table D.10 Reference Spectra (RS) Scenarios applied to each binary and ternary mixture (Taxa presented), with the matching RS scenario for each mixture highlighted in grey.

Mixture Code	Taxa Presented	Reference Spectra Taxa Selected		
		Blue	Green	Brown
		M. aeruginosa	C. cambricum	--
		M. aeruginosa	P. simplex	--
		D. lemmermannii	C. cambricum	--
A	<i>M. aeruginosa</i> + <i>C. cambricum</i>	M. aeruginosa	C. cambricum	Cryptomonas sp.
		D. lemmermannii	C. reinhardtii	A. formosa
		M. aeruginosa	C. cambricum	S. petersenii
		D. lemmermannii	C. cambricum	S. petersenii
		M. aeruginosa	C. cambricum	F. crotonensis

B	<i>M. aeruginosa</i> + <i>P. simplex</i>	M. aeruginosa	P. simplex	--
		D. lemmermannii	P. simplex	--
		M. aeruginosa	P. simplex	A. formosa
C	<i>S. rhodobaktron</i> + <i>P. simplex</i>	S. rhodobaktron	P. simplex	--
		S. rhodobaktron	P. simplex	F. crotonensis
		D. lemmermannii	P. simplex	F. crotonensis
D	<i>D. lemmermannii</i> + <i>A. formosa</i>	D. lemmermannii	--	A. formosa
		D. lemmermannii	C. reinhardtii	A. formosa
		M. aeruginosa	C. reinhardtii	A. formosa
E	<i>M. aeruginosa</i> + <i>A. formosa</i>	M. aeruginosa	--	A. formosa
		D. lemmermannii	C. reinhardtii	A. formosa
		M. aeruginosa	C. reinhardtii	A. formosa
F	<i>M. aeruginosa</i> + <i>Cryptomonas sp.</i>	M. aeruginosa	--	Cryptomonas sp.
		M. aeruginosa	C. cambricum	Cryptomonas sp.
		M. aeruginosa	--	S. petersenii
		D. lemmermannii	--	Cryptomonas sp.
		D. lemmermannii	C. reinhardtii	A. formosa
G	<i>S. rhodobaktron</i> + <i>F. crotonensis</i>	S. rhodobaktron	--	F. crotonensis
		S. rhodobaktron	P. simplex	F. crotonensis
		D. lemmermannii	P. simplex	F. crotonensis
		M. aeruginosa	C. cambricum	S. petersenii
H	<i>C. cambricum</i> + <i>A. formosa</i>	--	C. cambricum	A. formosa
		D. lemmermannii	C. cambricum	A. formosa
		M. aeruginosa	C. cambricum	A. formosa
I	<i>C. cambricum</i> + <i>Cryptomonas sp.</i>	--	C. cambricum	Cryptomonas sp.
		D. lemmermannii	C. cambricum	Cryptomonas sp.
		M. aeruginosa	C. cambricum	Cryptomonas sp.
		--	P. simplex	F. crotonensis
		M. aeruginosa	C. cambricum	S. petersenii
		M. aeruginosa	P. simplex	F. crotonensis
J	<i>P. simplex</i> + <i>F. crotonensis</i>	--	P. simplex	F. crotonensis
		M. aeruginosa	P. simplex	F. crotonensis
		D. lemmermannii	P. simplex	F. crotonensis
		--	P. simplex	S. petersenii
		--	C. cambricum	F. crotonensis
		--	C. cambricum	A. formosa
K	<i>D. lemmermannii</i> + <i>P. simplex</i> + <i>F. crotonensis</i>	D. lemmermannii	P. simplex	F. crotonensis
		M. aeruginosa	P. simplex	F. crotonensis
		D. lemmermannii	S. obliquus	F. crotonensis

		D. lemmermannii	P. simplex	S. petersenii
		Synechococcus sp.	C. cambricum	Cryptomonas sp.
		M. aeruginosa	C. reinhardtii	A. formosa
		D. lemmermannii	C. cambricum	S. petersenii
		M. aeruginosa	C. cambricum	S. petersenii
L	<i>M. aeruginosa</i> + <i>C. cambricum</i> + <i>S. petersenii</i>	D. lemmermannii	C. reinhardtii	A. formosa
		M. aeruginosa	C. cambricum	F. crotonensis
		D. lemmermannii	C. cambricum	S. petersenii
		M. aeruginosa	C. cambricum	Cryptomonas sp.

Table D.11 Average estimated algal group F_0 proportions (expressed as percentage of total F_0 signal) at different levels of relative taxon contribution, for taxon 1 in binary mixtures with matching RS applied. Symbols indicate estimated proportions different from true proportions by 5% (γ) and 10% (β), respectively.

True Proportion	A <i>MaCc</i>	B <i>MaPs</i>	C <i>SrPs</i>	D <i>DlAf</i>	E <i>MaAf</i>	F <i>MaCsp</i>	G <i>SrFc</i>	H <i>CcAf</i>	I <i>CcCsp</i>	J <i>PsFc</i>
0	0	1.3	3.8	0	0	0.8	0	0	6.7 γ	7.3 γ
10	10	14.4	14.1	5.9	9.2	11.3	8.9	0 γ	18.5 γ	13
25	26.4	28.1	26.8	24.9	25.2	26.2	23.5	18.7 γ	36.5 $\gamma\beta$	26.3
50	55.6 γ	51	47.8	51.7	53.7	51.2	45.4	50.7	60.8 $\gamma\beta$	47.5
75	84.1 γ	72.2	76.4	75.1	73.6	78.8	69.2 γ	77.9	81.3 γ	69.7 γ
90	100 γ	85 γ	93.2	91.2	94.3	97.1 γ	89	94	98.3 γ	92.1
100	100	95.4	100	100	100	100	100	100	100	100

γ indicates when the observed average proportion for a given algal group is not within 5% of the expected contribution

β indicates when the observed average proportion for a given algal group is not within 10% of the expected contribution

Table D.12 $F_v:F_m$ of pure culture ('true' $F_v:F_m$, first row and shaded) and relative difference in estimated $F_v:F_m$ (as percentage of pure culture $F_v:F_m$) at different levels of relative contribution in binary mixtures with matching RS applied. Symbols (γ) indicating significant differences in estimated $F_v:F_m$ from true $F_v:F_m$ based on 1-way ANOVA and Tukey's HSD post-hoc analysis ($p < 0.05$).

True Proportion	A1 Bl	B1 Bl	C1 Bl	D1 Bl	E1 Bl	F1 Bl	G1 Bl	H1 Gr	I1 Gr	J1 Gr
100	0.4	0.4	0.25	0.4	0.22	0.46	0.3	0.69	0.71	0.6
90	3.76 γ	-1.6	-9.41	-1.18	-47.58 γ	-3.26	-8.95	-0.53	-3.29	2.19
75	-8.4 γ	1.1	-4.05	-2.66	46.21 γ	-6.3 γ	-5.83	-1.6	-0.78	0.75
50	-9.02 γ	2.61	6.88	-14.79 γ	37.27 γ	-4.99 γ	-2.62	-5.3	7.36 γ	1.41
25	-12.97 γ	5.9	24.6 γ	-100 γ	-100 γ	-3.42	10.22	-76.82 γ	21.18 γ	3.15
10	-100 γ	15.75 γ	56.88 γ	-100 γ	-100 γ	2.39	-55.24 γ	-100 γ	28.89 γ	0.21
True Proportion	A2 Gr	B2 Gr	C2 Gr	D2 Br	E2 Br	F2 Br	G2 Br	H2 Br	I2 Br	J2 Br
100	0.62	0.61	0.63	0.56	0.63	0.67	0.58	0.58	0.65 *	0.57
90	7.34 γ	-0.16	1.81	1.64	1.57	-3.59	2.83	5.27	-83.66 γ	2.08
75	7.1 γ	-2.63	3.31 γ	7.36 γ	5.35 γ	-4.41	3.73	15.34	-100 γ	2.87
50	8.68 γ	-2.08	2.05	4.79	4.5 γ	-1.8	0.26	14.37	-19.11 γ	2.25
25	20.97 γ	-3.62	3.82 γ	1.11	5.88 γ	4.19	3.68	12.99	10.08 γ	-1.24
10	-100 γ	-14.36 γ	12.61 γ	-9.44 γ	43.5 γ	-39.66	5.18	-25.82	-65.33 γ	-39.53 γ

* $F_v:F_m$ determined using single-taxon RS for *Cryptomonas* sp.

Table D.13 $F_v:F_m$ of pure culture ('true' $F_v:F_m$, first row and shaded) and relative difference in estimated $F_v:F_m$ at different levels of relative contribution in ternary mixtures (K and L, Table 5.1), with symbols (γ) indicating significant differences in estimated $F_v:F_m$ from true $F_v:F_m$ based on 1-way ANOVA and Tukey's HSD post-hoc analysis ($p < 0.05$).

True Proportion	(K) <i>D.lemm</i> / <i>P.simp</i> / <i>F.croto</i>			(L) <i>M.aeru</i> / <i>C.camb</i> / <i>S.peter</i>		
	Bl	Gr	Br	Bl	Gr	Br
100	0.5	0.61	0.57	0.43	0.67	0.58
80:10:10	1.9	-100 γ	-14.7	-7.6	6.7 γ	-100 γ
50:25:25	2.2	-25.6	-11.9	-6.7	-3.5 γ	22.1 γ
33:33:33	1.9	21.4	-7.2	-13	-1.3	3.9
10:80:10	-38.3	6	-39 γ	-100 γ	1.3	-100 γ
25:50:25	1	12	-15.2	-36.9 γ	6.1 γ	-100 γ
10:10:80	8.3	-24.1	1.3	-84.9 γ	7.1 γ	3
25:25:50	-0.6	24.7	-7.1	-15	0.9	6.9

Table D.14 Pre-exposure $F_v:F_m$ and post-exposure relative $F_v:F_m$ from independently conducted binary mixture and monoculture irradiance exposure experiments. Average (\pm standard deviation). Letter/number represents mixture code and taxon number.

Suspension	Light treatment	A1	B1	C1	D1	E1	F1	G1	H1	I1	J1
Binary mixture	Pre (abs)	0.38 (± 0.02)	0.42 (± 0.02)	0.27 (± 0.01)	0.32 (± 0.01)	0.28 (± 0.01)	0.43 (± 0.01)	0.28 (± 0.04)	0.66 (± 0.01)	0.78 (± 0.01)	0.62 (± 0.01)
	P	0.8 (± 0.02)	0.87 (± 0.05)	0.32 (± 0.06)	0.82 (± 0.04)	0.89 (± 0.1)	0.52 (± 0.2)	0.47 (± 0.04)	0.92 (± 0.01)	0.83 (± 0.01)	0.93 (± 0.03)
	PA	0.51 (± 0.03)	0.67 (± 0.04)	0.12 (± 0.1)	0.67 (± 0.04)	0.64 (± 0.04)	0.41 (± 0.14)	0.1 (± 0.03)	0.84 (± 0.03)	0.79 (± 0.06)	0.78 (± 0.06)
	PAB	0.29 (± 0.04)	0.49 (± 0.02)	0.08 (± 0.03)	0.28 (± 0.07)	0.45 (± 0.06)	0.31 (± 0.05)	0.1 (± 0.03)	0.75 (± 0.04)	0.68 (± 0.03)	0.58 (± 0.04)
Mono-culture	Pre (abs)	0.42 (± 0.01)	0.42 (± 0.01)	0.3 (± 0.01)	0.39 (± 0.03)	0.42 (± 0.01)	0.42 (± 0.01)	0.3 (± 0.01)	0.69 (± 0.01)	0.69 (± 0.01)	0.59 (± 0.01)
	P	0.87 (± 0.01)	0.87 (± 0.01)	0.32 (± 0.06)	0.85 (± 0.04)	0.87 (± 0.01)	0.87 (± 0.01)	0.32 (± 0.06)	1.01 (± 0.02)	1.01 (± 0.02)	0.94 (± 0.01)
	PA	0.63 (± 0.04)	0.63 (± 0.04)	0.07 (± 0)	0.67 (± 0.1)	0.63 (± 0.04)	0.63 (± 0.04)	0.07 (± 0)	0.9 (± 0.01)	0.9 (± 0.01)	0.82 (± 0.04)
	PAB	0.49 (± 0.04)	0.49 (± 0.04)	0.05 (± 0.02)	0.31 (± 0.1)	0.49 (± 0.04)	0.49 (± 0.04)	0.05 (± 0.02)	0.83 (± 0.02)	0.83 (± 0.02)	0.65 (± 0.01)
		A2	B2	C2	D2	E2	F2	G2	H2	I2	J2
Binary mixture	Pre (abs)	0.68 (± 0.02)	0.59 (± 0.02)	0.64 (± 0.01)	0.59 (± 0.01)	0.6 (± 0.03)	0.67 (± 0.01)	0.6 (± 0.03)	0.65 (± 0.01)	0.45 (± 0.01)	0.58 (± 0.02)
	P	0.98 (± 0.03)	0.94 (± 0.03)	0.94 (± 0.02)	0.97 (± 0.09)	1.02 (± 0.08)	0.9 (± 0.02)	0.94 (± 0.05)	0.9 (± 0.03)	1.36 (± 0.11)	0.89 (± 0.02)
	PA	0.91 (± 0.04)	0.78 (± 0.03)	0.82 (± 0.03)	0.67 (± 0.03)	0.81 (± 0.1)	0.79 (± 0.03)	0.78 (± 0.05)	0.73 (± 0.03)	1.02 (± 0.43)	0.78 (± 0.01)
	PAB	0.86 (± 0.03)	0.61 (± 0.05)	0.6 (± 0.04)	0.6 (± 0.09)	0.74 (± 0.12)	0.67 (± 0.03)	0.64 (± 0.12)	0.56 (± 0.13)	0.83 (± 0.1)	0.67 (± 0.05)
Mono-culture	Pre (abs)	0.69 (± 0.01)	0.59 (± 0.01)	0.59 (± 0.01)	0.56 (± 0.03)	0.56 (± 0.03)	0.67 (± 0)	0.6 (± 0.02)	0.56 (± 0.03)	0.67 (± 0)	0.6 (± 0.02)
	P	1.01 (± 0.02)	0.94 (± 0.01)	0.94 (± 0.01)	0.82 (± 0.03)	0.82 (± 0.03)	0.95 (± 0.01)	0.96 (± 0.02)	0.82 (± 0.03)	0.95 (± 0.01)	0.96 (± 0.02)
	PA	0.9 (± 0.01)	0.82 (± 0.04)	0.82 (± 0.04)	0.62 (± 0.02)	0.62 (± 0.02)	0.87 (± 0.03)	0.85 (± 0.04)	0.62 (± 0.02)	0.87 (± 0.03)	0.85 (± 0.04)
	PAB	0.83 (± 0.02)	0.65 (± 0.01)	0.65 (± 0.01)	0.55 (± 0.05)	0.55 (± 0.05)	0.68 (± 0.02)	0.71 (± 0.05)	0.55 (± 0.05)	0.68 (± 0.02)	0.71 (± 0.05)

Table D.15 Pre-exposure $F_v:F_m$ and post-exposure relative $F_v:F_m$ from independently conducted ternary mixture and monoculture irradiance exposure experiments. Average (\pm standard deviation).

Suspension	Light Treatment	<i>Dlemm + Psimp + Fcroto</i>			<i>Maeru + Ccamb + Speter</i>		
		Bl	Gr	Br	Bl	Gr	Br
Ternary mixture	Pre (abs)	0.46 (± 0.03)	0.73 (± 0.03)	0.49 (± 0.04)	0.37 (± 0.02)	0.67 (± 0.01)	0.59 (± 0.01)
	P	0.84 (± 0.03)	1.13 (± 0.09)	0.93 (± 0.07)	0.75 (± 0.05)	0.93 (± 0.03)	0.76 (± 0.43)
	PA	0.43 (± 0.14)	1.05 (± 0.06)	0.74 (± 0.08)	0.36 (± 0.12)	0.89 (± 0.02)	0.45 (± 0.41)
	PAB	0.28 (± 0.1)	0.88 (± 0.07)	0.58 (± 0.1)	0.12 (± 0.11)	0.8 (± 0.05)	0.15 (± 0.2)
Mono-culture	Pre (abs)	0.39 (± 0.03)	0.59 (± 0.01)	0.6 (± 0.02)	0.42 (± 0.01)	0.69 (± 0.01)	0.62 (± 0.01)
	P	0.85 (± 0.04)	0.94 (± 0.01)	0.96 (± 0.02)	0.87 (± 0.01)	1.01 (± 0.02)	0.91 (± 0.02)
	PA	0.67 (± 0.1)	0.82 (± 0.04)	0.85 (± 0.04)	0.63 (± 0.04)	0.9 (± 0.01)	0.46 (± 0.15)
	PAB	0.31 (± 0.1)	0.65 (± 0.01)	0.71 (± 0.05)	0.49 (± 0.04)	0.83 (± 0.02)	0.25 (± 0.05)